



Terms and Conditions of Use of Digitised Theses from Trinity College Library Dublin

Copyright statement

All material supplied by Trinity College Library is protected by copyright (under the Copyright and Related Rights Act, 2000 as amended) and other relevant Intellectual Property Rights. By accessing and using a Digitised Thesis from Trinity College Library you acknowledge that all Intellectual Property Rights in any Works supplied are the sole and exclusive property of the copyright and/or other IPR holder. Specific copyright holders may not be explicitly identified. Use of materials from other sources within a thesis should not be construed as a claim over them.

A non-exclusive, non-transferable licence is hereby granted to those using or reproducing, in whole or in part, the material for valid purposes, providing the copyright owners are acknowledged using the normal conventions. Where specific permission to use material is required, this is identified and such permission must be sought from the copyright holder or agency cited.

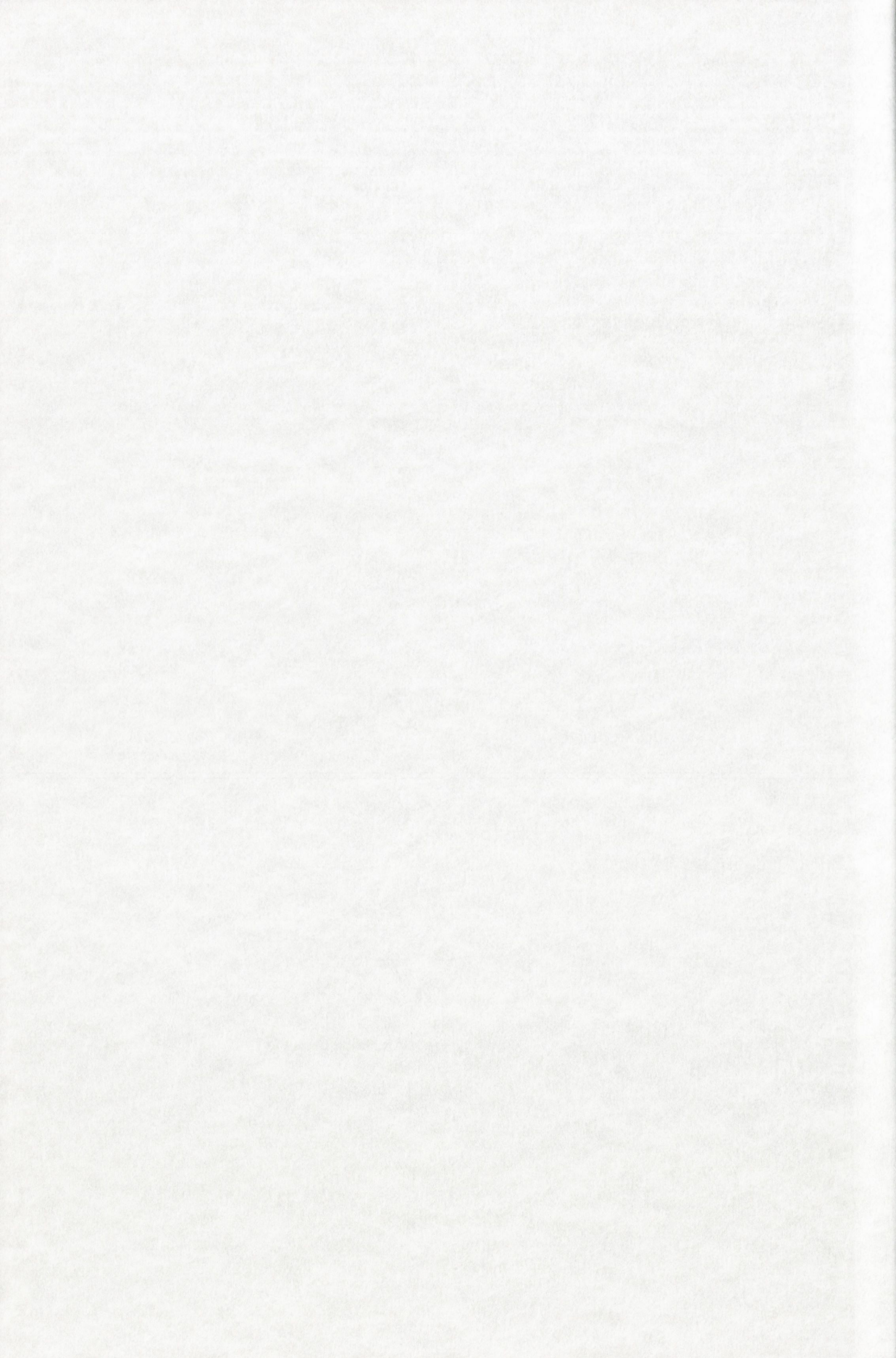
Liability statement

By using a Digitised Thesis, I accept that Trinity College Dublin bears no legal responsibility for the accuracy, legality or comprehensiveness of materials contained within the thesis, and that Trinity College Dublin accepts no liability for indirect, consequential, or incidental, damages or losses arising from use of the thesis for whatever reason. Information located in a thesis may be subject to specific use constraints, details of which may not be explicitly described. It is the responsibility of potential and actual users to be aware of such constraints and to abide by them. By making use of material from a digitised thesis, you accept these copyright and disclaimer provisions. Where it is brought to the attention of Trinity College Library that there may be a breach of copyright or other restraint, it is the policy to withdraw or take down access to a thesis while the issue is being resolved.

Access Agreement

By using a Digitised Thesis from Trinity College Library you are bound by the following Terms & Conditions. Please read them carefully.

I have read and I understand the following statement: All material supplied via a Digitised Thesis from Trinity College Library is protected by copyright and other intellectual property rights, and duplication or sale of all or part of any of a thesis is not permitted, except that material may be duplicated by you for your research use or for educational purposes in electronic or print form providing the copyright owners are acknowledged using the normal conventions. You must obtain permission for any other use. Electronic or print copies may not be offered, whether for sale or otherwise to anyone. This copy has been supplied on the understanding that it is copyright material and that no quotation from the thesis may be published without proper acknowledgement.



**The role of hyphae and hypha-associated genes in
the pathogenesis of
*Candida dubliniensis***

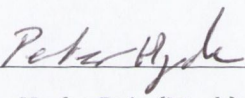
**A thesis submitted to the University of Dublin in fulfillment of the requirements
for the degree of Doctor of Philosophy by**

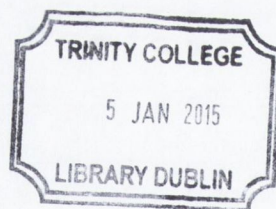
**Peter Hyde
March 2014**

**Microbiology Research Unit,
Division of Oral Biosciences,
Dublin Dental University Hospital,
University of Dublin,
Trinity College Dublin.**

Declaration

I hereby declare that this thesis has not previously been submitted for a degree at this or any other university, and that it represents my own unaided work, except where duly acknowledged in the text. I agree that this thesis may be lent or copied at the discretion of the librarian, Trinity College Dublin.


Peter Hyde, B.A. (Mod.) Microbiology



Thesis 10718

**“Sometimes you wake up. Sometimes the fall kills you.
And sometimes, when you fall, you fly”
-Neil Gaiman**

Summary

Candida albicans is a major cause of superficial and systemic fungal infections in humans. In contrast, its most closely related phylogenetic neighbour, *Candida dubliniensis*, causes disease much less frequently, despite sharing many characteristics. *Candida albicans* is capable of a reversible switch between an ellipsoid yeast form and an elongated filamentous form in response to various environmental cues. Morphological plasticity is considered to contribute to the virulence and pathogenesis of *C. albicans*. *Candida dubliniensis* shares this dimorphic trait, although the less pathogenic species forms true hyphae at much lower rates under infection-simulative conditions *in vitro* and *in vivo*. The development of true hyphae in *C. albicans* is highly regulated by complex interconnecting signalling pathways. Expression of hypha-specific genes is associated with *C. albicans* virulence. Notably, key virulence-associated hypha-specific genes (*CaALS3*, *CaHYR1*) are absent from the *C. dubliniensis* genome, contributing to the lack of virulence, relative to *C. albicans*. This study has attempted to dissect the importance of lower filamentation rates and hypha-specific genes in the pathogenesis of *C. dubliniensis*, and by extension, *C. albicans*.

By constructing *C. dubliniensis* mutant strains, expressing *CaALS3* or *CaHYR1*, under the control of a doxycycline-inducible integrated promoter, this study has explored the pathogenic contribution of *C. albicans* hypha-specific genes in a less virulent background. Construction of these heterologous expression *C. dubliniensis* strains presented challenges, highlighting limitations in current molecular cloning methods. Inducible gene expression was confirmed for *C. dubliniensis* strains harbouring *CaALS3* and *CaHYR1*. Phenotypic analysis of *C. dubliniensis* expressing *CaALS3* supported the role of *CaALS3* in adhesion to host epithelial cells, and its importance during the adhesion and invasion stages of infection. *Candida dubliniensis* expressing *CaHYR1* did not reveal an increase in fungal survival when cells were incubated with human neutrophils. Further investigation of protein localisation and abundance will help define the phenotypes observed.

The lower rate of filamentation displayed by *C. dubliniensis* is commonly associated with the reduced virulence exhibited by the species, compared to *C. albicans*. This study has suggested that although *C. dubliniensis* filamentation rates are lower than *C. albicans*, intra-species variation in ability to filament may play a role, or serve as an indicator of virulence potential. Adhesion to host tissues is a key step in the process of infection. *Candida dubliniensis* strain variation, rather than cell morphology, appeared to play a more important role in initial adhesion stages. However, damage of epithelial tissue monolayers was morphology-dependent, with *C. dubliniensis* hyphae causing higher levels of tissue damage than corresponding yeast cells. These findings support the importance of protein identity and quantity during adhesion, suggesting that intraspecies differential regulation of proteins is responsible for variation in adhesion efficiency. Tissue damage caused by *C. dubliniensis* hyphae likely resulted from a combination of protein-induced damage and active hyphal penetration. Further study to dissect these two invasion mechanisms in *C. dubliniensis* will reveal the dominant mechanism, and highlight any differences between *C. dubliniensis* and *C. albicans* hyphal-induced tissue damage.

Induction of hyphae is a dynamic reversible process and reversion of hyphae to yeast occurs over time. As a result of the lower filamentation efficiency of *C.*

dublinsiensis, previous studies have been limited by this reversion. As part of this current study, a method for *C. dublinsiensis* hyphal induction and morphological maintenance (>18 h) has been developed. Comparison of morphogenetic regulator expression patterns, in response to an established hyphal induction method and the newly developed method, has highlighted differences in expression of *NRG1*, *CPH1*, and *EFG1*, indicative of the reversion rates associated with both methods. Inter- and intra-species variation in gene expression was also observed, suggesting a link between epidemiological sources of strains. Future transcriptomic, proteomic, and infection model studies will benefit from the development of this novel method for *C. dublinsiensis* hyphal induction, enabling the accurate analysis of stable *C. dublinsiensis* true hyphae.

Mass spectrometric analysis of the *C. dublinsiensis* and *C. albicans* cell wall GPI-anchored protein repertoire, using the newly developed method for hyphal induction and maintenance, allowed comparison of cell wall protein identity, and relative abundance on yeast and hyphal cells. Similar to morphogenetic regulator expression analysis, inter- and intra-species differences were highlighted. Although *C. dublinsiensis* does not possess the virulence-associated proteins *CaAls3p* and *CaHyr1p*, a relatively virulent *C. dublinsiensis* isolate was found to express a hypha-specific protein (*CdFlo9p*), with predicted characteristics analogous to *CaAls3p* and *CaHyr1p*. Future investigation will determine whether *CdFlo9p* is responsible for higher *C. dublinsiensis* virulence levels and whether the expression of *CdFlo9p* represents an example of evolutionary adaptation in the absence of *CaAls3p* and *CaHyr1p*.

In order to better combat fungal infection as a result of *Candida*, it is important to understand the virulence-associated evolutionary adaptations experienced by *C. dublinsiensis* and *C. albicans*. The divergent evolutionary paths taken by the two *Candida* species have resulted in the establishment of *C. albicans* as an efficient opportunistic pathogen, while *C. dublinsiensis* rarely causes infection. This study has elaborated on the mechanisms underlying the lack of virulence of *C. dublinsiensis*, compared to its closest relative *C. albicans*, confirming that the combination of lower filamentation rates and lack of virulence-associated genes plays an important role in the reduced virulence of *C. dublinsiensis*. The development of an improved method for induction and maintenance of *C. dublinsiensis* hyphae will enable future research to more accurately assess the role of *Candida* filamentation in the pathogenesis of *Candida* spp.

TABLE OF CONTENTS

Acknowledgements	I
Abbreviations	III

Chapter 1. General introduction

1.1. The importance of fungal infections.....	2
1.1.1. Candidiasis	2
1.2. The <i>Candida</i> genus.....	3
1.2.1. Discovery of <i>Candida dubliniensis</i>	3
1.2.2. Population structure	5
1.2.3. Epidemiology of <i>Candida albicans</i> and <i>C. dubliniensis</i>	7
1.2.4. Antifungal resistance	7
1.3. Morphological plasticity of <i>C. albicans</i> and <i>C. dubliniensis</i>	8
1.3.1. <i>Candida</i> filamentation	9
1.3.2. Chlamydospores	10
1.3.3. Mating.....	11
1.3.4. Biofilm growth.....	12
1.4. Genomic comparison of <i>C. albicans</i> and <i>C. dubliniensis</i>	14
1.4.1. Gene family expansion and gene loss	14
1.4.2. Virulence-associated cell wall proteins	15
1.5. Aims of the current study.....	18

Chapter 2. General materials and methods

2.1. General microbiological methods.....	20
2.1.1. Strains and growth conditions.....	20
2.1.2. Chemicals and enzymes.....	21
2.1.3. Buffers and solutions	21
2.2. Isolation and analysis of nucleic acids from <i>Candida</i> cells.....	22
2.2.1. Extraction of genomic DNA from <i>Candida</i> cells.....	22
2.2.2. PCR amplification	23
2.2.3. Extraction of chromosomal DNA from <i>Candida</i> cells.....	23
2.2.4. Southern blot analysis of <i>Candida</i> DNA	24
2.2.5. Rapid lysis and extraction of <i>Candida</i> DNA for colony PCR.....	24
2.2.6. Harvesting RNA and synthesis of cDNA.....	25
2.2.7. qRT-PCR validation and analysis of gene expression	25
2.3. Recombinant DNA techniques	26
2.3.1. Isolation of plasmid DNA from <i>Escherichia coli</i>	26
2.3.2. Digestion and ligation of DNA fragments.....	26
2.3.3. Transformation of PIPES/CaCl ₂ -competent <i>E. coli</i> by heat shock.....	26
2.4. Hyphal induction of <i>C. albicans</i> and <i>C. dubliniensis</i>	27
2.4.1. Standard hyphal induction on solid media.....	27
2.4.2. Standard hyphal induction in liquid media.....	28

2.5. General tissue culture methods	28
2.5.1. Growth and maintenance of cell lines	28
2.5.2. Approved isolation of human buccal epithelial cells	29

Chapter 3. Construction and analysis of *C. dubliniensis* strains expressing *C. albicans* virulence genes

3.1. Introduction	31
3.1.1. <i>ALS</i> gene family.....	31
3.1.2. <i>IFF</i> gene family.....	33
3.1.3. Molecular cloning methods.....	34
3.1.4. Aims of this part of the study	37
3.2. Specific materials and methods	38
3.2.1. Restriction endonuclease-mediated cloning	38
3.2.1.1. Preparation of template DNA.....	38
3.2.1.2. PCR amplification and purification of <i>CaALS3</i> alleles.....	38
3.2.1.3. Isolation of plasmids.....	38
3.2.1.4. Digestion and ligation of DNA fragments	38
3.2.1.5. Transformation of <i>E. coli</i> competent cells.....	39
3.2.1.6. Screening of putative transformants by PCR amplification.....	39
3.2.2. PCR fusion and split marker cloning	40
3.2.2.1. Design of PCR fusion primers.....	40
3.2.2.2. PCR amplification of DNA fragments.....	40
3.2.2.3. Two step fusion procedure.....	40
3.2.2.4. Split-marker transformation of <i>C. dubliniensis</i>	41
3.2.2.5. Screening of putative transformants by PCR amplification.....	41
3.2.3. Non-integrative plasmid transformation	42
3.2.4. Constitutive gene expression cloning.....	42
3.2.4.1. Design of primers for <i>pENO.NAT</i> constitutive gene expression.....	42
3.2.4.2. DNA amplification and transformation of <i>C. dubliniensis</i>	43
3.2.5. Southern blot analysis of putative transformants.....	43
3.2.5.1. PCR amplification of DIG-labelled probe.....	43
3.2.5.2. Preparation of template DNA.....	44
3.2.5.3. Southern blot analysis	44
3.2.6. Analysis of gene expression by qRT-PCR	44
3.2.6.1. Induction of gene expression with doxycycline.....	44
3.2.6.2. Isolation of RNA and preparation of cDNA	44
3.2.6.3. Analysis of gene expression by qRT-PCR.....	45
3.2.7. Comparison of CdpNIM and CapNIM doxycycline-inducible gene expression systems.....	45
3.2.7.1. The impact of growth condition on gene expression.....	45
3.2.7.2. Investigation and quantification of inducible gene expression.....	45
3.2.8. Immunofluorescent detection of <i>CaAls3p</i>	46
3.2.9. Adherence of WÜ284.CaALS3 to human buccal epithelial cells.....	46
3.2.10. Survival of WÜ284.CaHYR1 against human neutrophil response.....	46
3.3. Results	48
3.3.1. Restriction endonuclease-mediated cloning of <i>CaALS3</i>	48
3.3.2. PCR fusion and transformation of WÜ284 with <i>CaALS3</i>	49
3.3.2.1. Analysis of <i>CaALS3</i> gene expression in WÜ284 transformed with CdpNIM.CaALS3.....	50
3.3.2.2. Comparative analysis of CdpNIM and CapNIM doxycycline-inducible gene expression.....	50
3.3.2.3. Analysis of <i>CaALS3</i> gene expression in WÜ284 transformed with CapNIM.CaALS3.....	51

3.3.2.4. Confirmation of chromosomal integration of <i>CapNIM.CaALS3</i>	51
3.3.2.5. Phenotypic analysis of WÜ284 cells expressing <i>CaALS3</i>	52
3.3.2.6. Detection of <i>CaAls3p</i> on the <i>Candida</i> cell surface.....	52
3.3.3. Restriction endonuclease-mediated cloning of <i>CaHYR1</i>	52
3.3.4. PCR fusion-mediated cloning of <i>CaHYR1</i>	53
3.3.4.1. Analysis of <i>CaHYR1</i> gene expression in WÜ284 transformed with <i>CapNIM.CaHYR1</i>	53
3.3.4.2. Confirmation of chromosomal integration of <i>CapNIM.CaHYR1</i>	53
3.3.4.3. Phenotypic analysis of WÜ284 cells expressing <i>CaHYR1</i>	54
3.3.5. Constitutive gene expression system using pENO.NAT.....	54
3.3.6. Non-integrative gene expression system using pADH1	54
3.4. Discussion.....	56
3.4.1. Molecular cloning methods.....	56
3.4.2. <i>ALS3</i> gene cloning and expression.....	57
3.4.3. <i>HYR1</i> gene cloning and expression.....	59
3.4.4. Future directions.....	59

Chapter 4. *Candida dubliniensis* hyphal induction, adhesion and tissue damage

4.1. Introduction.....	61
4.1.1. Filamentous diversity.....	61
4.1.2. <i>Candida</i> hyphal induction.....	63
4.1.3. Infection models	64
4.1.4. Strain variation.....	66
4.1.5. Aims of this part of the study	66
4.2. Specific materials and methods	68
4.2.1. Hyphal induction on solid media.....	68
4.2.1.1. Growth and maintenance conditions.....	68
4.2.1.2. Visualisation of hyphae.....	68
4.2.2. Hyphal induction in liquid media	68
4.2.2.1. Staining and morphological verification.....	68
4.2.2.2. Induction of hyphae following preculture in YEPD broth	69
4.2.2.3. Tissue culture medium (CDMEM) as a hyphal inducer.....	69
4.2.3. <i>Candida dubliniensis</i> strain growth rates.....	69
4.2.4. Adhesion to TR146 human buccal epithelial monolayers.....	70
4.2.4.1. Quantification of adhesive colony forming units.....	70
4.2.4.2. Direct visualisation of adherent cells	71
4.2.5. Morphology-associated tissue damage.....	71
4.3. Results.....	72
4.3.1. Hyphal induction on solid media.....	72
4.3.2. Cell morphology verification	73
4.3.3. Hyphal induction in liquid media	73
4.3.3.1. Morphological reversion in liquid media.....	74
4.3.3.2. Hyphal induction in tissue culture medium (CDMEM)	74
4.3.4. Strain variation and growth rates.....	75
4.3.5. Yeast and hyphal adherence to TR146 human buccal epithelial monolayers.....	75
4.3.6. Morphology-associated tissue damage.....	76
4.3.6.1. Visualisation of adherence and TR146 epithelial cell damage.....	77
4.4. Discussion.....	78
4.4.1. Induction of <i>C. dubliniensis</i> hyphae on solid media	78
4.4.2. Morphological identification and differentiation of hyphae.....	78
4.4.3. Induction of <i>C. dubliniensis</i> hyphae in liquid media	79

4.4.4. Morphology and fungal adherence to human epithelial cells	80
4.4.5. Fungal morphology and tissue damage	80
4.4.6. Future directions	82

Chapter 5. Improved *Candida dubliniensis* hyphal induction and maintenance

5.1. Introduction	84
5.1.1. <i>Candida</i> hyphal induction signals.....	84
5.1.1.1. Serum	84
5.1.1.2. <i>N</i> -acetylglucosamine.....	85
5.1.1.3. Quorum sensing and cell density.....	86
5.1.1.4. Nutrient sensing	88
5.1.1.5. Carbon dioxide	89
5.1.1.6. Carbon source.....	89
5.1.2. Hyphal commitment and reversion.....	90
5.1.3. Aims of this part of the study	91
5.2. Specific materials and methods	92
5.2.1. Development of an improved method for <i>C. dubliniensis</i> hyphal initiation and maintenance.....	92
5.2.1.1. Nutrient abundance.....	92
5.2.1.2. Oxygen and carbon dioxide	93
5.2.1.3. Quorum and environmental sensing	93
5.2.1.4. Carbon source availability.....	93
5.2.2. Optimal growth, hyphal induction and morphology maintenance.....	93
5.2.3. Analysis of morphogenetic regulator expression.....	94
5.2.3.1. Yeast morphology.....	94
5.2.3.2. Hyphal morphology	94
5.2.3.3. Experimental timepoints	95
5.2.3.4. Cell disruption and RNA extraction	95
5.2.3.5. Generation of cDNA.....	95
5.2.3.6. Primer design for qRT-PCR	95
5.2.3.7. Analysis of gene expression	96
5.3. Results	97
5.3.1. The impact of nutrients on <i>C. dubliniensis</i> hyphal induction.....	97
5.3.2. Oxygen and carbon dioxide	98
5.3.3. The role of quorum and environmental sensing.....	98
5.3.4. Carbon source and availability	99
5.3.5. Serum and <i>N</i> -acetylglucosamine induction of <i>C. dubliniensis</i> hyphae.....	100
5.3.6. Analysis of morphogenetic regulator response to growth and hyphal induction conditions.....	100
5.3.6.1. Negative regulator of glucose-controlled genes (<i>NRG1</i>).....	100
5.3.6.2. <i>Candida</i> pseudohyphal regulator (<i>CPH1</i>).....	100
5.3.6.3. Enhanced filamentous growth regulator (<i>EFG1</i>).....	101
5.4. Discussion	102
5.4.1. Development of an improved method for initiation and maintenance of <i>C. dubliniensis</i> hyphae.....	102
5.4.1.1. Nutrient limitation.....	102
5.4.1.2. Carbon dioxide and hyphae.....	103
5.4.1.3. Quorum and environmental sensing	104
5.4.1.4. Carbon source and availability as a hyphal inducing signal.....	105
5.4.1.5. Serum and <i>N</i> -acetylglucosamine induction of hyphae.....	105

5.4.2. Regulation of <i>Candida</i> filamentous dimorphism	107
5.4.2.1. <i>NRG1</i>	107
5.4.2.2. <i>CPH1</i>	108
5.4.2.3. <i>EFG1</i>	109
5.4.3. Future directions	110

Chapter 6. Comparative proteomic analysis of *C. dubliniensis* and *C. albicans* dimorphic cell wall proteins

6.1. Introduction.....	112
6.1.1. Cell wall composition.....	112
6.1.2. Glycophosphatidylinositol-anchored cell wall proteins.....	113
6.1.3. Protein detection in <i>C. albicans</i> and <i>C. dubliniensis</i>	114
6.1.4. <i>In silico</i> protein prediction	114
6.1.5. Mass spectrometric detection of protein	114
6.1.6. Aims of this part of the study	116
6.2. Specific materials and methods	117
6.2.1. Growth and morphology induction conditions	117
6.2.2. Effective cell disruption and isolation of cellular protein fractions	118
6.2.3. Sample preparation for mass spectrometry	120
6.2.4. Preparation of peptides	120
6.2.4.1. Disulphide bond reduction and alkylation.....	120
6.2.4.2. Tryptic digestion of cell wall proteins.....	120
6.2.4.3. Peptide processing	121
6.2.5. Quadropole Time of Flight mass spectrometry.....	121
6.2.5.1. Run conditions	121
6.2.5.2. Data analysis.....	121
6.2.6. Fourier Transform mass spectrometry	122
6.2.6.1. Run conditions.....	122
6.2.6.2. Data analysis.....	122
6.2.7. <i>In silico</i> protein prediction tools	122
6.3. Results.....	124
6.3.1. <i>In silico</i> protein prediction	124
6.3.2. Morphological induction and maintenance	124
6.3.3. Protein identification by Q-TOF mass spectrometry	125
6.3.4. Relative quantification of proteins by FTMS	126
6.3.4.1. Interspecies protein variation	126
6.3.4.2. Intraspecies protein variation	128
6.3.5. Gene expression analysis of a hypha-associated GPI-protein.....	129
6.4. Discussion.....	131
6.4.1. Comparison of <i>in silico</i> and <i>in vitro</i> GPI-protein identification	131
6.4.2. Identification of GPI-proteins by Q-TOF.....	132
6.4.2.1. Morphology-independent protein expression	132
6.4.2.2. Morphology-dependent protein expression	132
6.4.3. Methodology sensitivity and variation	134
6.4.4. Intra- and inter-species cell wall GPI-protein variation.....	134
6.4.5. Quantification and relative abundance of GPI-proteins	136
6.4.6. Cell wall GPI-proteins and vaccine development	137
6.4.7. Future directions	137

Chapter 7. General discussion

7.1. Molecular cloning methods	140
7.1.1. Species-specific adaptations and challenges	140
7.2. Filamentation of <i>C. dubliniensis</i> and <i>C. albicans</i>	141
7.2.1. Filamentation and strain variation	141
7.2.2. Morphology and virulence.....	141
7.2.3. Morphologically stable <i>C. dubliniensis</i> hyphae.....	142
7.2.4. A <i>C. dubliniensis</i> virulence-associated cell wall GPI-protein.....	143
7.3. Filamentation and evolutionary adaptation.....	144
7.3.1. Epidemiological source as an indicator of filamentous virulence.....	144
7.3.2. The importance of host factors.....	144
7.3.3. Evolutionary and pathogenic divergence	145
7.4. Future directions and concluding remarks	145
References	147

Index of figures

Page numbers refer to text page preceding the figure(s)

Figure	Title	Page
1.1.	Maximum likelihood phylogeny, showing selected members of the CTG and WGD clades of the genus <i>Candida</i>	3
1.2.	Population structure of <i>C. albicans</i> and <i>C. dubliniensis</i>	6
1.3.	Hypha-inducing environmental signals and signalling pathways	9
3.1.	Modular domain structure of <i>C. albicans</i> ALS family members	31
3.2.	Molecular gene cloning using a doxycycline-inducible differential gene expression system	39
3.3.	PCR fusion and split marker transformation cloning approach	40
3.4.	Constitutive gene expression system approach	43
3.5.	Comparison of doxycycline inducible gene expression systems	50
3.6.	Southern blot analysis showing chromosomal integration of gene expression cassettes	51
3.7.	Phenotypic analysis of <i>C. dubliniensis</i> induced to express <i>CaALS3</i>	52
3.8.	Immunofluorescent detection of <i>CaAls3p</i> on the surface of <i>Candida</i> cells	52
4.1.	Colony fringe microscopy of <i>C. dubliniensis</i> on solid hyphal inducing media	72
4.2.	Verification of cell morphology by visualisation of nuclear division and segregation patterns	73
4.3.	Induction of <i>C. dubliniensis</i> true hyphae in liquid media	73
4.4.	Induction and reversion of <i>C. dubliniensis</i> hyphae in WS medium	74
4.5.	Induction of <i>C. dubliniensis</i> and <i>C. albicans</i> hyphae in tissue culture medium (CDMEM)	74
4.6.	<i>Candida dubliniensis</i> and <i>C. albicans</i> strain growth rates	75
4.7.	Adherence of <i>C. dubliniensis</i> , and <i>C. albicans</i> yeast and hyphae to TR146 human epithelial monolayers	76
4.8.	<i>Candida dubliniensis</i> and <i>C. albicans</i> morphology-associated tissue damage	76
4.9.	Direct visualisation of <i>Candida</i> morphology and damage of TR146 human epithelial monolayers	77

Index of figures

Page numbers refer to text page preceding the figure(s)

Figure	Title	Page
5.1.	The impact of nutrients in preculture growth media on <i>C. dubliniensis</i> and <i>C. albicans</i> hyphal induction	97
5.2.	The impact of nutrient abundance during induction of <i>C. dubliniensis</i> and <i>C. albicans</i> hyphae	97
5.3.	Oxygen and carbon dioxide during <i>C. dubliniensis</i> and <i>C. albicans</i> hyphal induction	98
5.4.	The role of inoculation density during the <i>C. dubliniensis</i> filamentous transition	98
5.5.	Cyclic AMP as a hyphal inducing signal in <i>C. dubliniensis</i> and <i>C. albicans</i>	98
5.6.	The importance of carbon source and abundance during <i>C. dubliniensis</i> , and <i>C. albicans</i> hyphal initiation and maintenance	99
5.7.	Improved <i>C. dubliniensis</i> hyphal induction and maintenance	100
5.8.	Temporal analysis of morphogenetic regulator expression during the dimorphic transition	100
6.1.	The <i>C. albicans</i> cell wall	112
6.2.	Interspecies GPI-protein variation and GPI-protein abundance	127
6.3.	Analysis of <i>C. dubliniensis</i> and <i>C. albicans</i> hypha-associated <i>FLO9</i> gene expression	129
6.4.	Conservation of <i>FLO9</i> between <i>C. albicans</i> and <i>C. dubliniensis</i>	136

Index of tables

Page numbers refer to text page preceding the table(s)

Table	Title	Page
2.1.	List of <i>C. albicans</i> and <i>C. dubliniensis</i> strains used as part of this study	20
2.2.	List of oligonucleotide primers used as part of this study	23
4.1.	Induction of <i>C. dubliniensis</i> hyphae and strain variation on solid growth media	72
6.1.	Identification of GPI-proteins by Q-TOF mass spectrometry	125
6.2.	Interspecies comparison of GPI-protein abundance on <i>C. albicans</i> and <i>C. dubliniensis</i> cell walls	127

Acknowledgements

First of all I would like to thank my supervisor Prof. Derek Sullivan for his support. I particularly appreciate his encouragement to not only to travel during the course of my studies, but also to pursue the areas of research that I found to be important and interesting. Thanks also to Prof. Gary Moran and Dr. Judy Higgins for their help during the early stages of my project. I am grateful for the contributions from, and discussions with all the members of the *Candida* research group. For ordering reagents, equipment, and being told how messy my lab bench was, I don't know what I would have done without the assistance and organisation of our lab manager, Dr. Mary O'Donnell. I would not have been able to carry out any research without the funding support of the Health Research Board and Dublin Dental University Hospital.

I would like to thank all the past and present members of the Oral Bioscience, Microbiology Unit. Putting up with my endless science questions and always making me smile at coffee break made the past four years enjoyable, regardless of stress levels. In particular I would like to thank Aisling for being in the right place at the right time and putting me in contact with people who helped me through a difficult injury and transition. Thanks also to Emily and Sarah for all of their triathlon advice and helping me avoid doing something stupid and getting myself disqualified in the middle of a race.

I was lucky enough to have the opportunity to travel and meet some really great people. To all of the FINSysB members, the Aberdeen Fungal Group and the University of Amsterdam cohort, thank you for being so welcoming. Thanks to Megan and Jeanette for showing me the Scottish countryside outside of Aberdeen, and the Amsterdam group for showing me that in the Game of Thrones boardgame you either win, or you die. Or you get so confused by the rules that you just try to sabotage the closest player.

I especially want to thank Clemens Heilmann, and Prof. Frans Klis for an exciting collaboration, interesting conversations, and a reminder that the scientific research world is much bigger than our little corner in Dublin.

There are not many people who would put up with me, so I want to thank Fiona for sticking with me and putting up with all the random obsessions and coffee-fuelled hyperactivity. I am grateful to Fiona's parents, Denis and Maria, for supplying the coffee in the first place. To my sister Joanne, I don't have any purple and pink dots in this thesis but I hope you will settle for fluorescent blue ones. Finally, to my own parents, John and Rhona, the "cooking" (research) is going ok. Actually it's finished...

Abbreviations

.mgf	Mascot Generic File format
.pkl	Micromass Peak List file format
°C	Degrees centigrade
Δ	Deletion (of a gene or part of a gene)
~	Approximately
5-FC	5-Fluorocytosine/ 5-flucytosine
ACN	Acetonitrile
AIDS	Acquired immunodeficiency syndrome
ARS	Autonomously replicating sequence
ATP	Adenosine 5' -triphosphate
BEC	Buccal epithelial cell
bp	Base pair
BSA	Bovine serum albumin
cAMP	Cyclic adenosine monophosphate
CDMEM	Complete Dulbecco's modified Eagle's medium
cDNA	Complementary DNA
CEN	Centromeric
cfu	Colony forming unit
CFW	Calcofluor white
CGD	<i>Candida</i> Genome Database
CO ₂	Carbon dioxide
C _t	Cycle threshold
DAPI	4', 6-diamidino-2-phenylindole
DIG	Dideoxygenin
DMEM	Dulbecco's modified Eagle's medium
DMSO	Dimethyl sulphoxide

DNA	Deoxyribonucleic acid
DNase	Deoxyribonuclease
dNTPs	di-Nucleotide triphosphate
DOX	Doxycycline
DOX ₁₀₀	Doxycycline 100 µg/ml
DOX ₅₀	Doxycycline 50 µg/ml
DOX ₂₀	Doxycycline 20 µg/ml
DTT	Dithiothreitol
EDTA	Ethylenediamine tetraacetic acid
<i>et al.</i>	And others
FCS	Foetal calf serum
FTMS	Fourier Transform Mass Spectrometry
g	Gram
GlcNAc	<i>N</i> -acetylglucosamine
GMP	Guanosine monophosphate
GPI	Glycophosphatidylinositol
h	Hour(s)
HA	Haemagglutinin
His	Histidine
HIV	Human immunodeficiency virus
HPLC	High performance liquid chromatography
HSL	Homoserine lactone
<i>i.e.</i>	That is
IAA	Indole-acetic acid
IPTG	Isopropyl-β-thiogalactoside
ITS	Internally transcribed spacer
kb	kilobase

kg	Kilogram
kV	Kilovolt
L	Litre(s)
L _{AMP}	LB with 100 µg/ml ampicillin
LB	Luria Bertani (agar/broth)
LDH	Lactate dehydrogenase
M	Molar
mAb	Monoclonal antibody
MAPK	Mitogen activated Protein Kinase
Mb	Megabase
MCS	Multiple cloning site
mg	Milligram
MI	Morphological index
min	Minute
ml	Millilitre
MLST	Multilocus sequence typing
mM	Millimolar
MPA	Mycophenolic acid
mRNA	Messenger RNA
MRS	Major repeat sequence
MTL	Mating type-like
NAT ₁₀₀	YEPD (agar/broth) with 100 µg/ml
NAT ₂₀₀	YEPD (agar/broth) with 200 µg/ml
NCAC	Non- <i>Candida albicans Candida</i>
ng	Nanogram
nm	Nanometre
O ₂	Oxygen
OD _x	Optical density at x nm
ORF	Open reading frame

P:C:I	Phenol:Chloroform:Isoamyl alcohol
PAMP	Pathogen-associated molecular pattern
PBS	Phosphate Buffered Saline
PCR	Polymerase Chain Reaction
PDA	Potato dextrose agar
PI	Isoelectric point
PIPES	Piperazine- <i>N,N'</i> -bis(2-ethanesulfonic acid)
PMN	Polymorphonuclear
Q-TOF	Quadropole Time of Flight
qRT-PCR	Real Time Quantitative Reverse Transcriptase Polymerase Chain Reaction
r.p.m.	Revolutions per minute
RE	Restriction endonuclease
RHE	Reconstituted human epithelium
RNA	Ribonucleic acid
RNase	Ribonuclease
s	Second(s)
SDS	Sodium dodecyl sulfate
SLD	Synthetic low dextrose
TBE	Tris-borate EDTA
TE	Tris-EDTA
TFA	Tri-fluoro acetic acid
Tris	Tris (hydroxymethyl)aminomethane
T _x	Time (x)
UK	United Kingdom
USA	United States of America
UV	Ultraviolet

v/v	Volume per volume (ml/100ml)
w/v	Weight per volume (g/100ml)
WGD	Whole genome duplication
WS	Water with 10 % (v/v) FCS
<i>x g</i>	Gravitational force
X-Gal	5-bromo-4-chloro-3-indoyl β -D-galactopyranoside
YEPD	Yeast Extract Peptone Dextrose
YNB	Yeast nitrogen base with ammonium sulfate and amino acids
YNB -a.a.	Yeast nitrogen base without amino acids
YNB -a.a. - (NH ₄) ₂ SO ₄	Yeast nitrogen base without amino acids or ammonium sulfate
YNB-S	Yeast nitrogen base with FCS
YPDS	YEPD with 10 % (v/v) FCS
YPS	Yeast extract peptone sucrose
β	Beta
β Me	β -Mercaptoethanol
μ g	Microgram
μ l	Microlitre
μ m	Micrometre

Chapter 1

General introduction

1.1. The importance of fungal infections

Fungal infections are a significant personal and economic burden in nosocomial and community settings. In the United States of America (USA) during 1998, the economic cost of fungal infections has been estimated as costing approximately \$2.6 billion (Wilson *et al.*, 2002). Improvements in technology and medical therapies made during the last two decades have resulted in an ageing population, increasing the number of immunocompromised people who may be susceptible to fungal infections (Flevari *et al.*, 2013). Thus the economic cost as a result of duration of hospitalisation and antifungal treatments is likely to continue to increase. Fungal superficial and systemic infections are commonly caused by pathogenic *Candida* species. *Candida* has previously been reported as the fourth most common cause of systemic infections in hospitals in the USA, with associated mortality rates ranging from 15 % to 35 % (Pfaller & Diekema, 2007). Although the genus is composed of more than 150 distinct species of yeast, a very limited number of these are clinically relevant as human pathogens. The leading cause of candidaemia is *Candida albicans*, accounting for approximately 60 % of systemic *Candida* infections (Kibbler *et al.*, 2003). In England between 2004 and 2010, *C. albicans* was the cause of up to 69 % of neonatal invasive *Candida* infections (Oeser *et al.*, 2014). The frequency of isolation non- *C. albicans* *Candida* (NCAC) species such as *Candida glabrata*, *Candida parapsilosis*, *Candida tropicalis* and *Candida dubliniensis* is considered to be increasing (Krcmery & Barnes, 2002). As of 2002, isolation of NCAC species from incidences of candidaemia had doubled from an average rate of 25 % to 50 %. Additionally, a retrospective study of *Candida* bloodstream infections in western Saudi Arabia between 2002 and 2009 reported that NCAC were responsible for as much as 66 % of *Candida* systemic infections (Al Thaqafi *et al.*, 2014). The cause of this is not yet clear. However, frequency of isolation of certain species varies geographically (Pfaller *et al.*, 2010). For example, *C. glabrata* is isolated more frequently from patients in North America compared to Latin America. Whether this is a result of geographical effects, underlying population variation or a result of different clinical detection methods has yet to be resolved.

1.1.1. Candidiasis

Candida spp. are abundant in the wider environment and many species exist as harmless commensals of the mammalian oral, gastrointestinal and urogenitary tracts. They can become opportunistic pathogens when the normal function of the host immune system is

altered. Commonly, incidences of systemic and superficial candidiasis arise when the immune system is compromised by an underlying condition such as diabetes, acquired immune deficiency syndrome (AIDS), or cancer (Pfaller & Diekema, 2007). Hormonal changes as a result of pregnancy may also be a predisposing factor for vulvovaginal superficial candidiasis. Infants and the elderly are also susceptible to opportunistic infection with *Candida*. Additionally, therapeutic treatment with antibiotics or steroids can lead to overgrowth of *Candida*, increasing the risk of candidiasis (Banerjee *et al.*, 2008; Dimopoulos *et al.*, 2008; Fidel & Sobel, 1996). Infection of healthy people is rare. *Candida* species can be responsible for both superficial and systemic infections. Infection of the oral cavity as either pseudomembranous or erythematous candidiasis is the most common occurrence of candidiasis (Korting, 1989). This manifests as the localised appearance of creamy white raised lesions or inflamed red lesions on the mucosal surfaces of the mouth. These lesions are usually accompanied by pain and bleeding when scraped as the natural epithelial barrier has been disrupted by the action of fungi invading the substrata. This is often an indication of perturbation of the local host immune system, as evidenced by the high prevalence of oropharyngeal candidiasis in AIDS patients (Sullivan *et al.*, 2004).

1.2. The *Candida* genus

Candida spp. are ascomycetes, representing a genus composed of species which grow as asexual blastospores. A small number of these species have the ability to form pseudohyphae or true hyphae. Fitzpatrick *et al.* have shown that the *Candida* genus is actually a polyphyletic group within the order Saccharomycetales (Fig. 1.1) (Fitzpatrick *et al.*, 2006). Differences in codon usage during protein translation has identified two main groups of clinically relevant *Candida* species (Massey *et al.*, 2003; Papon *et al.*, 2012). The whole genome duplication (WGD) clade translates the CTG codon as leucine and the CTG clade is comprised of species that translate the CTG codon (CUG) as serine. The WGD clade contains the brewer's yeast *Saccharomyces cerevisiae*, and the second most frequent cause of candidiasis, *C. glabrata*, while the CTG clade contains the major pathogen *C. albicans* and NCAC species *C. tropicalis*, *C. parapsilosis* and *C. dubliniensis*.

1.2.1. Discovery of *C. dubliniensis*

The most closely related species to *C. albicans* is *C. dubliniensis* and both are considered to have evolved from an ancestral *C. tropicalis* (McManus & Coleman, 2014). In fact, until 1995, *C. dubliniensis* isolates were routinely identified as "atypical" isolates of *C. albicans*

as a result of an inability to distinguish between the two species due to phenotypic similarities. Most of these “atypical” isolates were recovered from severely immunodepressed patients suffering from AIDS, and HIV infection. Sullivan *et al.* conducted a study of isolates recovered from the oral cavities of AIDS patients from Ireland and Australia (Sullivan *et al.*, 1995). Phenotypic analysis of growth patterns on potato dextrose agar (PDA) and in yeast extract peptone dextrose (YEPD) broth at various temperatures was carried out. Assessment of carbohydrate assimilation profiles and investigation of production of germ tubes, pseudohyphae, and chlamydospores identified divergence of these “atypical” isolates from the phenotypic characteristics of *C. albicans* isolates. Genomic analysis using DNA fingerprinting with *C. albicans* probes, karyotype analysis and investigation of ribosomal RNA gene nucleotide sequences led Sullivan *et al.* to conclude that these “atypical” isolates in fact represented a distinct taxon which they suggested should be called *Candida dubliniensis*. An isolate (CD36) from the oral cavity of a HIV-infected patient who had presented with erythematous candidiasis was designated as the type strain. As a result of similar phenotypic and genotypic characteristics, it was hypothesised that prior to 1995, *C. dubliniensis* strains may have been misidentified as *C. albicans*. Retrospective analyses of *C. albicans* strain collections proved this to be true, presenting a challenging problem for the correct differentiation of *C. albicans* and *C. dubliniensis* in clinical samples (Jabra-Rizk *et al.*, 2000; Kim *et al.*, 2003).

Historically, rapid identification of *C. albicans* was primarily conducted using the germ tube test, based on detection of the serum-induced dimorphic switch between ellipsoidal blastospores and filamentous growth, resulting in polarised extension of an outgrowth (germ tube) from the yeast cell. However, *C. dubliniensis* also forms germ tubes in response to serum, complicating differentiation of the two distinct species. Growth of *Candida* on chromogenic media such as CHROMagar™ *Candida* allows primary screening and differentiation of *Candida* species (Odds & Bernaerts, 1994). As a result of the presence of chromogenic substrates in the medium *C. albicans* grow as light green, while *C. dubliniensis* grows as dark green colonies (Sullivan & Coleman, 1998). Although there have been suggestions that this chromogenic phenotype is weakened after sequential growth on CHROMagar™ *Candida*, Kirkpatrick *et al.* confirmed the suitability of CHROMagar™ *Candida* for use as a primary screening method (Kirkpatrick *et al.*, 1998). However, this approach includes incubation time, leading to a delay in results. Donnelly *et al.* described a rapid polymerase chain reaction (PCR) based test taking advantage of differences in the sequence of the *ACT1* gene to differentiate between *C. dubliniensis* and

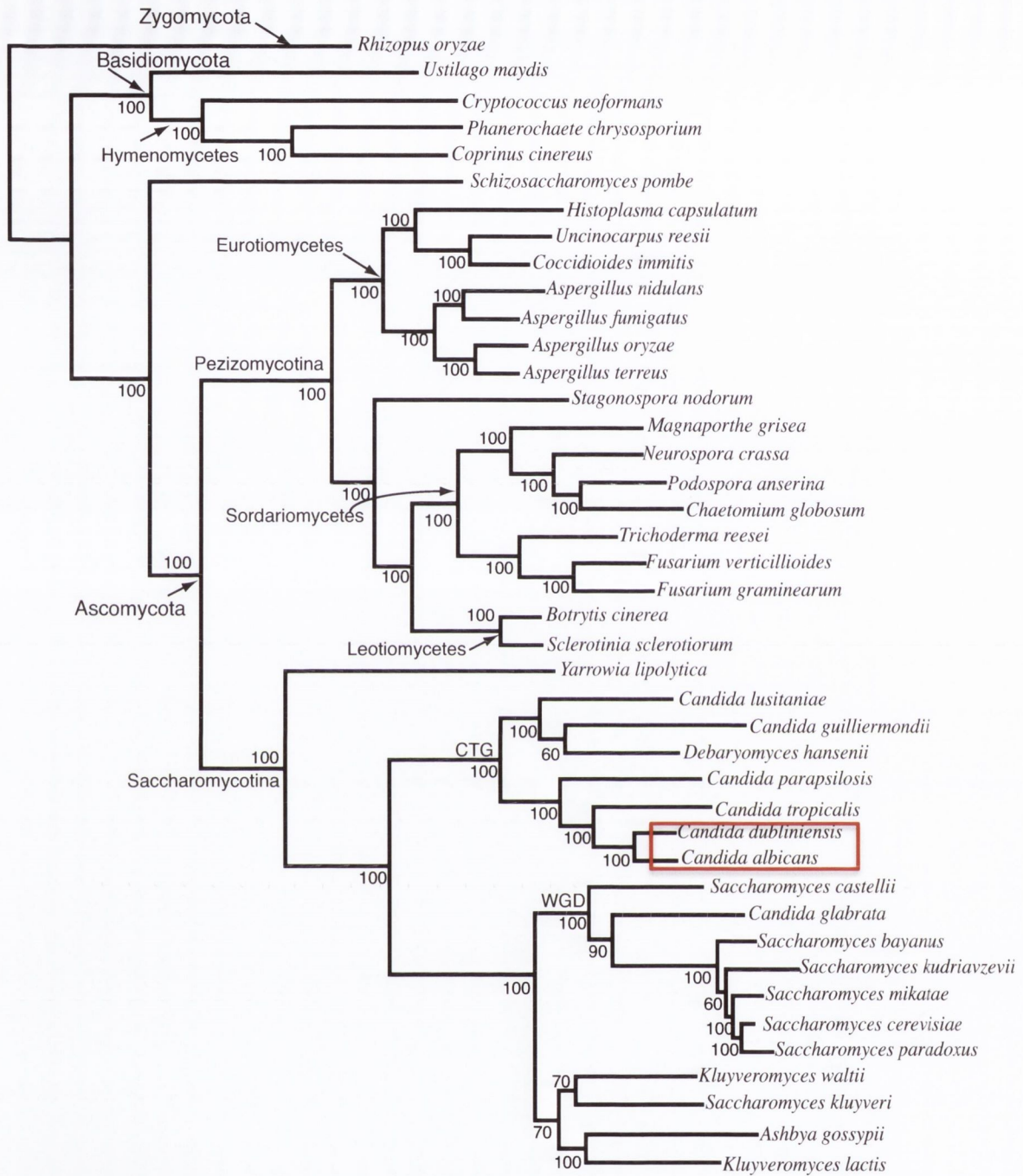


Figure 1.1. Maximum likelihood phylogeny, showing selected members of the CTG and WGD clades of the genus *Candida*. *Candida dubliniensis* is the closest phylogenetic neighbour to the opportunistic pathogen *Candida albicans*. Adapted from Fitzpatrick *et al.*, 2006.

C. albicans (Donnelly *et al.*, 1999). Crude isolation of DNA by a boiling method enabled rapid analysis of genomic material by PCR, amplifying a 288 bp amplicon specific to *C. dubliniensis*. The study also documented a relatively low level of intraspecies sequence variation, supporting the use of species identification by this method. Other identification methods such as thermotolerance at high temperatures (> 42 °C) may result in false negatives or positives (Pinjon *et al.*, 1998). *Candida albicans* was reported to grow successfully at elevated temperatures while *C. dubliniensis* struggled to grow. However, documentation of *C. albicans* isolates unable to grow at 45 °C has led to questions over the reliability of this method of presumptive identification (Kirkpatrick *et al.*, 1998). Technological advances have resulted in the development and use of mass spectrometry as a clinical diagnostic tool for identifying pathogenic organisms (Bader *et al.*, 2011; Zehm *et al.*, 2012). This technology is still in the early stages of evaluation and questions regarding reliability, cost and benefit still need to be addressed. Conceivably this method may be useful for distinguishing between *C. albicans* and *C. dubliniensis* species in a clinical setting.

1.2.2. Population structure

Strain variation is one of the determining factors influencing antifungal resistance in *C. albicans* and *C. dubliniensis*, with strains of specific lineages more likely to exhibit resistance to specific antifungals or chemicals such as 5-flucytosine. Although *C. albicans* possesses a cryptic sexual cycle, it is for the most part considered to be asexual, leading to a clonal method of reproduction (Odds, 2010). Evolution and elaboration of resistance mechanisms is mediated primarily by chromosomal rearrangements and mutations. Genetic diversity is limited by rates of recombination and chromosomal polymorphisms. Historically, strain analysis and epidemiological studies were performed using a variety of phenotypic profiling methods. Morphotype analysis, serotyping, carbohydrate assimilation profiles, and antifungal susceptibility testing all contributed to strain characterisation and analysis (Sullivan *et al.*, 1995). However, due to the lack of interlaboratory reproducibility of these phenotypic tests, more sophisticated molecular DNA-based techniques were developed (Hunter, 1991; Saghrouni *et al.*, 2013). Many typing methods have been used to characterise *Candida* although perhaps the most useful methods for analysis of population structure of *C. albicans* and *C. dubliniensis* have been restriction enzyme analysis and multilocus sequence typing (MLST). Restriction enzyme analysis relies on probing restriction endonuclease-digested DNA with specific probes. Analysis of *C. albicans* commonly used DNA-fingerprinting probes 27A or Ca3, with Ca3 providing better

discrimination between strains (Pujol *et al.*, 1997). Use of the Ca3 11 kb repetitive gene fragment identified five major *C. albicans* clades (I/ II/ III/ SA/ E) (Soll & Pujol, 2003). The distribution of strains between the clades is distinctive, with approximately 35 % of *C. albicans* isolates belonging to Group I, 31 % to Group II, and 19 % to Group III. Geographic location appears to play an important role in the distribution of *C. albicans* clonality. Analysis of South African isolates identified the presence of a large clonal population distinct from the three previously identified groups (Blignaut *et al.*, 2003). While isolates from Group I, II, and III were present in the population, there was enrichment for isolates comprising the Group SA, suggesting specific evolutionary adaptation to the local environment or host factors. A European-specific group was also identified with 26 % of isolates from an international study identifying as Group E when analysed by Ca3 fingerprinting (Pujol *et al.*, 2002). MLST analysis of between six to eight loci, targeting stable household genes further expanded knowledge of *C. albicans* population structure (Bougnoux *et al.*, 2002; Tavanti *et al.*, 2003). MLST analysis was found to agree with Ca3 fingerprinting, although clade E was divided into two subgroups (Tavanti *et al.*, 2005). One of the strongest benefits of typing methods such as Ca3 fingerprinting and MLST is the strength of interlaboratory reproducibility. MLST, in particular, benefits from the ease of dissemination of knowledge, as databases may be easily shared and analysed. Similar to *C. albicans* restriction enzyme-mediated analysis with a fingerprinting probe, analysis of *C. dubliniensis* isolates with the 16 kb Cd25 fingerprinting probe enabled analysis of population distribution and structures. Joly *et al.* found that, of three potential probes, Cd25 was species-specific and generated the most distinct fingerprinting patterns (Joly *et al.*, 1999). Two major *C. dubliniensis* clades were found by Cd25 fingerprinting. Analysis of internally transcribed spacer (ITS) regions found that ITS genotype I correlated with Cd25 group I isolates, while three ITS genotypes were associated with Cd25 group II isolates (Gee *et al.*, 2002). Further analysis of a collection of *C. dubliniensis* isolates from Egypt and Saudi Arabia identified an additional major Cd25 group composed of ITS genotype 3 and genotype 4 strains (Al Mosaid *et al.*, 2005). Complementary MLST analysis of *C. dubliniensis* has revealed the presence of three clades (McManus *et al.*, 2008). Clade 1 (C1) contains predominantly ITS genotype 1 strains while the second clade (C2) contains ITS genotype 2 isolates. Clade 3 (C3) from MLST analyses is composed of ITS genotype 3 and genotype 4 isolates. Overall, McManus *et al.* have shown that the population structure of *C. dubliniensis* is less divergent than *C. albicans* (Fig. 1.2). Although MLST broadly agrees with Cd25 fingerprinting, typing patterns as a result of karyotypic analysis displays significant

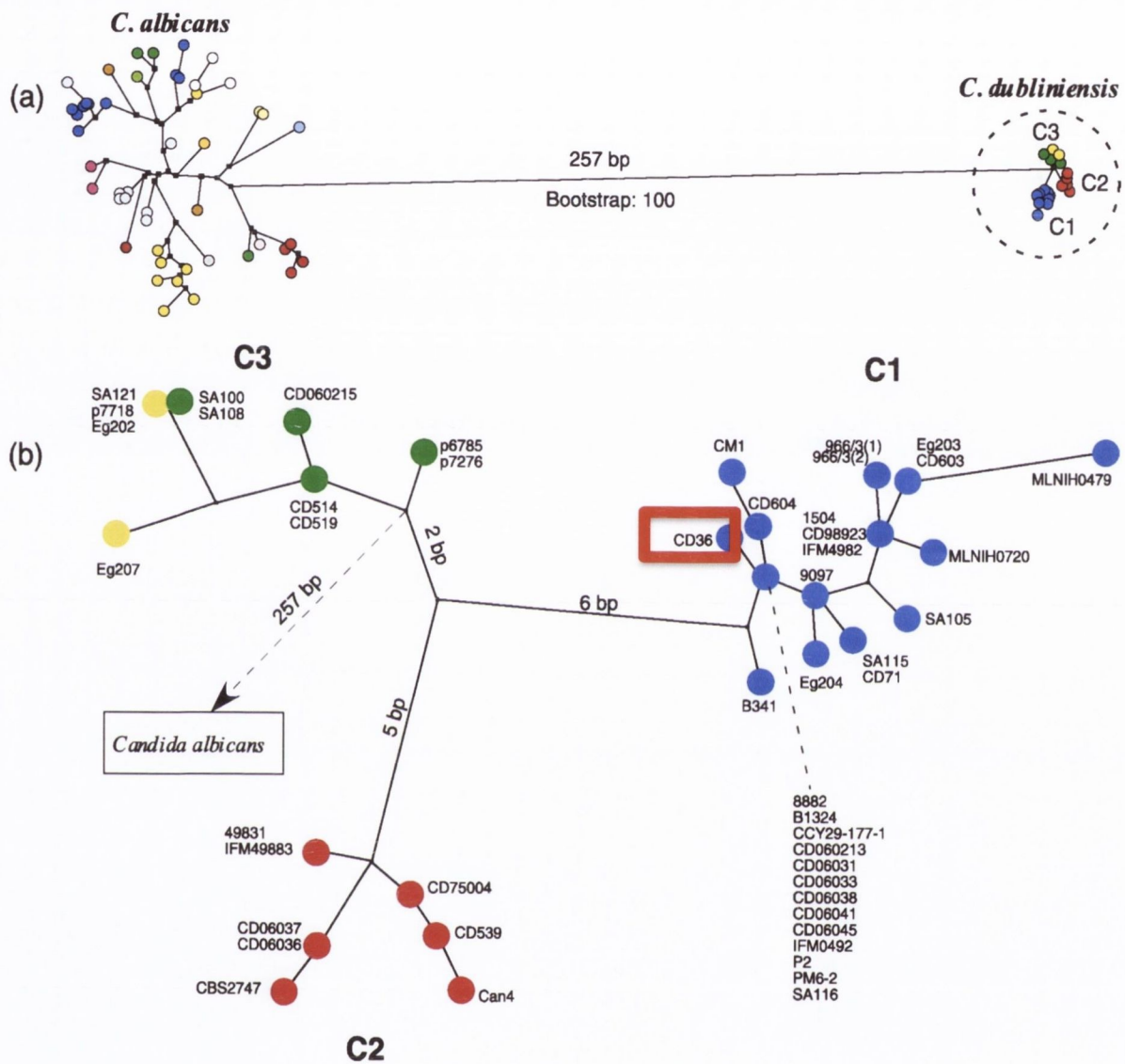


Figure 1.2. Population structure of *C. albicans* and *C. dubliniensis*. Maximum-parsimony tree based on MLST analysis of *C. albicans* and *C. dubliniensis* isolates showing greater divergence among *C. albicans* isolates. The *C. dubliniensis* type strain CD36 is highlighted. Adapted from McManus *et al.*, 2007.

differences (McManus & Coleman, 2014). This is considered to be a result of the lack of sequence variation in *C. dubliniensis* and may also be limited by the relatively small amount of isolates analysed so far.

1.2.3. Epidemiology of *C. albicans* and *C. dubliniensis*

Despite the close phylogenetic relationship and similarities in phenotypic characteristics, it is striking that there is such a difference in the virulence of *C. albicans* and *C. dubliniensis*. Although *C. albicans* may be responsible for approximately 60 % of systemic *Candida* infections, *C. dubliniensis* is commonly attributed to less than 2 % of systemic infections (Kibbler *et al.*, 2003; Sullivan *et al.*, 2005). Cases of candidiasis as a result of *C. dubliniensis* infection are predominantly associated with depression of the host's immune system, as evidenced by the increased frequency in isolation from the oral cavities of HIV-infected AIDS patients and diabetic individuals (Loreto *et al.*, 2010; Sullivan *et al.*, 2004). The natural niche of *C. albicans* is currently considered to be the oral cavity and gastrointestinal tract of humans, with potential reservoirs in other mammalian species (Barelle *et al.*, 2006; Edelmann *et al.*, 2005; Kumamoto, 2011). Although *C. dubliniensis* is also found in the oral cavity and gastrointestinal tract, it is a less successful coloniser and it has been suggested that *C. dubliniensis* has evolved to colonise an unknown niche (Moran *et al.*, 2012). In addition to human sources, *C. dubliniensis* has been recovered from avian and *Ixodida* (ticks) sources in close proximity, indicating a potential source of geographic transmission (Nunn *et al.*, 2007). However there is insufficient evidence to suggest that this is the natural *C. dubliniensis* niche and the direction of transfer has been suggested to be from human to bird (McManus *et al.*, 2009). It is possible that *C. albicans* and *C. dubliniensis* naturally colonise different niches, and the factors which contribute to the success of *C. albicans* colonisation of the human oral and gastrointestinal tract are also associated with the increased virulence of the species, relative to its phylogenetic neighbour, *C. dubliniensis*.

1.2.4. Antifungal resistance

As a result of frequent prophylactic use of azoles in the treatment of candidiasis, emergence of resistant strains to this class of antifungals is common (Pfaller, 2012). Upregulation of the drug efflux pumps Cdr1p and Cdr2p, and the major facilitator Mdr1p mediates resistance of *C. albicans* and *C. dubliniensis* to azoles (Mukherjee *et al.*, 2003). While upregulation of Mdr1p reduces susceptibility to fluconazole, Cdr1p and Cdr2p reduce susceptibility to fluconazole, itraconazole and ketoconazole (Moran *et al.*, 2002;

Wirsching *et al.*, 2000). *Candida* spp. also display resistance to treatment with 5-flucytosine (5-FC), a fluorinated derivative of the pyrimidine cytosine (Hope *et al.*, 2004). The mode of action of this antifungal is a result of inhibition of fungal protein synthesis. This occurs due to conversion of 5-flucytosine to 5-fluorouracil, subsequent phosphorylation and incorporation of the phosphorylated pyrimidine into RNA, leading to protein miscoding (Waldorf & Polak, 1983). Intrinsic resistance to 5-FC is common in specific clades, and acquisition of secondary resistance requires 5-flucytosine to be used in combination with an additional antifungal such as amphotericin B (Quinto-Aleman *et al.*, 2012; Vermes *et al.*, 2000). Typically, 5-flucytosine is used to treat only severe candidiasis associated with life-threatening infections such as endocarditis or meningitis (Hauser *et al.*, 2003). The limited clinical use of 5-FC is partly due to the frequency of emerging resistance, but also because the drug can have toxic effects on patients, causing serious side effects such as disruption of liver function, vomiting and diarrhoea. Resistance mechanisms appear to be clade-specific in *C. albicans* usually occurring as a result of amino acid substitutions in the proteins encoded by *FUR1* and *FCA1* (Dodgson *et al.*, 2004). Amphotericin B is a polyene antifungal that is commonly used in conjunction with 5-FC (Drew *et al.*, 2013). The combination therapy improves antifungal action, allowing lower dosages to be used, and reducing drug toxicity. Amphotericin B is considered to function by binding ergosterol in fungal cell membranes, forming a transmembrane channel, leading to leakage of intracellular ions and cell death (Baginski & Czub, 2009). It can be used either topically for superficial infections or intravenously for invasive infection. However, intravenous treatment is coupled with toxicity and side effects can range from nausea, hypotension and fatigue to nephrotoxicity (Laniado-Laborin & Cabrales-Vargas, 2009). Toxicity is reduced by using liposomal formulations of amphotericin B such as AmBisome[®] (Takemoto *et al.*, 2006).

1.3. Morphological plasticity of *C. albicans* and *C. dubliniensis*

There are a variety of phenotypic and genetic characteristics that likely contribute to the enhanced pathogenicity of *C. albicans* in the human host. However, as a result of the close evolutionary and genetic relationship between *C. albicans* and *C. dubliniensis*, the two species share many of these characteristics. Variations in regulation or functionality of these characteristics are likely to play a significant role in the differential virulence of the two *Candida* species.

1.3.1. *Candida* filamentation

Many clinically relevant *Candida* species are capable of dimorphism, growing either as an ellipsoid blastospore (yeast) or an elongated filament (hypha). Hyphae can be further differentiated as either pseudohyphae or true hyphae. Pseudohyphae are commonly observed as chains of elongated buds with constrictions at the site of septation whereas true hyphae are elongated filaments of uniform diameter with no evidence of constriction along the length of the filament (Merson-Davies & Odds, 1989). Remarkably, the only *Candida* species that have been observed to be capable of forming true hyphae are the closely related species *C. albicans*, *C. dubliniensis* and *C. tropicalis*, although *C. tropicalis* very rarely produces elongated hyphae (Gilfillan *et al.*, 1998; Suzuki *et al.*, 1991). As the dominant *Candida* pathogen, most studies concerning *Candida* filamentation have been conducted with *C. albicans* rather than *C. dubliniensis*. The rate at which the different species form true hyphae varies, with *C. albicans* rapidly producing large amounts of true hyphae in response to hypha-inducing signals. Some of these signals and the associated signaling pathways are presented in Fig. 1.3. However *C. dubliniensis* produces true hyphae at a much lower rate under similar growth conditions (Stokes *et al.*, 2007). Non-filamentous *C. albicans* strains were initially reported as being avirulent, leading to the hypothesis that the ability to produce true hyphae is an important virulence factor during *C. albicans* colonisation of the human host (Lo *et al.*, 1997). True hyphae were considered to be the invasive form of *C. albicans*, while yeast were associated with systemic and disseminated candidiasis. The role of pseudohyphae during colonisation or invasion has not been elaborated. Although the efficiency of *C. albicans* production of true hyphae has been associated with increased invasion and virulence, the characterisation of *C. albicans* strains unable to produce filaments has shown that some non-filamentous *C. albicans* strains may retain their virulence. Similarly, *C. albicans* mutant strains created to be constitutively filamentous have been observed to be less virulent than the wild type strains (Bendel *et al.*, 2003). Though there is a possibility that these observations may be an artifact of the genetic manipulation methods used, it has opened up the field to consider the complexity of hyphae and examine the true underlying cause of hyphal-associated virulence. *In vitro* studies of *C. dubliniensis* have shown much lower levels of hyphae produced, in conjunction with lower levels of invasion of host tissues, under conditions designed to mirror *in vivo* invasion (Spiering *et al.*, 2010). However, the difference in morphology between *C. albicans* and *C. dubliniensis* in infection models complicates interpretation of morphology-associated virulence. The discrepancy in morphology-

associated virulence between the two species is currently attributed to the reduced ability or propensity of *C. dubliniensis* to form true hyphae under invasion simulative conditions. The dimorphic transition is discussed in further detail in Chapter 4 and Chapter 5. The differential filamentation of *C. albicans* and *C. dubliniensis*, and the resultant virulence phenotypes are dealt with in Chapter 4, while the genetic regulatory mechanisms underlying filamentation are explored in Chapter 5.

1.3.2. Chlamyospores

In addition to filamentous morphologies, *C. albicans* and *C. dubliniensis* display the ability to grow as large, thick-walled, spherical cells called chlamyospores. As the only two species found to produce chlamyospores, *C. albicans* and *C. dubliniensis* were identified by growth of these cell types on media such as cornmeal, rice extract, or Pal's agar (Staib & Morschhauser, 2007). However, this was also a contributing factor in the historical misidentification of *C. dubliniensis* isolates as *C. albicans* (Sullivan *et al.*, 1995). Interestingly, only *C. dubliniensis* forms chlamyospores on Staib agar (Staib & Morschhauser, 2005a). The biological function of chlamyospores is unknown and the cells have rarely been observed *in vivo* (Chabasse *et al.*, 1988). On average, chlamyospores measure 6 μm in diameter but can grow up to an observed maximum of 10 – 12 μm diameter. Compared to an average diameter of 3 μm for yeast cells, chlamyospores are easily visibly differentiated from yeast cells. Chlamyospores have been observed on nutrient poor media, in conjunction with filamentous elements, forming from the tip of suspensor cells (Jansons & Nickerson, 1970a). The cells are double walled with the outer layer comprised of a thin, electron transparent layer and the inner layer composed of electron dense material (Shannon, 1981). The outer layer was later revealed to be composed mostly of β -1,3-glucan and chitin to a lesser degree (Jansons & Nickerson, 1970b). In contrast, the inner layer is thought to be composed of proteinaceous material. Various cellular elements have been observed including vacuolar and cytoplasmic organelles. Mitochondria and ribosomes have also been detected, although these organelles appear to disappear over time (Miller *et al.*, 1974). Additionally, nuclear division across the junction between the suspensor cell and chlamyospore has not yet been observed, raising questions regarding the pattern of nuclear segregation during replication (Vidotto *et al.*, 1996). Citiulo *et al.* showed that metabolic activity in chlamyospores was reduced over time with a significantly lower level of activity after 14 days compared to 5 days (Citiulo *et al.*, 2009). Metabolic activity in 30 day old chlamyospores was not detectable. Citiulo *et al.* also showed that chlamyospores were capable of budding, producing

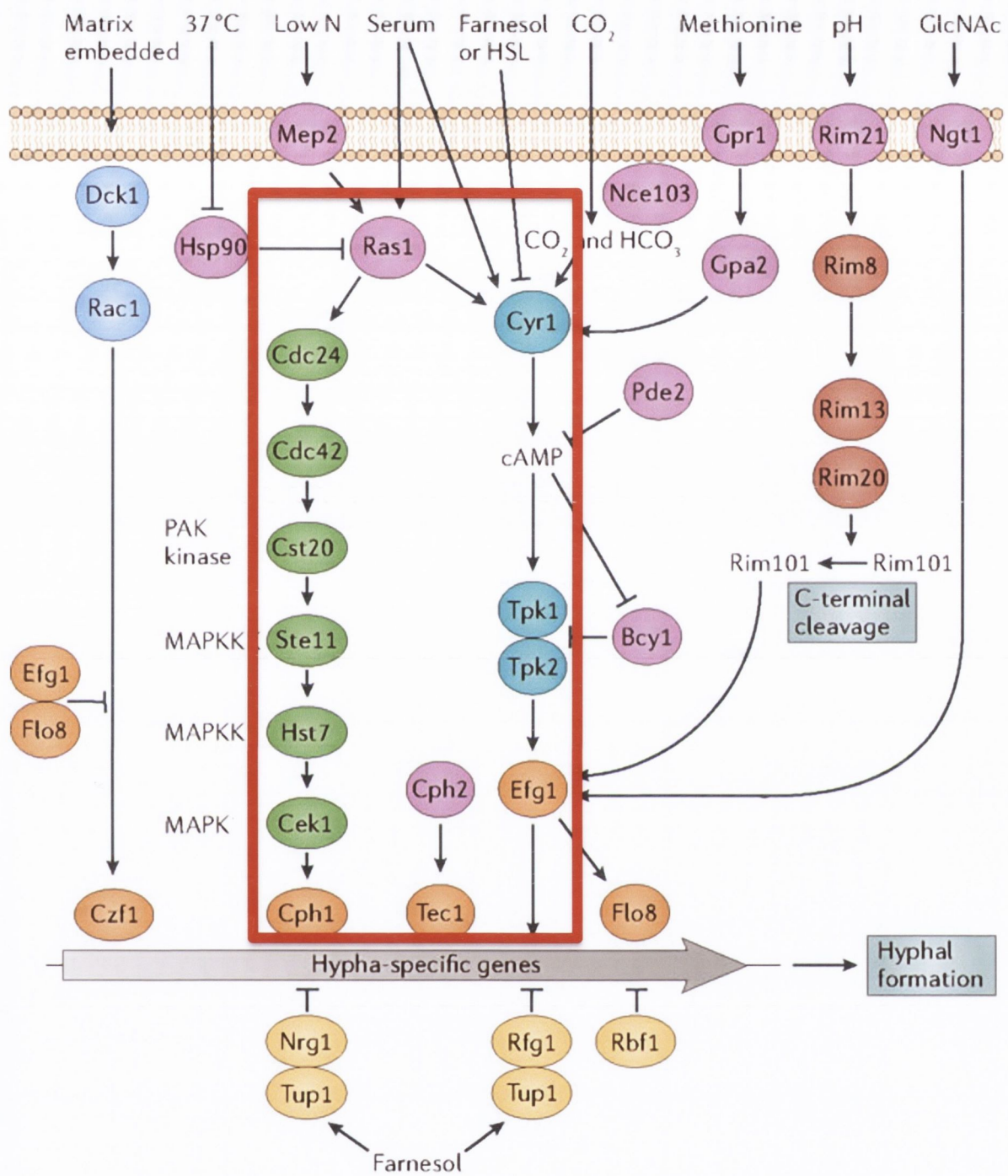


Figure 1.3. Hypha-inducing environmental signals and signalling pathways. A selection of known positive and negative hyphal induction signals, transduction pathways and effector proteins governing the *C. albicans* filamentous transition. Strong hyphal induction through the Ras1p signaling pathway is highlighted, showing induction of hypha-specific genes through the effector proteins Cph1p, and Efg1p. Adapted from Sudbery, 2011.

daughter yeast cells, and also germination to produce filamentous pseudohyphae and true hyphae. Palige *et al.* have identified two chlamyospore-specific genes shared by *C. albicans* and *C. dubliniensis* (Palige *et al.*, 2013). Both *CSP1* and *CSP2* encode chlamyospore-specific proteins localised to the cell wall and serve as a marker for chlamyospore growth. Whether the proteins function in a structural capacity or display some other function is unknown and is likely to be investigated in the future. Genetic regulation of chlamyospore production appears to share a number of similarities with regulation of filamentation. Nutrient limitation and the associated regulatory genes *NRG1* and *UME6* appear to play a role in the development of chlamyospores (Staib & Morschhauser, 2005b). The regulatory mechanisms governing the transition between the various morphological states in *Candida* are highly complex and interconnected, resulting in difficulty in dissecting the impact of each pathway on morphology and virulence.

1.3.3. Mating

In addition to the yeast to hypha transition, *Candida* are capable of mating and can undergo a process of reversible phenotypic switching between a white and opaque cell type (Nielsen & Heitman, 2007). So-called white cells are the commonly occurring ellipsoid yeast cells whereas opaque cells are elongated, bean shaped cells (Slutsky *et al.*, 1987). Opaque cells can be visually distinguished from white cells by microscopy, and macroscopically by using phloxine B to stain opaque cell colonies pink/red (Liu *et al.*, 2010). Both *C. albicans* and *C. dubliniensis* are diploid and display a cryptic meiotic program (Alby & Bennett, 2010). They possess mating type-like (MTL) loci, similar to other fungal mating type loci (Butler, 2010). The transcription factors *MTLa* and *MTL α* are responsible for determining mating type and phenotypic switching competency. Two forms, or idiomorphs, can be produced by each locus, similar to allelic variation (Butler *et al.*, 2004). From *MTLa*, *a1* and *a2* are produced, and $\alpha1$ and $\alpha2$ are produced from *MTL α* . A heterodimer is formed by *a1* and $\alpha2$ (*a1 α 2*), efficiently repressing switching and elaboration of other mating genes (Magee & Magee, 2000). Heterozygous cells are normally maintained in the white form and will only undergo meiosis if *a1* or $\alpha2$ are lost as a result of mitotic recombination, enabling phenotypic switching and mating (Wu *et al.*, 2007). Homozygous strains on the other hand are influenced by the activity of another transcription factor, encoded by *WOR1*, which acts as a master regulator of switching (Huang *et al.*, 2006). Activity of *WOR1* is usually repressed by the *a1 α 2* dimeric repressor. Activation of *WOR1* results in a positive feedback loop, supporting establishment and maintenance of the opaque, mating competent state. *WOR1* also represses expression of

EFG1, which usually supports growth of *Candida* as white yeast (Zordan *et al.*, 2007). Secreted pheromones activate mating with a-pheromone and α -pheromone activating mating response in their opposing mating type i.e. a-pheromone stimulates α/α mating and *vice versa*. Pujol *et al.* demonstrated that *C. albicans* and *C. dubliniensis* are capable of interspecies mating, and this was dependent on cell clumping to facilitate fusion (Pujol *et al.*, 2004). Surprisingly, the rate of interspecies mating was higher than that of *C. dubliniensis* intraspecies mating, although this is likely to be influenced by the higher rate of clumping displayed by *C. albicans* mating types. Mating type may also play a role in fungal survival in the human host. White cells have been shown to produce a chemoattractant which leads to attraction of human neutrophils and fungal engulfment while opaque cells do not produce the same chemical signal (Geiger *et al.*, 2004). White cells are associated with virulence in murine systemic models of candidiasis and opaque cells are considered to be more successful in colonising cutaneous surfaces. It is important to note that the environmental signals which have been found to induce mating include growth under elevated CO₂ and use of *N*-acetylglucosamine (GlcNAc) as a carbon source instead of glucose (Xie *et al.*, 2013). These are conditions which are intricately linked with dimorphism and represent a commonality between regulation of *Candida* filamentation and mating.

1.3.4. Biofilm growth

Microbial biofilms are highly abundant in nature and can cause serious problems in nosocomial settings. Biofilms are frequently characterised as a single or multi-species group of organisms growing as an adherent 3-dimensional structure (Hiyari & Bennett, 2011). Cells are commonly embedded in an extracellular matrix (Nobile *et al.*, 2009). Biofilms can colonise biotic and abiotic surfaces (Fanning & Mitchell, 2012). In the human host, microbial biofilms can contribute to deep-seated infections, providing an *in situ* reservoir for invading microbes. Biofilm establishment on indwelling medical devices such as catheters, prostheses, pacemakers and even dentures, in addition to growth on mucosal cell surfaces, presents a major problem in healthcare (Harriott & Noverr, 2011). Many clinically relevant *Candida* species are capable of forming biofilms (Silva *et al.*, 2011). In particular, *C. albicans* and *C. dubliniensis* efficiently produce biofilms (Alnuaimi *et al.*, 2013). The ability of clinical isolates to produce biofilm has been associated with higher levels of patient mortality (Ramage *et al.*, 2009; Viudes *et al.*, 2002). Distinct stages of biofilm development have been documented beginning with initial fungal adherence to a cell, followed by cell proliferation, maturation of the biofilm and dispersal of cells from

the biofilm surface (Finkel & Mitchell, 2011). In *C. albicans* and *C. dubliniensis*, initial attachment of yeast, or hyphal cells to surfaces is mediated by adhesive fungal cell wall proteins (Alsteens *et al.*, 2013; Staab *et al.*, 2013). Maturation of the biofilm includes production of an extracellular matrix and development of hyphae (Richard *et al.*, 2005). The matrix is commonly a mix of polysaccharide, carbohydrate, and proteinaceous or nucleic material (Finkel & Mitchell, 2011). As the biofilm matures, yeast cells are budded from the surface and disperse, enabling migration and colonisation of other surfaces (Robbins *et al.*, 2011). Yeast cells dispersed from biofilm have been observed to be more virulent in a murine model of disseminated candidiasis, suggesting a role for biofilm-associated epigenetic changes in increasing virulence (Uppuluri *et al.*, 2010). The genetic regulatory network governing the switch to a biofilm mode of growth has been examined for *C. albicans*, highlighting *BCR1*, *TEC1*, *EFG1*, *NDT80*, *ROB1*, and *BRG1* as playing dominant roles in regulation of biofilm growth (Nobile *et al.*, 2012). These genes are involved in the regulation of adhesin genes and are associated with filamentation, contributing further to the complex challenge of dissecting the link between filamentation and virulence. Cell interactions in biofilms are complex and depend on the nature of the biofilm. Quorum sensing plays an important role in the maturation of a biofilm (Deveau & Hogan, 2011; Nobile *et al.*, 2009). Multispecies biofilms often display modulation of cocolonising species activity through the action of secreted quorum sensing molecules such as homoserine lactones (bacteria) or farnesol (*Candida*) (Albuquerque & Casadevall, 2012; Mear *et al.*, 2013). These signaling molecules may have antagonistic or synergistic effects on the overall development of the biofilm. Biofilms present a number of challenges to treatment with antibiotics and antifungals (Taff *et al.*, 2013). One of the most significant barriers to treatment is the presence of an extracellular matrix (Bonhomme & d'Enfert, 2013). Diffusion of therapeutic drugs through the matrix depends on the composition and sequestration of drugs by matrix components is possible (Nett *et al.*, 2010). By the time drugs reach embedded cells, the drug concentration may have been reduced, leading to levels of activity lower than the required minimum dose. Additionally, delayed diffusion of drugs through the matrix allows cells to employ drug efflux pumps such as *CDR1*, *CDR2* and *MDR1*, which contribute to fluconazole resistance in *C. albicans* and *C. dubliniensis* (Mukherjee *et al.*, 2003). Upregulation of these genes also increases resistance to ketoconazole and itraconazole. Within a biofilm pockets of highly variable microenvironments exist. The morphological plasticity exhibited by *C. albicans* and *C. dubliniensis* in response to local environmental conditions enables the fungi to successfully adapt and take advantage of growth in a biofilm. Biofilms can also be a source of persister

cells which exhibit atypical responses to antifungals and environmental stresses, showing increased survival rates (Lewis, 2010). *Candida albicans* persister cells have been shown to contribute to oral carriage of the fungus, displaying high levels of drug tolerance (Lafleur *et al.*, 2010).

1.4. Genomic comparison of *C. albicans* and *C. dubliniensis*

Whole genome comparison of 16 species distributed between the CTG and WGD clades, in addition to specific comparative genomics of *C. albicans* and *C. dubliniensis* has highlighted important differences that are likely to influence *Candida* virulence in a human host. Analysis and assembly of the *C. albicans* genome has revealed a 15.9 Mb genome (Assembly 21), consisting of eight sets of chromosome pairs (Selmecki *et al.*, 2010). Similarly, *C. dubliniensis* possesses a 14.6 Mb genome, although the less virulent species possesses a complex karyotype with a mix of haploid and diploid chromosomes and obvious examples of chromosomal rearrangement (Magee *et al.*, 2008). Assembly of the *C. dubliniensis* genome from a consensus of chromosomal homologs was partly based on resemblance to *C. albicans*. There is a high level of similarity between the genomes of *C. albicans* and *C. dubliniensis*. When genes encoding proteins are compared in the two species, there is a high degree of identity, with 44.4 % of genes over 90 % identical, and 96.3 % of genes greater than 80 % identical (Jackson *et al.*, 2009). There is also a high degree of positional conservation supporting the close phylogenetic relationship between the two species. The major repeat sequence (MRS) is a set of repetitive sequences or DNA elements that are unique to *C. albicans* and *C. dubliniensis* (Magee *et al.*, 2008). All but one chromosome contains MRS elements, with chromosome R of *C. dubliniensis* and chromosome 3 of *C. albicans* lacking an MRS. The highly repetitive nature of the MRS is considered to result in karyotypic variation in the absence of a regular meiotic cycle. It is thought to be a source of recombination events and chromosomal translocation providing a mechanism for genomic diversity.

1.4.1. Gene family expansion and gene loss

Comparative genomics has emphasised enrichment of gene families that are common to clinically relevant pathogenic *Candida* species (Butler *et al.*, 2009). Several of these families are associated with hyphal morphogenesis indicating the importance of the dimorphic transition in *Candida* virulence. Remarkably, many of these families have been revealed to have undergone expansion in *C. albicans*. In contrast, *C. dubliniensis* has either failed to expand gene families or suffered loss of key genes, possibly indicating a path of

reductive evolution compared to *C. albicans* (Jackson *et al.*, 2009; McManus & Coleman, 2014). The *IFA* family is a group of genes encoding putative transmembrane proteins. The proteins are similar to leucine repeat-rich proteins from viruses. The *IFA* family in *C. albicans* is comprised of 31 members while *C. dubliniensis* possesses only 21 members. There is evidence of pseudogenisation in *C. dubliniensis* with many *IFA* members likely to be nonfunctional. Out of 21 members, 14 are predicted to be fragmentary in *C. dubliniensis* compared to only 6/31 in *C. albicans*. This represents one of the clearest examples of differing evolutionary patterns displayed by *C. albicans* and *C. dubliniensis*. Speciation has led to *C. albicans* expanding the *IFA* family through gene duplication while *C. dubliniensis* is actively in the process of loss of genes. The environmental selective pressures governing this pattern have yet to be elucidated.

Another example of family expansion in *C. albicans* occurs in the *TLO* gene family. While most *Candida* species possess one *TLO* gene, *C. albicans* has expanded its repertoire to 14 members. The *TLO* genes are located in close proximity to the telomeres and are currently thought to be components of the mediator complex, influencing general transcription (Zhang *et al.*, 2012). Notably, *C. dubliniensis* possesses two *TLO* genes and deletion of *CdTLO1* has been shown to negatively impact hyphal formation (Jackson *et al.*, 2009). Complementation of the *CdTLO1* mutant with *C. albicans* *TLO* genes (*CaTLO11/CaTLO12*) restores filamentation. The functional mechanism of the *C. dubliniensis* *TLO* genes is an area of active study and may expand on the interaction between *TLO* proteins, the mediator complex, and *Candida* filamentation.

Proteases are known to play important roles in adherence to an invasion of host tissues. Members of the large family of secreted aspartyl protease genes (*SAP*) have been shown to be upregulated during infection (Schaller *et al.*, 2000). *Candida dubliniensis* lacks orthologs of *SAP4*, *SAP5*, *SAP6*, and instead possesses Cd36_63420 which shows partial similarity to the three *C. albicans* *SAP* genes (Jackson *et al.*, 2009). The redundancy and diversity displayed by *C. albicans* *SAP* genes is likely to play a role in its increased ability to cause infection and invasion of host tissues.

1.4.2. Virulence-associated cell wall proteins

As the first point of contact between fungal and host cells, surface expressed cell wall proteins play a crucial role in the ability of the fungus to adhere to and potentially invade host tissues. Notably, cell wall proteins known to contribute to the pathogenesis of *C.*

albicans hyphae have been found to be absent or significantly divergent in *C. dubliniensis*. The *IFF* gene family has been associated with virulence (Bates *et al.*, 2007; Boisrame *et al.*, 2011). In particular, *HYR1* has been demonstrated to be rapidly upregulated in *C. albicans* hyphae, with an abundance of protein present on the hyphal cell surface (Bailey *et al.*, 1996; Heilmann *et al.*, 2011). It is therefore striking that *HYR1* is completely absent from the *C. dubliniensis* genome (Moran *et al.*, 2004). Deletion of the gene from the *C. dubliniensis* genome is supported by a residual identity at the locus corresponding to *HYR1*. The protein is currently thought to contribute to survival of the fungus when in contact with human neutrophils (Luo *et al.*, 2010). Thus, the absence of the gene from *C. dubliniensis* may contribute to the relative lack of pathogenicity, and the requirement for severe underlying host conditions for establishment of infection. The hyphal specific cell wall protein encoded by *HWPI* aids *C. albicans* attachment to host epithelial cells through a mechanism of mimicry (Staab *et al.*, 1999). The protein facilitates the formation of stable covalent attachments by mimicking host cell transglutaminase substrates. When transglutaminases on the surface of host cells contact the N-terminal domain of Hwp1p strong bonds are formed, enabling the fungus to strongly adhere to epithelial cells. In addition to invasive infection, this proves important for *C. albicans* biofilm formation and mating (Ene & Bennett, 2009; Nobile *et al.*, 2006). In contrast, *C. dubliniensis* possesses a truncated form of the gene displaying only 49 % nucleotide identity to *CaHWPI* (Moran *et al.*, 2004). Whether *CdHwp1p* is functional or not has yet to be proven, although it too is upregulated on induction of hyphal growth. However, alignment of the respective nucleotide sequences shows loss of N-terminal and C-terminal residues from *CdHWPI* relative to the *C. albicans* gene, raising questions about N-terminal-mediated functionality and presence of the protein on the *C. dubliniensis* cell surface, which is usually directed by a C-terminal signal sequence and attachment of a glycosylphosphatidylinositol-anchor to β -1,6-glucan in the *Candida* cell wall.

In *C. albicans*, one of the most well characterised cell wall protein-encoding gene families is the *ALS* family (Sheppard *et al.*, 2004). The family encodes adhesin proteins that enable *C. albicans* yeast and hyphae to adhere to a variety of host tissue types and ligands. *Candida albicans* possesses 8 *ALS* genes distributed across 3 chromosomes. *Candida dubliniensis* possesses only 6 *ALS* family members, lacking a direct ortholog of *CaALS3* and *CaALS5*. In *C. albicans*, *CaALS5* resulted from duplication of *CaALS1*. Although gene duplication has been commonly observed in *C. albicans*, it is also visible in *C. dubliniensis* as Cd36_64800, an adhesin-like gene of the *C. dubliniensis ALS* repertoire

arose from duplication of Cd36_65010 (Jackson *et al.*, 2009). Importantly *CaAls3p* has been identified as a *C. albicans* hyphal-specific adhesin and putative invasin, triggering uptake of fungal cells by a host cadherin-dependent mechanism (Phan *et al.*, 2007). Presumably this strongly contributes to the invasive ability of *C. albicans* hyphae, enabling the pathogenic *C. albicans* to gain access to tissue substrata and the host bloodstream, causing systemic infection. The absence of *ALS3* from the *C. dubliniensis* repertoire is therefore thought to play a significant role in the lack of invasive pathogenicity displayed by the related yeast.

1.5. Aims of the current study

Although *C. albicans* and *C. dubliniensis* possess similar characteristics and potential virulence factors such as mating, biofilm growth, and antifungal resistance, the main reason for the difference in virulence between the two species is currently considered to be predominantly due to differential filamentation, and the presence or absence of key virulence-associated genes. The intricate complexity between environmental sensing and *Candida* filamentation may determine *C. dubliniensis* virulence, as local host microenvironments present a wide range of nutrient availability and environmental stresses.

- Differentially express the *C. albicans* hypha-specific genes *CaALS3* and *CaHYR1* independently in a *C. dubliniensis* background, and investigate virulence-associated phenotypes.
- Analyse the impact of *C. dubliniensis* morphology on adhesion to, and tissue damage of, human epithelial cells.
- Develop an improved method for the initiation and maintenance of *C. dubliniensis* true hyphae, and examine the genetic regulation of morphologies induced under different growth conditions.
- Compare and contrast the morphology-associated cell wall proteomes of *C. albicans* and *C. dubliniensis*.

Chapter 2

General materials and methods

2.1. General microbiological methods

2.1.1. Strains and growth conditions

Unless otherwise stated, *Candida* isolates used in this study were obtained from the culture collection of the Microbiology Research Unit, Division of Oral Biosciences, Dublin Dental University Hospital, Lincoln Place, Dublin 2, Ireland (Table 2.1). *Candida* strains with the prefix HE- were obtained from the laboratory collection of Prof. Gottfredsson, Faculty of Medicine, University of Iceland, Iceland. *Escherichia coli* strains used during this study include XL10 gold (Stratagene (*endA1, glnV44, recA1, thi-1, gyrA96, relA1, lac, Hte Δ(mcrA)183, Δ(mcrCB-hsdSMR-mrr)173, tet^R, F'[proAB, lac]^qZΔM15, Tn10(Tet^R, Amy, Tn5(Kan^R)] and XL10 gold harbouring pBluescript II KS (-) (Stratagene, La Jolla, California, USA). *Escherichia coli* strains harboring the plasmids pADH1 and pALS3 were kindly supplied by Dr. S. Filler, Harbour-UCLA, Medical Centre, Torrance, California, USA. *Escherichia coli* harboring the plasmid pHYR1 was supplied by Prof. A.J. Brown, Aberdeen Fungal Group, University of Aberdeen, The Institute of Medical Sciences, Foresterhill, Aberdeen, Scotland, UK.*

All *Candida* strains were maintained routinely on Yeast Extract Peptone Dextrose (YEPD) medium (10 g/L yeast extract [Sigma-Aldrich, Tallaght, Dublin, Ireland], 20 g/L Bactopeptone [Difco], 20 g/L dextrose [Sigma], pH 5.5) Cells were grown at either 30 °C or 37 °C, statically (Gallenkamp, Leicester, UK), or in an orbital incubator (New Brunswick Scientific Company Inc., Edison, New Jersey, USA) rotating at 200 r.p.m. Strains were grown aerobically unless stated otherwise. Nourseothricin-resistant strains were cultured on YEPD agar containing nourseothricin (clonNAT, Werner Bioagents, Germany). *Candida dubliniensis* strains were grown on 100 µg/ml (NAT₁₀₀) and *C. albicans* strains were grown on 200 µg/ml (NAT₂₀₀). Uridine auxotrophic (*ura3Δ/ura3Δ*) *C. dubliniensis* strains were grown on YEPD supplemented with 100 µg/ml uridine.

Escherichia coli strains were maintained on either Luria-Bertani (LB) pH 7.4 agar or LB agar containing 100 µg/ml ampicillin (Penbritin, GlaxoSmithKline, Rathfarnham, Dublin 14, Ireland) (L_{amp}) at 37 °C.

Table 2.1. *Candida dubliniensis* and *C. albicans* isolates used in this study

Isolates	Country of origin	Sample	Source/Reference
Can 6	Canada	Oral	(Pinjon <i>et al.</i> , 1998)
CBS2747	Netherlands	Sputum	(Meis <i>et al.</i> , 1999)
CBS8500	Netherlands	Blood	(Meis <i>et al.</i> , 1999)
CBS8501	Netherlands	Blood	(Meis <i>et al.</i> , 1999)
CD36	Ireland	Oral	(Sullivan <i>et al.</i> , 1995)
CD38	Ireland	Oral	(Sullivan <i>et al.</i> , 1995)
CD41	Ireland	Oral	(Moran <i>et al.</i> , 1997)
CD506	Ireland	Oral	(Gee <i>et al.</i> , 2002)
CD539	United Kingdom	Oral	(Pinjon <i>et al.</i> , 1998)
CD57	Ireland	Vaginal	(Moran <i>et al.</i> , 1997)
CM1	Australia	Oral	(Sullivan <i>et al.</i> , 1995)
HE124	Iceland	Blood	(Asmundsdottir <i>et al.</i> , 2009)
HE163	Iceland	Blood	(Asmundsdottir <i>et al.</i> , 2009)
HE176	Iceland	Blood	(Asmundsdottir <i>et al.</i> , 2009)
HE183	Iceland	Blood	(Asmundsdottir <i>et al.</i> , 2009)
HE194	Iceland	Blood	(Asmundsdottir <i>et al.</i> , 2009)
HE199	Iceland	Blood	(Asmundsdottir <i>et al.</i> , 2009)
HE222	Iceland	Blood	(Asmundsdottir <i>et al.</i> , 2009)
HE237a	Iceland	Blood	(Asmundsdottir <i>et al.</i> , 2009)
HE237b	Iceland	Blood	(Asmundsdottir <i>et al.</i> , 2009)
HE247	Iceland	Blood	(Asmundsdottir <i>et al.</i> , 2009)
HE281	Iceland	Blood	(Asmundsdottir <i>et al.</i> , 2009)
HE283	Iceland	Blood	(Asmundsdottir <i>et al.</i> , 2009)
HE30	Iceland	Blood	(Asmundsdottir <i>et al.</i> , 2009)
HE38a	Iceland	Blood	(Asmundsdottir <i>et al.</i> , 2009)
HE57	Iceland	Blood	(Asmundsdottir <i>et al.</i> , 2009)
LP1	Ireland	Oral	(Gee <i>et al.</i> , 2002)
WÜ284	Germany	Oral	(Morschhauser <i>et al.</i> , 1999)
CdUM1A ^a	N/A	N/A	(Staib <i>et al.</i> , 2001)
SC5314	United States of America	Blood	(Gillum <i>et al.</i> , 1984)

^a Derivative of WÜ284 (*ura3Δ1::MPAR-FLIP/URA3*)

N/A Not applicable

Long-term strain storage was on plastic beads in Microbank (Pro-Lab Diagnostics, Richmond Hill, Ontario, L4B 1K3, Canada) cryogenic vials at -80 °C.

2.1.2. Chemicals and enzymes

Reagents and chemicals used were all of molecular biology-grade or analytical-grade sourced from Sigma-Aldrich, Roche (Roche Products [Ireland] Limited, Citywest, Dublin 24, Ireland), Promega (Promega Corporation, Madison, Wisconsin, USA) and Ambion (Bio-Sciences, Dun Laoghaire, Co. Dublin, Ireland). Enzymes, dNTPs, DNA molecular markers and DNA loading dyes were all obtained from Sigma Aldrich, Promega and New England Biolabs (Ipswich, MA, USA), stored at -20 °C and subsequently used according to manufacturer's instructions. Doxycycline hyclate was purchased from Sigma-Aldrich and stock solutions were stored in the dark at 4 °C for short-term storage. Both cyclic adenosine monophosphate (cAMP) and GlcNAc were purchased from Sigma-Aldrich and stored at -20 °C. Calcofluor white and 4',6-diamidino-2-phenylindole (DAPI) were purchased from Sigma-Aldrich and stored according to manufacturer's guidelines.

2.1.3. Buffers and solutions

Ultrapure water used for buffers and solutions was Milli-Q Biocel-purified water (resistivity 18.2 MΩcm) (Millipore, Carrigtwohill, Cork, Ireland). Molecular biology grade water was purchased from Sigma-Aldrich for resuspension of nucleic acids and PCR. Phosphate Buffered Saline (PBS) solution was prepared from PBS tablets (Difco, BD, Dun Laoghaire, Co. Dublin, Ireland) according to manufacturer's instructions, and sterilised by autoclaving. Tris-EDTA (TE) containing 10 mM Tris-HCL, 1 mM EDTA pH 8.0 was used as a buffer for storage of DNA. Tris-Borate EDTA (TBE) at a concentration of 20X containing 0.45 M Trizma base, 0.45 M boric acid and 0.01 M EDTA, was diluted in ultrapure water to a final concentration of 0.5X and used as the buffer for gel electrophoresis. Citrate phosphate buffer (200 mM) contained 58 ml of 0.4 M Na₂HPO₄ and 42 ml of 0.2 M citric acid. PIPES buffer was prepared with 60 mM CaCl₂, 10 mM PIPES, 15 % (v/v) glycerol, pH 7. Sodium dodecyl sulphate (SDS) extraction buffer was prepared with 50 mM Tris-HCL, 2 % (w/v) SDS, 100 mM Na-EDTA, 150 mM NaCl, pH 7.8 and stored at 30 °C. Prior to use 8 µl (per 1 L) of β-mercaptoethanol (βMe) was added. All solutions were stored at room temperature unless stated otherwise.

Lee's Medium was prepared by adding, in a 1 L final volume, 12.7 g of salts mix (5 g $(\text{NH}_4)_2\text{SO}_4$, 0.2 g $\text{MgSO}_4 \cdot 7\text{H}_2\text{O}$, 2.5 g K_2HPO_4 , 5.0 g NaCl), 4.714 g of L-amino acid mix (0.5 g L-alanine, 1.3 g L-leucine, 1.0 g L-lysine, 0.1 g L-methionine, 0.0714 g L-ornithine, 0.5 g L-phenylalanine, 0.5 g L-proline, 0.5 g L-threonine), 12.5 g of glucose (Lee *et al.*, 1975). The pH was adjusted to pH 4.5 and sterilised by filtration. Prior to use, this stock solution was supplemented with 1 ml/L 0.001 % (w/v) biotin (0.01 g/L), 1 ml/L 400 mM arginine (84.2 g/L L-arginine monohydrochloride), 1 ml/L 1 M trace metals stock I (203 g/L magnesium chloride hexahydrate, 147 g/L calcium chloride dehydrate), 1 ml/L 1 M trace metals stock II (0.6 g/L zinc sulphate heptahydrate, 2.7 g/L iron (III) chloride hexahydrate, 0.6 g/L copper sulphate pentahydrate).

2.2. Isolation and analysis of nucleic acids from *Candida* cells

2.2.1. Extraction of genomic DNA from *Candida* cells

Genomic DNA was isolated from *Candida* as described previously (Reuss *et al.*, 2004). *Candida* cells were cultured by incubation on YEPD agar at 37 °C for 2 days. Cells were inoculated in YEPD broth and incubated at 37 °C, 200 r.p.m. overnight. After 16 h the cells were centrifuged at 12, 000 $\times g$ for 3 min, washed in 1X PBS and resuspended in Breaking Buffer (2 % (v/v) Triton X-100, 1 mM EDTA, 1 % (w/v) SDS, 100 mM NaCl, and 10 mM Tris-HCl pH 8.0). Liquefied phenol, washed in Tris-buffer from Thermo Fisher Scientific Ltd. (Bishop Meadow Rd., Loughborough, UK) was used to prepare phenol:chloroform:isoamyl alcohol (PCI) in the ratio of 24:24:1. Resuspended cells in breaking buffer were added to an equal volume of PCI in screw-capped tubes (Sarstedt, Drinagh, Wexford, Ireland). The cells were broken in a Fastprep FP120 Cell Dismembrator (Thermo Fisher Scientific Ltd.). Isolated DNA was purified by cold ethanol precipitation using cold, 100 % (v/v) ethanol (200 proof, absolute) and 3 M sodium acetate. The solution was centrifuged at 13,000 $\times g$ at -4 °C and washed in 70 % (v/v) ethanol. The solution was centrifuged as described previously, the supernatant was removed and the purified pellet was allowed to dry at room temperature. The washed and dried DNA pellet was then resuspended in either TE buffer or ultrapure water for immediate downstream applications or storage at -20 °C.

2.2.2. PCR amplification

Oligonucleotide primers were custom synthesised by Sigma-Aldrich using standard synthesis conditions, dissolved to 100 μ M in molecular biology grade water (Sigma-Aldrich) and stored at -20 °C. Primers used in this study are listed in Table 2.2. Polymerase chain reaction amplification was carried out using either the GoTaq® system (Promega) or the Expand High Fidelity PCR system (Roche Diagnostics Ltd.) according to manufacturer's instructions unless explicitly stated.

Amplified products were visualised by electrophoresis using 0.8 % (w/v) agarose gels containing 1 % (v/v) GelRed™ (Biotium, Hayward, California, USA) for expected products over 1 kb or 2 % (w/v) agarose gels for expected products under 1 kb. TBE was used to cast agarose gels and as running buffer for electrophoresis. GelRed™-bound nucleic acid was visualised using a UV transilluminator (Ultra Violet Products Ltd., Cambridge, United Kingdom) at 345 nm.

PCR products were routinely purified using the Genelute™ PCR Clean-Up kit (Sigma-Aldrich) or the Wizard® SV Gel and PCR Clean-Up System (Promega). DNA sequencing was carried out commercially by Source Bioscience (Tramore, Co. Waterford, Ireland).

2.2.3. Extraction of chromosomal DNA from *Candida* cells

High-quality chromosomal *Candida* DNA was isolated using a gentle cell breaking method based on previously described methods (Gallagher *et al.*, 1992; Pearce & Howell, 1991). Briefly, this was conducted by incubating *Candida* cells on YEPD agar at 37 °C for 48 h. A single colony was inoculated in YEPD broth and incubated for 18 h at 37 °C in an orbital incubator at 200 r.p.m. After 18 h the broths were centrifuged at 4,000 $\times g$ for 10 min. The supernatant was removed, the cells were washed in 1X PBS, and then resuspended in 20 mM Citrate Phosphate Buffer, 40 mM EDTA, 1.2 M Sorbitol, pH 5.6. Protoplasting was achieved using Zymolyase 20T (Amsbio, AMS Biotechnology (Europe) Ltd., Abingdon, Oxford, UK) at 37 °C, 200 r.p.m. for 3 h. Protoplasts were harvested by centrifugation and lysed by resuspending in 10X TE buffer containing 10 % (w/v) SDS, to which potassium acetate (5 M) was added before incubation on ice for 30 min. The lysed cells were centrifuged (Sorvall SS-34

rotor) for 10 min at 8,500 r.p.m. (approximately 8,600 $\times g$). Nucleic acids and proteins were precipitated by adding ice-cold isopropanol. After centrifugation at 4 °C for 10 min, the pellet was allowed to dry at room temperature, and then resuspended in TE buffer. RNase A (10 µg/ml) and proteinase K (2 mg/ml) were used to digest RNA and proteins respectively. Purification of DNA was achieved by phenol/chloroform extraction, and precipitation using 100 % (v/v) ethanol and 3 M sodium acetate. DNA was resuspended in 1X TE buffer and stored at -20 °C.

2.2.4. Southern blot analysis of *Candida* DNA

Specific DNA probes were amplified with DIG DNA labeling mix (Roche Diagnostics Ltd.) and electrophoresed on 0.8 % (w/v) agarose alongside DIG Molecular Weight Marker II, DIG-labeled (Roche Diagnostics Ltd.) (Southern, 1975). Chromosomal *Candida* DNA was digested with *EcoRI* or *BglII* (Promega) and transferred to a positively charged nylon membrane (Roche Diagnostics Ltd.). DNA was cross-linked to the membrane using UV light and the membrane was allowed to air dry. Hybridisation of the DIG-labeled probe to the membrane was carried out according to manufacturer's instructions using DIG Easy Hyb Granules (Roche Diagnostics Ltd.). Anti-Digoxigenin-AP, Fab fragments (Roche Diagnostics Ltd.) were used to bind membrane-bound DIG-labeled probe. CDP-Star substrate (Sigma-Aldrich) was used as a chemiluminescent substrate and incubated in the dark with Biomax Light Film (Sigma-Aldrich). Film was developed using Kodak Fixer (Sigma-Aldrich) and Kodak Developer (Sigma-Aldrich).

2.2.5. Rapid lysis and extraction of *Candida* DNA for colony PCR

Rapid screening of potential transformant colonies was facilitated by the use of a reliable colony PCR screening method (personal communication, Dr. L. Holland, UCD). Briefly, this entailed picking a small amount of fresh colony using a P20 pipette tip and thoroughly resuspending it in 5 µl of molecular biology grade water in a PCR thin-walled tube (Sigma-Aldrich). The mixture was boiled in a thermocycler (G-storm GSI thermocycler, Life Technologies Corporation, California, USA) at 95 °C for 5 min. A standard GoTaq® PCR reaction mixture was added to the boiled sample and PCR amplification was carried out as follows: 35 cycles of 95 °C for 15 s, 55 °C for 15 s, 72 °C for 15 s. Amplimers were visualised on a 0.8 % (w/v) agarose gel as previously described.

Table 2.2. Oligonucleotide primers used during this study

Primer	Primer nucleotide sequence (5'-3')
ALS3F1SALI	GACCTGTCGACATTGTATAAACAACACTACCAACTG
ALS3R1BGLII	TGAAGATCTTCTAAAAAGGCGACTATGATG
HYR1F1SALI	GACCTGTCGACGGTAATAACAACATGAAAGTGG
HYR1BGLII	TGAAGATCTGGTTCAACTCATCACATGAATA
CDPNIMF1	TTGAGAGAGACCGTCAAAAAC
CAPNIMF1	GAGATGGAGCCGTCAAATATCC
PNIMF2	GACAATCTTGATTGGGCATTTG
PNIMR1	TCTACTTGGTTATGTGGTTTTGATCACATTATTATCCTTATTTATTTAACACATGGCATGGATGAACTATAC
PNIMR3	AAATCCATTTTGTGGTTTAATTGTTTCCATGGTTGTTTTATTCATGTGACACATGGCATGGATGAACTATAC
PNIMR2	GACAAATATATGAGTAACAATGTATATTGTTGTAGCATCTTTGTCGACTATTTATATTTG
PNIMR4	TAAGCAAAATTGTGAATATAAAGTTTGATACCACTTTCATCTTTGTCGACTATTTATATTG
ALS3F2	CAAATATAAATAGTCGACAAAGATGCTACAACAATATACATTGTTAC
ALS3R2	CCAGATTTCCAGATTTCCAGAATTTAGATCTTTATTTGTATAGTTCATCCATGCCATGTGTTAAATAAATAAGGATAATAATGTGAT
HYR1F2	CAAATATAAATAGTCGACAAAGATGAAAGTGGTATCAAACTTTATATTCACAAT
HYR1R2	CCAGATTTCCAGATTTCCAGAATTTAGATCTTTATTTGTATAGTTCATCCATGCCATGTGTACATGAATAAAACAACCATGGAAACA
JUNCF1	TGCCTTGGGTGGCTATTTTA
JUNCR1	TCGTTTCTGATGGGGCTTTTC
CARTTAF1	CTCATCCCTGGTCTTGGCTA
CARTTAR1	GGTTTGGTGGGGTATCTTCA
CDADH1F1	GCAAGATGTTACCTGCAACG
CDADH1R1	GGTGGTCCTGCAGACATTTT

Continued overleaf

Table 2.2. Continued

Primer	Primer nucleotide sequence (5'-3')
RPS1NAT1F1	GTAAAAACAAGAGATTGTCTAAAGGAAAGAAAGGATTAAGAAAGGTCGTTAGTATCGAATCGACAGC
RPS1NAT1R1	TTAAACAGATTCTAAACAACATCTTTAAACCAGAAGAACTTTCTTACCTTTTTCTTCTCTAAAAAGGCGACTATGATG
ENO1ALS3F1	CAGTTGGTAGTTGTTTATACAATTGTTGTAATATTCCTGAATTATC
ENO1ALS3R1	GATAATTCAGGAATATTACAACAATTGTATAAACTACCAACTG
RPS1F1	GTAAAAACAAGAGATTGTCTAAAG
RPS1R1	TTAAACAGATTCTAAACAACATC
EFB1F1	ATTGAACGAATTCTTGGCTGAC
EFB1R1	CATCTTCTTCAACAGCAGCTTG
qRTALS3F1	TGGAAGCTTCATCGCCTATC
qRTALS3R1	GCGATTGAGATTGGTTGGTT
qRTHYR1F1	TCTGGTTCCGAAAGTGGTTC
qRTHYR1R1	TTTTCCATCAAAGCCAGTCA
qRTNRG1F1	AAAGACCCAAGAAGAAAACA
qRTNRG1R1	CTGTGTTGTTGTCTGTTTCG
qRTCPH1F1	AGCAGAAATACCCGTGCTGT
qRTCPH1R1	ATCCCATGGCAATTTGTTGT
qRTEFG1F1	ACAGCCACCACTACCAGGTC
qRTEFG1R1	CACGTGTCATTTGGGCCACAT
qRTACT1F1	AGCTCCAGAAGCTTTGTTTCAGACC
qRTACT1R1	TGCATACGTTTCAGCAATACCTGGG

Oligonucleotide sequences for primer design were obtained from *Candida* genome database (CGD)
Restriction enzyme digestion sites are underlined

2.2.6. Harvesting RNA and synthesis of cDNA

RNA was isolated from *Candida* cells by mechanical disruption using a FP120 Fastprep bead beater and purified using the Qiagen RNeasy Mini kit (Qiagen, Manchester, UK) according to the manufacturer's directions. The isolated RNA was treated with Turbo DNase (Ambion, Bio-Sciences Ltd.) to digest and remove any double stranded DNA carry-over. RNA quality was assessed by gel electrophoresis and nucleic acid concentration was measured on a Nanodrop 2000C (Thermo Fisher Scientific). A total of 1 µg of DNase-treated RNA was used to reverse transcribe cDNA using the Superscript II First Strand Synthesis system (Invitrogen, Bio-Sciences Ltd.). Briefly, 1 µg RNA and 1 µl Oligo(dT)18 (500 µg/ml) (Promega) were heated to 70 °C for 10 min in a thermocycler and chilled on ice for 1 min. After 1 min, 4 µl of 5 x First Strand Buffer, 2 µl of 0.1 M DTT, and 1 µl of dNTP mix (10 mM) (Promega) were added to each reaction vessel and incubated at 42 °C for 2 min. 1 µl of Superscript II RT was added to each reaction vessel, with a final reaction volume of 11 µl, and reverse transcription was performed by holding the reaction vessels at 42 °C for 1 h. The reaction was inactivated at 70 °C for 15 min as per manufacturer's instructions and 20 µl molecular biology grade water was added before storing at -20 °C. The quality of cDNA was assessed by PCR using primers, EFB1F1 and EFB1R1, to check for the presence of contaminating gDNA.

2.2.7. qRT-PCR validation and analysis of gene expression

Fast SYBR Green Master Mix (Applied Biosystems, Bio-Sciences Ltd.) in a 15 µl total reaction volume was used in conjunction with an Applied Biosystems 7500 Real-Time PCR system to assay gene expression levels from cDNA samples. Output was analysed by the comparative C_t ($2^{\Delta\Delta C_t}$) method to calculate fold up- and down- regulation of expression of specific genes (Schmittgen & Livak, 2008). Primers used for qRT-PCR were first verified for comparative amplification efficiency to the endogenous control, *ACT1*. By using serial dilutions of genomic DNA template and plotting the resultant C_t values against the log of DNA concentration it was possible to calculate the amplification efficiency of each primer pair. Linear regression was used to calculate the slope of the line, and amplification efficiency was calculated according to the equation $m = -(1/\log E)$, where m is the slope of the line and E is the amplification efficiency value. Primer pairs were only used if the amplification efficiency was

within 10 % of the efficiency value for amplification of the housekeeping gene *CdACT1* or *CaACT1*.

2.3. Recombinant DNA techniques

2.3.1. Isolation of plasmid DNA from *Escherichia coli*

Escherichia coli was pre-grown on L_{amp} at 37 °C for 18 h. A single colony was inoculated into L_{amp} broth and grown at 37 °C in an orbital incubator overnight. After 18 h, the broths were centrifuged at 16,000 $\times g$, the supernatant was removed and the cells were washed in 1X PBS. Plasmids were isolated from washed cells using either the Plasmid Miniprep Kit (Sigma) or the Wizard Plasmid Extraction Kit (Promega) according to the manufacturer's instructions. Nucleic acid concentration was measured using a Nanodrop 2000C and stored at -20 °C.

2.3.2. Digestion and ligation of DNA fragments

Plasmid digestion patterns were predicted using the online NEBCutter tool (<http://tools.neb.com/NEBcutter2/index.php>). DNA was digested using restriction endonuclease enzymes sourced from Promega or New England Biosystems as recommended. Digested DNA was visualised by gel electrophoresis. The PCR Cleanup kit (Sigma) was used to purify the digested DNA of interest from the digestion mixture. Where necessary, DNA fragments were isolated by gel purification. This was conducted by gel electrophoresis of whole digestion mixes on 0.8 % (w/v) agarose gels, excising the band of interest from the gel and processing gel slices through the Wizard PCR and Gel Cleanup kit (Promega). Ligation of purified, digested DNA fragments was achieved using T4 DNA ligase (Promega) and allowing ligation to occur initially at 20 °C for 2 h, and then at 4 °C overnight.

2.3.3. Transformation of PIPES/CaCl₂-competent *E. coli* by heat-shock

Transformation of competent *E. coli* (XL10 gold) prepared with PIPES and CaCl₂ was conducted using a process based on previously developed methods (Sambrook & Russell, 2006). *Escherichia coli* XL10 gold was grown overnight in LB at 37 °C in a rotary incubator. After 18 h, the preculture was inoculated into fresh, prewarmed LB and incubated at 37 °C, 200 r.p.m. for approximately 2 h until mid-log phase of growth (OD₆₀₀ 0.4). The cells were chilled on ice for 1 h. The broth was centrifuged in

a Sorvall centrifuge (GSA rotor) at 400 r.p.m. (approximately 30 $\times g$) for 10 min at 4 °C. After removal of the supernatant, the cell pellet was gently resuspended in 30 ml ice cold 100 mM MgCl₂, and centrifuged again. Cells were resuspended in 100 ml ice cold CaCl₂ and chilled on ice for 10 min. Cells were centrifuged and washed in 50 ml ice cold PIPES buffer. After another round of centrifugation, the cells were resuspended in 20 ml PIPES buffer. The buffer was gently swirled while ice cold 80 % (v/v) glycerol was added to a final concentration of approximately 10 % (v/v). The competent cells were aliquoted into microfuge tubes and either snap-frozen in liquid nitrogen for storage at -80 °C or used directly in a transformation reaction.

Competent XL10 gold cells were thawed on ice. Ligation mixtures (30 μ l) were added directly to 200 μ l of chilled XL10 gold and chilled on ice for 5 min. The transformation reaction mixture was heat shocked at 42 °C for 2 min, chilled on ice for 2 min, and allowed to recover in 1 ml SOC broth (2 % (w/v) tryptone, 0.5 % (w/v) yeast extract, 10 mM NaCl, 2.5 mM KCl, 10 mM MgCl₂, 20 mM glucose) at 37 °C, 200 r.p.m. for 2 h to allow expression of antibiotic resistance genes. Approximately 100 μ l of recovered cells were plated on L_{amp} agar. The rest of the transformation mix was centrifuged at 16,000 $\times g$ for 3 min and the cell pellet was resuspended in 100 μ l SOC broth. This ~10X cell suspension was also plated on L_{amp} agar. All inoculated L_{amp} plates were incubated at 37 °C overnight.

2.4. Hyphal induction of *C. albicans* and *C. dubliniensis*

2.4.1. Standard hyphal induction on solid media

Spider agar was prepared using 1 % (w/v) nutrient broth, 1 % (w/v) mannitol, 0.2 % (w/v) K₂HPO₄, and 1.35 (w/v) % Bactoagar. Synthetic low dextrose (SLD) agar contained 0.17 % (w/v) Yeast nitrogen base without amino acids, 0.5 % (w/v) ammonium sulphate, 0.1 % (w/v) glucose, and 1.35 % (w/v) Bactoagar. Yeast nitrogen base serum (YNB-S) agar was prepared with 0.67 % (w/v) yeast nitrogen base with amino acids, 0.5 % (w/v) glucose, and 1.35 % (w/v) Bactoagar. The molten agar was supplemented with 10 % (v/v) foetal calf serum after sterilisation by autoclaving. Yeast extract peptone sucrose (YPS) agar was prepared with 1 % (w/v) yeast extract, 2 % (w/v) Bacto-peptone, and 1.35 % (w/v) Bactoagar. After

sterilisation this was supplemented with filter-sterilised sucrose at a final concentration of 2 % (v/v).

2.4.2. Standard hyphal induction in liquid media

Standard basal hyphal induction was initiated by nutrient-rich serum induction as described previously (O'Connor *et al.*, 2010). Briefly, this was carried out by inoculating fresh YEPD broth with a single *Candida* colony from a 48 h YEPD plate, and incubating the broth overnight at 37 °C, 200 r.p.m. After 18 h, the broths were centrifuged, the cells were washed in 1X PBS and counted using a Neubauer improved haemocytometer. Washed cells were inoculated in prewarmed YEPD with 10 % (v/v) FCS (YPDS) to a final density of 2×10^6 cells/ml. Hyphal induction broths were either incubated in 250 ml conical flasks in a rotary incubator, or statically, to prevent clumping, in 6-well multiwell plates at 37 °C. For improved *C. dubliniensis* hyphal induction, the same YEPD preculture approach was adopted, however, the induction medium was replaced with nutrient poor 10 % (v/v) FCS (O'Connor *et al.*, 2010). Yeast and hyphal cells were visualised and quantified using a Nikon E600 microscope and a Nikon TMS-F inverted microscope (Nikon).

2.5. General tissue culture methods

2.5.1. Growth and maintenance of cell lines

The immortalised human epithelial cell line TR146 was obtained from the collection of the Microbiology Research Unit, Division of Oral Biosciences, Dublin Dental University Hospital, Dublin 2, Ireland. Cells were stored in Nunc® Cryobank vials (Sigma-Aldrich) under liquid nitrogen vapour. Cells were stored at a density of 1×10^6 cells/ml in Dulbecco's Modified Eagle's Medium (DMEM) supplemented with 10 % (v/v) dimethyl sulphoxide (DMSO) as a cryoprotectant. Frozen cells were revived and grown in cell culture flasks in DMEM supplemented with 20 % (v/v) FCS at 37 °C under 5 % (v/v) CO₂. Cells were passaged with trypsin-EDTA (Sigma-Aldrich) as they reached ~80 % confluency. After the first passage from frozen, cells were maintained in Complete DMEM (CDMEM) medium (DMEM, 10 % (v/v) FCS). Cells used for experiments were all passaged less than twenty times.

2.5.2. Approved isolation of human buccal epithelial cells

Permission was gained from multiple volunteers to isolate keratinised human buccal epithelial cells. Samples from the oral cavity were obtained using sterile cotton swabs, transferring the swabs to sterile 1X PBS and swirling the swab to create a cell suspension (Jordan *et al.*, 2014). Samples from over 5 volunteers, for each experiment, were pooled, centrifuged at $2,000 \times g$ for 5 min, and washed twice in 10 ml 1X PBS. Washed cells were counted using an improved Neubauer haemocytometer and resuspended in 1X PBS to a density of 2×10^5 cells/ml. Cells were used immediately after isolation for each experiment.

Chapter 3

Construction and analysis of *Candida dubliniensis* strains expressing *Candida albicans* virulence genes

3.1. Introduction

3.1.1. ALS Family

The Adhesin-like-sequence family (*ALS*) is a group of genes that have received significant interest as key players in the pathogenesis of *C. albicans* infections. *Candida albicans* possesses 8 *ALS* genes encoding a set of GPI-anchored proteins with similar modular domain structures (Sheppard *et al.*, 2004). The genes are spread over three chromosomes, with *CaALS3* on Chromosome R, *CaALS6* and *CaALS7* on Chromosome 3 and the remaining members located on Chromosome 6 (Hoyer *et al.*, 1998a). Comparative genomics has shown that *C. dubliniensis* apparently possesses seven genes which show similarity to the *ALS* gene family (Hoyer *et al.*, 2001; Jackson *et al.*, 2009). Remarkably though, *C. dubliniensis* completely lacks an orthologue of the *ALS3* gene. In-depth analysis by Jackson *et al.* showed that the *C. dubliniensis* and *C. albicans* *ALS* family represented a mixture of positional orthologues, species-specific genes or sequence modifications arising after speciation. These characteristics may be an indication of different evolutionary pressures on each species and their response to adapt to specialised niches.

ALS-encoded proteins are modular and composed of three domains (Fig. 3.1) (Hoyer *et al.*, 2008). The C-terminal domain anchors the protein to the *Candida* cell wall via a GPI-anchor, while the middle region of each protein is comprised of varying numbers of tandem repeats (Hoyer, 2001). These tandem repeats are predicted to be highly glycosylated, and are considered to provide a flexible linker between domains, playing a role in final protein conformation and steric freedom. The N-terminal domain of *Als* proteins have been determined to be the functional domain, playing a role in adhesion to host substrates. *In silico* modeling of *Als*p N-terminal domains reveals a structure composed of anti-parallel beta sheets, linked by hypervariable immunoglobulin-like regions thought to relate to specificity of substrate binding (Sheppard *et al.*, 2004).

ALS-encoded proteins have been shown to play a role in binding of organisms to various host substrates such as laminin and fibronectin. Historically, studies have taken advantage of a combination of gene knockout strains in *C. albicans* and heterologous expression of select genes in the yeast *S. cerevisiae*. Studies have

analysed the response of these constructs in epithelial and endothelial infection models, in addition to substrate binding assays, revealing complex patterns of adhesion between various family members and host tissues and ligands (Hoyer *et al.*, 2008). In *C. albicans* knockout strains, interpretation of phenotypes has been complicated by the high level of sequence similarity and functional degeneracy observed throughout the *ALS* family (Hoyer *et al.*, 2008). There are also indications that the absence of one Als protein can alter the transcription levels of other *ALS* genes, leading to further skewing of results (Zhao *et al.*, 2005). Interpretation of results through heterologous expression systems in organisms such as *S. cerevisiae* may also be complicated by species-specific factors such as codon usage leading to variations in protein translation (Santos & Tuite, 1995).

Previous studies have highlighted *CaALS3* specifically as a significant factor in *C. albicans* adhesion to a number of tissues and host ligands, and subsequent internalisation. Gene knockout mutants of *CaALS3* have shown reduced adhesion to endothelial cells, buccal epithelial cells and FaDu epithelial monolayers (Oh *et al.*, 2005; Zhao *et al.*, 2004). Latex beads coated with recombinant *CaAls3p* are efficiently internalised by host cells, showing that *CaAls3p* is sufficient for invasion (Phan *et al.*, 2007). The tandem repeat linker region of *CaALS3* possesses allelic variability resulting in two different sized alleles in the sequenced strain, SC5314. The large allele of *CaALS3* in SC5314 contains 12 tandem repeats while the small allele contains nine tandem repeats. While the large allele is currently associated with full pathogenesis, studies have shown that the variability of pairing a large and small allele, and the respective sizes of the tandem repeats, may influence the virulence of *C. albicans* strains (Oh *et al.*, 2005). Internalisation is considered to be due to similarities between the N-terminal of *CaAls3p* and host cadherins (Moreno-Ruiz *et al.*, 2009; Phan *et al.*, 2005). Cadherins are transmembrane proteins that play an integral role in cell adhesion at adherens junctions between a number of different cell types. Mimicry of cadherins by *CaAls3p* enables not only adhesion to host cells but also uptake via endocytic recycling pathways (Zhu & Filler, 2010). *CaAls3p* has displayed the ability to bind ferritin, enabling *C. albicans* to harvest host iron from host cells and surrounding tissues (Almeida *et al.*, 2008). Concurrently, damage of epithelial cells by *C. albicans* is associated with uptake of iron by invading fungal cells. Interestingly, *CaAls3p* has been observed to be non-essential in a murine systemic

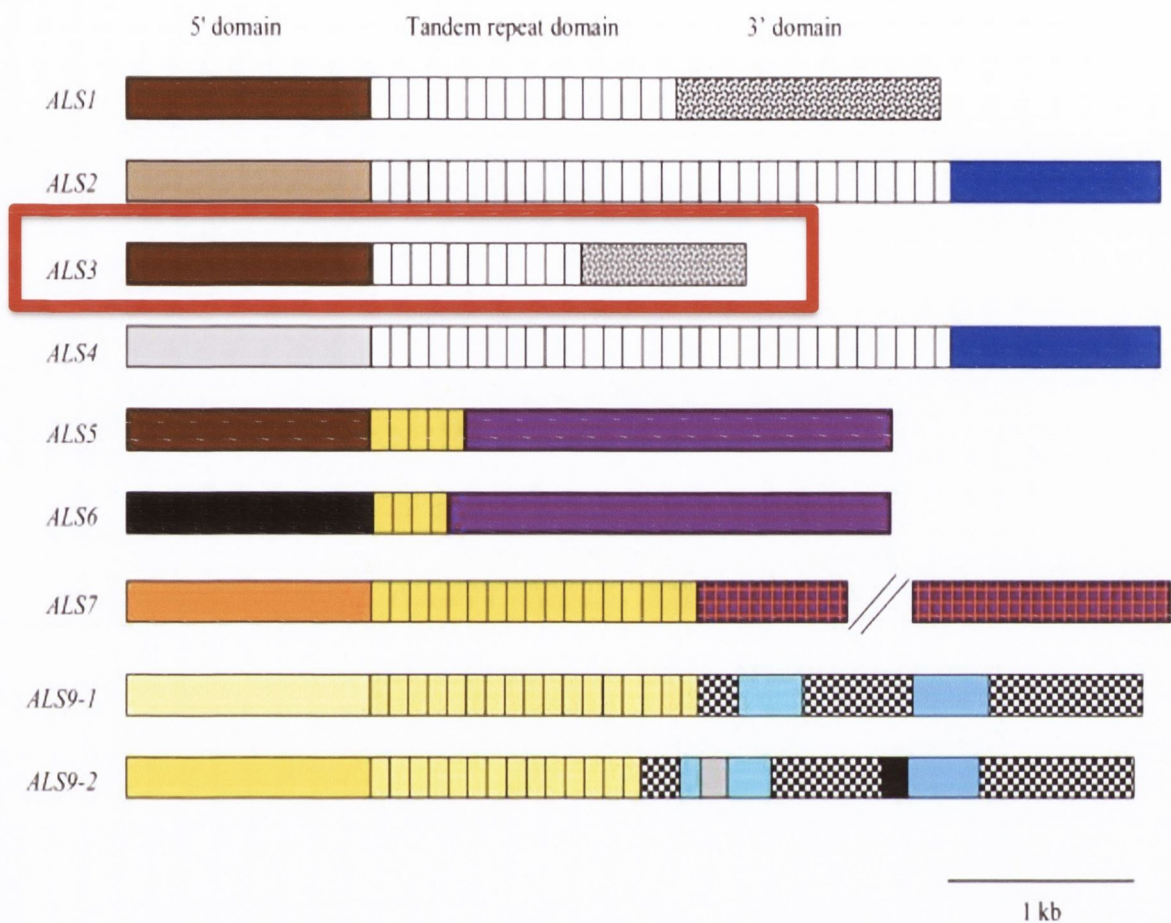


Figure 3.1. Modular structure of *C. albicans* ALS family members. Sequence and domain similarity is indicated by matching colour schemes. The target of this current study, *CaALS3*, is highlighted. Adapted from Hoyer *et al.*, 2008.

model of disseminated candidiasis, possibly highlighting its importance specifically during the adhesion and invasion stages of infection (Cleary *et al.*, 2011; Fu *et al.*, 2013).

Regulation of *CaALS3* is strongly linked to the hyphal morphology of *C. albicans* cells. Development of hyphae is associated with rapid upregulation of *CaALS3* (Kadosh & Johnson, 2005). Analysis of the natural promoter of *CaALS3* has revealed two important activation regions (Argimon *et al.*, 2007). One region appears to be responsible for transcription activation while the other region plays a role in the magnitude of the transcriptional response. The major morphological regulator *CaEfg1p* is essential for activation of the promoter while *CaCph1p*, the effector protein as part of the MAPK pathway, is also thought to play a role in the scale of the response (Moazeni *et al.*, 2012). The close association between *CaALS3* associated virulence, the hyphal morphology in *C. albicans*, and the absence of an *ALS3* gene or orthologue in the less filamentous, relatively non-pathogenic *C. dubliniensis*, have presented the protein as an attractive vaccine target and vaccine development studies are ongoing (Ibrahim *et al.*, 2006; Spellberg *et al.*, 2008; Spellberg *et al.*, 2006). Whether a *CaALS3*-specific vaccine would display activity against other *Candida* species capable of expressing *ALS* family of *ALS*-like proteins has yet to be determined although an *ALS3* vaccine appears to show some broad protection against the Gram-positive pathogen *Staphylococcus aureus* (Spellberg *et al.*, 2008).

3.1.2. *IFF* Family

The *C. albicans* *HYR/IFF* gene family is a group of genes which, similar to the *ALS* family, are hyphally regulated and thus associated with hyphal virulence (Kadosh & Johnson, 2005). The family in *C. albicans* consists of 12 genes, predicted to produce adhesin-like proteins. All but one member of the family possesses a conserved GPI-protein recognition pattern suggesting the proteins are localised in the cell wall, similar to members of the *ALS* family. The single protein lacking a GPI-attachment site is *Calff11p*, and is instead a secreted protein that has been associated with cell wall stability and virulence (Bates *et al.*, 2007). Boisrame *et al.* have experimentally demonstrated that most of the proteins encoded by the *HYR/IFF* family in *C. albicans* are located at the cell surface, either through GPI-linkages to β -1,6-glucan or are associated with the plasma membrane (Boisrame *et al.*, 2011). Extracellular exposure

of N-terminal functional domains has been determined to be related to the serine/threonine-rich region of the protein. Relatively little is known about the function of the majority of the members of this gene family.

Bailey *et al.* originally identified and characterised *CaHYR1* as a morphogenetically regulated gene, apparently encoding a non-essential hyphal cell wall protein (Bailey *et al.*, 1996). No altered phenotype was observed and *CaHYR1* was initially designated as a gene with unknown function. Subsequently, *CaHYR1* was identified as a putative virulence factor and potential vaccine target (Luo *et al.*, 2010). Indirect immunofluorescence showed an abundance of *CaHyr1p* on the surface of *C. albicans* hyphae confirming its identity as a hyphal cell wall associated protein. The *CaHyr1p* protein was found to be associated with resistance of *C. albicans* hyphae to human neutrophil-mediated killing. Heterologous expression of *CaHYR1* in *C. glabrata* supported resistance to fungal killing by human neutrophils (Fu *et al.*, 2013). Additionally, recombinant *CaHyr1p* N-terminus partially protected against systemic *C. albicans* infection in a murine model of disseminated candidiasis (Luo *et al.*, 2011). The mechanism of action contributing to this resistance has yet to be elaborated.

Candida dubliniensis possesses an orthologous *HYR/IFF* family. However, only 11 gene members are present in its genome. Notably, the less virulent *Candida* species does not possess an orthologue of the *HYR1* gene. As a putative virulence factor, the absence of this gene from the genome of *C. dubliniensis* may represent one of the factors for the reduced virulence of *C. dubliniensis* as an opportunistic human pathogen. Jackson *et al.* established that *CaHYR1* was not a duplication event that occurred after the evolutionary split of *C. albicans* and *C. dubliniensis* (Jackson *et al.*, 2009). Instead, deletion of *HYR1* from the *C. dubliniensis* genome was postulated, based on residual similarity at the corresponding locus. Thus, loss of *HYR1* from *C. dubliniensis* suggests evolutionary pressures distinct from those experienced by *C. albicans*.

3.1.3. Molecular cloning methods

While the concept of genetic cloning is well established, the discipline itself is constantly evolving and methods are improving. Processes such as PCR, creation of auxotrophic strains and antibiotic resistance as a selective agent have played pivotal

roles in the maturation of the technology. Genetic cloning in *Candida* faces a number of technical issues such as non-canonical codon usage, lack of selectable markers and poor transformation efficiency. Methods used in the baker's yeast *S. cerevisiae* have been adapted for use in *Candida* (Alani *et al.*, 1987). The *URA3* gene, encoding an orotidine-5-phosphate decarboxylase in *C. albicans* (Losberger & Ernst, 1989), was targeted to develop the method now known as URA-blaster mutagenesis (Fonzi & Irwin, 1993). This method was used for construction of a homozygous *ura3Δ/ura3Δ* auxotrophic strain, which requires supplementation with exogenous uridine for normal growth (Negredo *et al.*, 1997; Wilson *et al.*, 2000). In this way, complementation of the *ura3Δ/ura3Δ* strain with DNA containing a wild type *URA3* gene, along with any gene or construct of interest, enables efficient selection of transformant cells on minimal media lacking uridine. The URA-blaster method was first described by Fonzi *et al.* in 1993. Subsequently, however, it was discovered that strains constructed with the URA-blaster technique were not isogenic with their wild-type parent strains and may have undergone significant genomic rearrangements due to recombination (Brand *et al.*, 2004; Garcia *et al.*, 2001). In addition, complementation with *URA3* did not uniformly restore natural expression of the decarboxylase (Lay *et al.*, 1998). *URA3* expression and phenotypic effects vary depending on whether the gene is present in ectopic DNA, or chromosomal loci other than its natural locus such as *ENO1*, *ACT1* or *RPS1* (Murad *et al.*, 2000; Sundstrom *et al.*, 2002b; Wilson *et al.*, 2000). This has been found to affect the virulence of *C. albicans* strains and their derivatives in infection models (Cheng *et al.*, 2003). Interpretation of phenotypes of strains constructed using the URA-blaster method is thus complicated in a number of ways (Bain *et al.*, 2001). Recent attempts to restore *URA3* to its natural locus after cloning a gene of interest by *URA3* complementation may represent a viable method to confirm observed phenotypes (Gerami-Nejad *et al.*, 2013).

As a result of the challenges with utilising the *URA3* method, without causing peripheral deleterious effects, there have been many studies undertaken to identify alternative selectable markers, which do not themselves impact on fungal growth or virulence. A cassette for resistance to the aminoglycoside hygromycin B was developed as a dominant selectable marker. The hygromycin B phosphotransferase gene was amplified from *E. coli* and used as the core of a *C. albicans* cassette, which

successfully conferred resistance to the antibiotic (Basso *et al.*, 2010). However, the group discovered not only that hygromycin B required a buffered neutral pH in minimal medium for functionality, but that plasmid-transformed *C. albicans* strains, grown in the absence of hygromycin B, lost their plasmids over the course of 40 generations. Thus chromosomal integration is favoured in the case of hygromycin B resistance. An alternative selectable marker investigated for *C. albicans* antibiotic resistance is mycophenolic acid (MPA) (Goshorn & Scherer, 1989). The target of mycophenolic acid, inosine monophosphate dehydrogenase (*IMH3*), is an enzyme involved in nucleic acid synthesis promoting *de novo* biosynthesis of guanosine monophosphate (GMP). Kohler *et al.* used overexpression of *IMH3* from plasmids to demonstrate its use as a selectable marker in *C. albicans* (Kohler *et al.*, 1997). However, further studies in both *C. albicans* and *C. dubliniensis* have indicated that MPA-resistant transformants take longer to grow than wild-type, indicating a deleterious effect on fitness of the fungal cell (Wirsching *et al.*, 2000).

The most well established dominant selection method for *C. albicans* is resistance to the broad spectrum streptothricin class antibiotic, nourseothricin. This is achieved in one of two ways. Reuss *et al.* amplified the nourseothricin-resistance gene streptothricin acetyltransferase (*SAT1*) from *E. coli* harboring the bacterial transposon Tn1825 and placed it under the control of the *C. albicans* *ACT1* promoter (Reuss *et al.*, 2004). An alternative approach assembled a nourseothricin resistance element by amplifying the *NAT1* gene from *Streptomyces noursei* and placing it under the control of the *TEF1* promoter from *Ashbya gossypii* (Shen *et al.*, 2005). Both methods confer nourseothricin resistance and form the basis of many genetic cloning approaches in *Candida*.

In particular, the *SAT1* element is used as the dominant selectable marker in the tetracycline-inducible differential expression cassette, pNIM1 (Park & Morschhauser, 2005). While the Tet-Off system previously used with *C. albicans* allowed silencing of transcription with the addition of tetracycline to the growth medium, the Tet-On system used in pNIM1 allows for creation of *C. albicans* strains containing genes which may be toxic to the fungal cell (Gossen *et al.*, 1995). The default state of genes introduced under this system is transcriptionally off. Treatment with tetracycline allows transcription activation and investigation of protein functionality in ways

which could not be achieved using the Tet-Off system. This system was established by fusing a *C. albicans* reverse tetracycline-controlled transactivator (*cartTA*), under the control of *CaADH1*, to *SAT1*. A *rtTA*-dependent promoter, based on the *C. albicans* OP4 promoter coupled with seven copies of the Tet operator (*tetO*) activation sequence, was constructed to drive transcription of any gene of interest. Excision of a *GFP* element and replacement with a gene of interest allows transformation of *C. albicans* with a tetracycline-inducible differential expression system with selection of transformant cells based on nourseothricin resistance. The pNIM1 system was further developed for use with *C. dubliniensis*, replacing the *CaADH1* promoter sequence with the orthologous *CdADH1* sequence for improved integration into the *C. dubliniensis* *CdADH1* locus (Spiering *et al.*, 2010).

3.1.4. Aims of this part of the study

This part of the project aimed to express the hyphal-specific genes *CaALS3* and *CaHYR1* in both yeast and hyphal cells of the significantly less pathogenic *C. dubliniensis* in order to investigate the contribution of each individual gene to *Candida* pathogenesis.

3.2. Specific materials and methods

3.2.1. Restriction endonuclease-mediated cloning

3.2.1.1. Preparation of template DNA

Candida cells were grown initially on YEPD agar and subinoculated in YEPD broth and incubated as described in Chapter 2. Cells were washed in 1X PBS and cell walls were disrupted using the bead beater method. DNA was extracted using phenol-chloroform extraction and resuspended in 1X TE buffer. For PCR, genomic DNA was resuspended to a final concentration of 100 ng/ μ l.

3.2.1.2. PCR amplification and purification of CaALS3 alleles

DNA sequences for *CaALS3* were extracted from the *Candida* Genomic Database (CGD) and aligned with the sequence published by Zhao *et al.* (Zhao *et al.*, 2004). *CaALS3* small and large alleles were PCR amplified from SC5314 genomic DNA using Expand High Fidelity Polymerase (Roche). Primers used in this study are listed in Table 2.2. Primers ALS3F1SALI and ALS3R1BGLII were used in a PCR reaction; 94 °C for 2 min, 10 cycles of 94 °C for 15 s, 56 °C for 30 s, 68 °C for 3 min, 20 cycles of 94 °C for 15 s, 56 °C for 30 s, 68 °C for 3 min with an increase of 5 s per cycle. Final elongation was performed at 68 °C for 7 min. Mixed allelic amplimers were directly purified using the Genelute PCR Cleanup Kit (Sigma) and stored at -20 °C. Alternatively, PCR amplimers were electrophoresed on 0.8 % (w/v) agarose and individual products, i.e. small (3.2 kb) and large (3.5 kb) *CaALS3* alleles, were gel purified, and stored at -20 °C.

3.2.1.3. Isolation of plasmids

Escherichia coli cells harbouring plasmids were grown as described in Chapter 2. After washing cells in 1X PBS, cells were lysed and plasmids were extracted using the Wizard Plasmid Extraction kit (Promega). Plasmid DNA was stored at -20 °C.

3.2.1.4. Digestion and ligation of DNA fragments

Purified *CaALS3* alleles, mixed *CaALS3* allele suspensions, and plasmid DNA were digested with *Sal*I and *Bgl*II restriction endonuclease enzymes in a 37 °C waterbath for 2 h. Digested DNA was purified using the Genelute PCR cleanup kit (Sigma). In the

case of digested pNIM plasmid DNA, the excised *GFP* and plasmid DNA backbone were separated by electrophoresis of the mixed digested DNA on 0.8 % (w/v) agarose and gel purifying each DNA fragment with the Wizard PCR and Gel Cleanup kit (Promega). Various ligation reactions were carried out using T4 DNA ligase (Promega) according to manufacturer's guidelines, briefly described in Chapter 2. Each digested *CaALS3* preparation was ligated to either pBluescript or CdpNIM DNA backbone. Digested *GFP* was also re-ligated to digested CdpNIM backbone as a proof of concept experiment. Ligation mixes were used directly in transformation reactions (Fig. 3.2).

3.2.1.5. Transformation of *E. coli* competent cells

Competent *E. coli* XL10 gold cells were prepared with CaCl₂ as described in Chapter 2. Each 30 µl ligation mixture was added to 200 µl of chilled competent cells, heat-shocked, chilled and allowed to recover in SOC medium for 2 h at 37 °C, 200 r.p.m. Cells transformed with pBluescript fragments were inoculated on L_{amp} plates containing IPTG and X-Gal. Competent cells transformed with pNIM fragments were inoculated on Lamp agar. Inoculated agar plates were incubated at 37 °C overnight.

3.2.1.6. Screening of putative transformants by PCR amplification

Antibiotic selection was used to assay uptake of pBluescript harbouring the ampicillin resistance gene. Blue-white screening was used to initially identify any colonies in which the wild type pBluescript plasmid was disrupted. The appearance of blue colonies indicated successful ligation of *CaALS3* to the multiple cloning site (MCS) of pBluescript. Blue colonies were subinoculated on fresh L_{amp} agar. Plasmid DNA was extracted from each putative transformant and digested with *Sal*I and *Bgl*II to investigate the enzymatic digestion pattern. Circular, undigested plasmid DNA was used as template in a PCR reaction to screen for the presence of *CaALS3*, using primers ALS3F1SALI and ALS3R1BGLII.

Cells transformed with pNIM ligation mixes were subinoculated onto fresh L_{amp} agar, plasmids were extracted and screened by both digestion and PCR in the same way as pBluescript.

3.2.2. PCR fusion and split marker cloning

3.2.2.1. Design of PCR fusion primers

Fusion primers were designed, based on the sequence of CapNIM and the *CaALS3* sequence, similar to primers previously used by Martin *et al.* to generate an *EED1* expression cassette (Martin *et al.*, 2011a).

3.2.2.2. PCR amplification of DNA fragments

The CdpNIM DNA sequence was divided into three fragments (Fig. 3.3). Fragment 1, containing *CdADH1*, *cartTA*, and *SAT1*, was PCR amplified from circular CdpNIM1 plasmid using primers CDPNIMF1 and either PNIMR1 for *CaALS3* or PNIMR3 for *CaHYR1*. Fragment 2, containing *pTet*, and *CdADH1*, was PCR amplified from CdpNIM1 using primers PNIMF2 and PNIMR2 for *CaALS3* or PNIMF2 and PNIMR4 for *CaHYR1*. Taking the place of *GFP* in pNIM, *CaALS3* was amplified either from SC5314 or the *CaALS3* long allele was amplified specifically from pALS3 (Dr. S. Filler, UCLA), using primers ALS3F2 and ALS3R2. This primer pair amplified the *CaALS3* gene with long oligonucleotide tails to allow both PCR fusion to fragment 2 and homologous recombination with fragment 1 during transformation of *C. dubliniensis*. The same method was used for amplification of CapNIM fragments, using circular CapNIM plasmid as PCR template, differing only in the amplification of fragment 1 using forward primer CAPNIMF1 instead of CDPNIMF1. The second gene of interest, *CaHYR1*, was amplified from SC5314 genomic DNA template using primers HYR1F2 and HYR1R2 with long oligonucleotide tails similar to the *CaALS3* method.

3.2.2.3. Two step fusion procedure

Fragment 2 was fused to each gene of interest (*CaALS3* or *CaHYR1*) by two-step PCR amplification. To avoid PCR errors, high fidelity polymerase was used in each stage of the process. The first stage was performed as a short reaction in the absence of primers, during which complementary oligonucleotide tails on each fragment were allowed to bind to each other similar to the annealing stage of a standard PCR reaction. The reaction conditions for this stage were 94 °C for 2 min, 15 cycles of 94 °C for 15 s, 56 °C for 30 s, 68 °C for 4 min, followed by final elongation at 68 °C for 7 min. The second phase of the fusion reaction was carried out in the presence of primers that would amplify the desired full-length product. This was done using 1 µl

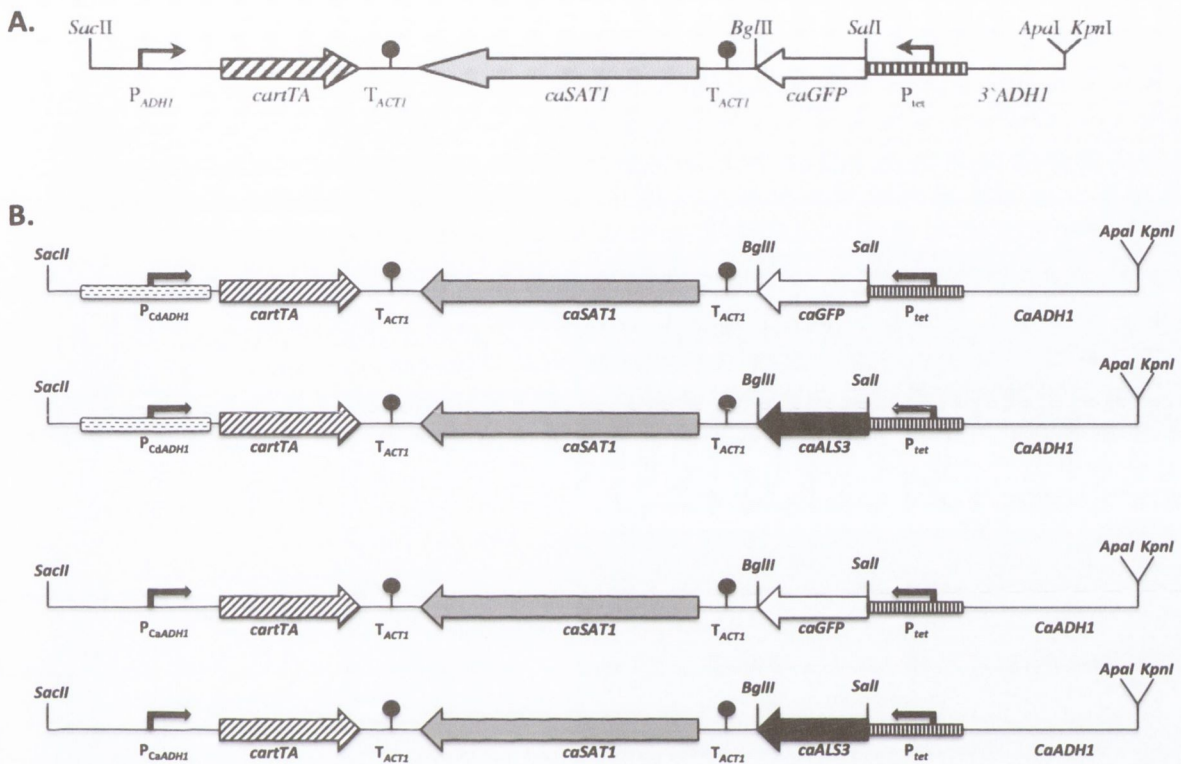


Figure 3.2. Molecular gene cloning using a doxycycline-inducible differential gene expression system. (A) Tetracycline-inducible expression system pNIM1 (CapNIM). (B) Derivatives of both CapNIM and CdpNIM for tetracycline-inducible expression of *CaALS3* or *GFP*. Restriction enzyme sites *Bgl*II and *Sal*I allow excision of *GFP* and insertion of a gene of choice (*CaALS3*/*CaHYR1*). Restriction enzyme sites *Sac*I and *Apa*I/*Kpn*I allow linearisation of the expression cassette from circular plasmid and integration into the *C. albicans* or *C. dubliniensis ADH1* locus. Schematic diagrams not to scale. Adapted from Park *et al.*, 2005.

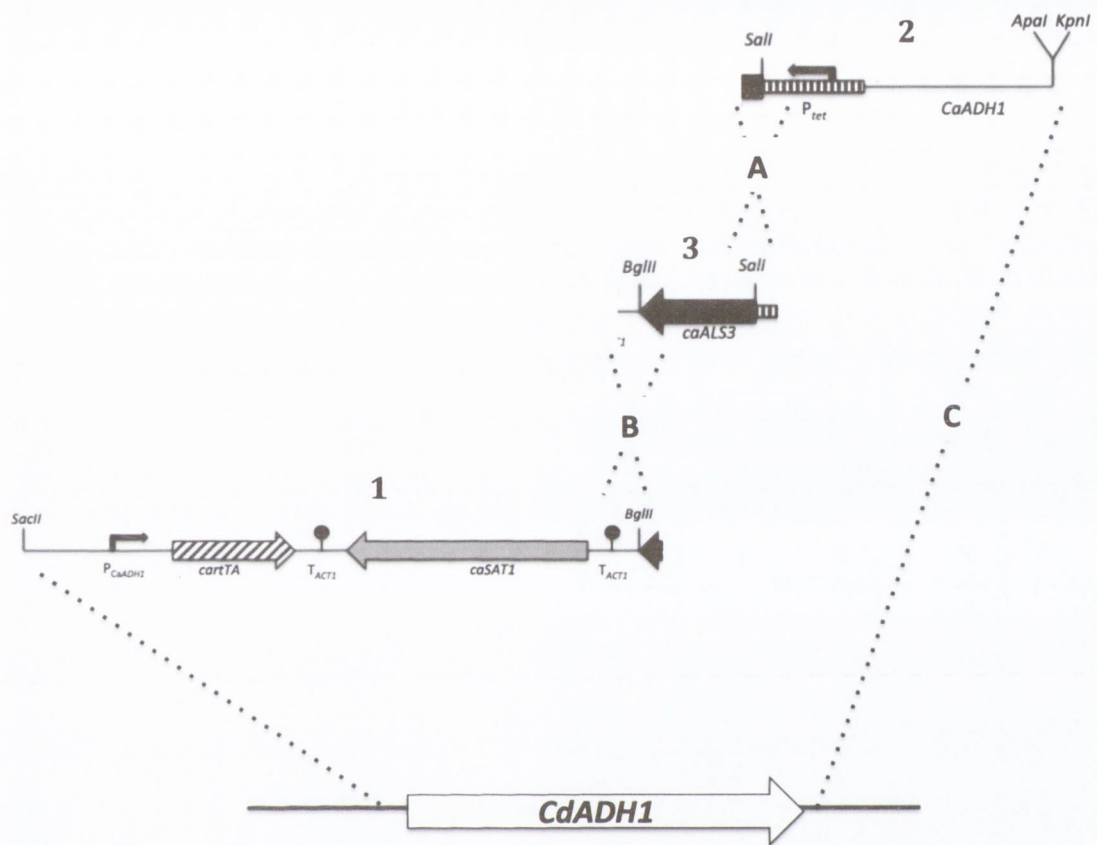


Figure 3.3. PCR fusion and split marker transformation cloning approach. Fragment 1 was composed of the downstream *ADH1* sequence, *cartTA* and *SAT1*. Fragment 2 contained $pTet$ and the upstream *ADH1* sequence. Fragment 3 contained the gene of interest, in this case *CaALS3*. (A) PCR fusion of *CaALS3* to $pTet$. (B) Homologous recombination event during transformation, joining *CaALS3/pTet* to the *cartTA/SAT1* fragment. (C) Directed integration of the inducible expression cassette into one of the *CdADH1* alleles.

of raw PCR product from the first-stage reaction as template for the second-stage reaction. The cycling conditions used for the second stage were 94 °C for 2 min, 10 cycles of 94 °C for 20 s, 56 °C for 30 s, 68 °C for 4 min, 20 cycles of 94 °C for 20 s, 56 °C for 30 s, 68 °C for 4 min increasing by 5 s per cycle, followed by final elongation at 68 °C for 7 min. The *CaALS3*/fragment 2 fusion product was amplified using primers PNIMF2 and ALS3R2. The *CaHYR1*/Fragment 2 fusion product was amplified with the primer pair PNIMF2 and HYR1R2. Where necessary, gel purified products were concentrated by evaporation of solvent in a Labconco Centrivap Concentrator (Labconco, Kansas City, Missouri, USA).

3.2.2.4. Split-marker transformation of *C. dubliniensis*

Electrocompetent WÜ284 cells were prepared as described in Chapter 2. Competent cells were chilled on ice. Purified pNIM fragment 1, containing the marker for antibiotic resistance, was combined with fused DNA, containing the gene of interest and tetracycline-responsive operator sequences, in 10 µl molecular biology grade water and chilled on ice. The mixed DNA solution was combined with 200 µl of electrocompetent WÜ284 and transferred to an electroporation cuvette. Directly after electroporation, 1 ml of warm YEPD broth was added to the cells. Broths were incubated at 30 °C, 200 r.p.m. for 3 h to allow for expression of antibiotic resistance from *SAT1*. After cell recovery, 100 µl from each broth was transferred to NAT₁₀₀ plates. The remaining broth was centrifuged and resuspended in 100 µl YEPD. This was also transferred to NAT₁₀₀ plates. Transformed *Candida* cells were incubated at 30 °C for four to five days.

3.2.2.5. Screening of putative transformants by PCR amplification

Nourseothricin-resistant WÜ284 colonies were subinoculated on fresh NAT₁₀₀ plates and incubated at 37 °C for two days. Genomic DNA was isolated from these colonies by growing them overnight in YEPD broth, disrupting the cells in a bead beater and extracting DNA by the phenol-chloroform method. For PCR, DNA concentration was adjusted to 100 ng/µl in molecular biology grade water. Screening of transformants was carried out by attempting to PCR amplify key DNA sequences. Screening was performed for the presence of *CaALS3* or *CaHYR1*, the junction at which heterologous recombination was determined to occur, and the presence of the transactivator *cartTA*. The *CaALS3* gene was amplified using primers ALS3F2 and ALS3R2. The

CaHYR1 gene was amplified using the primer pair HYR1F2 and HYR1R2. The recombination junction site was amplified using primers JUNCF1 and JUNCR1, and the *cartTA* reverse transactivator was amplified with primer pair CARTTAF1 and CARTTAR1 (Table 2.2).

3.2.3. Non-integrative plasmid transformation

Circular plasmid DNA was isolated from *E. coli* strains harbouring plasmids pADH1 and pALS3 as described in Chapter 2. A *URA3* deficient WÜ284 strain was maintained on YEPD agar supplemented with 100 µg/ml uridine (Staib *et al.*, 2001). Competent WÜ284 (*ura3Δ/ura3Δ*) cells were prepared and transformed by electroporation as outlined in Chapter 2. Transformants were allowed to recover in YEPD broth supplemented with 100 µg/ml uridine for 1 h at 37 °C and then transferred to YEPD agar lacking exogenous uridine and incubated at 30 °C for 7 days. Transformed cells were grown in YEPD broth overnight at 37 °C, 200 r.p.m. Cells were centrifuged and total DNA was extracted using a bead beater and phenol-chloroform extraction. Isolated DNA from putative transformants was screened by PCR for the presence of *CaALS3* using primers ALS3F1SALI and ALS3R1BGLII.

3.2.4. Constitutive gene expression cloning

3.2.4.1. Design of primers for *pENO.NAT* constitutive gene expression

Primer sequences for the promoter and antibiotic resistance module from *pENO.NAT* were designed based on primers used by Milne *et al.* to construct an expression plasmid (Milne *et al.*, 2011). Long oligonucleotide tails were added to these basic primer sequences, both to facilitate integration into the upstream sequence of *CdRPS1* (*CdRP10/Cd36_02890*), and to allow for recombination with a *CaALS3* fragment by fusion PCR. The *CaALS3* fragment was amplified using *ALS3* complementary oligonucleotide sequences for fusion PCR and integration into the downstream sequence of *CdRPS1*. Primer3Plus (<http://www.bioinformatics.nl/cgi-bin/primer3plus/primer3plus.cgi/>) was used in each case to optimise the primer sequences against the possibility of dimer formation or secondary structures forming during PCR.

3.2.4.2. DNA amplification and transformation of *C. dubliniensis*

Plasmid DNA was extracted from *E. coli* harbouring pENO.NAT (Milne *et al.*, 2011). The antibiotic resistance and enolase promoter sequence (pENO.NAT) was amplified from circular plasmid DNA using primers RPS1NAT1F1 and RPS1NAT1R1. *CaALS3* was amplified from pALS3 using primers ENO1ALS3F1 and ENO1ALS3R1. PCR products were purified with the Genelute PCR Cleanup kit (Sigma). Both DNA fragments were combined in a two-step PCR fusion reaction similar to the approach used for pNIM fusion constructs. Primers RPS1F1 and RPS1R1 were used for the second stage amplification reaction (Fig. 3.4).

Transformation of electrocompetent WÜ284 was conducted similar to the method described in section 3.2.2.4. In this case, the single fusion product, pENO.ALS3, was used to transform WÜ284. A variety of DNA concentrations were used during electroporation. Cells were allowed to recover in YEPD broth at 30 °C for 3 h. Recovered cells were inoculated on NAT₁₀₀ plates and incubated at 30 °C for four to five days.

3.2.5. Southern blot analysis of putative transformants

3.2.5.1. PCR amplification of DIG-labelled probe

In order to detect both the wild type *CdADH1* allele, and the allele into which constructs would integrate, a *CdADH1*-specific probe was generated for Southern blotting. A restriction endonuclease fragment map was predicted using NEBCutter (<http://tools.neb.com/NEBcutter2/>) for DNA flanking the *CdADH1* locus after digestion with either restriction enzymes *EcoRI* or *BglII*. A probe for *CdADH1* was targeted to a fragment which would generate different digestion patterns based on the presence or absence of a pNIM cassette. The *CdADH1* probe was amplified with primer pair CDADH1F1 and CDADH1R1 in a PCR reaction using GoTaq[®] polymerase and DIG-labelled dNTPs. The reaction cycling conditions were 94 °C for 1 min, 30 cycles of 94 °C for 30 s, 56 °C for 30 s, 72 °C for 2 min, followed by elongation at 72 °C for 10 min. DIG-labelled probe was stored at -20 °C.

3.2.5.2. Preparation of template DNA

As cell disruption using a bead beater sheared DNA to a significant degree (data not shown), a more sensitive method for isolation of chromosomal DNA was used to extract DNA for Southern Blotting. Chromosomal DNA was extracted, digested and transferred to a positively charged membrane according to the method described in Chapter 2.

3.2.5.3. Southern blot analysis

Southern blotting was carried out according the manufacturer's recommendations for DIG Easy-hyb granules (Roche). The *CdADH1* DIG-labelled probe was hybridised to the membrane, which was then washed, blocked, and treated with anti-digoxigenin-AP Fab fragments to bind membrane bound DIG-labelled probe. Chemiluminescent substrate was added and Biomax light film (Kodak) was used to visualise the DIG-labelled restriction endonuclease fragment pattern. Membranes were stored between blotting paper in a sealed plastic bag at 4 °C.

3.2.6. Analysis of gene expression by qRT-PCR

3.2.6.1. Induction of gene expression with doxycycline

Verified WÜ284.CaALS3 transformants were incubated on YEPD plates at 37 °C for 48 h. Single colonies were inoculated into YEPD broths containing 20 µg/ml (DOX₂₀), 50 µg/ml (DOX₅₀) or 100 µg/ml (DOX₁₀₀) of doxycycline hyclate. Doxycycline broths were incubated at 37 °C, 200 r.p.m. overnight. After 16 h 5 µl from each overnight culture was subinoculated in fresh DOX broths and grown overnight at 37 °C, 200 r.p.m. DOX broths were centrifuged at 16,000 *x g* for 3 min and washed in 1X PBS. The supernatant was removed and cells were either used directly for RNA isolation or snap-frozen under liquid nitrogen and stored at -20 °C.

3.2.6.2. Isolation of RNA and preparation of cDNA

RNA was isolated from cells using a combination of mechanical disruption with a bead beater and extraction of RNA with the Qiagen RNeasy kit (Qiagen) as outlined in Chapter 2. cDNA was generated from 1 µg of DNase-treated RNA with Superscript Reverse Transcriptase II according to manufacturer's instructions. cDNA was stored at -20 °C.

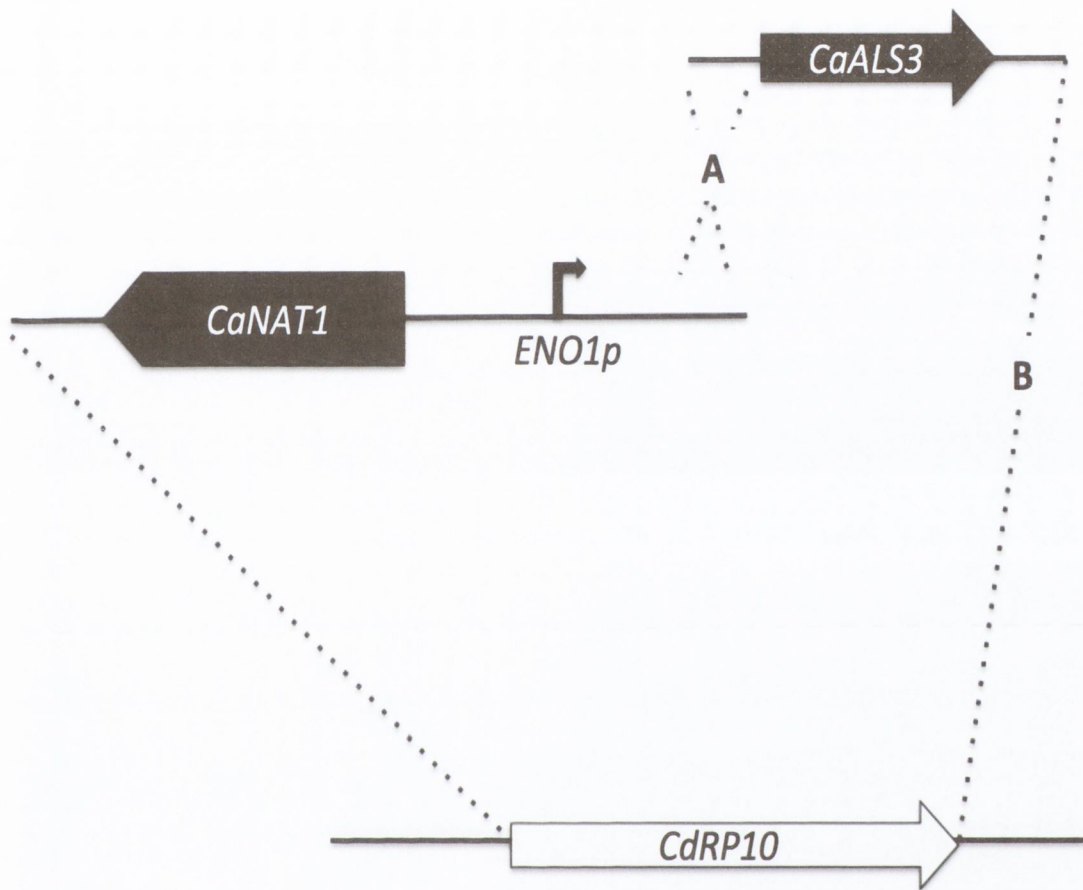


Figure 3.4. Constitutive gene expression approach. Expression cassette for pENO.NAT-controlled constitutive expression of *CaALS3* in *C. dubliniensis*. (A) PCR fusion of *CaALS3* fragment to the enolase promoter fragment. (B) Directed integration into the *C. dubliniensis* *CdRPS1* (*CdRP10*) locus.

3.2.6.3. Analysis of gene expression by qRT-PCR

Doxycycline-induced gene expression was analysed by qRT-PCR conducted on cDNA. All qRT-PCR experiments were run on an Applied Biosystems 7500 Real-Time PCR system. Fast SYBR Green (Applied Biosystems) was used in 15 µl reaction volumes with 0.5 µl (100 ng) of cDNA template and 0.75 µl of each primer. Primers used for qRT-PCR analysis can be found in Table 2.2. The housekeeping gene, *ACT1* (Cd36_12690), was used as an internal endogenous control for each reaction. The C_t value of each individual reaction was defined as the cycle number at which fluorescence of the SYBR green dye crossed a calculated threshold. This allowed calculation of average C_t values and comparison of $2^{-\Delta\Delta C_t}$ values according to the method described by Schmittgen and Livak (Schmittgen & Livak, 2008).

3.2.7. Comparison of CdpNIM and CapNIM doxycycline-inducible gene expression systems

3.2.7.1. The impact of growth condition on gene expression

The strength of doxycycline-inducible gene expression was assessed by comparing production of fluorescent protein from a WÜ284 strain harbouring the CdpNIM.GFP cassette with a SC5314 strain harbouring the CapNIM.GFP cassette. Strains were initially grown on YEPD agar at 37 °C for 48 h. Single colonies were subinoculated into DOX₂₀ or DOX₅₀ broths and incubated at either 30 °C or 37 °C in an orbital incubator overnight. After 16 h, broths were centrifuged at 16,000 $\times g$ for 3 min and washed in 1X PBS. Cells were resuspended in sterile distilled water to a standard optical density (OD₆₀₀ 2.0).

3.2.7.2. Investigation and quantification of inducible gene expression

PBS-washed doxycycline-induced cells were directly observed under GFP filter fluorescence microscopy using a Nikon Eclipse E600 epifluorescence microscope equipped with a high power mercury lamp (Nikon) and an Endow GFP Bandpass Emission filter combination (Nikon).

Serial dilutions of PBS-washed doxycycline-induced cells were prepared in 96 well plates. GFP fluorescent intensity was measured using a Tecan plate reader with

485/535 nm filters. Statistical analysis was carried out using Prism statistical software (Prism 5 for MacOSX, V5.0).

3.2.8. Immunofluorescent detection of *CaAls3p*

Immunodetection of *CaAls3p* with monoclonal antibody (mAb) was kindly carried out by personnel in the laboratory of Dr. S. Filler, UCLA, according to flow cytometry methods described previously using a polyclonal antibody raised against a purified recombinant N-terminal domain fragment of *CaAls3p* (rAls3p) (Phan *et al.*, 2007).

3.2.9. Adherence of WÜ284.CaALS3 to human buccal epithelial cells (BECs)

Fungal strains from 48 h YEPD agar plates were grown overnight in YEPD broth supplemented with DOX₅₀ or DOX₁₀₀ at 37 °C, 200 r.p.m. Cells were centrifuged at 16,000 $\times g$ for 1 min, washed in 1X PBS and resuspended to a final density of 1×10^7 cells/ml. Human buccal epithelial cells were isolated from fresh cheek swabs supplied by multiple volunteers. Cell samples were pooled in 20 ml 1X PBS, centrifuged at 2,000 $\times g$ for 5 min, washed with 1X PBS and resuspended to 2×10^5 cells/ml. Yeast and BECs were combined at a ratio of 50 yeast to a single BEC. The cells were incubated at 37 °C, 200 r.p.m. for 2 h. After coincubation the cells were transferred to a 10 ml syringe barrel containing a 12 μ m pore filter (Millipore) prewashed with 1X PBS. The cell suspension was allowed to pass through the filter under the force of gravity. The filter was washed by passing through 20 ml 1X PBS. The filter was removed, stained with calcofluor white, mounted on a glass slide and visualised by microscopy under an ultraviolet filter. At least 100 human BECs were counted and the number of adherent yeast cells were recorded in each case.

3.2.10. Survival of WÜ284.CaHYR1 against human neutrophil response

Human polymorphonuclear (PMN) cells were isolated and prepared according to the method used by Sheth *et al.* previously (Sheth *et al.*, 2011). Cells were counted and resuspended in pre-warmed RPMI-1640. Fungal cells from 48 h YEPD agar plates were grown overnight in either YEPD broth or YEPD broth supplemented with DOX₅₀ at 30 °C with agitation. The following day, fresh broths were inoculated to a density of 0.2 OD₆₀₀, and grown at 30 °C until the culture reached a density of 0.6 - 0.8 OD₆₀₀. Fungal cells were washed in 1X PBS and resuspended in RPMI-1640. Fungal cells were added to human PMNs in a ratio of 10:1 in 2 ml tubes and incubated for 2 h at

37 °C under 5 % (v/v) CO₂. An equal aliquot of fungal cells was transferred to YEPD agar in triplicate and incubated at 30 °C overnight. PMN cells in coculture with fungal cells were lysed by addition of 100 µl 0.25 % (w/v) SDS at 30 °C for 10 min. The cultures were mixed with ice cold water (900 µl) and incubated with 50 U DNaseI in 100 µl 10X PBS for 15 min at 30 °C. A 50 µl aliquot of each culture at a 1:10 dilution in water was transferred to a YEPD agar plate and incubated at 30 °C overnight. Fungal colony forming units (cfu) on YEPD plates were counted and expressed as a percentage of the initial inoculum i.e. % survival.

3.3. Results

3.3.1. Restriction endonuclease-mediated cloning of *CaALS3*

In order to express the *CaALS3* gene in a *C. dubliniensis* background, restriction enzyme digestion of expression plasmids, ligation of *CaALS3* to the plasmid, and subsequent transformation of *C. dubliniensis* WÜ284 with the linearised plasmid was used for chromosomal integration and stable, inducible gene expression (Fig. 3.3).

As allelic variation of *ALS3* is postulated to influence virulence, with the large allele more strongly associated with pathogenesis, both *ALS3* alleles were investigated (Oh *et al.*, 2005). Small and large alleles of *CaALS3* amplified from *C. albicans* SC5314 yielded DNA fragments of approximately 3.2 kb and 3.5 kb respectively, reflecting the known variability of the tandem repeats corresponding to the linker region of the protein. Treatment of the purified PCR-amplified products with restriction endonuclease enzymes *Bgl*II and *Sal*I created overhangs to facilitate ligation to similarly treated plasmid. Digestion of plasmid CdpNIM1 with *Bgl*II and *Sal*I, and gel purification, resulted in isolation of the plasmid backbone from a 700 bp *GFP* DNA fragment. Ligation of the digested *CaALS3* fragments, in molecular weight-adjusted ratios of 1:1, 1:3, and 1:10, to 200 ng of the vector backbone, and transformation of *E. coli* XL10-gold yielded only two transformant colonies growing on L_{amp} agar plates. Screening of isolated plasmids from these transformants by PCR yielded negative results for the presence of *CaALS3*. Similarly, digestion of the transformant plasmids with *Bgl*II and *Sal*I yielded only DNA bands corresponding to the plasmid backbone and *GFP*. This ligation and transformation reaction was repeated on more than 3 separate occasions without success. The CdpNIM plasmid also contained pBluescript sequences for propagation in *E. coli*, resulting in a linear backbone size of almost 9.5 kb. In an attempt to avoid ligation inefficiencies related to the size of the plasmid backbone, and aid plasmid propagation, *CaALS3* was also ligated to the MCS of pBluescript (3 kb). Digestion of pBluescript with *Sal*I linearised the plasmid created one “sticky” overhang for ligation. A *Bgl*II cleavage site is not present in the pBluescript MCS. Thus, ligation was carried out as a combination of blunt end and overhang ligation. DNA ligation, transformation of *E. coli* XL10 gold, and screening of transformant colonies by blue-white screen yielded three transformants after second generation growth on blue-white screening plates. Initial screening by PCR of

plasmids isolated from transformants suggested weak amplification of *CaALS3* from one of the transformants. However, screening of the plasmid by digestion pattern was inconclusive as a result of the small size difference between linear pBluescript (3.0 kb) and *CaALS3* (3.2 kb and 3.5 kb). The ligations and transformation reactions were repeated on several occasions. Although transformants were isolated by blue-white screening, subsequent PCR screening of plasmids for the presence of *CaALS3* yielded weak amplimers of incorrect size. Complementary screening of transformants by digestion with *Sall* and *BglII* also yielded unexpected results. Instead of isolation of two bands corresponding to linear pBluescript and *CaALS3*, only one DNA fragment of 3.0 kb length was observed. This result was uniform for all isolated transformants. Despite many ligation and transformation attempts, it appeared impossible to successfully clone *CaALS3* into CdpNIM1 as no CdpNIM.*CaALS3* plasmids could be retrieved from transformed *E. coli* XL10.

3.3.2. PCR fusion and transformation of WÜ284 with *CaALS3*

In vitro assembly of a CdpNIM.*CaALS3* cassette was achieved by a PCR fusion strategy similar to that used by Martin *et al.* (Martin *et al.*, 2011a). Primers incorporating long oligonucleotide tails were used to amplify *CaALS3* and facilitate both fusion of PCR products and homologous recombination during transformation (Fig. 3.4). Although highly specific primer pairs were used to amplify the respective fragments of CdpNIM, gel purification was necessary due to the high level of secondary primer binding. Fusion of *CaALS3* with the *pTet* fragment from CdpNIM in a two step PCR fusion reaction resulted in a 4.9 kb fragment which was then combined with the reverse transactivator fragment, *cartTA* (4.5 kb), containing the dominant selectable marker *SAT1*. These fragments were used to transform *C. dubliniensis* WÜ284 by electroporation. Over the course of multiple transformation attempts a variety of DNA concentrations were used. Transformation efficiency was low, requiring high concentrations of DNA for transformation (0.5 µg – 10 µg). For example, using a total of 2 µg of transforming DNA by electroporation yielded approximately 10 to 20 colonies when grown on nourseothricin agar. Transformants yielding the expected PCR amplimer patterns were identified by PCR screening of isolated genomic DNA for *CaALS3*, the *cartTA* transactivator, and by amplifying across the internal CdpNIM recombination junction integral to the split marker-transformation strategy. Integration efficiency of *CaALS3* into the *C. dubliniensis* genome was approximately 30

%, while further screening to ensure the presence of the *cartTA* reduced this percentage for integration of the entire CdpNIM.CaALS3 cassette. This is exemplified by a single transformation event using 2 µg total DNA which yielded a total of 18 colonies on NAT₁₀₀. Screening of the 18 transformants displayed 12 positive for the *cartTA* transactivator, 6 positive for *CaALS3* and only four positive for recombination of the split fragments to yield the full length cassette.

3.3.2.1. Analysis of *CaALS3* gene expression in WÜ284 transformed with CdpNIM.CaALS3

Transformants containing CdpNIM.CaALS3 were assayed for doxycycline-inducible gene expression by qRT-PCR. When treated with DOX₂₀ transformants showed an increase in gene expression ranging between 4-fold and 15-fold upregulation (data not shown). However, comparison of transcript abundance relative to the highly-expressed endogenous control *ACT1* showed a maximum *CaALS3* abundance of 0.09 when treated with DOX₂₀ relative to *ACT1*. As *CaALS3* is a highly expressed cell surface protein, this low level of expression was determined to be unacceptably low.

3.3.2.2. Comparative analysis of CdpNIM and CapNIM doxycycline-inducible gene expression

Comparison of the CdpNIM.GFP cassette, integrated in *C. dubliniensis* WÜ284, with the CapNIM.GFP cassette integrated in *C. albicans* SC5314 displayed significant differences in green fluorescent protein expression (Fig. 3.5). Both visual microscopy, using a fluorescent filter, and measurement of fluorescent intensity at 505 nm, confirmed that doxycycline induced expression from the CdpNIM was much weaker than that of its *C. albicans* counterpart. As a ratio of fluorescent intensity units, CdpNIM expressed less than 2 % of the amount of fluorescent protein as CapNIM when cells were grown at 30 °C in the presence of DOX₂₀. At 37 °C, this ratio increased to only 13.4 % fluorescent protein abundance from CdpNIM relative to CapNIM. In this way, protein abundance not only differs between the expression systems but the degree of variation is also dependent on temperature. As the only difference between the CdpNIM cassette and the parent CapNIM cassette is the *ADH1* promoter, this suggests a previously unknown difference in the basal expression level of *ADH1* between the two *Candida* species. As the *ADH1* promoter in both pNIM cassettes is responsible for driving transcription of the reverse tetracycline transactivator *cartTA*,

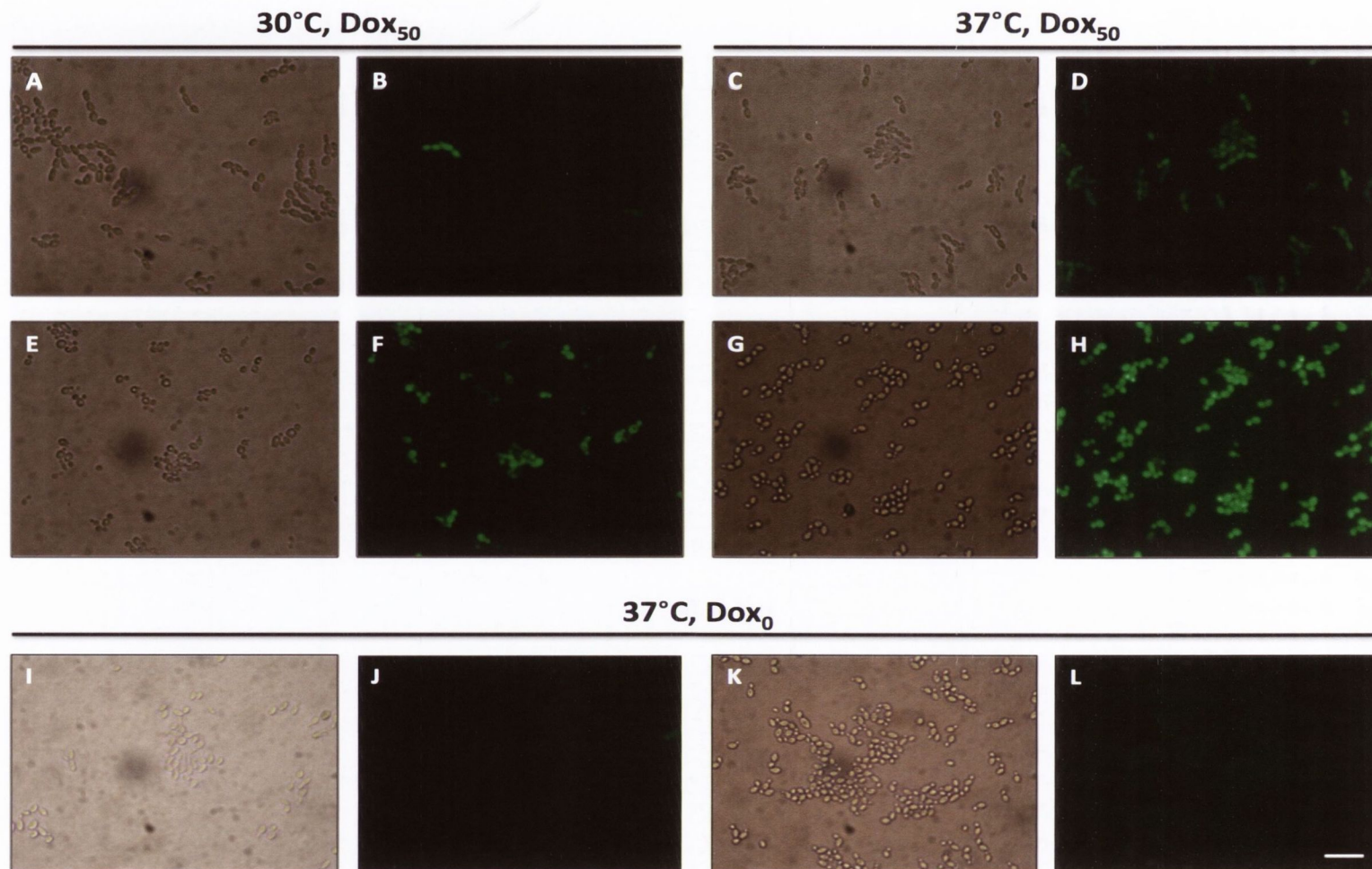


Figure 3.5. Comparison of doxycycline-inducible gene expression systems. Variation of green fluorescent protein was dependent on both temperature and gene expression system. Cells treated with doxycycline and washed with phosphate buffered saline were visualised by light microscopy and fluorescent microscopy to highlight the difference between GFP generation using two different gene expression systems. Panels (A)-(D) WÜ284.CdpNIM (E)-(H) SC5314.CapNIM. Panels (I)-(J) show WÜ284.CdpNIM and (K)-(L) SC5314.CapNIM not treated with doxycycline. Scale bar represents 10 μ m.

it is likely that the difference in gene expression in response to doxycycline is, in the case of CdpNIM, negatively impacted by the relative lack of abundance of the transactivator protein resulting in the reduced dissociation of repressor from the tetO operator sequences. As *CaALS3* and *CaHYR1* are both documented as highly expressed GPI-anchored proteins on the surface of *C. albicans* hyphae CdpNIM was deemed insufficient for the requirements of this study. Thus, attempts were refocused on using CapNIM as the doxycycline-inducible expression system in *C. dubliniensis* WÜ284. An identical PCR fusion and split marker transformation strategy was used for *CaALS3*, with the CapNIM *cartTA* fragment amplified from CapNIM plasmid. Integration efficiency into the *CdADH1* locus was low necessitating high concentrations of transforming DNA. As a representation of cloning efficiency, one split marker transformation of WÜ284 with CapNIM.CaALS3 yielded 9 transformants growing on nourseothricin agar after electroporation and recovery in YEPD broth. PCR screening for the presence of *CaALS3* showed five positive transformants. When screening for the *cartTA* region, only two were positive, although these transformants were also positive for the recombination junction of the two transforming DNA fragments.

3.3.2.3. Analysis of *CaALS3* gene expression in WÜ284 transformed with CapNIM.CaALS3

Analysis of doxycycline-induced *CaALS3* RNA expression by qRT-PCR showed higher levels of *CaALS3* expression in the CapNIM constructs compared to the CdpNIM constructs (data not shown). One CapNIM.CaALS3 transformant expressed *CaALS3* at 4.8 times the expression of *ACT1* as measured by comparative C_t values. Conversely, the other transformant expressed 0.4 times the amount of *CaALS3* RNA as *ACT1* RNA transcript when treated with DOX₂₀.

3.3.2.4. Confirmation of chromosomal integration of CapNIM.CaALS3

Correct integration of CapNIM.CaALS3 (WÜ284.ALS3) into the *CdADH1* locus of the transformant with the highest *CaALS3* RNA expression was confirmed by Southern blot analysis (Fig. 3.6a). Probing *EcoRI*-digested DNA, generated from high quality chromosomal DNA with a 370 bp *CdADH1* probe, detected a single visible DNA fragment of 3.5 kb for homozygous *CdADH1*. Two visible DNA fragments were detected for *C. dubliniensis* strains with heterozygosity at the *CdADH1* locus. The

positive control *C. dubliniensis* strain containing CdpNIM.GFP displayed the native *CdADH1* band and a 10.5 kb band corresponding to the DNA fragment containing the *GFP* expression cassette. The WÜ284.ALS3 transformant identified as expressing high levels of *CaALS3* as part of the CapNIM cassette also displayed two bands when the *CdADH1* locus was probed. In addition to the native *CdADH1* digested fragment, a 13.3 kb DNA fragment was observed, confirming the presence of the CapNIM.CaALS3 cassette integrated into the *CdADH1* locus.

3.3.2.5. Phenotypic analysis of WÜ284 cells expressing *CaALS3*

Induction of *CaALS3* expression by treatment with doxycycline increased adhesion of *C. dubliniensis* yeast to human buccal epithelial cells in a dosage dependent manner (Fig. 3.7). Results were expressed as the number of fungal cells bound to a total of 100 human BECs after washing away non-adherent fungal cells. Although treatment with doxycycline triggered a large increase in the binding of cells expressing *CaALS3* to human BECs, there was also an increase in the number of wild type WÜ284 cells binding to the BECs. Visualisation of adherent *C. dubliniensis* cells suggested a higher probability of binding of self-aggregated fungal cells to the human BECs.

3.3.2.6. Detection of *CaAls3p* on the cell surface of *C. dubliniensis*

Immunodetection of *CaAls3p* protein generated by doxycycline-inducible gene expression was kindly carried out by the laboratory of Dr. S. Filler, UCLA, using flow cytometry methods in conjunction with a polyclonal antibody raised against the N-terminal domain of recombinant *Als3p* (Phan *et al.*, 2007). Although treatment of the selected strain with DOX₅₀ or DOX₁₀₀ enabled detection of *CaAls3p* on the cell surface, the amount of protein detected, relative to WÜ284 wild-type was very low, and barely detectable in comparison to *C. albicans* SC5314 wild-type *CaAls3p* levels in hyphae (Fig. 3.8).

3.3.3. Restriction endonuclease-mediated cloning of *CaHYR1*

The *CaHYR1* gene was amplified from SC5314 genomic DNA with *Bgl*III and *Sal*I cleavage sites similar to the approach used for *CaALS3*, yielding a DNA fragment of approximately 2.8 kb. Purified *CaHYR1* DNA was digested and ligated to linearised CdpNIM. From a reaction of insert to vector ratio of 1:1 and 1:3, a total of 7 transformants were retrieved after transformation of *E. coli* XL10-gold and growth on

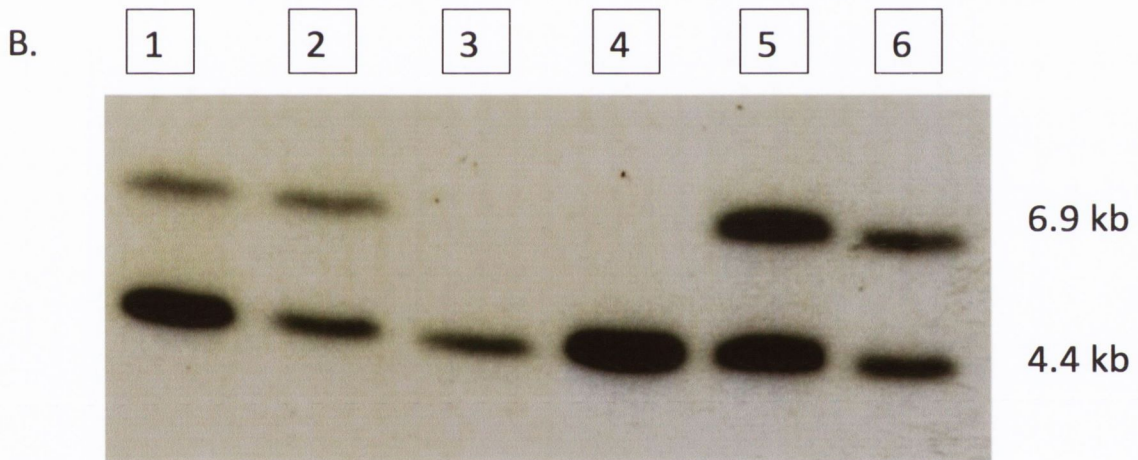
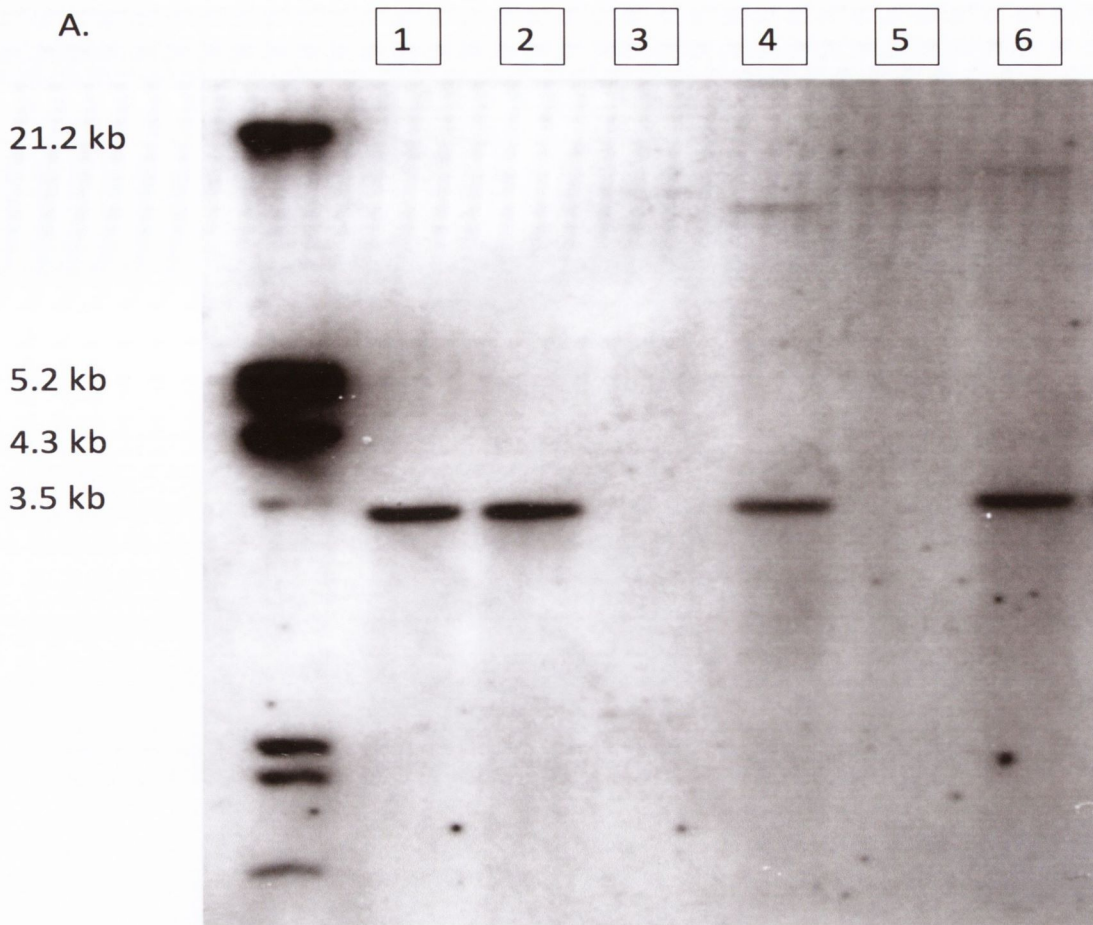


Figure 3.6. Southern blot analysis showing chromosomal integration of gene expression cassettes. (A) *EcoRI*-digested DNA probed with a DIG-labelled *CdADH1* probe. The molecular weight ladder used was DIG Molecular Weight Marker II. Native *CdADH1* locus was visualised as a 3.5 kb band. The lane order is 1. WÜ284 2. CD36 3. SC5314 4. WÜ284.CdpNIM 5. SC5314.CapNIM 6. WÜ284.CaALS3. (B) *HindIII*-digested DNA probed with DIG-labelled *CdADH1* probe. Native *CdADH1* was observed as a 4.4 kb band. Loci disrupted by pNIM-derivatives displayed a secondary, larger band (6.9 kb). Lane order is 1. WÜ284.CaHYR1a 2. WÜ284.CaHYR1b 3. WÜ284 4. CD36 5. WÜ284.CdpNIM 6. WÜ284.CaALS3.

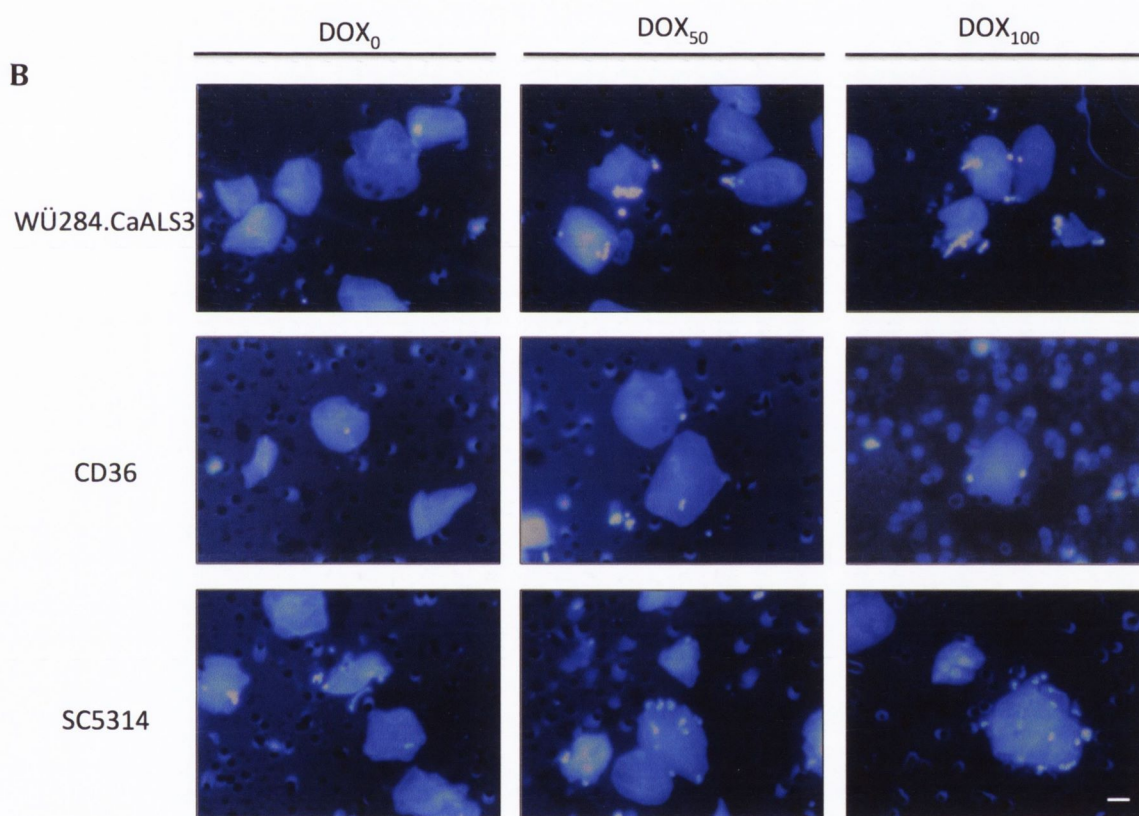
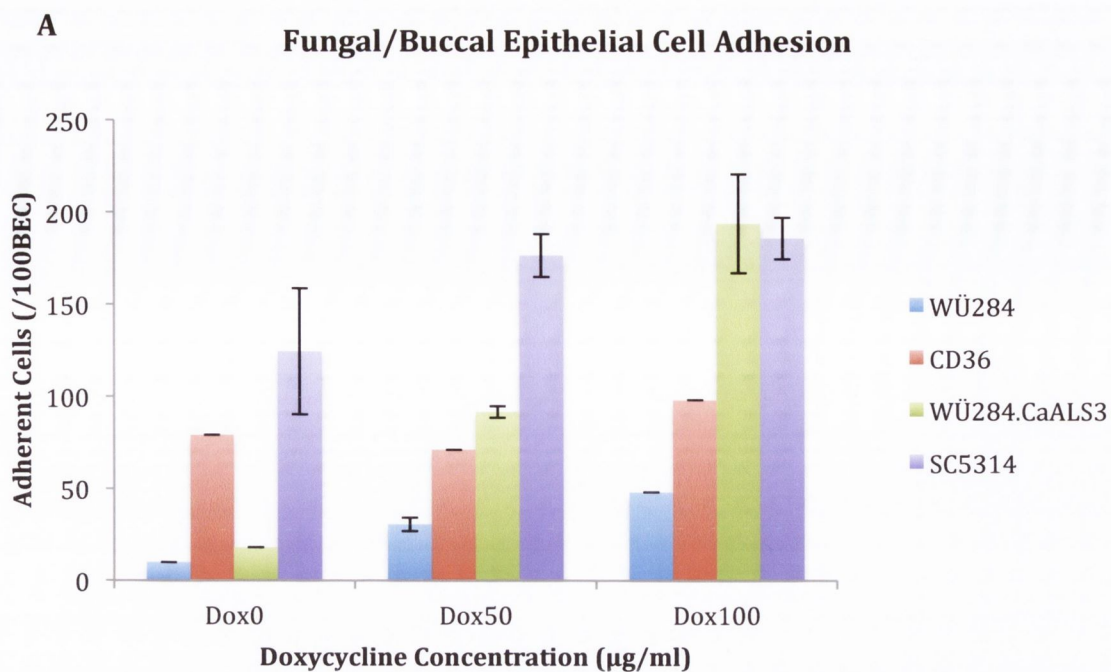


Figure 3.7. Phenotypic analysis of *C. dubliniensis* induced to express *CaALS3*.

(A) Inducible over-expression of *CaALS3* in *C. dubliniensis* WÜ284 resulted in a dosage dependent increase in adhesion to human buccal epithelial cells. Data was collected from three biological replicates. (B) Visualisation of fungal cells adhering to human BECs. Induction of *CaALS3* expression in a *C. dubliniensis* background increased adherence of WÜ284 yeast to human epithelial cells. Scale bar represents 10 µm.

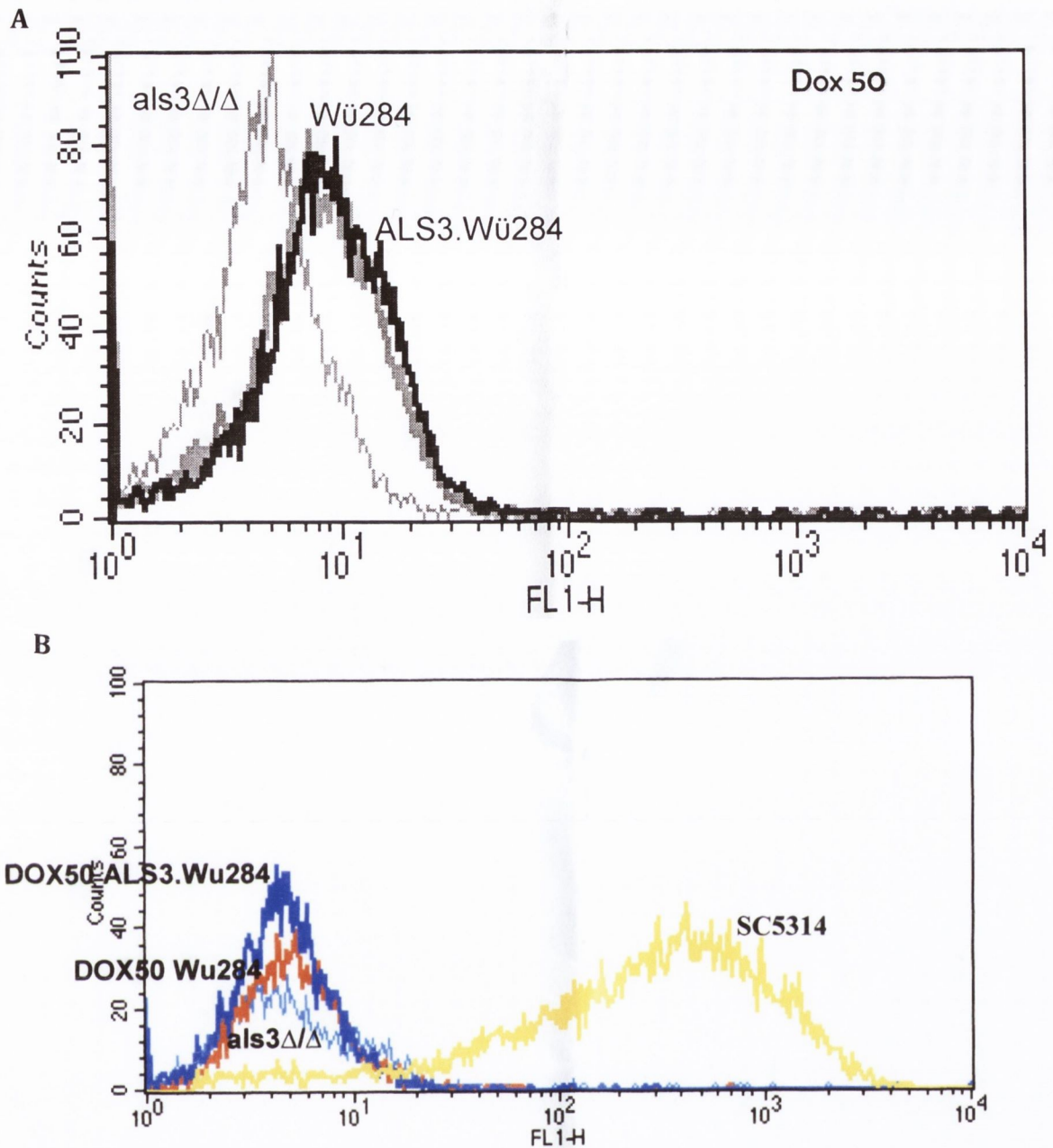


Figure 3.8. Immunofluorescent detection of *CaAls3p* on the surface of *Candida* cells. Immunodetection of *CaAls3p* on the surface of DOX₅₀-treated (A) *Candida dubliniensis* WÜ284.CaALS3 showing a small increase in *CaAls3p* levels relative to wild type WÜ284, signified by a nominal increase in fluorescent intensity (FL1-H). Both *C. dubliniensis* samples show an increase in background fluorescence relative to a *C. albicans* SC5314 *als3Δ/als3Δ* derivative. (B) *CaAls3p* produced by WÜ284.CaALS3 was observed to be much lower than native *CaAls3p* abundance on SC5314 hyphae which demonstrated high levels of fluorescent intensity due to abundant binding of antibody to *CaAls3p*.

L_{amp} agar. Screening of transformant plasmids by enzymatic digestion did not result in any positive transformants.

While a proof of concept ligation and transformation experiment replacing gel-purified *GFP* in the CdpNIM plasmid readily yielded correct transformants, neither *CaALS3* nor *CaHYR1* plasmids could be retrieved by restriction enzyme-mediated cloning in *E. coli*. As a consequence, an alternative cloning method was investigated.

3.3.4. PCR fusion-mediated cloning of *CaHYR1*

The split marker method with CapNIM as the expression system was also used to create *C. dubliniensis* strains expressing *CaHYR1*. The CapNIM fragment containing the *cartTA* transactivator with oligonucleotide tails complementary to *CaHYR1* was PCR amplified from CapNIM circular plasmid. The gel purified fragment was combined with the *CaHYR1* fusion fragment in a split marker transformation of WÜ284 and transformants were retrieved on nourseothricin agar. A total of six CapNIM.CaHYR1 *C. dubliniensis* transformants were determined to be correct by PCR screening for the *CaHYR1* gene, the *cartTA* transactivator, and the recombination junction.

3.3.4.1. Analysis of *CaHYR1* gene expression in WÜ284 transformed with CapNIM.CaHYR1

Analysis of *CaHYR1* gene expression indicated two of the transformants displayed doxyxycycline-inducible gene expression when treated with DOX₂₀. Under matching conditions, both of the identified transformants expressed levels of *CaHYR1* RNA approximately equal (1.0) to that of the highly expressed *ACT1* by the comparative C_t method (data not shown). This level of transcript abundance when treated with DOX₂₀ was determined to be sufficient for analysis to continue.

3.3.4.2. Confirmation of chromosomal integration of CapNIM.CaHYR1

Correct integration of the CapNIM.CaHYR1 cassette into the WÜ284 *CdADH1* locus was confirmed by Southern blot analysis (Fig. 3.6b). High quality chromosomal DNA was extracted and digested with *Bgl*III in contrast to the digestion pattern obtained for investigating CapNIM.CaALS3 constructs. However, an identical *CdADH1* probe was used to investigate CapNIM.CaHYR1 constructs. This digestion pattern yielded a wild type *CdADH1* locus fragment of 4.4 kb, while an allele containing CapNIM cassettes

also yielded a 6.9 kb fragment, confirming the correct integration of the cassette into the *C. dubliniensis* genome.

3.3.4.3. Phenotypic analysis of WÜ284 cells expressing CaHYR1

Currently the only experimental phenotype associated with *CaHYR1* functionality is increased survival against human PMN cells. Thus the *in vitro* survival of the CapNIM.CaHYR1 *C. dubliniensis* mutant strain during coincubation with human neutrophils was investigated. However, results from four individual neutrophil donors did not show any significant reproducible difference between survival of the *CaHYR1*-expressing mutant strain, induced with DOX₅₀, and the wild-type parent strain WÜ284 (data not shown).

3.3.5. Constitutive gene expression system using pENO.NAT

As both *C. dubliniensis* and *C. albicans* pNIM doxycycline-inducible expression systems are targeted to integrate into the *ADH1* locus, an alternative integration locus was investigated. The *CdRPS1* (*CdRP10/Cd36_02890*) locus was chosen as it has previously been used successfully in other *Candida* gene expression studies (Stokes *et al.*, 2007). A fusion PCR method was used to create a simple constitutive expression cassette containing the *NAT1* nourseothricin resistance marker, and *CaALS3* under the control of the powerful *CaENO1* promoter (Fig. 3.4). The cassette was designed with flanking *CdRPS1* sequences for directed integration into the *CdRPS1* locus. Although the approximately 6.0 kb expression cassette was assembled successfully by fusion PCR, transformation of *C. dubliniensis* WÜ284 was unsuccessful and no transformant colonies were obtained.

3.3.6. Non-integrative gene expression system using pADH1

Although a number of problems are presented by using *URA3* as a selective marker in homozygous *ura3Δ/ura3Δ* null strains an approach using the plasmid pALS3 and its parent plasmid pADH1 was attempted to express *CaALS3* ectopically in a *C. dubliniensis* strain. Transformation of a *ura3Δ/ura3Δ* WÜ284 strain with pALS3 by electroporation yielded only four transformant colonies. Three of these colonies grew weakly after patching the transformants onto fresh minimal media lacking uridine. Plasmid isolation from the three colonies, and PCR screening for the presence of *CaALS3* confirmed existence of the plasmid within the *C. dubliniensis* transformants.

However, these colonies continued to grow extremely poorly when transferred to fresh minimal media for single colony purification. After only a couple of generations the transformants failed to grow at all on minimal media lacking uridine suggesting rapid loss of the pALS3 plasmid. This is consistent with loss of the plasmid in other *Candida* species (personal communication, Dr. S. Filler, UCLA). Therefore, no stable *C. dubliniensis* strains containing plasmid pALS3 could be maintained successfully.

3.4. Discussion

This part of the study attempted to express the *C. albicans* virulence associated genes *CaALS3* and *CaHYR1* in a relatively non-virulent *Candida* background capable of filamentation (*C. dubliniensis*), albeit at a much lower level. Although *C. dubliniensis* mutants were recovered, expressing each of these virulence-associated genes individually, complications during protein detection and phenotypic testing resulted in an outcome that did not satisfactorily fulfill the aims of the study.

3.4.1. Molecular cloning methods

In particular, a variety of problems were presented by heterologous expression of *CaALS3* in a *C. dubliniensis* background. Previous studies, which have successfully expressed the gene and protein in other organisms, have experienced difficulties in strain stability over time (personal communication, Dr. S. Filler, UCLA). These difficulties appear to be reduced by using a *CEN/ARS* type plasmid containing a species-specific autonomously replicating sequence (*ARS*) and centromeric (*CEN*) sequence for stable, low copy plasmid replication (Liachko & Dunham, 2013; Taxis & Knop, 2006). Expression of *CaALS3* in *C. glabrata* was achieved by Fu *et al.* using a plasmid (pGRB2.2) which contained *C. glabrata*-specific *CEN/ARS* sequences (Fu *et al.*, 2013). Although the non-integrative expression plasmid pADH1 contains a *C. albicans* *ARS* (*CARS*) sequence it does not contain a *CEN* sequence (Bertram *et al.*, 1996). It is not clear whether a plasmid containing a *C. albicans* *ARS* may experience the same benefit in plasmid stability during replication when transferred to a different organism. In addition, conservation of centromeric sequences appears to differ greatly between *C. albicans* and *S. cerevisiae* (Sanyal *et al.*, 2004). Padmanabhan *et al.* reported that no conservation existed between *C. albicans* and *C. dubliniensis* *CEN* sequences by genomic analysis and that the loci may be the most rapidly evolving loci in the two species (Padmanabhan *et al.*, 2008). Further study would improve development of tools for creating mutant strains and analysing gene expression with relation to functional phenotypes.

This study has indirectly highlighted significant difference in gene expression between *C. albicans* and *C. dubliniensis*. Expression of *GFP* as part of the *CdpNIM* expression cassette, regulated by the *CdADH1* promoter, appeared to be much lower

than that observed in the CapNIM expression cassette under the control of the *CaADH1* promoter. In *C. albicans*, *CaAdh1p* has been shown to catalyse the production of ethanol in anaerobic environments (Bertram *et al.*, 1996). The protein has shown alternative cellular localisation during the dimorphic switch with *CaAdh1p* on the surface of yeast and in the cytosol of hyphae (Hernandez *et al.*, 2004; Urban *et al.*, 2003). Notably, expression was found to be decreased in *C. albicans* biofilms (Mukherjee *et al.*, 2006). Thus the low level of expression from *CdADH1* may indicate an increased tendency for *C. dubliniensis* to grow as a multicellular biofilm. It would be informative to investigate and compare any differential regulation in the expression of *ADH1* in *C. albicans* and *C. dubliniensis* planktonic cells and biofilm-associated cells. This study has also underlined the importance of promoter strength in gene expression studies. The *CdpNIM* expression cassette has previously been used to express *CaSFL2* in *C. dubliniensis* (Spiering *et al.*, 2010). The study found a relatively weak phenotype that, in hindsight, may be related to the weaker transcription from the *CdADH1* promoter. This work deserves to be revisited to assess the level of protein abundance in relation to the observed phenotype.

3.4.2. *ALS3* gene cloning and expression

Genomic integration of expression cassettes, such as pNIM, negates the need for optimisation of plasmid stability. The high rate of failure for recovery of *C. dubliniensis* transformants expressing *CaALS3* suggests that integration of the gene into the *C. dubliniensis* genome may have deleterious effects on the fitness of the organism. The ability of *CaAls5p*, *CaAls1p* and *CaAls3p* to form amyloid plaques has been documented elsewhere (Otoo *et al.*, 2008). Amyloid plaques are formed by the aggregation of insoluble protein fibers (Pinney & Hawkins, 2012). Atomic force microscopy studies have supported the hypothesis that this characteristic may improve the adhesive ability of the organism in both self-aggregation and binding to host ligands (Alsteens *et al.*, 2009). Although *CaAls3p* is naturally expressed on the surface of *C. albicans* hyphae it is not clear whether the proteins may interact and form amyloid plaques within the cell cytosol before they are translocated across the cell membrane and anchored in the cell wall. Historically, there have been no suggestions or evidence that *CaAls* proteins associate with chaperone proteins but it is conceivable that chaperone activity may hold the nascent protein in a folded state, which would prevent the exposure of amyloid forming sequences before the cell is

anchored to the cell wall. However, this does not explain the apparent success of groups in achieving *CaAls3p* expression on the surface of *S. cerevisiae* and *C. glabrata*.

In the case of *S. cerevisiae* expressing *CaAls3p*, Nobbs *et al.*, expressed protein fragments using a Gateway expression vector (Nobbs *et al.*, 2010). The resultant protein was a fusion of the *CaAls3p* N-terminal and tandem repeat domain to a haemagglutinin (HA) tag, a *C. glabrata* adhesin domain (Epa1p), and the anchor domain of a *S. cerevisiae* cell wall protein (Cwp2p). Fluorescent immunoprecipitation with an anti-HA antibody localised the fusion protein to the cell wall. The investigators did not report any protein folding differences arising from the complexity of the constructed fusion protein. Similarly, immunofluorescent detection of *CaAls3p* *C. glabrata* strains harbouring the pGRB2.2-*Als3* plasmid using an anti-*Als3* antibody raised against the N-terminal domain of *CaAls3p* localised the protein to the cell surface (Fu *et al.*, 2013). However, Miranda *et al.* have shown that differences in translation of CUG as either serine or leucine play an important role in the adhesive phenotype mediated by *CaAls* proteins (Miranda *et al.*, 2013). It is important to note that both *C. albicans* and *C. dubliniensis* belong to the CTG clade and predominantly translate CUG as serine. However, *C. glabrata* and *S. cerevisiae* use the standard genetic code and thus translate CUG predominantly as leucine (Papon *et al.*, 2013). Miranda *et al.* have shown that *CaALS3* possesses two CTG codons in its N-terminal domain and consequently may theoretically produce four variant proteins depending on predominant CUG translation patterns. This impact of this translation characteristic has yet to be experimentally investigated in *C. dubliniensis*. However, it is apparent that *CaAls3p* expressed heterologously may suffer from mistranslation, leading to protein production and cell surface expression that displays considerable identity variation from *CaAls3p* naturally expressed on the surface of *C. albicans* hyphae. It is not clear whether the *S. cerevisiae* and *C. glabrata* heterologous expression systems corrected *CaALS3* CTG codons for translation as serine instead of leucine.

Although little *CaAls3p* was detected by antibody binding and flow cytometry on the surface of *C. dubliniensis* cells constructed as part of this study, an increase in fungal adherence to human BECs was detected. It appears that even the presence of a very small amount of *CaAls3p* on the surface of *C. dubliniensis* yeast cells enhances

adhesion to epithelial cells, supporting the role of *CaAls3p* in *Candida* pathogenesis. Importantly *CaAls3p* is also a putative invasin (Liu & Filler, 2011). Further studies are required to investigate whether the low level of *CaAls3p* expression is sufficient for internalisation of *C. dubliniensis* yeast by epithelial cells. Expression of *CaALS3* in *C. dubliniensis* cells may also impact other forms of growth such as biofilms. Additional phenotypic characteristics will be investigated in future studies and infection models.

3.4.3. *HYR1* gene cloning and expression

In the absence of a suitable antibody to detect cell surface localisation of *CaHyr1p* in *C. dubliniensis* cells expressing *CaHYR1* RNA, investigation of fungal survival in coculture with human neutrophils was carried out. Protection against killing by human PMNs is posited to be one of the phenotypic characteristics of *CaHyr1p* expression (Luo *et al.*, 2010). In this case, no significant difference was observed between *C. dubliniensis* wild type WÜ284 and the mutant strain expressing *CaHYR1* (data not shown). While it appears that *CaHYR1* expression in *C. dubliniensis* does not confer protection against PMN activity it is possible that protein expression on the cell surface may be insufficient to contribute to a functional phenotype. Development of a *CaHyr1p* specific antibody would enable verification of protein localisation to the cell surface and estimation of protein abundance.

3.4.4. Future directions

In order to successfully investigate the function of virulence associated *C. albicans* proteins by heterologous expression in *C. dubliniensis* a number of methodology improvements are necessary. As both *CaAls3p* and *CaHyr1p* are highly abundant proteins on the surface of *C. albicans* hyphae it would be beneficial to have similar quantities of protein detectable on the *C. dubliniensis* cell surface. Detection of *CaHyr1p* is currently an obstacle. Development of a specific antibody or tagging the protein with a histidine (His) or HA tag would be extremely useful in future studies. Finally, there are a number of assumptions based on similarities between *C. albicans* and *C. dubliniensis* that require experimental verification and elaboration including CUG translation, protein glycosylation, secretion and protein trafficking pathways.

Chapter 4

***Candida dubliniensis* hyphal induction, adhesion and tissue damage**

4.1. Introduction

4.1.1. Filamentous diversity

Both *C. albicans* and *C. dubliniensis* are capable of dimorphism and can adapt to their local environment by transitioning between ellipsoid yeast and elongated filaments. In fact, three distinct morphological states have been identified and associated with this reversible dimorphic switch (Odds, 1985; Saville *et al.*, 2003). Yeast, pseudohyphae and true hyphae can be produced by *C. albicans* and *C. dubliniensis* in response to various environmental cues (Biswas *et al.*, 2007).

Yeast cells are spheroidal in shape and generally measure approximately 3.0 – 4.0 μm (Merson-Davies & Odds, 1989). These blastopores divide primarily by asexual reproduction (Nielsen & Heitman, 2007). Budding from a mother cell produces a daughter cell, which can bud new cells while still attached to the mother cell, or separately after cytokinesis and cell separation (Chaffin, 1984). True hyphae are elongated, tubular cells of uniform diameter along the extending structure (Merson-Davies & Odds, 1989). They are formed when yeast cells produce a polarised outgrowth called a germ tube as a result of environmental stimuli. The germ tube continues to extend from the tip as the cell progresses through the cell cycle (Staebell & Soll, 1985). A hyphal culture can develop into an intricate hyphal mycelium and form a multicellular biofilm (Kumamoto, 2002; Nobile & Mitchell, 2006). Pseudohyphae display similar physical properties to both yeast and true hyphal cells. In certain conditions, yeast mother cells bud a cell with the appearance of a germ tube. However, as pseudohyphal filaments develop, constrictions appear at the septae, creating a filament with non-uniform diameter (Merson-Davies & Odds, 1989). Both *C. albicans* and *C. dubliniensis* may form pseudohyphae with varying degrees of superficial similarity to either yeast or true hyphal cells.

In reality, *C. albicans* and *C. dubliniensis* often form cell cultures comprised of a mixture of these morphological forms and thus identification of each cell type can be problematic. In mixed culture, visual differentiation of pseudohyphae and true hyphae can be difficult due to their similar appearances in many growth environments (Sudbery *et al.*, 2004). In 1989, Merson-Davies and Odds described the morphological index (MI) method to identify and quantify both pseudo- and true

hyphae (Merson-Davies & Odds, 1989). This required making measurements of the length of the germ tube, the diameter of the septal junction, and the maximum diameter of the extending filament. While this is a reliable method, it is not particularly feasible to manually analyse large panels of strains over multiple time points due to the time required for making measurements. A similar way of differentiating hyphae is by measuring the minimum width of the filament (Sudbery *et al.*, 2004). *Candida albicans* true hyphae have been shown to possess a diameter of approximately 2.0 μm when grown on a variety of common growth media. In contrast, pseudohyphae display a minimum diameter of approximately 2.8 μm (Sevilla & Odds, 1986). However, making measurements may be subjective and also depend on the equipment. Thus identification and differentiation often requires validation.

A number of cell cycle differences between the various morphological forms have been identified and have been useful in differentiating between yeast, pseudohyphae and true hyphae (Berman, 2006; Sudbery, 2011). Key findings include patterns of septum formation, nuclear division and cell cycle progression. The primary septum in yeast and pseudohyphal cells forms between the mother and daughter cell junction (Soll *et al.*, 1978). In true hyphae the primary septum forms within the germ tube (Sudbery, 2001). Nuclear division in both yeast and pseudohyphae takes place across the junction of the mother and daughter cell before the daughter nuclei migrate into each cell. However, the first nuclear division in true hyphae has been shown to occur within the germ tube, after migration of the nucleus into the filament. The nuclei migrate back through the germ tube or to the apical compartment as the cell cycle progresses (Finley & Berman, 2005; Warena & Konopka, 2002). This knowledge provides an unambiguous validation method for visual differentiation of true hyphae and pseudohyphae. Nuclear material can be readily stained with DAPI, excited by ultraviolet light, and detected under a blue filter at approximately 460 nm (Hazan *et al.*, 2002; Kapuscinski, 1995). While this work has been developed and elaborated in *C. albicans*, based on cell cycle studies in *S. cerevisiae*, few extrapolations have been experimentally confirmed in *C. dubliniensis*. Due to the reduced tendency of *C. dubliniensis* to form true hyphae, and the increased likelihood of pseudohyphal growth under conventional filament-inducing conditions, it is necessary to extend cell cycle progression studies to *C. dubliniensis*.

The various *C. albicans* morphologies have been connected to different stages of infection. Yeast cells have been associated with systemic candidiasis and hyphae are commonly linked to host cell adhesion and invasion (Thompson *et al.*, 2011). However, the role of pseudohyphae in host colonisation and opportunistic infection has yet to be elucidated. Thus, it is clearly important to understand the properties of each cell type to understand their distinct roles in infection.

4.1.2. *Candida* hyphal induction

The differential virulence of *C. albicans* and *C. dubliniensis* is often attributed to the lower tendency of *C. dubliniensis* to form true hyphae (Stokes *et al.*, 2007; Vilela *et al.*, 2002). A number of studies have demonstrated the reduced capacity of *C. dubliniensis* to filament on conventional hyphal-inducing media commonly used for induction of *C. albicans* hyphae. Gilfillan *et al.* investigated the ability of two *C. albicans* and four *C. dubliniensis* strains to filament on treatment with either serum, GlcNAc or with a combined pH and temperature shift (Gilfillan *et al.*, 1998). Compared to the *C. albicans* strains, the *C. dubliniensis* strains displayed a delayed response in induction of germ tubes. *Candida dubliniensis* filamentation under the conditions tested reportedly achieved high levels (> 80%) over time. Critically, no distinction was apparently made between pseudohyphae and true hyphae. Stokes *et al.* improved on this work by analysing the hyphal induction patterns of four *C. albicans* strains and 11 *C. dubliniensis* strains (Stokes *et al.*, 2007). The study investigated filamentation in nine different hyphal-inducing media. All of the *C. albicans* strains formed greater than 50 % germ tubes under all the conditions tested. However much lower levels of filamentation were observed for the *C. dubliniensis* isolates. Less than 30 % (n = 11) of the strains displayed over 50 % filamentation in all but one of the hyphal-inducing media. The nutrient poor medium, water and serum (WS), composed of 10 % (v/v) serum, supported high levels of *C. dubliniensis* filamentation after 6 h incubation, indicating the importance of nutrient limitation for formation of *C. dubliniensis* hyphae. O'Connor *et al.* later determined that addition of peptone, glucose, or a combination of both to WS media, attenuated the hyphal inducing effect of the WS medium (O'Connor *et al.*, 2010). The group also elaborated on the importance of preculturing conditions, showing that growing *C. dubliniensis* isolates initially in a nutrient-limited medium such as Lee's medium contributed to the efficiency of hyphal

formation when cells were transferred to hyphal-inducing media. In summary, methods for successful induction of *C. albicans* hyphae do not necessarily lead to efficient *C. dubliniensis* hyphal formation. However, the reverse may be true i.e. methods for inducing *C. dubliniensis* hyphae appear to be sufficient for effective induction of *C. albicans* hyphae. In this way, specific environmental or experimental hyphal induction conditions naturally trigger different rates of hyphal formation, and presumably hyphal gene expression, in *C. albicans* and *C. dubliniensis*.

4.1.3. Infection models

A plethora of infection models are available for *Candida* research. Each model possesses its share of benefits and limitations. Infection models based on the relatively simple organisms *Caenorhabditis elegans* (roundworm), *Danio rerio* (zebrafish), *Galleria mellonella* (honeycomb moth), *Drosophila melanogaster* (fruitfly), *Bombyx mori* (silkworm), are useful for preliminary investigations (Alarco *et al.*, 2004; Chao *et al.*, 2010; Fuchs *et al.*, 2010; Matsumoto *et al.*, 2013; Pukkila-Worley *et al.*, 2009). However, they do not accurately mimic the infection process of *Candida* in a mammalian host. Mammalian host site-specific infection models have been developed to simulate systemic candidiasis, vaginal candidiasis, oral mucocutaneous infections, and orogastrointestinal carriage and invasion (Arendrup *et al.*, 2002; Naglik *et al.*, 2008a; Szabo & MacCallum, 2011). Host factors play a significant role in these models and experimental variation between studies may drastically influence the outcomes and conclusions generated (Netea *et al.*, 2008; Wachtler *et al.*, 2012).

In vivo, *Candida* cells are most closely associated with the adhesion and invasion of epithelial mucosal tissue that lines the orogastrointestinal tract (Mukherjee *et al.*, 2005; Zhu & Filler, 2010). For that reason, a number of immortalised epithelial cell lines have been used historically to investigate the ability of *C. albicans* yeast and hyphae to adhere to, invade, and cause cellular damage of epithelial cells. The cervical adenocarcinoma (HeLa), colorectal adenocarcinoma (Caco-2), pharyngeal squamous cell carcinoma (FaDu), and buccal squamous cell carcinoma (TR146) cell lines are commonly used for *Candida* infection studies (Dalle *et al.*, 2010; Park *et al.*, 2009). The buccal epithelial cell line TR146, in particular, has been developed to create the reconstituted human epithelium (RHE) model (Schaller *et al.*, 2006). The RHE model is a three-dimensional, differentiated tissue mounted on a scaffold in order to better

simulate a host tissue and the *Candida* invasion process. In this model *C. albicans* hyphae have been shown to readily invade both TR146 and RHE, *C. dubliniensis*, in contrast, has been shown to display only localised invasion and limited tissue damage (O'Connor *et al.*, 2010). The cell line growth medium, which usually contains serum, appears to play a significant role in this phenotype as *C. albicans* filaments efficiently in cell culture media such as DMEM and RPMI, and concurrently expresses hyphal-specific genes and proteins under these conditions (Wachtler *et al.*, 2012). However, *C. dubliniensis*, with its reduced tendency to form hyphae, does not filament to the same degree in cell culture media and, unsurprisingly, is usually found predominantly as yeast cells in epithelial cell infection models. In this way, analysis of morphology-specific or morphogenetically-regulated phenotypic outcomes in infection models is complicated and attributing damage to species morphology or specific protein function is challenging.

Nevertheless, significant data regarding the differential virulence of *C. albicans* and *C. dubliniensis* has been collected. Stokes *et al.* investigated the ability of *C. dubliniensis* and *C. albicans*, individually and in concert, to infect and colonise the stomach and intestine of mice in an orogastrintestinal model of infection (Stokes *et al.*, 2007). The group found that up until day 6 of the experiment there was no difference in the presence or absence of *Candida* from mice infected with *C. albicans* SC5314 or *C. dubliniensis* CD36 individually. However, between day eight and day ten, no CD36 was detected. Similar results were also observed for mice coinoculated with both SC5314 and CD36 in a competition experiment. By day 10 *C. dubliniensis* was not observed at all. Investigation of dissemination of *Candida* showed SC5314 in the stomach of all the mice and showed dissemination to the liver by the end of the experiment. In contrast, only 40 % of the mice infected with CD36 still displayed the fungus in their stomach. Likewise, 40 % of the mice inoculated with *C. dubliniensis* tested positive for dissemination to the liver. O' Connor *et al.* attempted to characterise the morphology of *C. dubliniensis* cells infecting RHE (O'Connor *et al.*, 2010). By combining preculture of *Candida* in Lee's medium with a pH and temperature shift, the study showed that *C. dubliniensis* WÜ284 pseudohyphal and hyphal cells possessed the capacity to cause localised invasion, and a significant increase in tissue damage after 24 h. In both cases, the magnitude of invasion and cell damage was much lower in magnitude than the phenotype displayed by *C. albicans* hyphae. This supports the findings of Spiering

et al. describing damage of RHE infected with *C. albicans* or *C. dubliniensis* over 12 h, showing significantly lower levels of tissue damage caused by *C. dubliniensis* CD36 compared to *C. albicans* SC5314 (Spiering *et al.*, 2010).

4.1.4. Strain variation

The first *C. dubliniensis* strain to be sequenced was CD36 and the findings, including a comparative study between the *C. albicans* and *C. dubliniensis* genome, highlighted differences between the two species (Jackson *et al.*, 2009). Although CD36 is considered a good representative of the species, the strain WÜ284 has been used historically as the “lab-strain”. It is relatively easily manipulated and a *ura3Δ/ura3Δ* mutant WÜ284 strain is available (Staib *et al.*, 2001). Both *C. dubliniensis* strains have been used interchangeably in infection models and are superficially quite similar. However, strain variation in *C. dubliniensis* has been suggested to play a significant role in virulence. A number of *C. dubliniensis* strains isolated by Asmundsdottir *et al.* from systemic infections have shown relatively high levels of virulence in a systemic murine model of infection (Asmundsdottir *et al.*, 2009). The study presented data from three *C. albicans* strains and nine *C. dubliniensis* strains, from either Genotype 1 or Genotype 2, that had been originally isolated from bloodstream infections. As a result of the study, it was concluded that intraspecies variation, rather than interspecies differences, had a more significant impact on differential virulence. It was acknowledged that isolation of *C. dubliniensis* from systemic infections may impact the perceived virulence of *C. dubliniensis*. Systemic isolates may be enriched for virulence promoting properties leading to an inaccurate representation of the species as a whole. This current study investigated the propensity a number of *C. dubliniensis* strains from the Icelandic strain variation study, in conjunction with a panel of *C. dubliniensis* strains from alternative sources and genotypes. The ability to these *C. dubliniensis* strains to form filaments was investigated and any correlation between filamentation rates, adhesion, or invasion of host epithelial tissue was explored.

4.1.5. Aims of this part of the study

The reduced efficiency of *C. dubliniensis* filamentation relative to *C. albicans* under many growth conditions has been shown previously (Moran *et al.*, 2007; O'Connor *et al.*, 2010; Stokes *et al.*, 2007). While *C. dubliniensis* has also been shown to be

generally less virulent than *C. albicans*, Asmundsdottir *et al.*, recently reported two *C. dubliniensis* strains, listed here as HE30 and HE38a, that displayed similar virulence to a *C. albicans* strain (IS-7) in a murine model of systemic infection (Asmundsdottir *et al.*, 2009). This part of the current study attempted to investigate whether increased virulence in *C. dubliniensis* strains correlated with an increased tendency to form hyphae under known hyphal-inducing conditions.

4.2. Specific materials and methods

4.2.1. Hyphal induction on solid media

4.2.1.1. Growth and maintenance conditions

Candida isolates used for this study are listed in Table 2.1. Strains were initially grown on YEPD at 37 °C for 48 h. Single colonies were then inoculated on a range of solid hyphal inducing media and incubated at 30 °C or 37 °C. Spider agar, SLD agar, YNBS agar and YPS agar were all used to investigate the ability, or tendency of *C. dubliniensis* strains (n = 19) to form filaments in response to commonly used hyphal inducers.

4.2.1.2. Visualisation of hyphae

Colonies were examined visually in a number of ways. A Flash & Go - Automatic Colony Counter (IUL, Barcelona, Spain) was used to obtain micrographs of entire agar plates. Colony fringe morphology was visualised with a Nikon TMS-F inverted microscope (Nikon) and micrographs were taken with a Nikon Coolpix 4500 camera (Nikon). Transverse slices of agar were visualised by chilling inoculated agar plates at 4 °C and slicing transverse sections. These sections were then mounted on microscope slides and fixed in place under a cover slip. Sections were visualised using a Nikon TMS-F inverted microscope (Nikon).

4.2.2. Hyphal induction in liquid media

4.2.2.1. Staining and morphological verification

Prior to staining, cells were washed in 1X PBS to reduce auto-fluorescence caused by growth medium components. *Candida* cells were routinely stained with calcofluor white (CFW) to highlight the chitinous structure of fungal elements. Approximately 2 µg/ml of CFW was used to highlight the chitin-rich cell walls of fungi. Cell nuclei were stained using DAPI. Approximately 1.5 µg/ml DAPI was used to stain nuclear material. Stained cells were visualised by fluorescence microscopy under UV light using a Nikon Eclipse E600 epifluorescence microscope equipped with a high power mercury lamp (Nikon).

Due to the wide spectrum of hyphal phenotypes in *C. dubliniensis*, and *C. albicans*, identification of true hyphae and distinction from pseudohyphae was determined by the location of active nuclear division. Pseudohyphal growth was indicated by nuclear division across the mother-daughter junction between mother yeast cell and daughter germ tube. True hyphae were identified by migration of the nucleus into the germ tube and nuclear division occurring within the germ tube itself.

4.2.2.2. Induction of hyphae following preculture in YEPD broth

Induction of hyphae by preculture in YEPD broth and subsequent induction in YEPD and 10 % (v/v) FCS (YPDS) was performed as described in Chapter 2. In general this method was used for hyphal induction in *C. albicans* and weak hyphal induction in *C. dubliniensis* strains.

Hyphal induction with YEPD preculture and induction in water with 10 % (v/v) FCS (WS) was used to trigger strong induction of *C. dubliniensis* and *C. albicans* hyphae, as described previously (O'Connor *et al.*, 2010).

4.2.2.3. Tissue culture medium (CDMEM) as a hyphal inducer

Standard growth and maintenance of human tissue monolayers was carried out using CDMEM as the maintenance medium. This growth medium contains FCS, which is known to be a strong inducer of hyphae. The degree of hypha formation during *Candida* growth in CDMEM was visualised by growing *Candida* cells initially in YEPD broth overnight at 30 °C, 200 r.p.m. After 16 h the cells were centrifuged, washed in 1X PBS, and resuspended in CDMEM, or 10 % (v/v) CDMEM for increased hyphal growth, to a final density of 1×10^6 cells/ml. Cells in CDMEM or 10 % (v/v) CDMEM were incubated at 37 °C and cell morphology was visualised at various timepoints.

4.2.3. *Candida dubliniensis* strain growth rates

Yeast growth rates were measured to assess any significant differences in fitness of yeast grown in nutrient-rich YEPD medium. Cells were pregrown on YEPD agar for 48 h. Single colonies were inoculated in YEPD broth and grown at 37 °C, 200 r.p.m. overnight. After 16 h cells were washed in 1X PBS and inoculated at a final density of 2×10^6 cells/ml in prewarmed YEPD broth in 24 well plates. Broths were incubated at 30 °C, 37 °C, or 42 °C, in a Genios plate reader (Tecan UK Ltd., Reading, UK), with

shaking. Cell density was measured at 540 nm periodically and growth curves were plotted from experiments performed in duplicate.

4.2.4. Adhesion to TR146 human buccal epithelial monolayers

4.2.4.1. Quantification of adhesive colony forming units

Adhesion of fungal cells to human epithelial TR146 monolayers was undertaken according to the method described by Rotrosen *et al.* (Rotrosen *et al.*, 1985). Briefly, TR146 cells were cultured in 75 cm² Corning Cell-bind flasks (Sigma-Aldrich) at 37 °C in a 5 % (v/v) CO₂ static incubator. Dulbecco's Modified Eagle Medium (DMEM) was supplemented with 10 % (v/v) FCS and 1 % (v/v) penicillin-streptomycin to form complete DMEM (CDMEM). The growth medium CDMEM was used for cell line growth and maintenance. Monolayers were allowed to reach approximately 80 % confluency and treated with Trypsin-EDTA to detach the monolayer from the flask surface. Detached cells were washed in DMEM and resuspended in CDMEM. An aliquot of suspended cells were stained with trypan blue to aid cell counting with an improved Neubauer haemocytometer. Approximately 1 x 10⁶ cells/ml were seeded in 6 well plates and incubated until 90 % confluency was attained.

Candida strains from 48 h old YEPD agar plates were grown overnight in YEPD broth at 37 °C, 200 r.p.m. *Candida* cultures were pelleted by centrifugation at 12000 x g, 3 min, washed in 1X PBS, and resuspended in 1 ml PBS. Cells were suitably diluted and cell density was counted with an improved Neubauer haemocytometer.

Confluent TR146 monolayers were washed with fresh CDMEM and the medium was removed. A suspension of 100 *Candida* cells in 2 ml CDMEM or 10 % (v/v) CDMEM was transferred to TR146 monolayer wells in triplicate and incubated at 37 °C, 5 % (v/v) CO₂ for 1 h. The same number of cells, in a 100 µl volume, was added to YEPD agar plates in triplicate and incubated at 37 °C for 24 h. After 1 h coincubation of *Candida* cells with TR146 monolayers, the medium was removed, the monolayers were gently washed with 10 ml 1 x PBS in 2 ml aliquots, with rotation of the plate to remove any non adherent fungal cells. Each monolayer was overlaid with 2 ml molten YEPD cooled to 37 °C. Monolayer plates with YEPD overlay were incubated at 37 °C overnight. After approximately 24 h, cfu for each well were counted, averaged and

expressed as a percentage of the average cell count from the control YEPD agar plates.

4.2.4.2. Direct visualisation of adherent cells

The morphology of adherent cells was investigated by inoculating TR146 epithelial cell monolayers grown on glass coverslips in 6 well plates with *Candida* cells similar to the method described in Section 4.2.4.1. However, instead of overlaying the 1X PBS-washed infected monolayers with YEPD, the monolayer-coated coverslips were fixed in 4 % (v/v) paraformaldehyde, stained with CFW, and mounted on microscope slides for direct visualisation under a UV microscope filter.

4.2.5. Morphology-associated tissue damage

The effect of *Candida* cells on TR146 human epithelial cell monolayers was investigated by measuring the release of cellular lactate dehydrogenase (LDH) from damaged epithelial cells using the CytoTox 96 Non-Radioactive Cytotoxicity Assay (Promega). Human epithelial TR146 monolayers were grown and maintained as outlined in Section 4.2.4.1. Prior to coincubation with *Candida* cells, TR146 monolayers grown in 96 well plates were washed with either CDMEM or 10 % (v/v) CDMEM. *Candida* cells were initially grown in YEPD broth overnight and resuspended in either CDMEM or 10 % (v/v) CDMEM as described in Section 4.2.2.3. Monolayers were inoculated with 100 µl of *Candida* cells at a density of 1×10^5 cells/ml. Infected monolayers were incubated at 37 °C, 5 % (v/v) CO₂ for 4 h. The CytoTox 96 Non-Radioactive Cytotoxicity Assay (Promega) was carried out according to manufacturer's instructions. This was performed by centrifuging the infected monolayers after 4 h incubation and transferring 50 µl of the supernatant to a sterile 96 well plate. Substrate mix was added to the supernatant and incubated in the dark at room temperature for 30 min. The enzymatic reaction was halted by adding the supplied stop solution to each well. Absorbance was measured at 480 nm using a Genios plate reader (Tecan UK Ltd., Reading, UK). Absorbance data were corrected for volume and background absorbance. Results were expressed as % cytotoxicity generated by the manufacturer's recommended calculation, based on corrected absorbance values $((\text{Effector} - \text{Effector Spontaneous} - \text{Target Spontaneous}) / (\text{Target Maximum} - \text{Target Spontaneous}))$.

4.3. Results

4.3.1. Hyphal induction on solid media

Candida dubliniensis strains are known to show variation in their ability to produce hyphae. The ability and propensity of a panel of 19 *C. dubliniensis* strains to produce filamentous colonies on defined solid media was investigated (Table 4.1). This panel included strains known to show enhanced virulence in a murine model, and strains known to produce filaments with varying degrees of efficiency. When grown on the standard, nutrient rich medium YEPD, at 30° C, 7/19 strains produced filamentous colonies after five days of growth (Fig. 4.1). While growth of *Candida* on YEPD predominantly yields yeast colonies, elaboration of filaments may be influenced by pH variation and nutrient availability over extended periods of time (> 5 days), within unbuffered YEPD medium. Growth on nutrient-rich YPS agar yielded only four strains displaying growth as filamentous colonies. Of these four filamentous strains, three were also filamentous on YEPD. Growth on SLD agar generated filamentous growth in 7/19 strains investigated, although the filamentous phenotype was weak in three of the strains observed. The positive effect of nutrient limitation on the initiation of filamentation in *C. dubliniensis* strains is weaker in media containing either glucose as a carbon source, or ammonium sulphate as a nitrogen source. This is consistent with the findings of O' Connor *et al.* which documented attenuation of *C. dubliniensis* filamentation in media supplemented with glucose and peptone (O'Connor *et al.*, 2010). Growth on Spider agar displayed the highest abundance of filamentous colonies, with 17 strains producing hyphal fringing around the colony borders. Only two *C. dubliniensis* strains, CD36 and HE222, failed to produce filamentous colonies under these conditions. Although Spider medium contains peptone, glucose and yeast extract in low concentrations, its ability to trigger filamentation in *C. dubliniensis* is clearly powerful. Visualisation of colony morphology by microscopy confirmed the observations of *C. dubliniensis* colonies grown on Spider agar. The filamentous fringe appeared more pronounced when colonies were grown on Spider medium at 30 °C relative to 37 °C. While WÜ284 embedded in YPS agar displayed a high proportion of filamentous cells along the colony radius, HE30 displayed a phenotype of fewer hyphal cells overall, with an abundance of yeast cells decorating extending filaments. In summary, transverse sections of colonies embedded in YPS agar revealed a

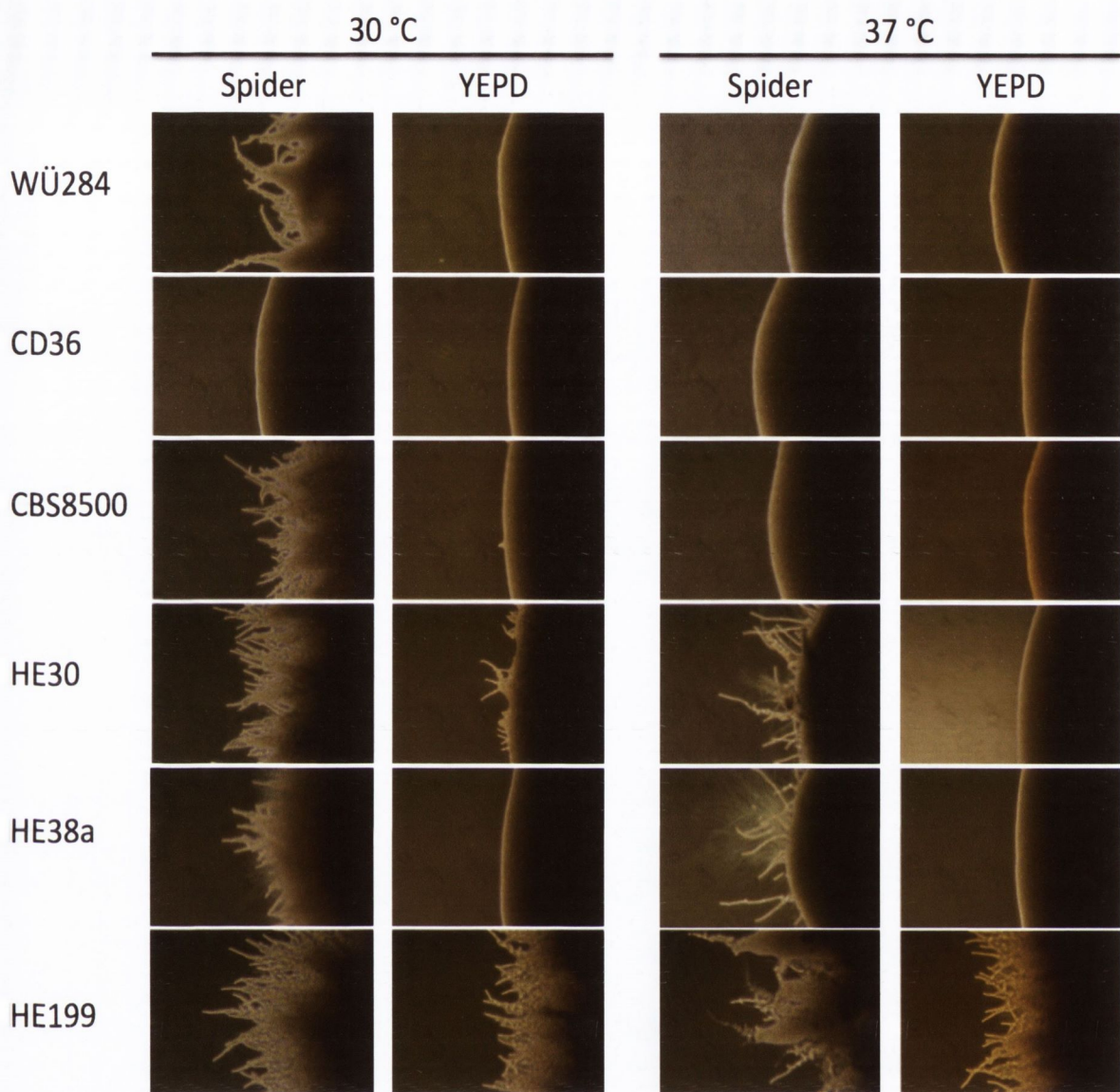


Figure 4.1. Colony fringe microscopy of *C. dubliniensis* on solid hyphal inducing media. Visualisation of *C. dubliniensis* colony fringing displayed intraspecies variation in the morphological response to YEPD and Spider growth medium. Micrographs were obtained after 5 days of incubation at 30 °C and 37 °C.

Table 4.1. Induction of *C. dubliniensis* hyphae and strain variation on solid growth media.

	YEPD	YPS	SLD	Spider
WÜ284	-	-	-	+
CBS8500	-	-	-	+
LP1	-	+	-	-/+
CD36	-	-	-	-
HE30	-	-	-	++
HE38a	-	-	-/+	++
HE57	-	-	+	++
HE124	+	+	-	-/+
HE163	-	-	+	+
HE176	-	-	-	++
HE183	-	-	-	-/+
HE194	+	+	-/+	+
HE199	++	++	-/+	++
HE222	-	-	-	-
HE237a	+	-	-	+
HE237b	+	-	-	+
HE247	-	-	-	++
HE281	+	-	+	++
HE283	+	-	+	++

Candida dubliniensis strains were incubated on different growth media at 30 °C for five days. Hyphal growth was inspected visually and scored as; - smooth, non-filamentous colonies, -/+ partly filamentous colonies, + filamentous colonies, ++ highly filamentous colonies.

complex network of yeast and hyphal cells throughout the filamentous colony, with morphological distribution varying depending on strain (data not shown).

4.3.2. Cell morphology verification

Identification of *C. dubliniensis* true hyphae by any method other than estimation according to the morphological index has not been described previously. Although filamentous forms were observed on solid hyphal-inducing agar, distinction between pseudohyphae and true hyphae is problematic. Hyphal virulence has historically been associated with *C. albicans* true hyphae. In order to identify, and distinguish between *C. dubliniensis* pseudo- and true- hyphae, various morphological forms, grown in liquid media, were stained with DAPI. This nuclear staining method was used to correlate apparent morphology with known nuclear division patterns. Staining of *C. dubliniensis* HE199 mixed morphology cultures identified not only yeast budding, with nuclear division occurring across the mother-daughter cell junction, true hyphae, but also pseudohyphae, in which nuclear division was visualised at the junction of the mother cell and elongating germ tube (Fig. 4.2). True hyphae were readily observed in *C. albicans* SC5314 hyphal cultures, with nuclear division occurring within the germ tube. Visual identification of true hyphae under magnification usually relies on recognition of a uniform diameter along the length of the filament, and can be subjective. Nuclear staining provided validation and improved reliable distinction between pseudohyphae and true hyphae. For the first time, this study describes and verifies the pattern of nuclear division in *C. dubliniensis* filamentous cells.

4.3.3. Hyphal induction in liquid media

Candida dubliniensis cells grown initially in YEPD broth overnight and inoculated in serum-containing broth displayed strain-specific levels of development of true hyphae after 2 h incubation in YPDS. Quantification of true hyphae by counting 100 cells for each strain yielded percentages ranging from 0 % to approximately 40 %, when hyphae were induced in YPDS (Fig. 4.3). As expected, initiation of *C. dubliniensis* hyphae was much stronger when WS was used as the induction medium. The lowest percentage of *C. dubliniensis* true hyphae observed using WS was approximately 20 %, displayed by CAN6, while the highest percentage was observed in HE281 with approximately 95 % true hyphae. In each *C. dubliniensis* strain investigated, induction

of hyphae was weaker than the response displayed by *C. albicans* SC5314. Variation within this range displayed by the other *C. dubliniensis* strains revealed a diverse response to hyphal induction with WS. Although hyphal induction was uniformly stronger in WS medium than YPDS, no unifying pattern between strains could be determined. An example of this is the contrasting phenotypes of HE124 and CAN6. Hyphal induction of CAN6 in YPDS was stronger than HE124. However, hyphal induction of CAN6 in WS was much weaker than HE124.

4.3.3.1. Morphological reversion in liquid media

Induction of *C. dubliniensis* true hyphae and maintenance of population morphology over time was investigated. Nutrient levels and extracellular signals in an actively growing culture are dynamic and this is reflected by the abundance of specific cell morphologies within any given population. Closer investigation of nine representative *C. dubliniensis* strains, chosen due to the range of filamentation ability, and *C. albicans* SC5314, once again showed variation in the strength of hyphal induction between strains. However, all of the strains, except one, displayed a similar pattern of hyphal percentages increasing over time until 3 h after induction in WS (Fig. 4.4). After this point, the hyphal percentage decreased and tended to decrease over time (> 3 h) as the ratio of yeast to hyphae in each culture increased (data not shown). Other than HE57, this pattern was common to the *C. dubliniensis* strains and the *C. albicans* reference strain.

4.3.3.2. Hyphal induction in tissue culture medium (CDMEM)

Growth and maintenance of TR146 epithelial cell monolayers is commonly performed using CDMEM as a growth medium. Although CDMEM does contain serum, it is a relatively nutrient-rich medium. Nutrient limitation has been shown to be important for *C. dubliniensis* hyphal induction. Growth of *C. dubliniensis* strains in CDMEM at 37 °C under atmospheric oxygen showed low levels of hyphal initiation after 1 h (Fig. 4.5). These levels were similar to that observed during a growth medium shift from YEPD to YPDS. *Candida albicans* SC5314 readily formed filaments under these conditions after 1 h. As the dominant morphology within the *C. dubliniensis* populations were yeast cells, with a small amount of hyphae, this was designated as a medium for preparing “yeast-primed” *C. dubliniensis* cells. In order to improve the proportion of hyphal cells in *C. dubliniensis* cultures for *in vitro* infection models, the

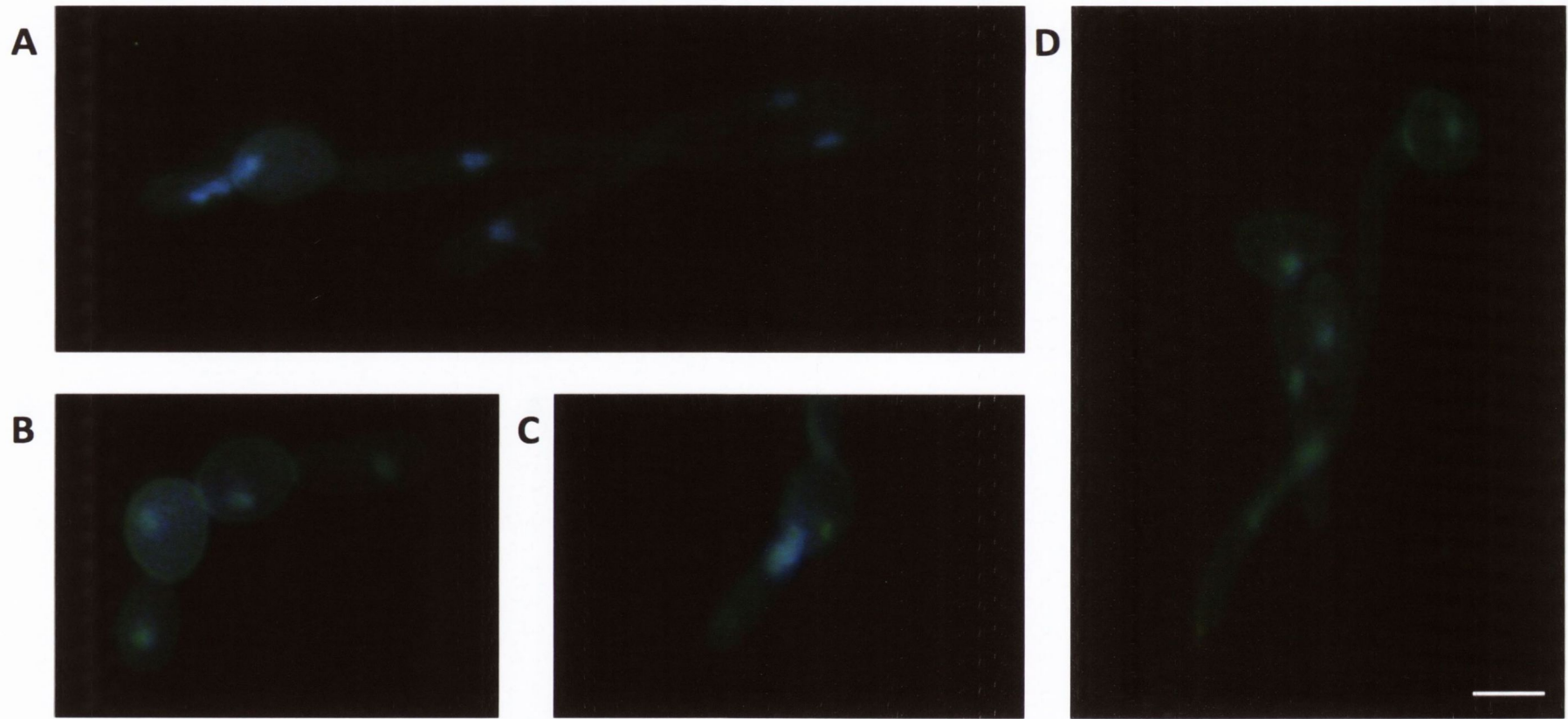


Figure 4.2. Verification of cell morphology by visualization of nuclear division and segregation patterns. Staining of PBS-washed cells using 1.5 μg DAPI was performed in order to highlight the nuclear elements of dividing and elongating cells. Distinct patterns of nuclear division corresponded to distinct morphological states. (A) Strain HE199 displayed true hyphae and yeast budding. (B) WÜ284 yeast cells. (C) HE199 pseudohypha, with nuclear division taking place across the mother-daughter junction. (D) SC5314 growth as yeast and true hyphae, distinguished by nuclear division within the germ tube. Scale bar represents 3 μm .

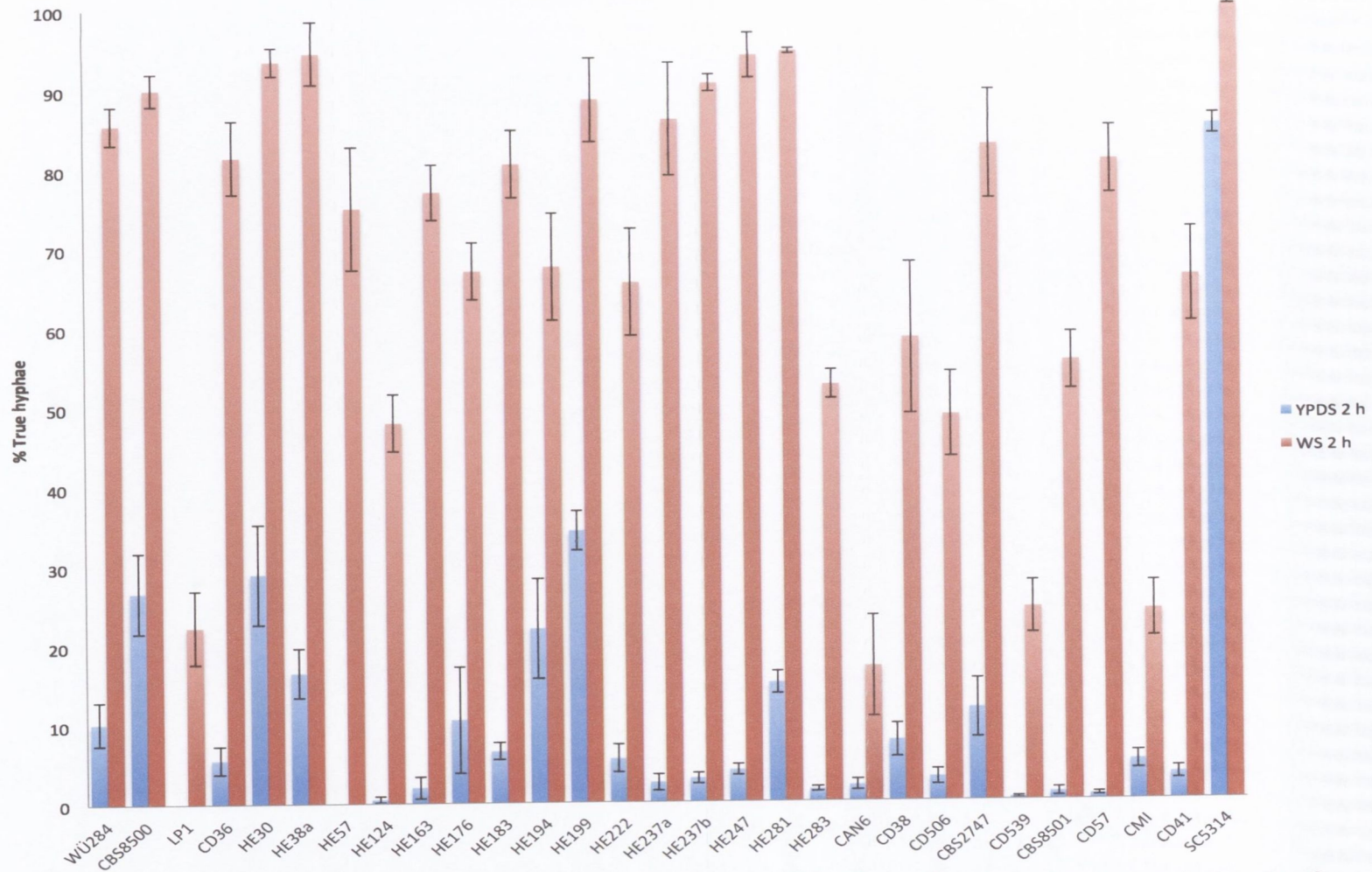


Figure 4.3. Induction of *C. dubliniensis* true hyphae in liquid media. Intraspecies variation in *C. dubliniensis* morphological response to weak (YPDS) or strong (WS) hyphal inducing media after 2 h. True hyphae were expressed as a percentage after counting at least one hundred fungal cells in each experimental sample. Data was collected from at least three biological replicates. For comparison with *C. albicans*, SC5314 was included as a reference.

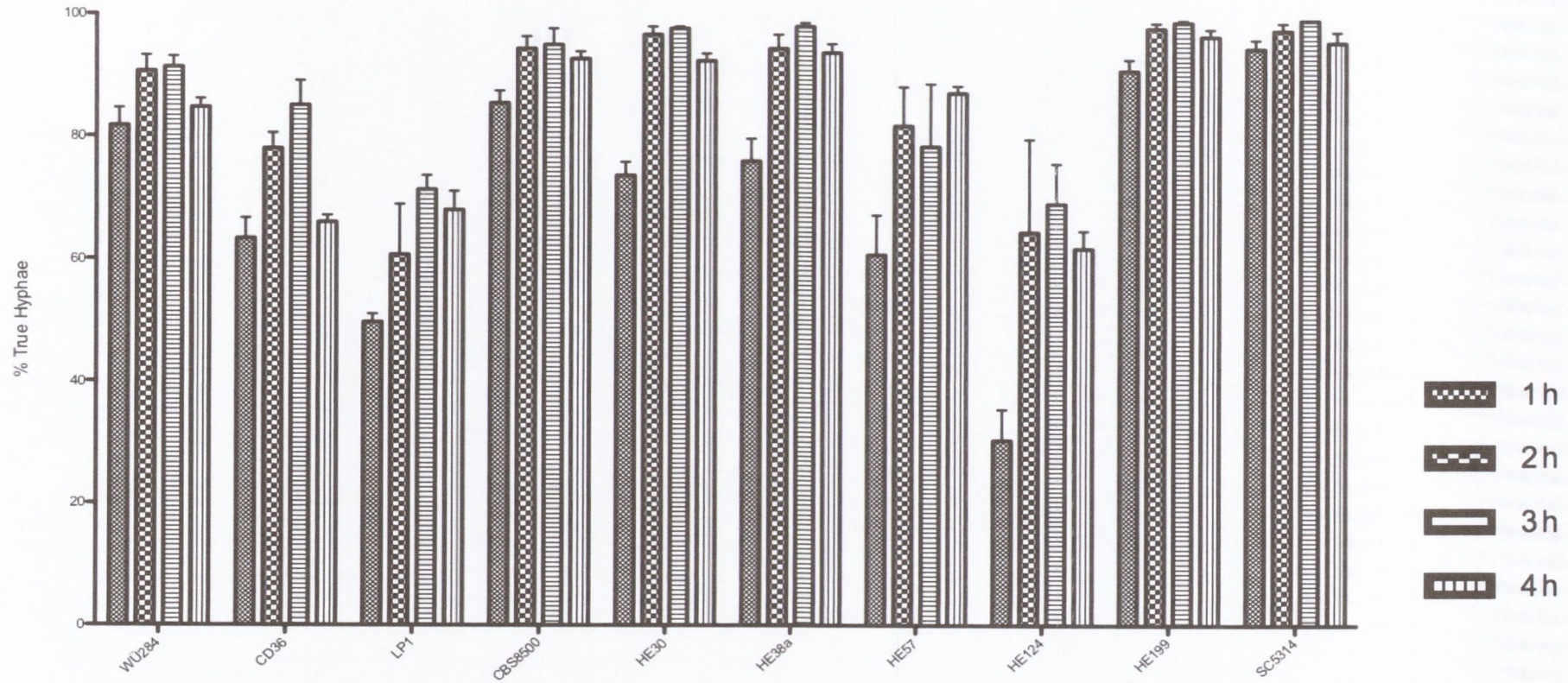


Figure 4.4. Induction and reversion of *C. dubliniensis* hyphae in WS medium. Strong induction of *C. dubliniensis* hyphae peaked at 3 h after hyphal induction with WS medium. Reversion of hyphae to yeast began to occur after 3 h. SC5314 was included as a *C. albicans* reference strain. 100 cells were counted and proportion of true hyphae was expressed as a percentage. Data represent the mean of three biological replicates.

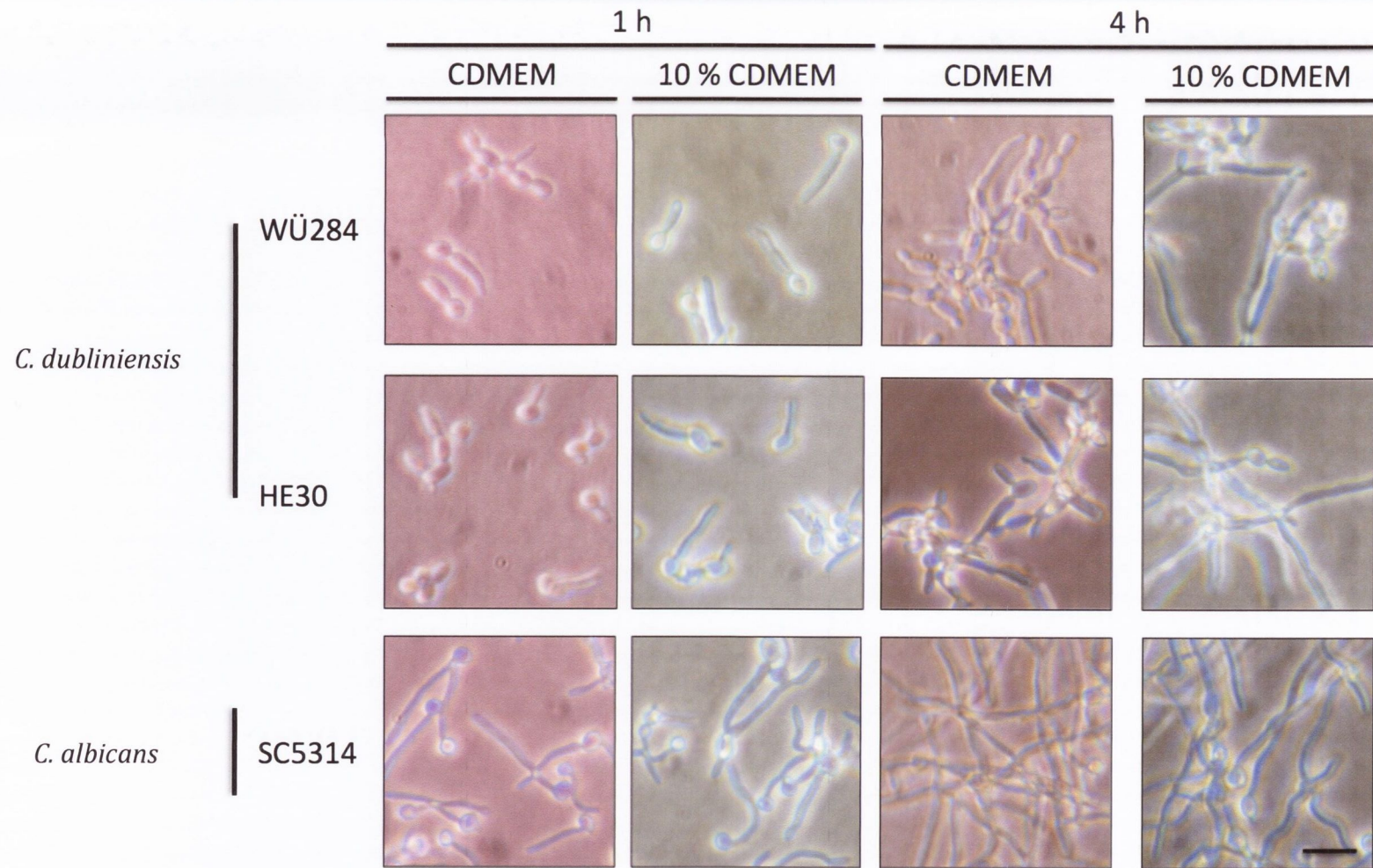


Figure 4.5. Induction of *C. dubliniensis* and *C. albicans* hyphae in tissue culture medium (CDMEM). Induction of *C. dubliniensis* and *C. albicans* hyphae with CDMEM was poor after 1 h, with significant morphological reversion after 4 h in both *C. dubliniensis* cultures. Hyphal initiation was more effective using relatively nutrient limited 10 % CDMEM. *Candida albicans* SC5314 readily produced hyphae in both growth media. Scale bar represents 10 μ m.

theme of nutrient starvation was extrapolated and 10 % (v/v) CDMEM was investigated as a *C. dubliniensis* hyphal inducing medium. Analogous to WS, 10 % (v/v) CDMEM provided relatively minimal nutrients for *Candida* growth in addition to serum to trigger hyphal induction. After 1 h growth in 10 % (v/v) CDMEM, instead of CDMEM, all the *C. dubliniensis* strains investigated displayed germ tube growth. After 4 h growth the proportion of *C. dubliniensis* hyphae in 10 % (v/v) CDMEM was much higher than observed in CDMEM, reaching approximately 60 %. However, hyphal proportions did not reach the same magnitude triggered by growth in WS. For infection model assays, hyphal induction with 10 % (v/v) CDMEM as the growth medium was used to prepare “hyphal-primed” *Candida* cells.

4.3.4. Strain variation and growth rates

As the *C. dubliniensis* Icelandic (HE-) isolates are relatively uncharacterised it was necessary to measure their growth rates under standard growth conditions to investigate any fitness defects or variations. Growth in YEPD broth at 30 °C displayed doubling times ranging between 105.2 and 127.8 min (Fig. 4.6). Analysis of the doubling times by 1-way ANOVA showed no significant difference ($P > 0.05$) between the isolates investigated. Similarly, growth in YEPD at 37 °C showed no statistical difference ($P = 0.07$) between growth rates by 1-way ANOVA. However, visualisation of the optical density data indicates a divergent pattern for HE199. This is likely reflective of measurement method limitations due to the increased tendency of HE199 to form germ tubes and self-aggregate even under normally non-inducing conditions. Unfortunately automated measurement methods are unreliable for measuring cell density of mixed morphology cultures. Other than HE199, the other isolates investigated displayed similar growth curves indicating similar fitness under the conditions tested.

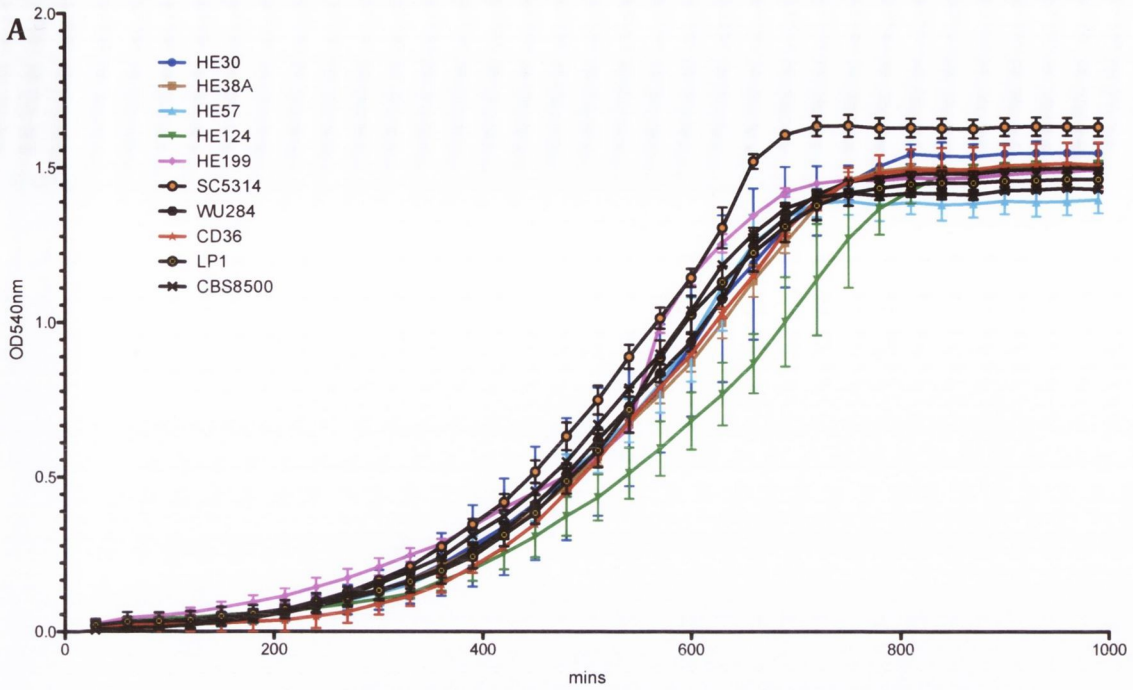
4.3.5. Yeast and hyphal adherence to TR146 human buccal epithelial monolayers

Adherence of “yeast-primed” (weak filamentation) and “hyphal-primed” (enhanced filamentation) *Candida* cells to TR146 epithelial cell monolayers was investigated by the method of Rotrosen *et al.* (Rotrosen *et al.*, 1985). As cellular adhesion is considered to be a relatively rapid process the assay was performed after 1 h coincubation of *Candida* and TR146 cells. The ability of *C. dubliniensis* cells to adhere

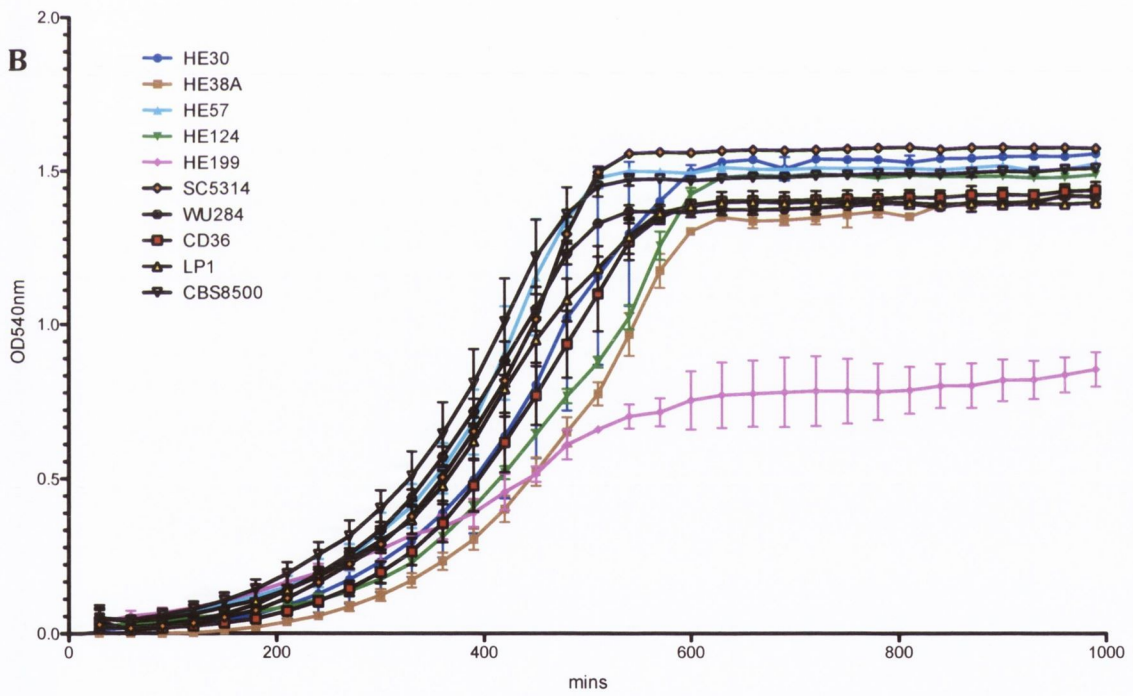
to epithelial cell monolayers was not influenced by morphology. Both yeast and hyphal cells appeared to adhere equally well to TR146 monolayers (Fig. 4.7). In contrast, when *C. albicans* cells were incubated with TR146 monolayers in CDMEM, the number of adherent cells was much higher than observed when the assay was performed in 10 % (v/v) CDMEM. This may be due to a lack of assay sensitivity regarding self-aggregating hyphal cells due to cfu being the unit of measurement in this case. The *C. dubliniensis* strain HE199 may have been affected, as it forms hyphae readily in both conditions used in the assay. While cellular morphology did not appear to result in any difference of each *C. dubliniensis* strain to adhere to TR146 monolayers, the variation in adhesive ability between strains was substantial. The adherence values ranged between approximately 50 % and 85 %. It is perhaps noteworthy that *C. dubliniensis* strains which displayed a higher propensity for forming hyphae (CBS8500 and HE30) also showed naturally higher adhesion values than less filamentous strains such as CD36 and LP1. The significance of this finding would be supported by analysis of a much larger group of both *C. albicans* and *C. dubliniensis* strains. In this way, intra-species variation seems to play an important role in the differential ability of *C. dubliniensis* strains to adapt, and adhere to the epithelial cell monolayer.

4.3.6. Morphology-associated tissue damage

The tissue damage inflicted by *Candida* morphologies on the TR146 monolayer was quantified by measuring the release of lactate dehydrogenase from damaged epithelial cells. The data were summarised as % cytotoxicity for interrogation (Fig. 4.8). The tissue damage inflicted was uniformly lower for “yeast-primed” cells compared to “hyphal-primed” cells after 4 h coincubation with TR146 monolayers. With the exception of HE199, the tissue damage caused by *C. dubliniensis* “yeast-primed” cells did not exceed 6 %. Although the damage triggered by “hyphal-primed” *C. dubliniensis* cells increased for each strain, the cellular damage did not exceed 8 % after 4 h coincubation. In contrast, *C. albicans* SC5314 “yeast-primed” cells inflicted less than 3 % damage, while “hyphal-primed” cells triggered substantial damage, leading to approximately 30 % cytotoxicity after 4 h. It is therefore clear that there is vastly differing potential for tissue damage between *C. albicans* yeast and hyphal morphologies.



	WU284	CD36	LP1	CBS8500	HE30	HE38A	HE57	HE124	HE199	SC5314
Doubling Time	122.4	109.1	105.2	125.0	127.0	126.4	121.6	127.2	107.7	127.8



	WU284	CD36	LP1	CBS8500	HE30	HE38A	HE57	HE124	HE199	SC5314
Doubling Time	117.1	92.82	113.9	123.4	94.19	86.13	102.1	99.25	160.9	93.85

Figure 4.6. *Candida dubliniensis* and *C. albicans* strain growth rates. (A) Doubling time (mins) of *C. albicans* and *C. dubliniensis* strains in YEPD broth at 30 °C showed little difference in doubling times. (B) Growth in YEPD broth at 37 °C highlighted abnormal growth of HE199, reflecting the increased tendency of HE199 to filament. Data was collected from two biological replicates.

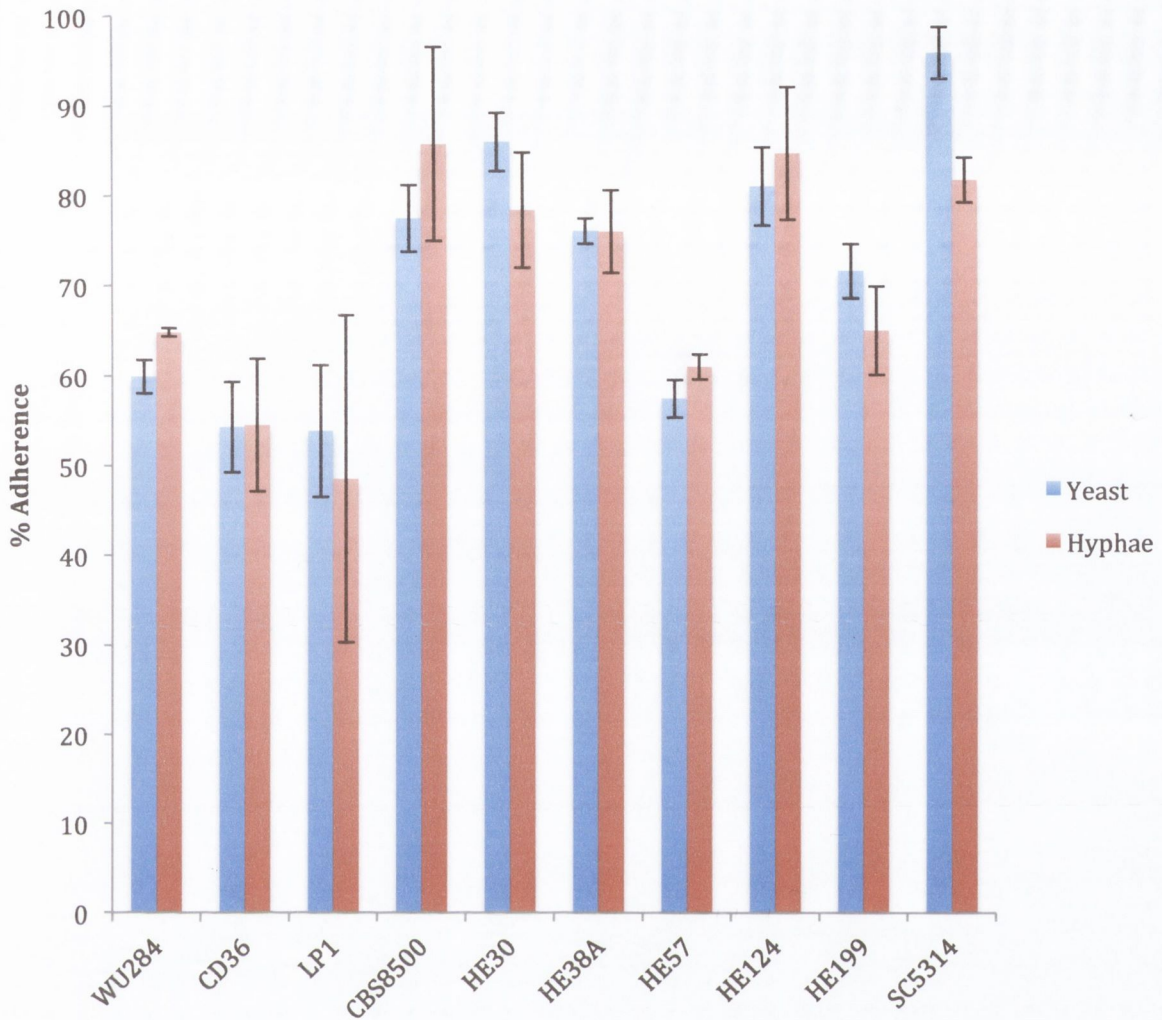


Figure 4.7. Adherence of *C. dubliniensis*, and *C. albicans* yeast and hyphae to TR146 human epithelial monolayers. *Candida dubliniensis* strains were incubated with TR146 epithelial monolayers for 1 h. Percentage adherence was measured as adherent cfu relative to the initial inoculum. Yeast cultures were incubated in CDMEM, while hyphal cultures were incubated in 10 % (v/v) CDMEM. Data represent the mean of three biological replicates.

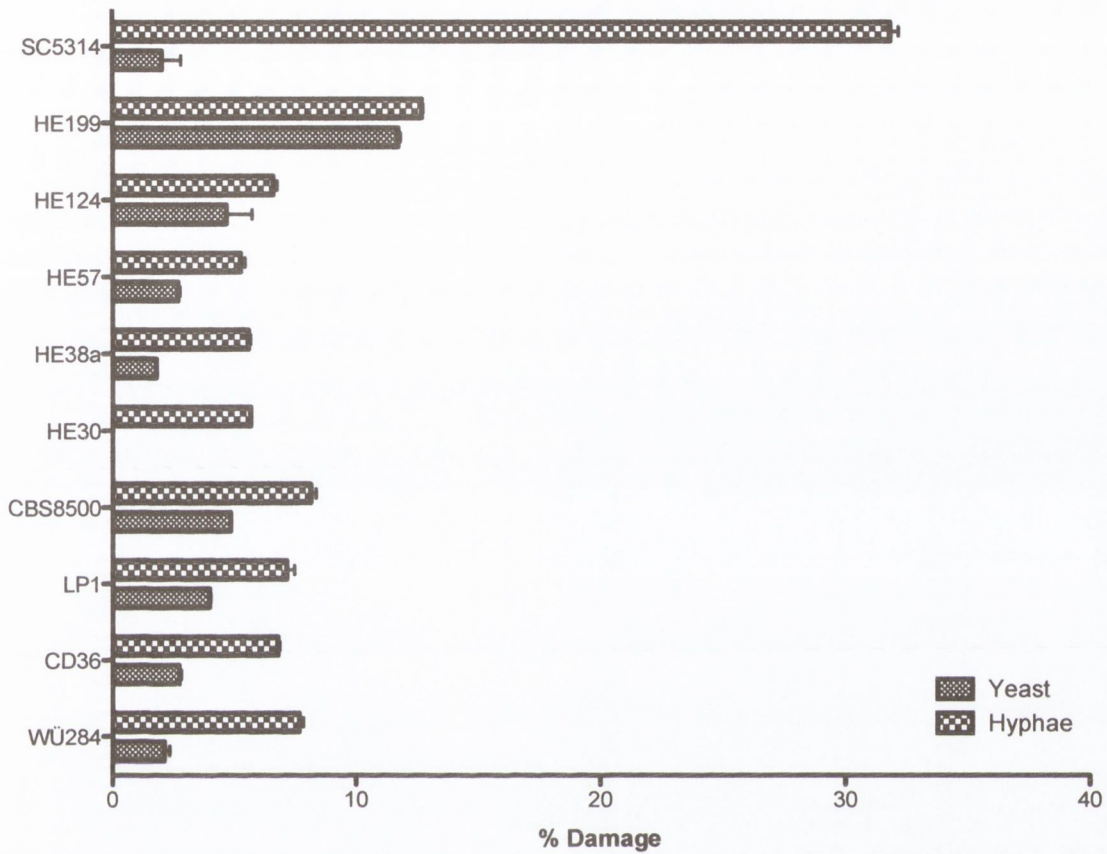


Figure 4.8. *Candida dubliniensis* and *C. albicans* morphology-associated tissue damage. Damage of TR146 epithelial monolayers, indicated by release of lactate dehydrogenase, as a result of coincubation with either *C. dubliniensis* or *C. albicans* for 4 h, showed a morphology-dependent phenotype. Growth in CDMEM resulted in predominantly yeast *C. dubliniensis* cultures while growth in 10 % (v/v) CDMEM produced cultures enriched for hyphal cells after 4 h. Data presented are the average of three biological replicates.

4.3.6.1. Visualisation of adherence and TR146 epithelial cell damage

Epithelial monolayers grown on glass slides and infected with “yeast-primed” *Candida* in CDMEM were washed in 1X PBS stained with CFW to elucidate the morphology of adherent cells. After 1 h of coincubation at 37 °C, 5 % (v/v) CO₂, *C. dubliniensis* (WÜ284 and HE30) appeared to adhere to epithelial monolayers when more than one cell clustered together (Fig. 4.9). Adherent *C. dubliniensis* cells were observed in cell clusters suggesting that the species requires the activity of multiple cells in a localised area to gain a foothold during cellular adhesion. Adherent cell clusters were also observed for *C. albicans* SC5314, although individual cells producing germ tubes were also detected after non-adherent cells were washed from the monolayer. This phenotypic pattern was similar after 3 h. After 18 h, TR146 cellular damage was visible as areas devoid of stained cells and, as a result of the cytotoxic effect of the invading fungal cells, parts of the damaged monolayer were washed away with non-adherent fungal cells. However, remaining patches of monolayer and adherent fungal cells clearly demonstrated the morphology of adherent cells. *Candida dubliniensis* cells were observed exclusively as yeast cells after 18 h and relatively little damage was inflicted to the TR146 monolayer. *Candida albicans* SC5314 adherent cells were present predominantly in the hyphal form and the cytotoxic damage inflicted to the TR146 monolayer was extensive. In this way, adherence of *C. dubliniensis* cells to TR146 epithelial cell monolayers appears to be dependent on local cell density rather than morphology, while *C. albicans* adherence may be influenced by both cell density and morphology.

4.4. Discussion

4.4.1. Induction of *C. dubliniensis* hyphae on solid media

The ability to produce hyphae is commonly investigated using a variety of hyphal inducing media. The dimorphic switch is a highly complex mechanism with a high degree of redundancy, responding to many different environmental signals. It has been shown previously that *C. dubliniensis* responds strongly to nutrient abundance and is more likely to form filaments under starvation conditions (O'Connor *et al.*, 2010). Although *C. albicans* also forms hyphae under starvation conditions it is capable of efficient filamentation in nutrient-rich growth media such as YEPD supplemented with serum. When *C. dubliniensis* strains were grown on solid hyphal-inducing media it was observed that induction of filamentation was more efficient on Spider agar rather than SLD. Spider agar is hypothesised to regulate dimorphism through the mitogen activated protein kinase (MAPK) pathway (Liu *et al.*, 1994). Almost all of the *C. dubliniensis* strains formed hyphae when grown on Spider agar. This may indicate a high degree of MAPK pathway sensitivity in *C. dubliniensis* that has yet to be explored. Growth of *C. dubliniensis* on solid hypha-inducing agar failed to identify a single strain that was capable of strong filamentous growth on all of the conditions tested. Both HE194 and HE199 produced varying degrees of filamentation on the media tested. Further study using systemic and orogastrointestinal infection models is required to ascertain whether these two *C. dubliniensis* strains display atypical virulence. The *C. dubliniensis* strains (HE30 and HE38a) identified by Asmundsdottir *et al.* as being relatively virulent in a murine model of systemic infection displayed slightly higher levels of filamentation on the solid media investigated compared to *C. dubliniensis* reference strains WÜ284 and CD36, suggesting a correlation between hypha formation and virulence.

4.4.2. Morphological identification and differentiation of hyphae

Differentiation of true hyphae, pseudohyphae, and yeast has historically been based on gross morphology (Merson-Davies & Odds, 1989). The morphology index is a powerful tool in making this distinction, but unfortunately, when working with large populations, or multiple samples over a time-course, this methodology is limited. Interpretation of morphology may be subjective as a wide range of filamentous phenotypes can be observed. Therefore it was important to confirm morphological

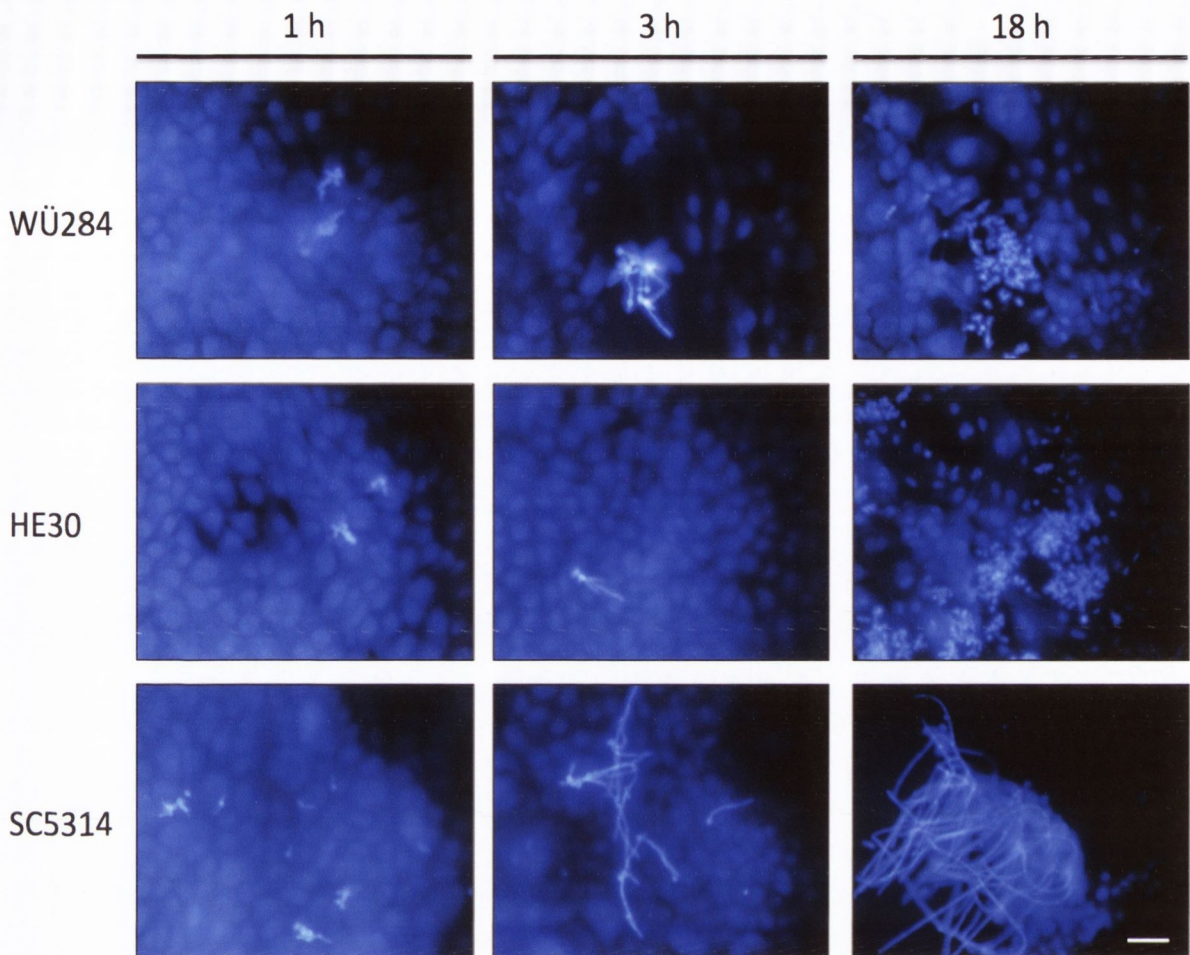


Figure 4.9. Direct visualisation of *Candida* morphology and damage of TR146 human epithelial monolayers. *Candida* cells were coincubated with TR146 monolayers grown on glass slides. Fungal cells were washed with PBS, fixed, and stained with calcofluor white to visualise chitin-rich fungal cell walls. Some background staining of TR146 epithelia was observed. Cells were coincubated in CDMEM at 37 °C under 5 % (v/v) CO₂. Adherent SC5314 displayed efficient hyphal induction after 1 h and maintained the hyphal morphology over 18 h. Damage of the monolayer was apparent as sections had been damaged and dislodged during washing of non-adherent cells. Adherent *C. dubliniensis* cells did not efficiently form hyphae after 1 h, and displayed a mixture of morphologies after 3 h. Adherent *C. dubliniensis* cells after 18 h coincubation with TR146 monolayers were predominantly in the yeast morphology. Tissue damage of TR146 monolayer infected with *C. dubliniensis* was not as extensive as observed with *C. albicans*. Scale bar represents 20 µm.

designations by a complementary method. Although patterns of nuclear replication and segregation have been investigated in *C. albicans*, this area of study has not been explored in *C. dubliniensis* (Sudbery *et al.*, 2004). This study provides the first experimental evidence of similar nuclear segregation patterns in filamentous *C. dubliniensis*. Correlation of nuclear division patterns with observed morphologies provided validation of differentiation of *C. dubliniensis* pseudo- and true hyphae in liquid culture as part of the current study. The use of DAPI for staining nuclear material may also prove useful in the future for investigating filamentous growth in other non-*C. albicans* *Candida* (NCAC) species. For example, *C. tropicalis* has also been shown to be capable of producing true hyphae, albeit at an even lower rate than *C. dubliniensis* (Fitzpatrick *et al.*, 2010; Jayatilake *et al.*, 2008). In order to better understand filamentation and its role in *Candida* virulence, it would be advantageous to investigate filamentation in NCAC in a systematic, non-subjective manner, utilising knowledge of nuclear segregation patterns for differentiation of filamentous morphologies.

4.4.3. Induction of *C. dubliniensis* hyphae in liquid media

Hyphal induction in liquid YPDS and WS media displayed a wide range of filamentation levels for *C. dubliniensis*. It is unclear whether this represents natural variation, or whether the strains investigated as part of the current study may be enriched for the ability to form filaments due to their isolation from systemic infections or superficial sites in the human host rather than environmental sources. A larger systematic study with isolates from different sources may elucidate further on any link between strain source and filamentation. The same may be true for *C. albicans*. This part of the study investigated filamentation of the most well studied *C. albicans* strain SC5314 for comparison of *C. dubliniensis* filamentation rates. However, for a more discriminatory investigation of *Candida* filamentation as a whole, additional *C. albicans* strains from various sources would need to be analysed to assess the natural range of filamentation. Currently, this work has yet to be approached in a large-scale systematic manner. Importantly, hyphal induction in liquid media allowed improved assessment of the efficiency of formation of true hyphae. Notably HE30 and HE38a displayed levels of filamentation higher than both WÜ284 and CD36, which are commonly used as *C. dubliniensis* reference strains. In summary, the *C. dubliniensis* strains designated as being “virulent” displayed higher

than normal levels of hyphae, indicating a possible link between *C. dubliniensis* hyphae and virulence.

4.4.4. Morphology and fungal adherence to human epithelial cells

The ability of *C. dubliniensis* strains to adhere to epithelial cells has been investigated previously and has been found to be highly variable depending on strains and growth conditions (Biasoli *et al.*, 2010; Gilfillan *et al.*, 1998). One factor in common with these studies is that the *C. dubliniensis* cells were in the yeast form and the adherent properties of *C. dubliniensis* hyphae have not been examined. By incubating *C. dubliniensis* in either CDMEM or 10 % (v/v) CDMEM it was possible to obtain *C. dubliniensis* populations which contained either low or high proportions of hyphae, respectively. Growth in nutrient-rich CDMEM yielded *C. dubliniensis* cultures with minimal levels of hyphae, while incubation in 10 % (v/v) CDMEM triggered stronger hyphal induction and resulted in cultures enriched for hyphae. The impact of the morphology of *C. dubliniensis* on adherence to epithelial cells was assessed. No detectable difference in adherence to TR146 epithelial cells was observed between *C. dubliniensis* cultures enriched for either yeast or hyphae. In support of previous studies, intra-species variation in adherence played a more important role than morphology in the initial stages of adherence (1 h). It is possible that morphology may play a more significant role at later stages of colonisation and infection. Although upregulation of adhesion-associated genes has been shown to be rapid in *C. albicans* and *C. dubliniensis* cells undergoing the transition to hyphae, little has been experimentally verified regarding the distribution and abundance of *C. dubliniensis* putative adhesive proteins, such as CdHwp1p, on the cell surface (Kadosh & Johnson, 2005).

4.4.5. Fungal morphology and tissue damage

Analysis of damage triggered by yeast and hyphal *C. dubliniensis* cells showed that LDH release from epithelial cells, as an indicator of tissue damage, was greater in *C. dubliniensis* hyphal cells compared to yeast cells. However, the levels of damage observed for *C. dubliniensis* hyphal cells were much lower than observed for *C. albicans* hyphae. However, it is important to note that under the growth conditions investigated, *C. dubliniensis* hyphal formation was still not equivalent to *C. albicans* hyphal formation. There are a number of mechanisms posited to be responsible for

hypha-associated cell damage. Active penetration and endocytosis have been shown to contribute to invasion of host cells by *C. albicans* (Dalle *et al.*, 2010). While proteins such as *CaAls3p* facilitate uptake of *C. albicans* by a host cadherin-dependent mechanism during the early stages of infection, active extension of elongating hyphae into cells through physical force has been demonstrated to play a dominant role within 3 h of infection (Phan *et al.*, 2007; Wachtler *et al.*, 2012). Active penetration of hyphae into host cells is poorly understood and is likely a result of a number of contributing factors including thigmotropism, hyphal extension kinetics and the elaboration of *Candida* proteases to weaken the host cell membrane (Mayer *et al.*, 2013; Wachtler *et al.*, 2011). These are all areas of study that have yet to be investigated in *C. dubliniensis*. Considering the clear difference in efficiency of elaboration of hypha formation between the two *Candida* species, it is likely that additional differences exist between *C. albicans* and *C. dubliniensis* hyphae, such as elongation kinetics and tropism. Regardless, further analysis is required to define the transcriptomic and protein expression profile of *C. dubliniensis* yeast and hyphal cells under the conditions investigated. It is highly probable that the lack of hyphal virulence-associated proteins, such as *CaAls3p* and *CaHyr1p*, from the *C. dubliniensis* protein repertoire contributes strongly to the relative lack of hyphal pathogenicity. In addition, *C. dubliniensis* lacks some secreted aspartyl proteases (*SAP5*, *SAP6*) and possesses a truncated form of *HWP1* that encodes a hyphal adhesin in *C. albicans* (Jackson *et al.*, 2009; Moran *et al.*, 2012). It is not known whether *CdHWP1* encodes a functional protein. Little is known about the composition of the *C. dubliniensis* cell wall in either morphology, and is therefore an obvious area of focus for future study. Nevertheless, this part of the current study has shown that when *C. dubliniensis* hyphae were induced to form hyphae, at a higher rate than previously investigated, there was an increase in tissue damage. However, this apparent increase was much lower than that observed for *C. albicans* cells induced to undergo the transition from yeast to hyphae. It is worth noting that the “virulent” *C. dubliniensis* strains HE30 and HE38a did not display an increase in tissue damage relative to similarly treated WÜ284 or CD36, suggesting that the previously observed “virulence” was specific to the experimental conditions of the murine systemic model, and may not be relevant to the epithelial tissue interface. Use of other infection models or cell types may highlight virulent phenotypes not observed as part of this study.

4.4.6. Future directions

In summary, a wide range of filamentation was observed for *C. dubliniensis* strains under *in vitro* filamentation conditions. Increased propensity for filamentation appeared to correlate with reported strain virulence. Adhesion to epithelial monolayers mirrored this observation, with “virulent” *C. dubliniensis* strains exhibiting increased levels of adherence relative to commonly used reference strains. However, this adherence was not dependent on morphology under the conditions investigated, suggesting a role for a morphology-independent mechanism during the early stages of *C. dubliniensis* attachment to epithelial cells. Morphology did play a minor role in the causation of tissue damage, as *C. dubliniensis* strains displayed an increase in damage when cells were induced to filament at a relatively high rate. However, the resultant increase in damage was much lower than observed for *C. albicans* SC5314 and even the “virulent” *C. dubliniensis* HE30 and HE38a did not result in similar levels of damage when induced to form hyphae. In the case of *C. dubliniensis* hyphae it appears that the lack of hypha-associated virulence genes contributes strongly to the relative lack of hyphal virulence. Further analysis of the mechanisms by which *C. dubliniensis* hyphae cause tissue damage will determine whether the damage observed as part of this study was due to mechanical extension of hyphae into host cells or protein-mediated.

Chapter 5

Improved *Candida dubliniensis* hyphal induction and maintenance

5.1. Introduction

5.1.1. *Candida* hyphal induction signals

5.1.1.1. Serum

The routine diagnostic test for *C. albicans* is performed by inoculating *Candida* cells into bovine serum and incubating the cultures for two to three hours at 37 °C (Mackenzie, 1962). Cells displaying filaments after this time period are routinely identified as *C. albicans*. However, most *C. dubliniensis* strains will also filament with varying efficiency under these conditions and thus, many *C. dubliniensis* strains were originally, and continue to be, misidentified as *C. albicans* (Sullivan *et al.*, 1995). Although diagnostic and typing methods have significantly improved since this germ tube test was first established, the mechanisms responsible for *Candida* hyphal formation are still not completely understood (McManus & Coleman, 2013). In particular, the complexity and variation of human and animal sera present a challenge (Statland *et al.*, 1976). While certain studies have stated that glycoproteins, specifically muramyl dipeptides similar to bacterial peptidoglycan, are the hyphal-inducing signal present in sera, it is clear that this may not be the only effector molecule (Piispanen & Hogan, 2008). Glycoproteins are a large family of molecules comprised of oligosaccharide molecules covalently bonded to polypeptide chains. Within glycoproteins there is a high level of potential variation in oligosaccharide composition. Glucose, mannose, galactose, fucose, and many other carbohydrate moieties are able to bond to peptide groups (Dell & Morris, 2001). The manner in which the covalent bond forms varies with both *n*- and *o*-glycosylation possible (Ruddock & Molinari, 2006). The ratios of serum components commonly vary between batches making it a difficult task to assign direct hyphal-inducing effects to various components of serum (Statland *et al.*, 1976). For this reason it is highly desirable to replace serum with defined molecules or compounds which will perform a similar role in the reliable and reproducible induction of *Candida* hyphae.

Serum is currently thought to activate hyphal induction pathways by activating both *RAS1* and the adenylyl cyclase gene *CYR1* independently (Wang & Xu, 2008). Ras1p itself, reinforces *CYR1* activity by binding to a conserved N-terminal RAS-association domain, while muramyl dipeptide-like molecules bind to a leucine-rich repeat

sequence domain (Fang & Wang, 2006; Wang & Xu, 2008). Increased *CYR1* activity results in an increase in cAMP synthesis, which in turn stimulates hyphal associated gene expression through activation of *EFG1* (Leberer *et al.*, 2001; Rocha *et al.*, 2001). Activation of *RAS1* appears to be key in the dimorphic switch in *C. albicans* as it regulates both the cAMP and MAPK major signal transduction pathways, thus indicating why serum is such a potent inducer of hyphal growth.

5.1.1.2. *N*-acetylglucosamine

N-acetylglucosamine (GlcNAc) is a glycoprotein that has been identified as a defined hyphal inducer. It is a highly abundant molecule that is present in human serum, bacterial cells and fungi.

Both Gram-positive and Gram-negative bacteria produce peptidoglycan as an integral part of their cell wall. Peptidoglycan is composed of alternating subunits of GlcNAc and *N*-acetylmuramic acid (Lovering *et al.*, 2012). Peptidoglycan is regularly shed into the extracellular environment (Nigro *et al.*, 2008). In this way, it can act as a signaling molecule between bacteria or other organisms (Kuss *et al.*, 2011). *Candida albicans* is commonly found as a commensal on mucosal surfaces in the gastrointestinal or urogenital tracts and may encounter extracellular peptidoglycan at these sites (Bougnoux *et al.*, 2006). In complex interspecies biofilms it is hypothesised that peptidoglycan released by bacteria may induce *C. albicans* to form hyphae, leading to invasion of host tissues (Wang & Xu, 2008).

GlcNAc is also an integral part of fungal cell walls. The inner cell walls of *Candida* are composed of a layer of chitin bound to glucan by β -1,3- and β -1,6- glycosidic linkages (Munro *et al.*, 2001). This serves as a base layer anchoring mannan fibrils and GPI-anchored proteins. Fungal chitin itself is a polymer based on multiple units of GlcNAc. While other parts of the cell wall are quite stable, chitin is rapidly synthesised and turned over as the cell responds to its growth environment (Munro *et al.*, 1998). Degradation of chitin provides another source of GlcNAc in the extracellular environment. Sensing of GlcNAc has been found to trigger two main signal transduction responses. The transporter Ngt1p internalises GlcNAc and the cAMP cascade is activated in a similar fashion to serum induction (Alvarez & Konopka, 2007). In addition, genes for GlcNAc catabolism are induced, providing the building

blocks for chitin synthesis (Gunasekera *et al.*, 2010; Kumar *et al.*, 2000). Surprisingly, genes historically associated with galactose metabolism were found to also be upregulated on exposure to GlcNAc (Kamthan *et al.*, 2013). However, Martchenko *et al.* have shown that the regulon originally responsible for regulation of the Leloir galactose metabolism pathway has been subverted in *C. albicans* and is no longer responsible for galactose metabolism (Martchenko *et al.*, 2007). Interestingly *Candida GAL1*, *GAL7* and *GAL10* possess a binding sequence for Cph1p in their promoter regions and may play an important role in the dimorphic switch. A *C. albicans GAL10* null mutant has been found to display increased filamentation (Singh *et al.*, 2007). While GlcNAc has been shown to efficiently induce filamentation in *C. albicans*, there are relatively few publications describing the response of *C. dubliniensis* to GlcNAc.

5.1.1.3. Quorum sensing and cell density

Cell density has been shown to play an important role in microbial cell communication (Boyer & Wisniewski-Dye, 2009). While it is known that *C. albicans* and *C. dubliniensis* undergo cell-signaling interactions, the importance of cell density in a growing and morphologically developing population has not been explored fully (Hogan *et al.*, 2004; Martins *et al.*, 2007). Large variations exist between the cell inocula used in infection model methods. While these variations in cell density may be necessary depending on the infection model, it is not clear what effect the inoculum density may have on the dimorphic characteristics of the organisms being inoculated. *Candida* strains investigated in the murine systemic model are commonly inoculated with approximately 2×10^6 cells/ml (Asmundsdottir *et al.*, 2009; Sundstrom *et al.*, 2002a). The initial inoculum is much higher in the murine orogastrointestinal model in which 2×10^8 fungal cells are introduced orally (Clemons *et al.*, 2006). *In vitro* models, such as the three dimensional RHE model, use approximately 2×10^6 cells (Naglik *et al.*, 2008b). Similarly, the basic *in vitro* 6-well plate assay for *Candida* hyphal formation commonly uses 2×10^6 cells/ml as an initial inoculum (Stokes *et al.*, 2007). Under many of these infection model conditions *C. dubliniensis* is found to filament poorly relative to *C. albicans* and this is frequently viewed as the reason for lower invasion and virulence levels displayed by *C. dubliniensis* (Moran *et al.*, 2012; Stokes *et al.*, 2007). However, cell-cell interactions are not fully understood and thus the impact of inoculum variations on the *C. dubliniensis* dimorphic switch has not been defined.

Cyclic adenosine monophosphate (cAMP) is an important signal transduction molecule. It is derived from ATP and thus serves as an indicator of free energy in cells (Chen *et al.*, 2011). It has been found to play a prominent role in the initiation of *C. albicans* hyphal formation as a core component of the *RAS1* signalling pathway (Hogan & Sundstrom, 2009). Generation of cAMP by the adenylate cyclase Cyr1p in turn leads to activation of protein kinase A (PKA) and transcription of hyphal specific genes through *EFG1* activity (Rocha *et al.*, 2001). Both Cyr1p and cAMP have been found to function in a feedback loop on *RAS1* activity, indicating interaction between free energy levels and maintenance of hyphal induction (Piispanen *et al.*, 2013). Addition of exogenous cAMP to *C. albicans* cells has been used to improve initiation of hyphal formation, while mutants with hyperactive *CYR1* have also been shown to exhibit hyperfilamentous phenotypes (Lindsay *et al.*, 2012; Moran *et al.*, 2007). *Candida dubliniensis*, however, does not appear to share this cAMP-sensitive phenotype. Addition of 10 mM cAMP to exponential phase *C. dubliniensis* WÜ284 cells in medium containing proline had no apparent effect, indicating significant divergence between the hyphal initiation mechanisms of *C. albicans* and *C. dubliniensis* with relation to free energy levels (Moran *et al.*, 2007).

Farnesol and farnesoic acid are widely recognised as autoregulatory quorum sensing molecules. Farnesol has been shown to coordinate cell behavior in complex populations by inhibiting the yeast to hypha transition (Albuquerque & Casadevall, 2012; Weber *et al.*, 2010). In complex structures such as biofilms this is important for adaptive development and maturation of the biofilm (Deveau & Hogan, 2011; Ganguly *et al.*, 2011). Although this organic molecule has been studied in *C. albicans* there is little understanding of its function in *C. dubliniensis*. Henriques *et al.* have demonstrated that relatively low levels of farnesol are sufficient to inhibit the formation of *C. dubliniensis* hyphae under hyphal inducing conditions without impacting the growth rate of the yeast (Henriques *et al.*, 2007). The mechanism by which farnesol acts on *C. albicans* is not fully defined but it is thought to act through inhibition of *CYR1* (Deveau *et al.*, 2010). In this way, the maintenance of hyphal morphology is repressed leading to reversion of hyphal cells to yeast cells.

While it is apparent that farnesol efficiently represses the formation of hyphae in *C. dubliniensis*, less is known about tyrosol. Tyrosol is also a quorum sensing molecule (De Sordi & Muhlschlegel, 2009). However, it appears to have an opposite effect to that of farnesol. In *C. albicans*, tyrosol has been shown to aid initiation of hyphal formation and reduce the length of the lag phase in growing cells (Chen *et al.*, 2004). This induction effect can be negated by farnesol indicating a dynamic balance between positive and negative autoregulation by QS molecules. Currently, the effect of tyrosol on initiation of *C. dubliniensis* hyphae has not been investigated and thus represents another gap in the understanding of the dynamics of *C. dubliniensis* dimorphism.

5.1.1.4. Nutrient sensing

Nutrient abundance, and nitrogen availability in particular, is known to have an effect on *Candida* dimorphism. Nutrient rich YEPD cultures commonly grow in the yeast phase unless supplied with an additional hyphal induction signal such as elevated temperature, or acidic pH. In *C. albicans*, the ammonium permease, Mep2p, is known to sense extracellular nitrogen levels (Biswas & Morschhauser, 2005). In cases of nitrogen limitation, hyphae are induced through activation of *RAS1* by the C-terminal domain of Mep2p. In this way, nitrogen limitation appears to impact hyphal induction through both the MAPK and PKA major morphological pathways.

Candida dubliniensis especially shows a strong response to nitrogen, as supplementation of WS hyphal inducing medium with 2 % (w/v) peptone has previously been demonstrated to reduce *C. dubliniensis* hypha formation (O'Connor *et al.*, 2010). O' Connor *et al.* have shown that addition of BSA as a whole protein analogue, or nitrogen supplementation with 100 mM ammonium sulphate resulted in a reduction in *C. dubliniensis* hyphal formation while having no deleterious effect on *C. albicans* hyphal formation. Clearly, there is a difference in either the environmental sensing mechanisms or nutrient availability response between *C. albicans* and *C. dubliniensis*.

Bastidas *et al.* have shown that Tor1p, a highly conserved eukaryotic kinase, regulates expression of a number of genes including *NRG1* (Bastidas *et al.*, 2009). Among its multiple functions, Tor1p appears to interpret nutrient levels and repress starvation

responses (Bastidas *et al.*, 2009; Sullivan & Moran, 2011). Thus *TOR1* activity contributes to repression of starvation-related hyphal induction. Addition of rapamycin to *C. dubliniensis* cells, blocking *TOR1* activity, results in the relief of repression of hyphal induction (Sullivan & Moran, 2011). The disparity between dimorphic switching of *C. albicans* and *C. dubliniensis*, under nutrient rich and nutrient limited conditions, likely plays an important role in the difference in virulence and commensalism between the two species.

5.1.1.5. Carbon dioxide

Carbon dioxide is central to a number of phenotypes displayed by *C. albicans*. It is involved in the white to opaque switch in mating-competent cells (Huang *et al.*, 2009). More importantly, for this study, elevated CO₂ levels induce hypha formation in *Candida* species (Hall *et al.*, 2010; Klengel *et al.*, 2005). This hypha-inducing signal is omnipresent in the environment. Recently it has gained attention as additional morphologies linked to high-CO₂ conditions have been discovered and described in *C. albicans*. “Fingers” and “tentacles” join hyphae on the list of potential virulent morphologies as they are observed under elevated CO₂ conditions (Daniels *et al.*, 2012). This is a striking find considering CO₂ saturation is estimated to be 5 % (v/v) and 20 % (v/v) in tissues and the gastrointestinal tract respectively (Daniels *et al.*, 2012). CO₂ is understood to activate hyphal induction through the interaction of carbonate ions with Cyr1p (Hall *et al.*, 2010). Consequently, hyphal development, as a result of CO₂ sensing, is mediated by the cAMP/PKA pathway.

While *C. dubliniensis* routinely experiences high CO₂ conditions in the host and infection models, little is known about the specific adaptive response to CO₂ (Moran *et al.*, 2007). Assumptions are inferred from *C. albicans* data but, as with other hypha inducing signals, many of these have yet to be experimentally tested.

5.1.1.6. Carbon source

The standard growth medium for *Candida* is nutrient-rich YEPD. This medium contains 2 % (w/v) glucose as the carbon source. Lee’s medium also contains glucose as the carbon source, although Lee’s medium only contains 1.25 % (w/v) glucose. Ene *et al.* have demonstrated the impact that growth on alternative carbon sources can have on not only the *C. albicans* cell wall but also on virulence and host responses

after growth on 2 % (w/v) lactate (Ene *et al.*, 2013). Similar to *C. albicans*, *C. dubliniensis* cells are commonly maintained on glucose-rich media prior to many kinds of experiments. Previously Gilfillan *et al.* had investigated *Candida* adherence attributes after growth on either glucose or galactose, finding no difference in adherence to BECs between *C. albicans* and *C. dubliniensis* after growth on galactose (Gilfillan *et al.*, 1998). This study used 500 mM galactose and assayed the adherence of yeast cells specifically. Work since then has shown that microsupplementation of *C. dubliniensis* cells with low levels of galactose can reduce expression of *NRG1*. Although galactose can serve as a carbon source, supplementation with low levels of the monosaccharide appear to activate a starvation response (Citiulo *et al.*, 2009). As already mentioned, metabolism of galactose in *Candida* is poorly understood as the genes associated with its metabolism in other yeast such as *S. cerevisiae* appear to be responsible for alternative functions (Martchenko *et al.*, 2007). Galactose-induced genes *GAL1*, *GAL7* and *GAL10* seem to play a role in the dimorphic switch in association with Cph1p. Currently this is poorly understood in both *C. dubliniensis* and *C. albicans* and is an area that requires further study with respect to the dimorphic switch.

5.1.2. Hyphal commitment and reversion

The dominant trend observed during *C. dubliniensis* hyphal induction is the transient induction of short-term hyphae, followed by reversion and proliferation of yeast form cells. The commitment phenomenon has been described in *C. albicans* as the window of opportunity in which a hyphal cell either commits to the filamentous form or reverts to blastospore growth (Chaffin & Wheeler, 1981; Mitchell & Soll, 1979). Similarly, this appears to be the case with *C. dubliniensis*, as even hyphal cells efficiently induced by WS treatment begin to revert to yeast form approximately 3 h after induction. Due to this phenomenon it is difficult to interrogate experimental data such as microarray transcriptome data (O'Connor *et al.*, 2010). Cells treated with hyphal inducing media appear to be in a state of flux and, while transcriptome data gives a snapshot of the cell at a particular time, this is part of a dynamic developmental program that ultimately reverts to yeast growth. For this reason, in order to study *C. dubliniensis* hyphae, it is highly desirable to bypass the reversion of *C. dubliniensis* hyphae to yeast in order to achieve stable, committed *C. dubliniensis*

hyphae. In this way it is possible to achieve data for absolute morphologies as opposed to cells in a fluctuating state of change between one form and another.

5.1.3. Aims of this part of the study

This part of the study attempted to identify and investigate the factors influencing the formation, maintenance and reversion of *C. dubliniensis* hyphae. This was done in order to obtain stable, committed *C. dubliniensis* hyphae for analysis of the role of major morphological regulators during the filamentous transition.

5.2. Specific materials and methods

5.2.1. Development of an improved method for *C. dubliniensis* hyphal initiation and maintenance

5.2.1.1. Nutrient abundance

Cells were prepared by growth on YEPD agar at 37 °C for 48 h. A single colony was isolated and inoculated in either YEPD broth or Lee's pH 4.5 broth and grown at 30 °C with shaking for 18 h. After 18 h, cells were washed with 1X PBS and inoculated in hyphal induction medium at a density of 1×10^5 cells/ml, unless otherwise stated.

Hyphal formation in *C. dubliniensis*, and *C. albicans*, was triggered and maintained using a medium developed from that used for induction of *C. albicans* hyphae by (Heilmann *et al.*, 2011). The nutrient medium, here referred to as DUBLIN medium, was prepared as a 10X stock solution composed of 0.7 % (w/v) Yeast nitrogen base, without amino acids or ammonium sulfate (YNB –a.a. –(NH₄)₂SO₄), and 75 mM MOPS buffered to pH 7.4. Nitrogen was added directly to the solution by addition of 5 mM GlcNAc. Unless otherwise stated, GlcNAc represented the sole nitrogen source in DUBLIN medium. Hyphal induction solutions were prepared from the buffered stock solution as required.

Yeast Nitrogen Base lacking amino acids but containing ammonium sulphate (YNB – a.a.) was used in place of YNB (–a.a. –(NH₄)₂SO₄), to assay the importance of nitrogen availability and limitation during *C. dubliniensis* hyphal formation. Varying concentrations (0.1X, 0.5X, 1X, 2X) of DUBLIN medium were tested both for hyphal initiation and hyphal maintenance over extended time periods. *Candida albicans* and *C. dubliniensis* cultures were assessed microscopically after 6 h and 18 h for the presence and proportion of yeast and hyphae. WS medium was used as a reference for comparison of short-term hyphal initiation efficiency.

5.2.1.2. Oxygen and carbon dioxide

Oxygenated conditions were generated by growing cultures under atmospheric oxygen in either static or orbital incubators.

Carbon dioxide-enriched conditions were prepared by growing cultures statically in a CO₂ incubator under 5 % (v/v) CO₂ or in a rotary incubator, within an anaerobic gas jar containing a CO₂ gas pack generating between 5 % - 8 % (v/v) CO₂.

5.2.1.3. Quorum and environmental sensing

The influence of initial cell density on the efficiency of hyphal formation was assayed by varying the inoculation density of cells being transferred to hyphal inducing media. DUBLIN medium (1X) was inoculated with cells to a final density of 2×10^3 , 2×10^4 , 2×10^5 , or 2×10^6 cells/ml and grown for 18 h

The contribution of cAMP to *C. dubliniensis* hyphal formation was assessed by addition of exogenous cAMP (500 nmoles/ 1000 nmoles/ 2000 nmoles) to 1X DUBLIN medium (+ (NH₄)₂SO₄).

Tyrosol was investigated as a potential hyphal inducer in *C. albicans* and *C. dubliniensis*. Tyrosol was added to hyphal inducing media in 20 µM increments up to a final concentration of 100 µM.

5.2.1.4. Carbon source availability

In order to assess the effects of carbon source availability on hyphal formation, various carbon sources were added to 1X DUBLIN medium in the form of simple carbohydrates. Glucose, sucrose, or galactose was added to hyphal induction medium to a final concentration of 0.1 % (w/v) or 0.5 % (w/v). Cultures were grown for 18 h and assessed microscopically.

5.2.2. Optimal growth, hyphal induction and morphology maintenance

The WS- and DUBLIN-induction methods were combined to explore the long-term efficacy of a solution designed to specifically target short-term hyphal initiation and long-term hyphal maintenance. In order to achieve this, *Candida* cells were incubated in 1X DUBLIN medium, with 0.1 % (w/v) galactose, and further supplemented with

10 % (v/v) FCS. Cultures were incubated under 5 % (v/v) CO₂ for 18 h. Culture morphology was assessed microscopically.

The ability of this DUBLIN/FCS medium to induce and maintain *C. dubliniensis* hyphae on agar plates was investigated. Agar plates containing DUBLIN medium, supplemented with 0.1 % (w/v) galactose and 10 % (v/v) FCS, and 2 % (w/v) bactoagar were prepared. PBS-washed cells from overnight *Candida* cultures grown in Lee's pH 4.5 at 30 °C were transferred to DUBLIN/FCS agar and incubated at 37 °C under 5 % (v/v) CO₂ for 3 days.

Due to the complexity and redundancy of interacting hyphal inducers in *C. albicans* it was necessary to not only isolate hyphal induction signals for *C. dubliniensis*, but also combine them in a number of ways in order to assess the contribution of each inducer to both hyphal formation and maintenance.

5.2.3. Analysis of morphogenetic regulator expression

5.2.3.1. Yeast morphology

Yeast cells were grown under standard YEPD growth conditions. Briefly, yeast cells were taken from a 48 h YEPD plate and grown aerobically with shaking in glucose-rich YEPD broth for 18 h at 37 °C.

5.2.3.2. Hyphal morphology

WS induction was chosen to be the historical reference condition as microarray data for *C. dubliniensis* cells induced to form hyphae under this condition are available (O'Connor *et al.*, 2010). Cells were prepared as described in Chapter 4. Briefly, cells from a 30 °C YEPD preculture were washed in 1X PBS, inoculated in WS (1 x 10⁵ cells/ml) preheated to 37 °C and grown aerobically with shaking for 18 h at 37 °C.

DUBLIN/FCS induction was used as an alternative, improved method for inducing stable, committed *C. dubliniensis* true hyphae. To this end, the growth and induction conditions matched those already discussed for DUBLIN/FCS induction. Briefly, cells were pregrown in Lee's medium pH 4.5 at 30 °C, harvested, washed in 1X PBS and inoculated in preheated DUBLIN induction medium supplemented with 0.1 % (w/v)

galactose and 10 % (v/v) FCS. Cultures were grown statically at 37 °C under 5 % (v/v) CO₂ for 18 h.

5.2.3.3. *Experimental timepoints*

In order to collect data over an extended time period, cells from yeast or hyphal cultures were harvested, washed in 1X PBS, and snap frozen in liquid nitrogen at 0, 1, 3, 6, 18 h time points. Cells from either the YEPD or Lee's pH 4.5 overnight precultures represented the T₀ timepoint. Cells frozen in liquid nitrogen were stored at -80 °C for subsequent breaking and RNA extraction.

5.2.3.4. *Cell disruption and RNA extraction*

Cells were disrupted by mechanical breakage using a Biospec Mini Bead Beater-24. Cells were subjected to three rounds of disruption at 3000 r.p.m. for 1 min each. Broken cells were chilled on ice between each successive breaking round. Otherwise, RNA was extracted in the same way as described in Chapter 2. RNA was eluted from the RNeasy Mini Kit column and nucleic acid concentration was measured prior to storage at -20 °C.

5.2.3.5. *Generation of cDNA*

A total of 1 µg of RNA, in each case, was used to generate cDNA according to the method outlined in Chapter 2. However, in this case, the improved Superscript Reverse Transcriptase III (Invitrogen) kit was used. Quality of cDNA was assessed by PCR using primers EFB1F1 and EFB1R1 to test for the presence of contaminating gDNA.

5.2.3.6. *Primer design for qRT-PCR*

A small selection of genes encoding major regulators known to play a role in the control of morphogenesis was chosen to represent the regulatory pathways responsible for the phenotypes observed, using different morphological induction media. Three major morphological-associated genes (*EFG1*, *CPH1* and *NRG1*) were chosen to present a view of both positive and negative regulation of the dimorphic switch. Primers for qRT-PCR were designed using Primer3 (<http://bioinfo.ut.ee/primer3/>). Primer pairs were chosen for potential ability to bind both *C. albicans* and *C. dubliniensis* DNA. Due to the sensitivity of qRT-PCR a

cutoff of a single primer nucleotide mismatch was established. Amplification efficiency of primer pairs was tested as outlined in Chapter 2. Similar amplification efficiency to *ACT1* amplification was confirmed in each case. Primers used in this study are listed in Table 2.2.

5.2.3.7. Analysis of gene expression

Gene expression was analysed using an Applied Biosystems 7500 Fast Real-Time PCR System in conjunction with Fast SYBR Green Master Mix. In a 15 μ l final volume, 7.5 μ l Fast SYBR Green was added to 0.75 μ l of each forward and reverse primer, and 0.5 μ l cDNA generated from extracted RNA. PCR cycling conditions used were 95 °C for 30s, and 40 cycles of 95 °C for 15 s, 60 °C for 15 s, 72 °C for 30 s. Fluorescence data was collected during the amplification step. Both threshold and mean C_t values were automatically calculated by the SDS v2.0.x software (Applied Biosystems). In each reaction, *ACT1* was used as the internal endogenous control. Data were converted from .csv files and exported as .xlsx files for analysis. Comparative threshold values were averaged over three replicate wells. Change in gene expression was visualised as the fold change in transcript abundance over time by calculating the $2^{\Delta\Delta C_t}$ value and plotting this against the timepoints assayed (Schmittgen & Livak, 2008). Data from T_0 correspond to gene expression levels from YEPD- or Lee's- precultured cells. Thus, all subsequent fold changes in expression at later time points are relative to the state of the cells from the initial inoculum. *ACT1* is routinely used as an endogenous control so gene expression relative to *ACT1* was also calculated to give perspective of relative transcript abundance within cells.

5.3. Results

5.3.1. The impact of nutrients on *C. dubliniensis* hyphal induction

The importance of suitable preculture conditions for the establishment and maintenance of *C. dubliniensis* hyphae was tested by initially growing cells in either nutrient-rich YEPD or nutrient-poor Lee's medium (Fig. 5.1). *Candida dubliniensis* cells grown in YEPD and inoculated in WS showed low levels of filamentation after 18 h of growth. Blastospores were the predominant morphotype under these growth conditions. In contrast, *C. dubliniensis* cells, particularly WÜ284, grown initially in Lee's medium and then inoculated in WS showed slightly higher levels of filamentation than their YEPD-grown counterparts after 18 h. Under matching conditions, *C. albicans* cells readily formed hyphae in both cases and the dominant morphology after 18 h was hyphal growth with only a small percentage of yeast present. Quantification of yeast and hyphal ratios was difficult after 18 h growth and for this reason qualitative assessments were made after analysing at least 5 microscopic fields of view.

Using DUBLIN medium (+ $(\text{NH}_4)_2\text{SO}_4$), as the hyphal inducing medium instead of WS, displayed similar results, with yeast being dominant in *C. dubliniensis* cultures pregrown in YEPD. *Candida dubliniensis* cells grown in Lee's medium showed a small decrease in the number of blastospores present after 18 h growth in DUBLIN medium (+ $(\text{NH}_4)_2\text{SO}_4$), and a corresponding increase in hyphal extension and proliferation. *Candida albicans* cells grown in either YEPD or Lee's medium and inoculated in DUBLIN medium (+ $(\text{NH}_4)_2\text{SO}_4$) displayed high levels of hyphal growth in either case, confirming the importance of nutrient levels for the formation of *C. dubliniensis* hyphae specifically.

To further investigate the importance of nutrient availability during active hyphal induction, cells were pregrown in Lee's medium and inoculated in 0.1X, 0.5X, 1X, 2X (v/v) DUBLIN medium, lacking ammonium sulphate and amino acids (Fig. 5.2). When cultured in 5 % (v/v) CO_2 growth for 6 h and 18 h, it is clear that the 0.1X nutrient formulation, representing a nitrogen and carbon-limited growth medium, allowed efficient conversion of *C. dubliniensis* yeast to hyphae. When nutrient levels were increased in 2X (v/v) medium formulation, it became apparent that, compared to 6 h

growth, after 18 h the number of blastospores present in the final culture steadily increased. This may represent impaired maintenance of hyphae, resulting in an increase in reversion to yeast and subsequent yeast proliferation. *Candida albicans* SC5314 cells do not appear to revert to blastospore growth under matching conditions.

5.3.2. Oxygen and carbon dioxide

The impact of carbon dioxide on the initiation and maintenance of *C. dubliniensis* hyphae was tested by incubating cells in WS or DUBLIN medium under either static aerobic or 5 % (v/v) CO₂ growth conditions (Fig. 5.3). *Candida dubliniensis* cells displayed more filamentous cells after 18 h when incubated under 5 % (v/v) CO₂, regardless of the nature of the inducing growth medium, suggesting a role in hyphal morphology maintenance. *Candida albicans* also displayed an increase in the proportion of hyphae present in the final culture grown under 5 % (v/v) CO₂ after 18 h growth. *Candida albicans* cells induced in DUBLIN medium under 5 % (v/v) CO₂ proliferated almost entirely as a hyphal network.

5.3.3. The role of quorum and environmental sensing

This study showed that initial inoculation density plays an important role in the maintenance of *C. dubliniensis* filamentous growth. When the initial inoculating density was varied from 1 x 10³ cells/ml to 1 x 10⁶ cells/ml, it was clear that with higher inoculation densities, *C. dubliniensis* cells displayed increased yeast growth over time (Fig. 5.4). Both WÜ284 and CD36 showed a high proportion of hyphae in the final culture when inoculated at an initial density of 1 x 10³ cells/ml. This hyphal proportion decreases when the initial inoculum is increased by a factor of 10, resulting in a more significant yeast presence with each increase.

Addition of exogenous cAMP was tested in conjunction with DUBLIN medium (+ (NH₄)₂SO₄) to investigate if this resulted in improved induction of *C. dubliniensis* hyphae (Fig. 5.5). Under the conditions tested, addition of 500 nmoles or 1000 nmoles cAMP, showed little difference in hyphal proportion in the final culture after 18 h. After addition of 2000 nmoles cAMP there was a small increase in the proportion of *C. dubliniensis* hyphae present. Although the proportion of *C. albicans* hyphae was much higher under these conditions, there appeared to be a

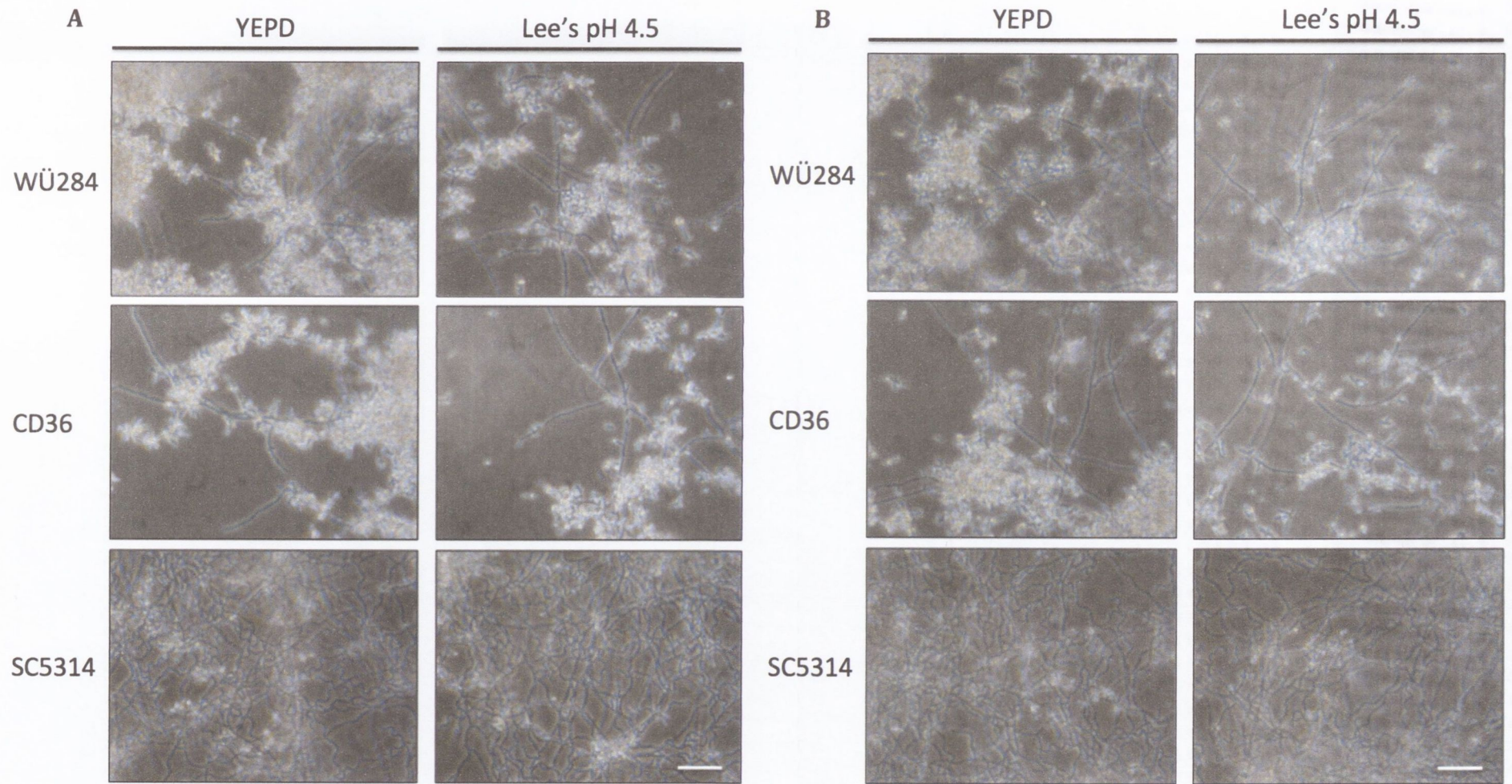


Figure 5.1. The impact of nutrients in preculture growth media on *C. dubliniensis* and *C. albicans* hyphal induction. (A) *Candida albicans* and *C. dubliniensis* cells grown initially in nutrient-poor Lee's medium produce more hyphae than cells precultured in YEPP. Micrographs taken after 18 h growth in (A) WS or (B) DUBLIN medium (+ $(\text{NH}_4)_2\text{SO}_4$). Scale bar represents 20 μm .

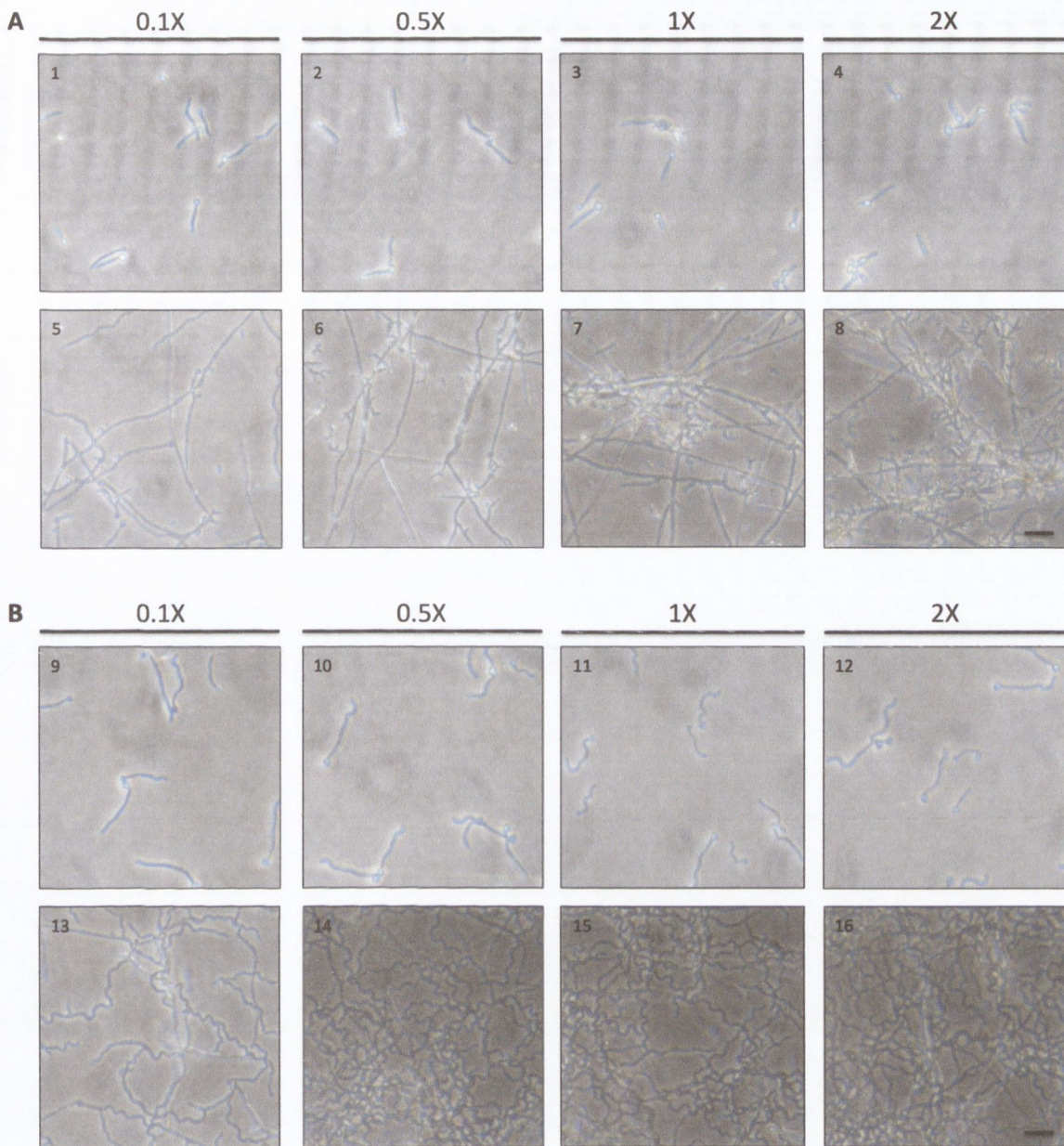


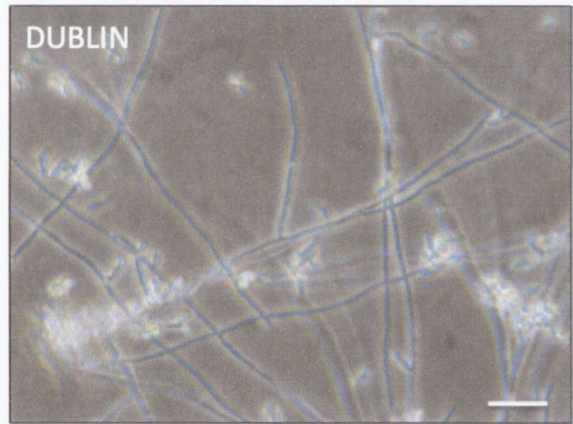
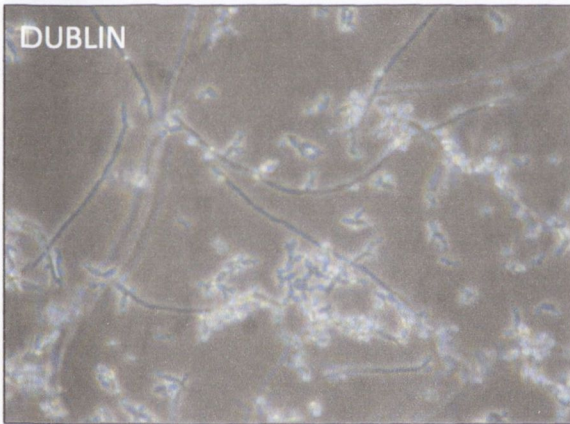
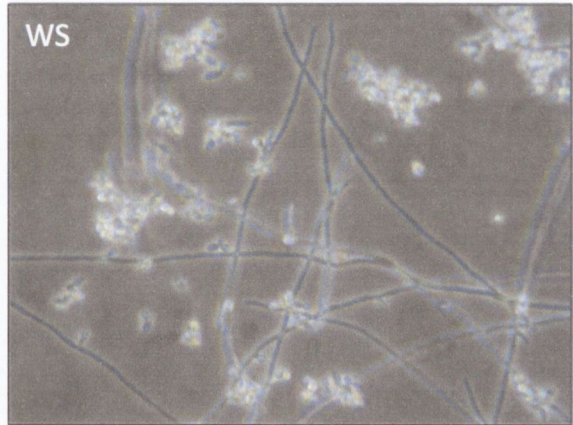
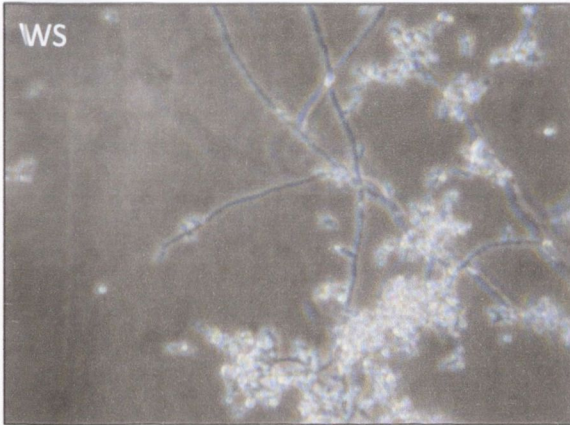
Figure 5.2. The impact of nutrient abundance during induction of *C. dubliniensis* and *C. albicans* hyphae. (A) WÜ284 and (B) SC5314 hyphae were induced in 0.1X, 0.5X, 1X, or 2X DUBLIN medium for 18 h. The proportions of yeast and hyphae were inspected visually. Micrographs were taken after 6 h (1) – (4), (9) – (12) and 18 h (5) – (8), (13) – (16). Scale bar represents 10 μ m.

CD36

A

O₂

CO₂



Continued overleaf

B

SC5314

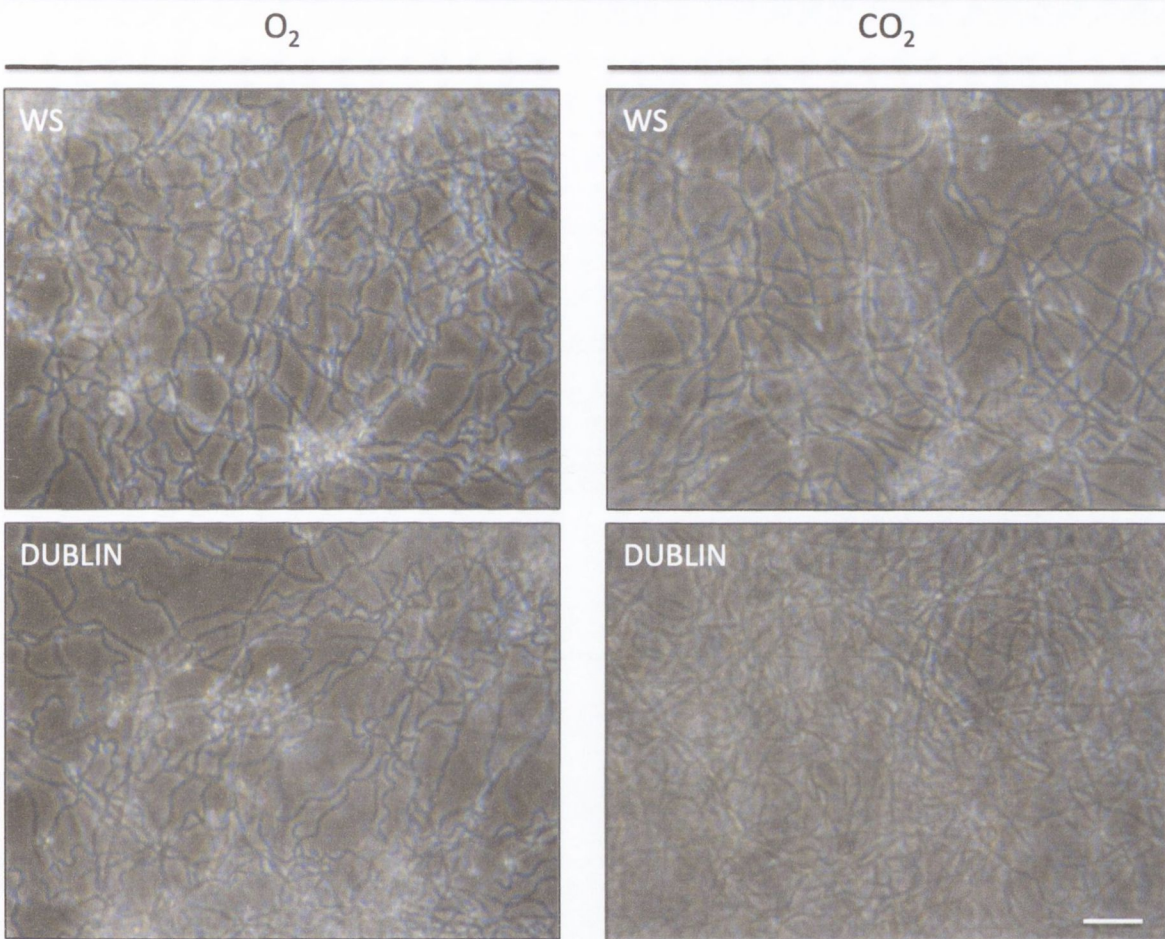


Figure 5.3. Oxygen and carbon dioxide during *C. dubliniensis* and *C. albicans* hyphal induction. *Candida albicans* and *C. dubliniensis* were induced to form hyphae in WS or DUBLIN medium under atmospheric oxygen or 5 % (v/v) CO₂. (A) The combination of WS and atmospheric oxygen resulted in poor hyphal maintenance in CD36 after 18 h. In contrast, the combination of DUBLIN medium and CO₂ enabled good maintenance of CD36 hyphae. (B) SC5314 did not require the combination of DUBLIN medium and CO₂ to efficiently form hyphae, although small numbers of yeast were present in WS-induced SC5314 cultures grown under atmospheric oxygen indicating a small degree of morphological reversion after 18 h. Scale bar represents 20 μm.

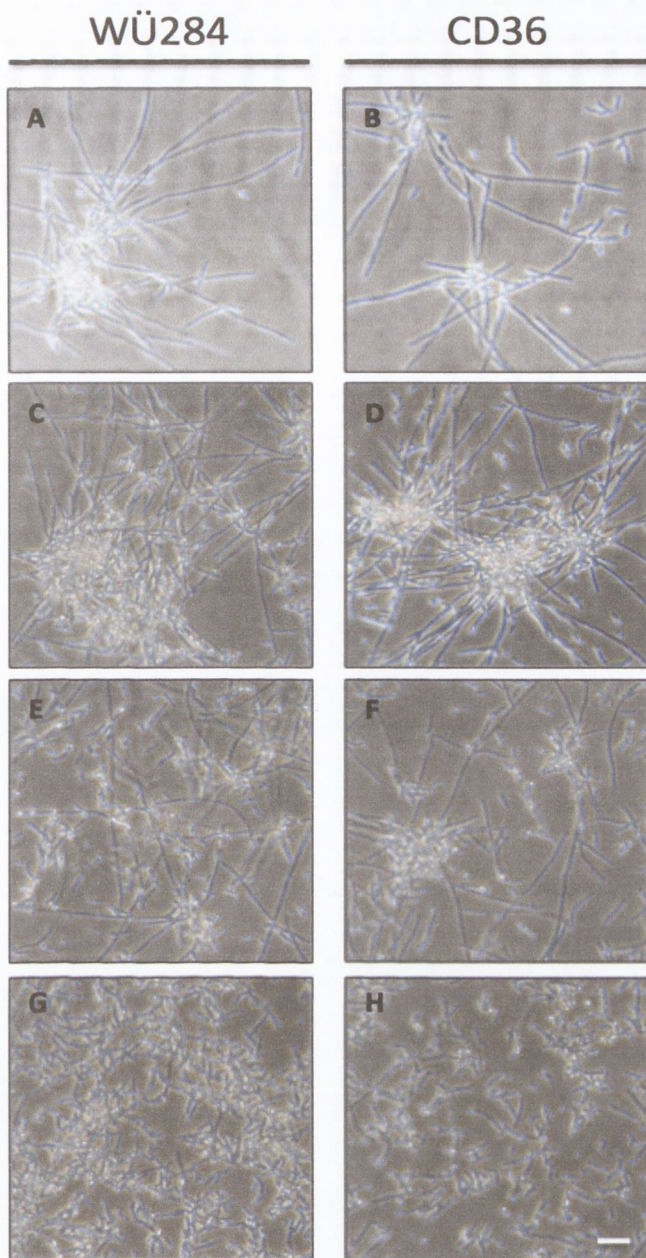


Figure 5.4. The role of inoculation density during the *C. dubliniensis* filamentous transition. The initial density of *C. dubliniensis* cells being inoculated into DUBLIN hyphal inducing medium was varied to assess the impact of quorum sensing on the dimorphic switch. (A), (B) 1×10^3 , (C), (D) 1×10^4 (E), (F) 1×10^5 or (G), (H) 1×10^6 cells/ml were inoculated into DUBLIN medium and incubated for 18 h. Both WÜ284 and CD36 exhibited the same response producing higher proportions of hyphae in cultures that were inoculated at a low cell density, and a greater proportion of yeast in cultures inoculated at a higher cell density. Scale bar represents 10 μm .

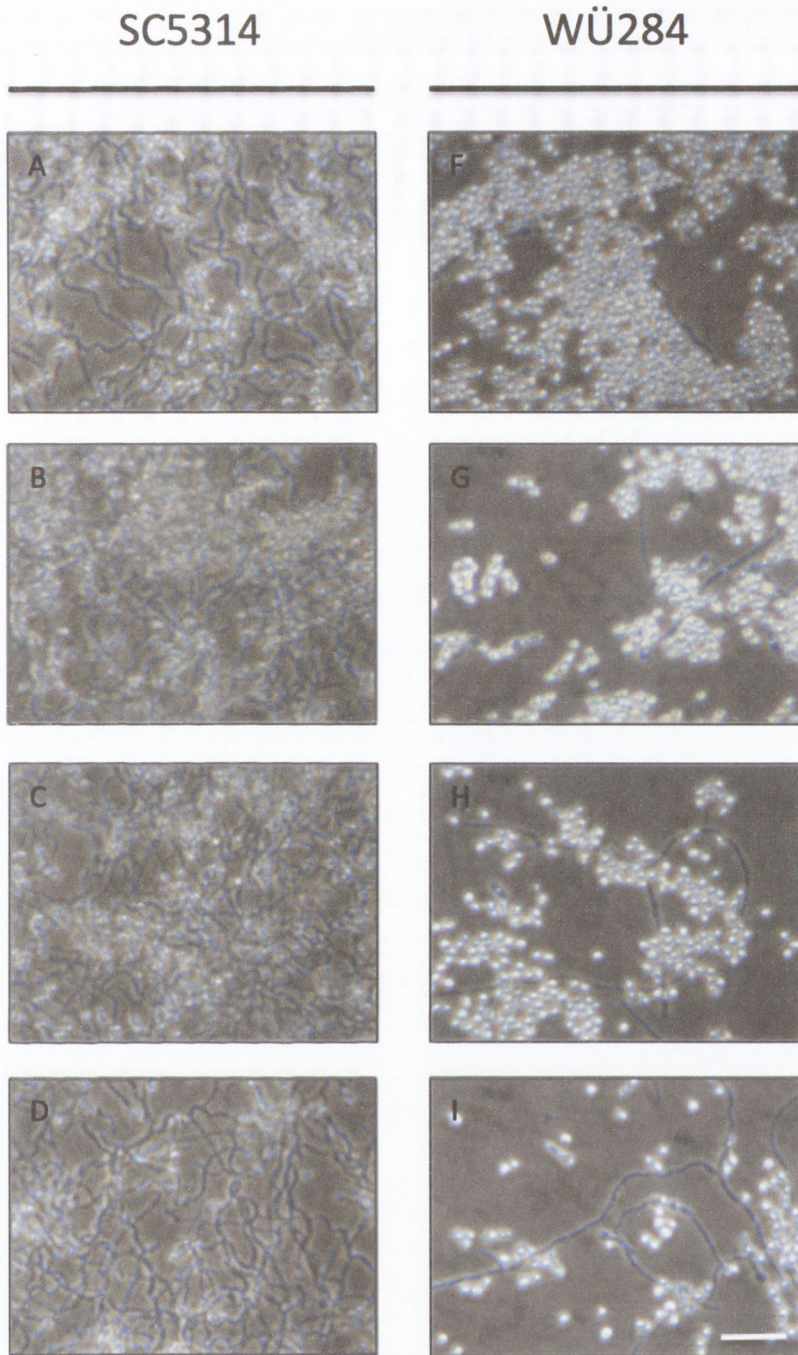


Figure 5.5. Cyclic AMP as a hyphal inducing signal in *C. dubliniensis* and *C. albicans*. *Candida albicans* and *C. dubliniensis* stationary phase cells were supplied with exogenous cAMP; (A), (F) untreated, (B), (G) 500 nmoles, (C), (H) 1000 nmoles, (D), (I) 2000 nmoles. Additionally the cells were incubated in DUBLIN medium (+ $(\text{NH}_4)_2\text{SO}_4$) at 37 °C under 5 % (v/v) CO_2 for 72 h. Scale bar represents 20 μm .

corresponding decrease in the number of yeast present in the final culture when treated with 2000 nmoles cAMP.

Tyrosol is hypothesised to have a hyphal inducing effect. However, adding exogenous tyrosol to *C. dubliniensis* hyphae induced with DUBLIN medium (+ $(\text{NH}_4)_2\text{SO}_4$), supplemented with 0.1 % (w/v) galactose, and incubated under 5 % (v/v) CO_2 , appeared to show no difference to the untreated control. Up to 100 μM tyrosol was added in 20 μM increments with no apparent difference in hyphal formation or maintenance under the conditions tested. This was true for both WÜ284 and CD36 (data not shown).

5.3.4. Carbon source and availability

Addition of glucose as a carbon source to DUBLIN medium resulted in a dramatic increase in biomass yield (Fig. 5.6). However, this was due, in part, to an increase in the proportion of *C. dubliniensis* yeast present in the final culture for media supplemented with either 0.1 % (w/v) or 0.5 % (w/v) glucose. This increase in blastospores was not observed with *C. albicans* cells, as final cultures were predominantly hyphal.

Supplementation of 1X DUBLIN medium with either 0.1 % (w/v) or 0.5 % (w/v) sucrose enabled higher biomass yields. While glucose supplementation resulted in an increase in the proportion of yeast, sucrose supplementation gave rise to a significant proportion of hyphae present in the final culture. However, many of these filamentous forms displayed the hallmarks of pseudohyphal growth such as non-uniform extension along the length of short filamentous chains.

DUBLIN medium showed both improved biomass yield and higher levels of hyphae when supplemented with 0.1 % (w/v) galactose. Addition of 0.5 % (w/v) galactose appeared to yield higher numbers of yeast indicating a delicate balance between *C. dubliniensis* hyphal induction and nutrient requirements with regards to carbon source.

5.3.5. Serum and *N*-acetylglucosamine induction of *C. dubliniensis* hyphae

By combining many induction signals and conditions it is possible to trigger and maintain morphologically pure communities of *C. dubliniensis* hyphae over extended time periods. Preculturing *C. dubliniensis* in Lee's medium pH 4.5 at 30 °C aerobically overnight, inoculating at a density of 1×10^5 cells/ml in 1X DUBLIN medium prewarmed to 37 °C and incubating under 5 % (v/v) CO₂ at 37 °C yielded ≥ 95 % hyphal cultures after 18 h. This hyphal proportion was further improved by supplementing the hyphal induction medium with 10 % (v/v) FCS (Fig. 5.7). This addition greatly increased the biomass yield. This method was shown to be valid for reliable long-term hyphal induction of the *C. albicans* reference strain SC5314.

5.3.6. Analysis of morphogenetic regulator response to growth and induction conditions

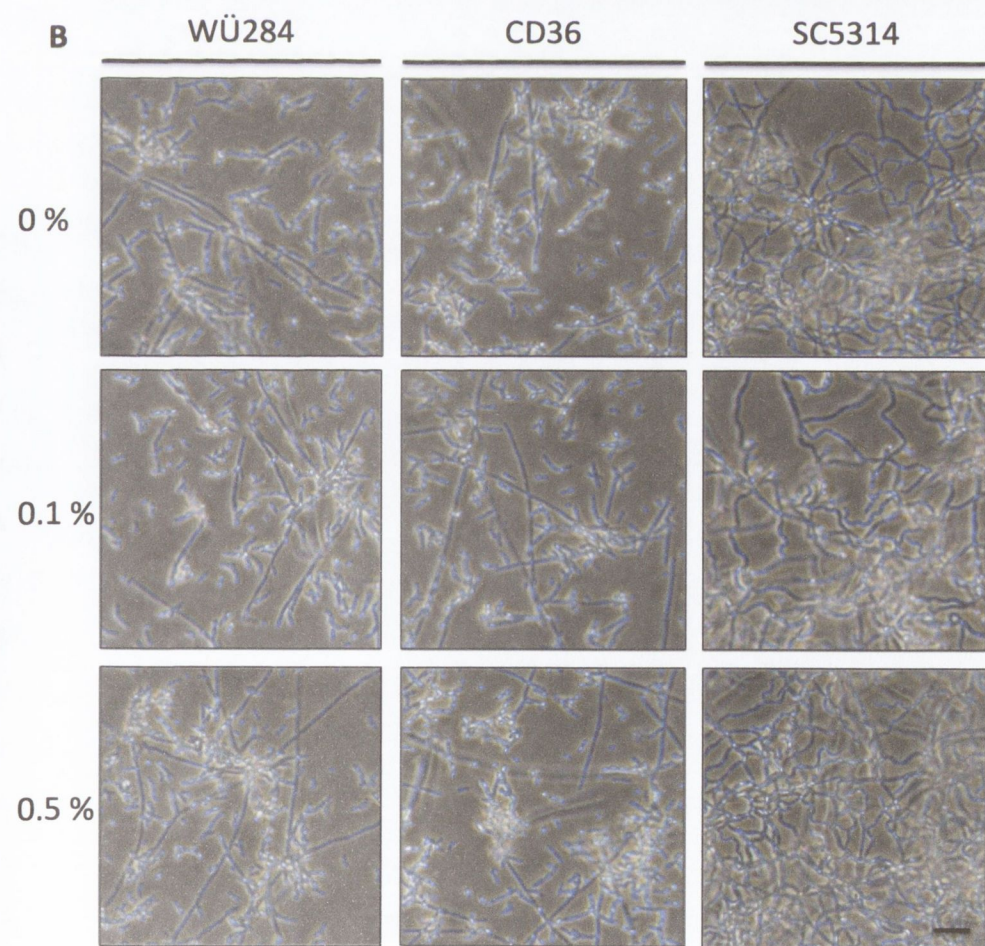
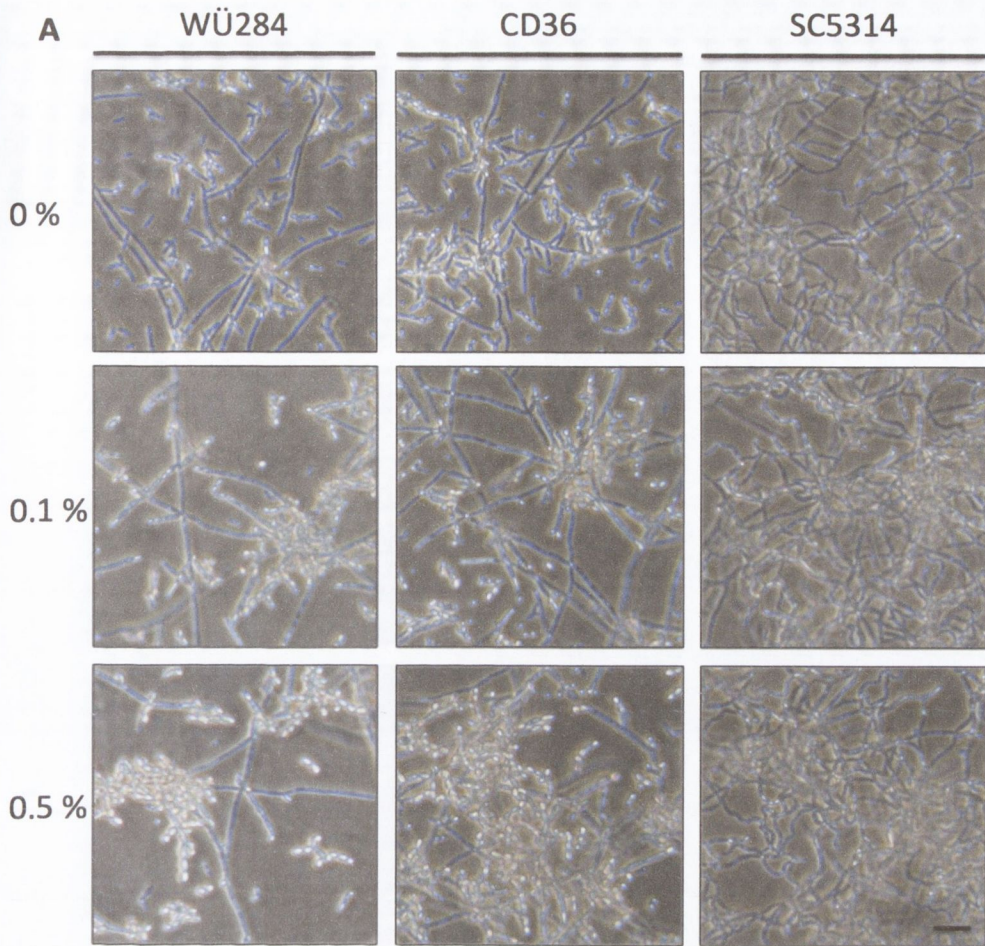
5.3.6.1. Negative regulator of glucose-controlled genes (*NRG1*)

Evaluation of *NRG1* levels in *C. albicans* and *C. dubliniensis* yeast and hyphae show rapid, transient decreases in *NRG1* expression for all conditions tested (Fig. 5.8a). Both *C. albicans* and *C. dubliniensis* yeast cultures showed reductions in expression after just 1 h. The magnitude of downregulation of *NRG1* expression was similar for both *C. dubliniensis* strains under each growth condition. However, the magnitude of downregulation of *NRG1* in DUBLIN-induced SC5314 hyphae was much larger than WS-induced hyphae. In all cases, downregulation of *NRG1* was transient, and slowly recovered over the course of 18 h.

5.3.6.2. *Candida* pseudohyphal regulator (*CPH1*)

Expression of *CPH1* in *C. dubliniensis* and *C. albicans* YEPD-grown yeast cells exhibited roughly comparable expression profiles over 18 h (Fig. 5.8b). The pattern of *CPH1* expression in SC5314, WÜ284 and HE30 yeast revealed slight downregulation of *CPH1* after 1 h, followed by increasing levels of *CPH1* transcript over time.

The pattern of *CPH1* expression was similar for SC5314 and HE30 hyphae, regardless of the induction medium used. Hyphal induction in either WS or DUBLIN medium resulted in an increase in *CPH1* levels after just 1 h and maintenance of expression levels over the course of 18 h. In contrast, WÜ284 hyphae induced in WS displayed



Continued overleaf

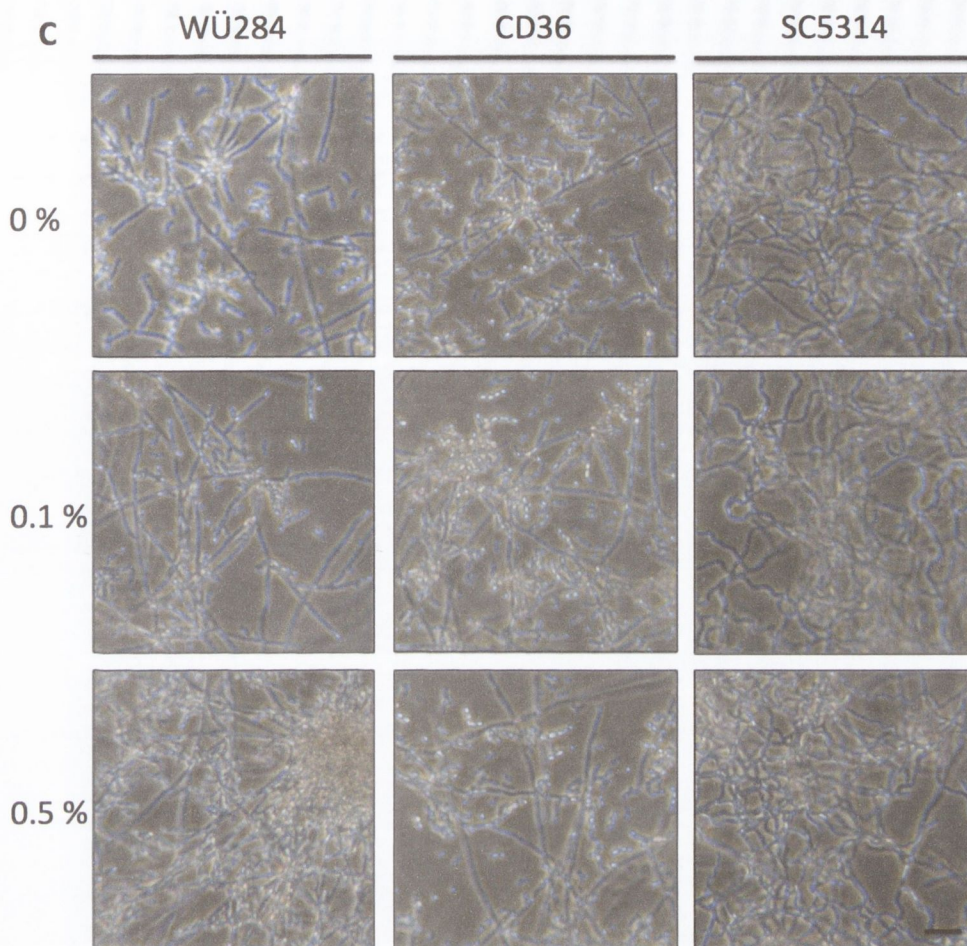


Figure 5.6. The importance of carbon source and abundance during *C. dubliniensis* and *C. albicans* hyphal initiation and maintenance. *Candida albicans* and *C. dubliniensis* were incubated in DUBLIN medium supplemented with 0.1 % (w/v) or 0.5 % (w/v) carbon source. The carbon sources investigated were (A) glucose, (B) sucrose, and (C) galactose. Supplementation of the hyphal inducing medium with glucose resulted in a significant proportion of yeast cells in *C. dubliniensis* cultures after 18 h. Addition of sucrose yielded fewer yeast cells in the hyphal cultures, although many of these hyphae bore the physical characteristics of pseudohyphae. Overall, supplementation with galactose improved *C. dubliniensis* hyphal maintenance after 18 h. However, *C. dubliniensis* hyphal induction and maintenance was dependent on carbon source concentration, as higher concentrations resulted in larger proportions of yeast by visual assessment. Scale bars represent 10 μm

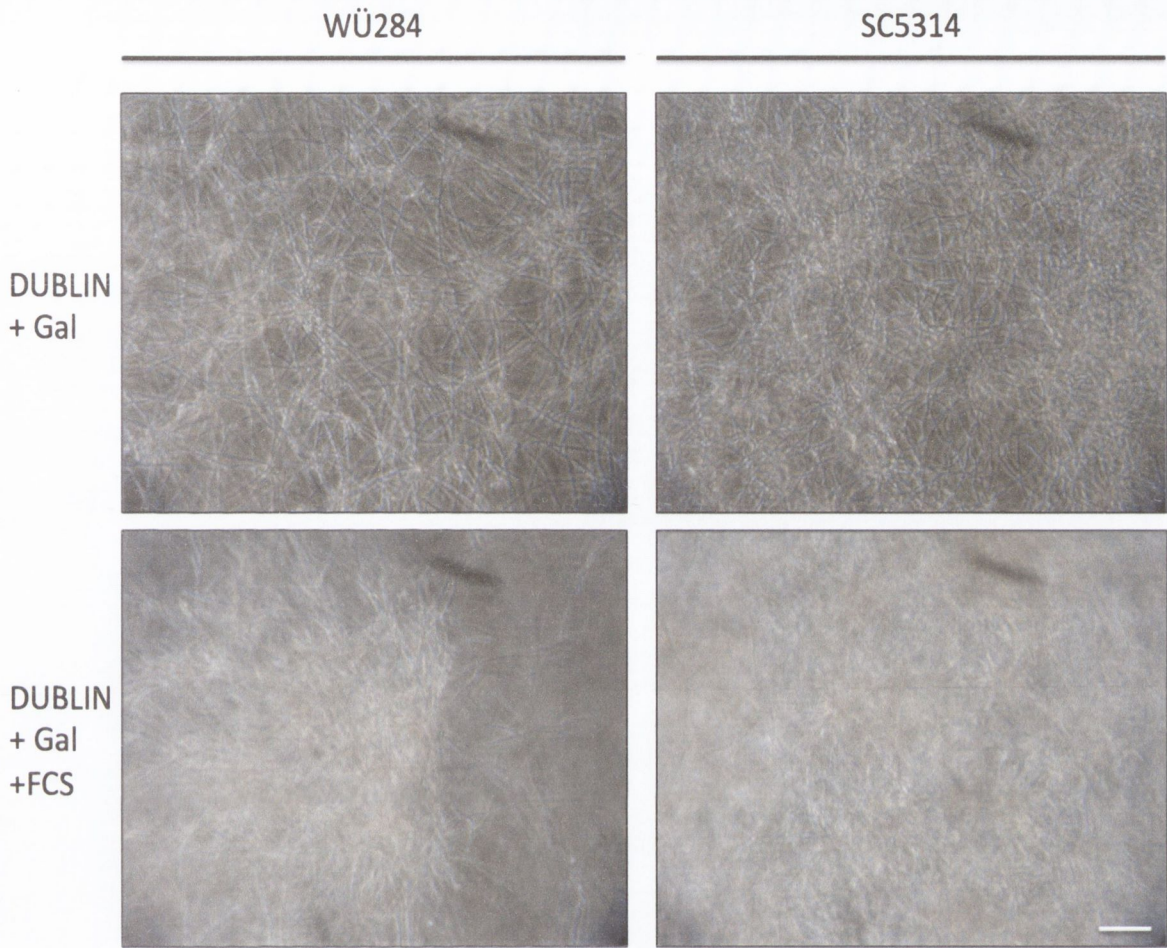


Figure 5.7. Improved *C. dubliniensis* hyphal induction and maintenance. Induction of *C. dubliniensis* and *C. albicans* hyphae and morphological maintenance over 18 h was achieved using DUBLIN medium supplemented with 0.1 % (w/v) galactose, under 5 % (v/v) CO₂ at 37 °C, in combination with preculture in Lee's pH 4.5 medium under atmospheric oxygen at 30 °C. Biomass was increased by addition of 10 % (v/v) FCS in the final hyphal induction medium. Scale bar represents 20 µm.

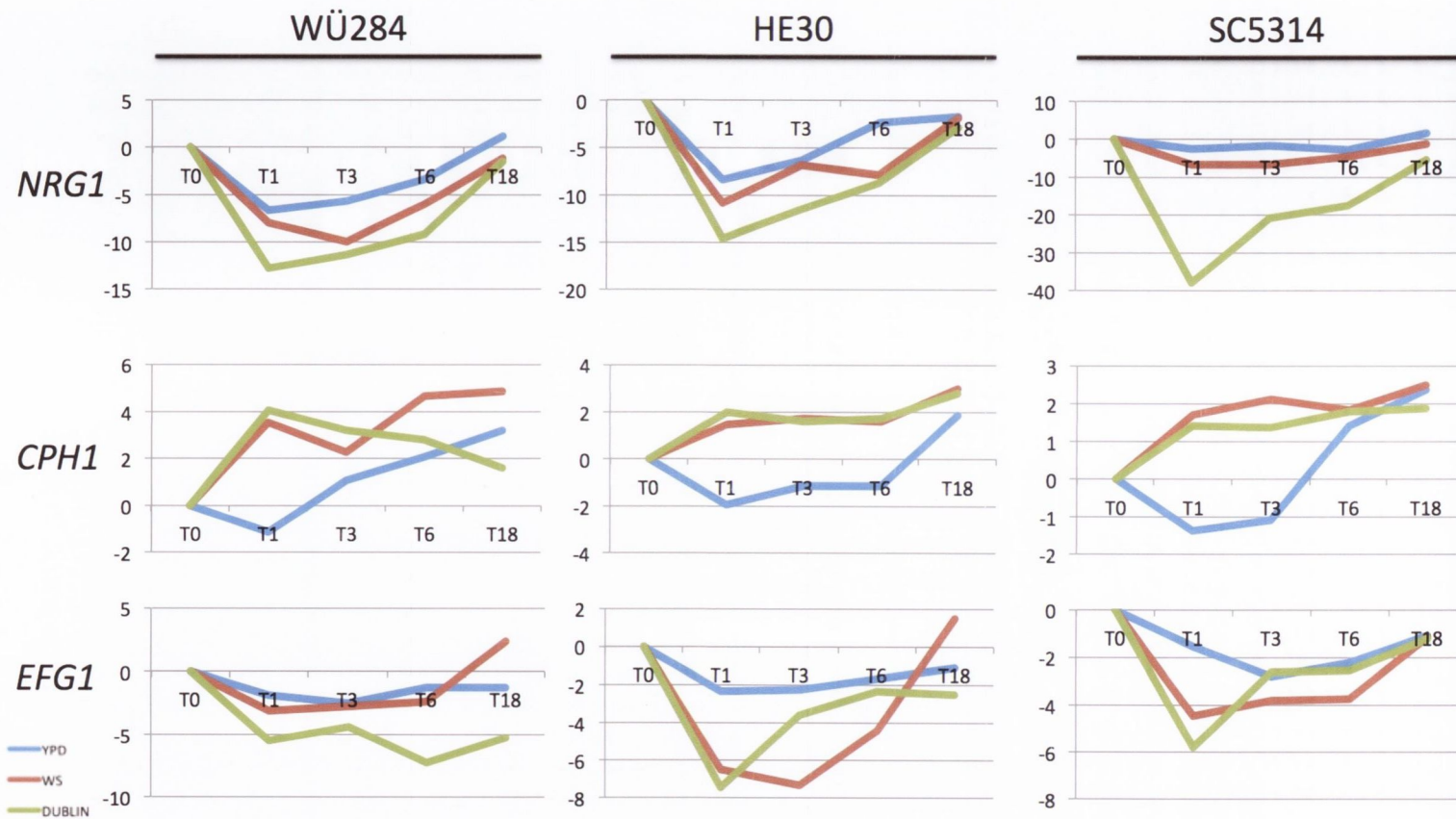


Figure 5.8. Temporal analysis of morphogenetic regulator expression during the dimorphic transition. *Candida albicans* and *C. dubliniensis* were induced to form yeast (YEPD medium) or hyphae (WS or DUBLIN medium). Gene expression analysis (qRT-PCR) assaying expression of *NRG1*, *CPH1*, and *EFG1* was carried out on cells grown for 0, 1, 3, 6, and 18 h. Data is presented as fold change values ($2^{-\Delta\Delta C_t}$) relative to 0 h i.e. gene expression levels in the cell inoculum.

increased levels of *CPH1* at T₁ but levels dropped between T₁ and T₃, before increasing again until T₁₈. Similarly, WÜ284 hyphae induced in DUBLIN medium increased after 1 h and subsequently displayed relatively decreased levels at T₃. However, *CPH1* levels continued to decrease consistently until T₁₈.

5.3.6.3. Enhanced filamentous growth regulator (*EFG1*)

Analysis of *EFG1* expression in *C. albicans* and *C. dubliniensis* cultures grown in YEPD medium showed an initial 2-fold decrease in expression levels relative to the stationary phase inoculum cells (Fig. 5.8c). Between T₁ and T₁₈, after inoculation in fresh growth medium, there was less than a 2-fold deviation from this expression level.

Expression of *EFG1* in hyphal cells varied depending on the hyphal induction method used. Hyphal SC5314 cells, induced by WS displayed a decrease in *EFG1* expression after 1 h. Levels of *EFG1* were maintained until T₆, at which point, *EFG1* transcript levels increased dramatically. Hyphal *C. dubliniensis* cells induced in WS medium showed a slight variation of this pattern. The most similar was WÜ284 hyphal cells in which *EFG1* expression decreased after 1 h, was maintained until T₆, and increased thereafter. In contrast to *C. albicans* SC5314, the final level of *EFG1* expression in WÜ284 hyphae induced by WS was positive, relative to the initial inoculum. Induction of HE30 hyphae with WS also revealed a decrease in *EFG1* expression after 1 h. However *EFG1* transcript levels continued to decrease until T₃, after which *EFG1* levels increased substantially.

Induction of hyphae with DUBLIN medium highlighted differences in the regulatory response to variation of induction signals. Hyphal SC5314 cells induced with DUBLIN medium displayed a larger decrease in *EFG1* expression levels at T₁ compared to induction with WS. However, after 3 h *EFG1* levels were similar to SC5314 yeast cells grown in YEPD, and *EFG1* expression levels increased thereafter, similar to YEPD-grown cells. HE30 hyphae induced in DUBLIN medium showed a similar pattern to SC5314 DUBLIN-induced hyphae, with downregulation of *EFG1* expression peaking at T₁ before decreasing in magnitude. However, WÜ284 hyphae induced in DUBLIN-medium displayed an overall reduction in expression of *EFG1* over the course of 18 h.

5.4. Discussion

5.4.1. Development of an improved method for initiation and maintenance of *C. dubliniensis* hyphae

This study has achieved, for the first time, efficient induction and effective maintenance of *C. dubliniensis* true hyphae over extended time periods (18 h). Until this point, experimental data for *C. dubliniensis* hyphae have been plagued by the significant presence of yeast and pseudohyphal cells within the population analysed (O'Connor *et al.*, 2010). While it has been shown previously that initiation and maintenance of *C. albicans* true hyphae can be achieved relatively simply, with only a few hyphal induction signals, it was necessary to combine many induction signals and conditions in order to achieve a similar outcome for the less filamentous *C. dubliniensis* (Stokes *et al.*, 2007). Each hyphal induction signal contributes in varying degrees to the *C. dubliniensis* hyphal state, presumably by activating various genes and pathways responsible for the morphogenic switch. While the data presented here are predominantly qualitative, due to the investigative nature and requirements of developing a reliable method for hyphal induction, the distinct contributions of each inducing signal may potentially be dissected quantitatively in the future. Regardless, it is clear that each inducing signal contributes to varying degrees to the filamentous state of *C. dubliniensis*, and perhaps *C. albicans*.

5.4.1.1. Nutrient limitation

Induction of *C. dubliniensis* true hyphae has been shown previously to be inhibited by nutrient abundance in both the preculture conditions and also in the hyphal inducing medium (O'Connor *et al.*, 2010). Preculture of *C. dubliniensis*, and *C. albicans*, in the nutrient-limited, defined Lee's medium increased short-term (up to 4 h) hyphal induction in YPDS relative to cells precultured in YEPD. The current study attempted to confirm this phenotype after extended time periods (18 h) using WS as the hyphal inducing medium. Conversion of hyphae to yeast over 18 h was substantial in WS. However *C. dubliniensis* cells grown initially in YEPD appeared to display higher levels of yeast cells than those precultured in Lee's medium. Investigation of the phenotype, with improved hyphal maintenance in DUBLIN medium, revealed similar results. Cells grown initially in Lee's pH4.5, and induced to form hyphae in DUBLIN medium,

displayed greater numbers of *C. dubliniensis* hyphal cells in comparison to cells precultured in YEPD. This supported the importance of nutrient limitation in precultures in not only hyphal initiation, but also subsequent hyphal maintenance in *Candida* populations. It is not clear whether the increased levels of hyphae observed after 18 h was a result of the combination of greater rates of initial hyphal induction in nutrient limited media with standard rates of reversion from hyphae to yeast, or whether the preculture conditions had some uncharacterised epigenetic effect on the hyphal reversion rate of *C. dubliniensis* hyphae to yeast. These qualitative investigations did not identify any significant difference in *C. albicans* hyphal induction as a result of preculture methods. This was due mainly to the high efficiency of hyphal initiation of *C. albicans*, resulting in few yeast cells observable in either condition tested. Variation of nutrient availability in the DUBLIN induction medium revealed that increasing both carbon and nitrogen availability in *C. dubliniensis* cultures correlated with an increase in the number of blastospores in the culture between 6 h and 18 h. *Candida albicans* cells filamented equally well regardless of nutrient levels under the conditions investigated. O' Connor *et al.* have previously documented the role of nutrients in the regulation of the morphogenic regulators *UME6* and *NRG1* with respect to *C. dubliniensis* dimorphism (O'Connor *et al.*, 2010). The current study suggests that the starvation response appears to play an important role not only in the initiation of *C. dubliniensis* true hyphae influenced by *UME6* and *NRG1* regulation but also in the maintenance of hyphal extension over time. It is not clear whether the different sensitivity displayed by *C. albicans* and *C. dubliniensis* to nutrient availability is a result of variation of environmental sensing through receptors such as Mep2p or Tor1p, or difference in downstream signaling pathways. The development of a hyphal induction medium for long-term induction of *C. dubliniensis* hyphae has created the opportunity to further investigate this disparity in the future. This discrepancy likely points to evolutionary differences as a result of the local niche or environmental conditions experienced by the two *Candida* species.

5.4.1.2. Carbon dioxide and hyphae

This study has confirmed that CO₂ plays a role not only in the initial induction of hyphae, but more importantly in the maintenance of the hyphal state. Carbon dioxide is a key factor not only in many infection models but also in the host gastrointestinal and urogenital tracts. Therefore it is noteworthy that CO₂ is such a potent signal for

triggering and maintaining the yeast to hyphal switch in both *C. albicans* and *C. dubliniensis*. The role of CO₂ in mediating hyphal development in *C. albicans* has been characterised, and activation of the Ras/cAMP pathway by CO₂ and carbonate ions has been documented. While this pathway has been explored in *C. albicans*, little has been confirmed regarding CO₂ activation of the Ras/cAMP pathway in *C. dubliniensis* and its potential similarities to its more filamentous relative *C. albicans*. This study has shown that CO₂ initiates and maintains growth of *C. dubliniensis* true hyphae although the mechanism governing this phenotype has yet to be confirmed. It is not clear whether an environment constantly enriched with CO₂ supports hyphae through sustained stimulation of the Ras/cAMP pathway alone, or whether it activates more than one pathway to maintain *C. dubliniensis* hyphal growth. The discovery of additional filamentous phenotypes such as “tentacles” and “fingers” in *C. albicans* under saturated CO₂ conditions suggests that carbon dioxide may play a role in additional signaling pathways that we are not aware of yet (Daniels *et al.*, 2012). Whether *C. dubliniensis* has the potential to develop these additional filamentous morphologies has yet to be investigated.

5.4.1.3. Quorum and environmental sensing

Quorum sensing molecules such as farnesol from *Candida*, or homoserine lactones (HSL) produced by bacteria have been shown to inhibit the yeast to hyphal switch. Antagonism of the Ras/cAMP pathway by these quorum sensing molecules triggers important behavioural and phenotypic modifications in single-species cultures and mixed-species biofilms (Langford *et al.*, 2009; Mear *et al.*, 2013). Both production and sensing of biological signaling molecules is influenced by *Candida* cell density (Hornby & Nickerson, 2004). This study has shown that, in single species cultures, cell density influences the development and maintenance of morphologically pure hyphal cultures. High initial cell densities reduced the long-term production of hyphal cells, presumably due to antagonistic molecules such as farnesol being produced in high concentrations, causing reversion of hyphae to yeast cells. Attempts to offset this inhibition by supplying exogenous tyrosol did not have any significant effect at the concentrations used. Little is known about the effect of tyrosol on *C. dubliniensis* and it is possible that higher concentrations may be required to abolish the inhibitive effect of farnesol on the yeast to hyphal switch. Exogenous supplementation of stationary phase cells with cAMP, in order to stimulate molecules downstream of the

Ras/cAMP pathway, similarly displayed no effect on the initiation and maintenance of *C. dubliniensis* true hyphae. Exponential phase *C. dubliniensis* cells previously displayed no increase in filamentation when treated with cAMP (Moran *et al.*, 2007). It appears that cAMP supplementation alone does not represent an effective signal for inducing *C. dubliniensis* cells to form filaments. It is not clear which mechanism is responsible for the reduced initiation and maintenance of *C. dubliniensis* hyphae at higher initial cell densities. However, regardless of the mechanism, the high degree of variation in inocula, as shown by this study, is likely to have a significant impact on experimental outcomes and conclusions of infection model studies investigating the dimorphic shift in both *C. dubliniensis* and *C. albicans*.

5.4.1.4. Carbon source and availability as a hyphal inducing signal

Supplementation of DUBLIN medium with a carbon source in order to increase biomass after 18 h growth yielded surprising results. Glucose supplementation resulted in high levels of *C. dubliniensis* yeast cells in the final culture, as seen to a lesser degree in *C. albicans* hyphal cultures grown for 18 h. Addition of sucrose weakly supported maintenance of *C. dubliniensis* filamentation after 18 h. A stronger filamentous phenotype in *C. dubliniensis* was observed when galactose was added. Although carbon sources in growth media are usually supplied at 2 % (w/v), microsupplementation with low levels of sugars has been shown to reduce *NRG1* levels in *C. dubliniensis* cells (Citiulo *et al.*, 2009). The interplay between hexose sugar sensing and signaling as it relates to filamentation in *C. albicans* is extremely complex and has been recently reviewed (Horak, 2013). Extrapolation of similarities indicate that low levels of galactose may support filamentation in a number of ways including activation of Ngt1p, Hgt4p, and Cph1p, leading to both initiation and maintenance of hyphae. However, functional similarities between orthologous genes in *C. dubliniensis* requires verification. Construction of a library of *C. dubliniensis* mutants would be a useful tool for investigating the impact of galactose on *C. dubliniensis* morphology. Further elucidation of these sensing mechanisms may help define risk factors in patients that may be susceptible to *C. albicans* and *C. dubliniensis* infections.

5.4.1.5. Serum and N-acetylglucosamine induction of hyphae

Serum is a highly complex medium and compositional variation between batches is common. Formation of hyphae in the relatively less filamentous *C. dubliniensis* is

sensitive to serum batch compositional variations. For this reason, among others, it was highly desirable to formulate a serum-free medium for induction of *C. dubliniensis*. Development of a serum-free media for *C. dubliniensis* hyphal induction was greatly influenced by the preparation of a defined medium for stable long-term induction of *C. albicans* hyphae, which was based on the monosaccharide GlcNAc found in serum (Heilmann *et al.*, 2011). Although GlcNAc was historically considered to be unsuitable for hyphal induction of *C. dubliniensis* strains, this study has shown that the molecule instead plays a major role in the maintenance of hyphae induced by alternative initiation signals (Gilfillan *et al.*, 1998; Stokes *et al.*, 2007). This supports the hypothesis that complex, serum-rich media may activate hyphal induction through multiple morphogenetic regulation pathways, while isolated GlcNAc stimulates hyphal induction and maintenance in a more specific manner. Initiation of *C. albicans* hyphae by GlcNAc is hypothesised to primarily act through Ngt1p stimulation of Efg1p and subsequent elaboration of hyphal specific genes (Alvarez & Konopka, 2007). If the same signaling pathway is true for *C. dubliniensis*, this suggests that CdEfg1p may not play a dominant role in initiation of *C. dubliniensis* true hyphae, but may contribute to maintenance of hyphae under strong induction conditions. Remarkably, galactose metabolism is also activated by GlcNAc, and the *GAL* operon has been shown to interact with the morphogenetic regulator Cph1p (Martchenko *et al.*, 2007). However this interaction is not well understood and the interaction of the *GAL* operon functionality with *Candida* filamentation has yet to be fully defined. Unfortunately, growth of *Candida* cells in nutrient-limited DUBLIN medium (- $(\text{NH}_4)_2\text{SO}_4$) containing GlcNAc, even when supplemented with galactose, resulted in low growth rates and low biomass after 18 h. Supplementation of the DUBLIN medium (- $(\text{NH}_4)_2\text{SO}_4$, 0.1 % (w/v) galactose) with 10 % (v/v) FCS resulted in a much higher biomass by visual estimation and measurement of dry weight (data not shown). Although the morphological purity was approximately 95 % hyphal after 18 h without addition of FCS, subsequent addition of FCS improved this percentage even further, likely due to the combined effects of additional hyphal initiation and maintenance signals. Serum has also been shown to bind farnesol efficiently, potentially ameliorating the inhibitory effect of the quorum sensing molecule on the yeast to hyphal switch in both *C. albicans* and *C. dubliniensis* (Mosel *et al.*, 2005). In this way, there are multiple potential mechanisms underlying serum-mediated induction of *Candida* hyphae. Further dissection of these mechanisms is required to

truly understand the role of serum during *in vitro* and *in vivo* *Candida* infections. This part of the study succeeded in identifying conditions under which *C. dubliniensis*, and *C. albicans* could be induced to form true hyphae and maintain this morphology for extended time periods (>18 h) without significant reversion to the yeast form, opening up possibilities for the future analysis of *Candida* filamentation and its role in virulence.

5.4.2. Regulation of *Candida* filamentous dimorphism

Initiation and maintenance of hyphae is the outcome of complex interactions between positive and negative morphogenetic regulators. The expression patterns of the major morphogenetic regulators *NRG1*, *EFG1* and *CPH1*, over 18 h were analysed. Results for WS-induced WÜ284 hyphae support previously described microarray data (O'Connor *et al.*, 2010). All *Candida* cells grown in YEPD remained in the yeast form for the duration of the experiment. While *C. albicans* SC5314 cells grown in either WS or DUBLIN medium were observed predominantly as hyphal cells, *C. dubliniensis* cells grown in WS medium displayed transient hyphal growth, with reversion visibly occurring between 3 h and 6 h. Only when incubated in DUBLIN medium were *C. dubliniensis* WÜ284 and HE30 cells capable of maintaining the hyphal morphology over 18 h. Thus, the current study was able to analyse both yeast and hyphal committed morphologies, in addition to cultures reverting between each morphology. Investigation of the underlying regulatory patterns involved in hyphal maintenance and yeast reversion enabled elaboration of a potential regulatory profile for *C. dubliniensis*, and *C. albicans*, dimorphism. The data obtained as part of this study represented a single biological replicate, and therefore it is necessary to either perform additional replicate experiments, or use the data obtained here as a pilot study for further transcriptomic experiments.

5.4.2.1. *NRG1*

The DNA-binding protein, Nrg1p, represses *Candida* filamentation in concert with Tup1p (Murad *et al.*, 2001). Null*mutants have been observed to display filamentous phenotypes under non-inducing conditions (Braun *et al.*, 2001). Survival of mice infected with *C. albicans* yeast, in which *NRG1* expression has been overexpressed, has been shown to be higher in a murine model of disseminated candidiasis,

highlighting the importance of *NRG1* expression, and the filamentous switch in the pathogenesis of *C. albicans* (Saville *et al.*, 2003).

Relief of *NRG1*-mediated transcriptional repression is known to be important for elaboration of hyphae in both *C. albicans* and *C. dubliniensis* (Moran *et al.*, 2007). It is currently unknown whether the magnitude of downregulation of *NRG1* activity results in comparable phenotypic outcomes between *C. dubliniensis* and *C. albicans*. However, this study suggests that the relationship between morphology and the magnitude of *NRG1* downregulation varied according to *Candida* species. While downregulation of *NRG1* in WS was larger for both *C. dubliniensis* WÜ284 and HE30, relative to that measured for *C. albicans* SC5314 at early time points, it was clear that SC5314 cultures were more filamentous in appearance. At later time points, corresponding to *C. dubliniensis* reversion of hyphae to yeast, there was little observable difference between *C. dubliniensis* and *C. albicans* *NRG1* expression levels. This reinforces the dynamic nature of positive and negative regulation of the dimorphic switch in *C. dubliniensis* and *C. albicans*. The increased efficiency of DUBLIN medium, for initiation and maintenance of *Candida* hyphae, was indicated by the consistently lower levels of *NRG1* expression in both *Candida* species over the course of 18 h.

5.4.2.2. *CPH1*

As part of the MAPK pathway, *CPH1* influences filamentation, mating and metabolism (Huang *et al.*, 2008). Its role as a major morphogenetic regulator was confirmed as a null mutant displayed both reduced filamentation and virulence (Liu *et al.*, 1994). Invading *Candida* cells lacking *CPH1* illicit an abnormal host cytokine response, indicating the importance of the gene for normal fungal cell wall proteins and secreted products (Korting *et al.*, 2003).

Levels of *CPH1* expression displayed divergent results in WÜ284 and HE30 according to the hyphal induction method used, indicating previously undescribed intraspecies variation in the regulation of morphology. Expression of *CPH1* in HE30 demonstrated similarity to SC5314 response to hyphal inducing media, with little variance in expression levels between WS-treated and DUBLIN-treated cells. However, transcript levels showed divergence between WS- and DUBLIN- treated WÜ284 cells after 3 h.

In contrast to the stable decrease in *CPH1* in DUBLIN-treated cells, *CPH1* transcript levels in WS-treated cells increased after 3 h. This difference in *CPH1* regulation is perhaps an indicator of the mechanisms governing reversion of *C. dubliniensis* hyphae to yeast over time as HE30 was consistently found to filament slightly more readily than WÜ284. The similarity of HE30 *CPH1* expression during filamentation to *C. albicans* SC5314 may correlate filamentation rates with the relatively high virulence of the *C. dubliniensis* HE30 strain.

5.4.2.3. *EFG1*

In *C. albicans*, *EFG1* was initially identified as a major morphogenetic regulator as a null mutant displayed reduced filamentation and virulence (Stoldt *et al.*, 1997). Further study has discovered that it experiences rapid negative autoregulation (Tebarth *et al.*, 2003). Overexpression of the gene also has the ability to repress formation of true hyphae. In *S. cerevisiae*, Efg1p acts as both an activator and repressor. Doedt *et al.* showed that Efg1p activity is modulated by its APSES partner Efh1p to regulate the dimorphic switch in *C. albicans* (Doedt *et al.*, 2004). This has yet to be proven to also be the case in *C. dubliniensis*.

It is likely that *EFG1* expression plays a significant role in the balance between hyphal maintenance and reversion in *C. albicans* and *C. dubliniensis*. Expression of *EFG1* in SC5314 was downregulated from transcript levels in the initial inoculum, consistent with its role as a repressor of transcription. In both WS- and DUBLIN-treated hyphae, *EFG1* was downregulated relative to YEPD-treated yeast cells presumably allowing transcription of hyphal specific genes. However, the magnitude of this downregulation was reduced over time, before returning to relatively neutral levels after 18 h in all media tested. The *EFG1* expression profile generated by *C. dubliniensis* WÜ284 and HE30 hyphae displayed downregulation of *EFG1* after 1 h in both hyphal-inducing media. Hyphal HE30 cells grown in DUBLIN medium experienced a large decrease in *EFG1* transcript levels after only 1 h. This was apparently transitory as *EFG1* levels increased rapidly after 3 h, stabilising thereafter. Similarly, HE30 hyphae induced by growth in WS experienced strong downregulation after 1 h. However, this downregulation was maintained for 3 h, after which, transcript levels of *EFG1* swiftly increased, showing upregulation after 18 h relative to *EFG1* expression in the initial inoculum. Hyphal cells of WÜ284 grown in WS medium initially experienced a small

decrease in *EFG1* expression, followed by a marked increase after 6 h. Hyphal WÜ284 induced in DUBLIN medium displayed downregulation of *EFG1* over the course of 18 h with some minor fluctuations throughout. Further transcriptome studies, utilising the improved *C. dubliniensis* hyphal induction method, would help define the impact of the observed regulatory patterns on the wider transcriptome, and proteome. Reversion of *C. dubliniensis* hyphae in WS is, in summary, associated with large variations in *EFG1* expression between 3 h and 6 h after hyphal induction, while hyphal maintenance apparently coincides with relatively stable levels of *EFG1* in *Candida* cells during the same time period.

5.4.3. Future directions

For the first time this study has enabled the analysis of stable, committed *C. dubliniensis* hyphae over extended time periods by developing a growth medium for efficient and effective induction and maintenance of *C. dubliniensis* hyphae. This has enabled intra- and interspecies analysis of morphogenetic regulation markers, revealing possible divergence in regulation patterns between *C. dubliniensis* and *C. albicans*, and also between two different strains of *C. dubliniensis*. The described findings implicate multiple morphological regulatory mechanisms contributing to the differential virulence observed between these two *Candida* species. Detailed analysis of downstream hypha-specific genes and further transcriptomic analyses of *C. dubliniensis* hyphae induced using this improved method will contribute to understanding of *Candida* filamentation and the role it plays in virulence.

Chapter 6

Comparative proteomic analysis of *Candida dubliniensis* and *Candida albicans* dimorphic cell wall proteins

6.1. Introduction

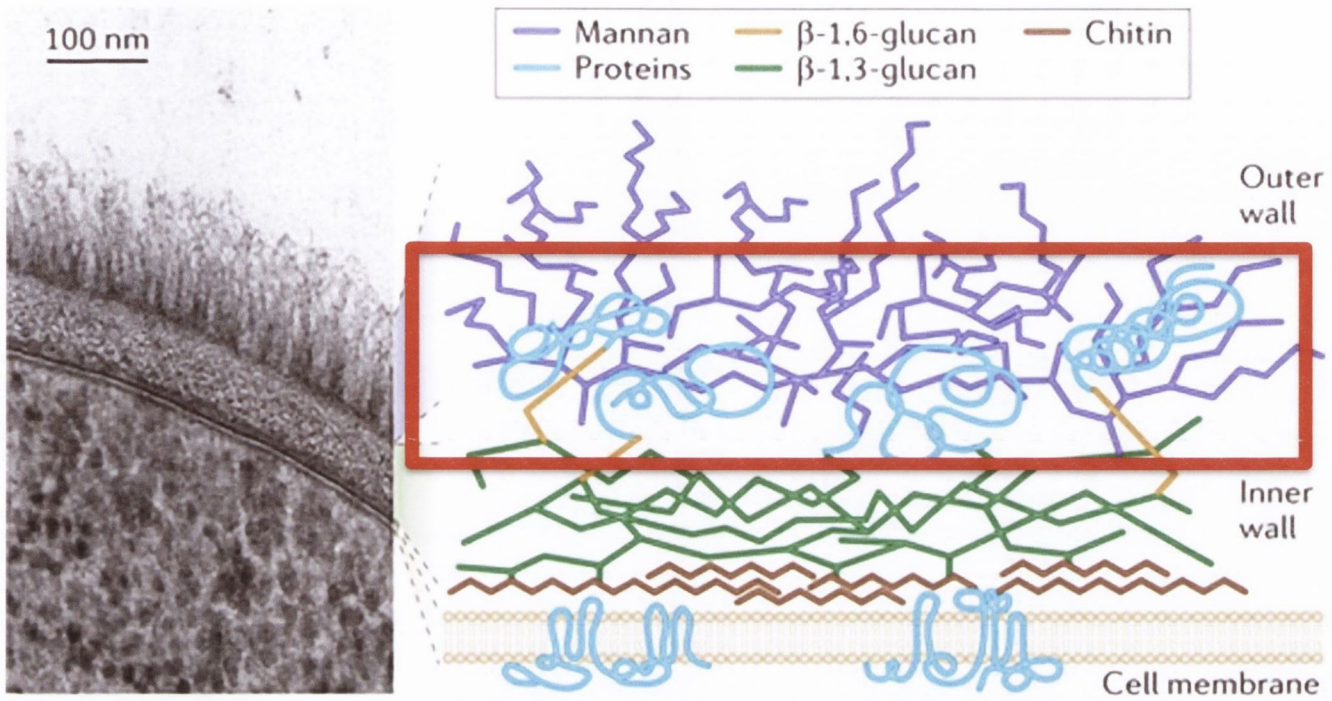
6.1.1. Cell wall composition

The *Candida* cell wall is multifunctional and serves as the interface between the fungus and the host. It provides a rigid cellular structure, protection from physical and antifungal stresses, and houses adhesins, allowing for cellular recognition of and attachment to specific substrates (Luo *et al.*, 2013). Two distinct layers protect the cell membrane. The inner wall consists of a polysaccharide network of chitin and β -1,3-glucan while the outer layer is comprised of β -1,6-glucan and decorated mannoproteins (Fig. 6.1) (Gow *et al.*, 2012).

A chitinous, rigid skeleton forms the basis of the inner cell wall (Kapteyn *et al.*, 2000). Although the total dry weight of chitin in cells is approximately 20 times lower than of β -1,3-glucan, the polymer composed of GlcNAc subunits plays an important role (Klis *et al.*, 2001). Elevated levels of chitin appear to contribute to *C. albicans* resistance to treatment with the echinocandin caspofungin (Walker *et al.*, 2013). Interestingly, levels of chitin have been shown to vary during the dimorphic switch (Munro *et al.*, 1998). *Candida albicans* hyphae have been reported to contain up to 5 times the amount of chitin in their cell walls compared to yeast cells.

The outer wall is anchored to the inner wall by covalent attachment of β -1,6-glucan to β -1,3-glucan in the inner wall (Free, 2013). While β -1,3-glucan forms a relatively rigid layer attached to chitin through covalent attachment and protein crosslinking, β -1,6-glucan acts as a flexible linker to glycosylphosphatidylinositol (GPI) outer wall proteins. Greater degrees of freedom may improve protein-substrate interactions and reduce the possibility of steric hindrance. GPI-anchored proteins are covalently bound to β -1,6-glucan and tend to be highly decorated with mannose chains (Hall & Gow, 2013). These post-translational modifications have been shown to alter recognition of cell wall glycoproteins by the host immune response.

While *C. albicans* and *C. dubliniensis* are highly related on a genetic level, there is a lack of knowledge regarding the *C. dubliniensis* cell wall ultrastructure. Inferences are made from *S. cerevisiae* and *C. albicans* data, but little experimental data exists for *C. dubliniensis* cell wall structure and protein localisation. It has been previously



Nature Reviews | Microbiology

Figure 6.1. The *C. albicans* cell wall. Schematic diagram of the multiple layers of the *C. albicans* cell wall, with mannosylated cell wall proteins forming the first point of interaction between the fungal cell and the environment. The location of mannosylated GPI-anchored proteins has been highlighted for clarity. Adapted from Gow *et al.*, 2012.

documented that *C. dubliniensis* yeast grown at 25 °C and 37 °C maintain a constant cell surface hydrophobicity associated with the appearance of its outer fibrillar layer (Jabra-Rizk *et al.*, 1999). In contrast, *C. albicans* grown at 37 °C displayed an increase in fibrillar length and density relative to growth at 25 °C. Hazen *et al.* later determined that much of this hydrophobicity phenotype, and associated substrate binding, was due to the expression pattern of a single cell wall-associated protein, *CdCsh1p* and its *C. albicans* homolog *CaCsh1p* (Hazen, 2004). However, this work was conducted in yeast cells and little is known about the cellular structure or cell wall proteins of *C. dubliniensis* hyphae compared to *C. albicans* hyphae.

6.1.2. Glycophosphatidylinositol-anchored cell wall proteins

It is widely accepted that GPI-anchored cell wall proteins are not only the most abundant group of *Candida* cell wall proteins but are most closely associated with virulence. Signal sequences at either terminus of the synthesised peptide are responsible for trafficking and processing of the peptide (Mayor & Riezman, 2004). The N-terminal signal sequence directs the peptide to the endoplasmic reticulum (Richard & Plaine, 2007). Cleavage of the carboxy-terminal peptide sequence allows attachment of a preformed GPI-anchor. It is not fully understood which signal is responsible for protein retention at the plasma membrane side of the cell wall, as opposed to transfer of proteins through the inner wall and subsequent covalent binding to GPI-attachment sites on β -1,6-glucan. Although the peptide sequence flanking the GPI-anchor is thought to play a role in this distinction, there is not yet sufficient evidence for this (Boisrame *et al.*, 2011).

In addition to cellular carbohydrate components, many *C. albicans* GPI-anchored cell wall proteins are recognised as immunogenic pathogen-associated molecular patterns (PAMPs) (Fradin *et al.*, 2000; Mora-Montes *et al.*, 2011). In particular, hyphal-associated GPI-proteins such as *CaAls3p*, *CaHyr1p*, and *CaHwp1p* are associated with virulence, and represent attractive vaccine targets (Edwards, 2012). These proteins display modular domains commonly observed in many cell wall GPI-proteins, with a carboxy-terminal GPI-anchor, a highly repetitive, glycosylated linker mid-region and a functional N-terminal domain (Klis *et al.*, 2009). As the first line of contact with host cells (other than secreted factors), cell wall GPI-proteins have been found to play important roles in adhesion, invasion and colonisation of host tissues.

In order to understand how these virulence-associated proteins contribute to disease, it is crucial to investigate and understand protein localisation on the cell surface of both *C. albicans* and *C. dubliniensis*, yeast and hyphae.

6.1.3. Protein detection in *C. albicans* and *C. dubliniensis*

Although comparative genomics have highlighted the genetic differences between *C. albicans* and *C. dubliniensis* little experimental data exists regarding *C. dubliniensis* proteins. While the existence of *C. dubliniensis* proteins such as chlamyospore-specific proteins, *CdCsp1p* and *CdCsp2p*, the hydrophobicity-associated protein, *CdCsh1p*, and the multidrug transporter, *CdCdr2p*, have been confirmed, many more inferences from genomic and transcriptomic data require investigation (Hazen, 2004; Moran *et al.*, 1998; Palige *et al.*, 2013). With regards to *C. dubliniensis* GPI-anchored cell wall proteins, Hoyer *et al.* have shown that *C. dubliniensis* cell wall protein extracts react to “Anti-Als” antibodies raised against the N-terminus of *CaAls5p*, indicating the presence of *CdAls* protein on the surface of *C. dubliniensis* cells (Hoyer *et al.*, 2001). Comparative genomics analysis has shown that although *C. dubliniensis* is missing *ALS3* from its genome, other *ALS* members, encoding proteins with similarity to their *C. albicans* counterparts, are present and this family of proteins likely mediates cell adhesion and substrate binding.

6.1.4. *In silico* protein prediction

Due to the lack of experimental evidence regarding the composition of the *C. dubliniensis* proteome it is necessary to make some predictions about the GPI-anchored cell wall proteome as a reference. ORF translations based on the sequenced *C. dubliniensis* strain CD36 and *C. albicans* strain SC5314 are both available through CGD and these resources are commonly used for *in silico* analysis (Inglis *et al.*, 2012). Known properties of GPI-anchored proteins such as signal sequences, GPI-attachment sites, isoelectric point and a lack of transmembrane helices allow filtering of peptide sequences using computational tools for *in silico* analysis (de Groot & Brandt, 2012).

6.1.5. Mass spectrometric detection of protein

Existing *C. dubliniensis* protein detection studies have predominantly used immunodetection and GFP-fusion strains to identify protein localisation (Ragni *et al.*, 2011). Difficulties in producing and obtaining *C. dubliniensis*-specific antibodies may

delay progression of protein detection studies. Mutant strains created by fusing fluorescent reporters to genes for protein tracking and detection is a commonly used method. However, detection occurs in an experimentally mutated strain and the method may produce artifacts. In order to avoid experimental artifacts in mutant derivatives it is preferable to analyse wild-type strains to detect natural protein localisation. One of the ways to achieve this is to use mass spectrometry to investigate various cellular fractions (de Groot *et al.*, 2004). Many mass spectrometry detection methods exist for identification and quantification of proteins. Both quadropole time-of-flight (Q-TOF) and Fourier transform mass spectrometry (FTMS) have recently been used successfully to analyse the wall proteome and secretome of *C. albicans* grown under various environmental conditions (Heilmann *et al.*, 2011; Sorgo *et al.*, 2010).

Q-TOF-based peptide identification is based on the premise of peptide fragment mass fingerprinting (Shevchenko *et al.*, 2000). Whole protein mixtures are digested with a specific protease, such as trypsin, and the resultant peptides are separated by chromatography, and analysed in a mass spectrometer. This yields both mass (MS) data and fragmented peptide mass (MS/MS) data. The resultant data are compared to potential mass data calculated by software such as MASCOT (Matrix Science). *In silico* calculations are generated from a user-supplied database of peptide sequences, and incorporates many criteria such as protease digestion patterns and protein modifications such as glycosylation. Comparison of experimental MS and MS/MS data with potential mass data yields most likely matches. This method can be used with complex protein mixtures and does not require any special peptide labeling. However, this method is best used for peptide identification only. Highly abundant peptides, such as those found in repetitive GPI-proteins are sampled preferentially and thus has the potential to skew any attempt to quantify protein abundance.

FTMS uses labelling of peptides with stable isotopes to obtain accurate MS and MS/MS data (Scigelova *et al.*, 2011). Replacement of the common ^{14}N nitrogen stable isotope in proteins with the stable ^{15}N nitrogen isotope by metabolic labeling allows growth of microbial cultures with ^{15}N incorporated into the proteome (Heilmann *et al.*, 2011). The difference between ^{14}N and ^{15}N labeled peptides is detected by a defined mass shift. The increased resolution and sensitivity of FTMS enables accurate

identification of paired ^{14}N and ^{15}N isotope peaks, allowing relative quantification of peptides ($^{14}\text{N}/^{15}\text{N}$). Although FTMS, paired with ^{15}N labeling, is much more sensitive than label-free methods, metabolic labeling requires growth over extended time periods (18 h) to ensure efficient incorporation of ^{15}N nitrogen into all proteins.

6.1.6. Aims of this part of the study

The dimorphic shift in *C. albicans* and *C. dubliniensis* is a dynamic event. Heilmann *et al.* succeeded in obtaining both yeast and pure hyphal cultures with *C. albicans* and presented data for the associated proteomes (Heilmann *et al.*, 2011). Using hyphal induction and maintenance methods developed and described in Chapter 5, it was possible to obtain and analyse *C. dubliniensis* proteomic data associated with the dimorphic shift. By using improved hyphal induction methods it is possible to assess the accuracy and success of *in silico* predictions, obtain a morphology-specific *C. dubliniensis* GPI-anchored cell wall proteome, and make some useful comparisons with this proteome. In this way a comparative analysis of intra- and interspecies cell wall proteomes can be performed, enabling an assessment of the contribution of the presence, and relative quantity, of specific GPI-anchored cell wall proteins to the differential virulence of *C. albicans* and *C. dubliniensis*.

6.2. Specific materials and methods

6.2.1. Growth and morphology induction conditions

The strains chosen for analysis of cell wall GPI-anchored protein repertoire were the *C. dubliniensis* strains WÜ284 and HE30. The *C. dubliniensis* strain WÜ284 is commonly used as a laboratory strain (Morschhauser *et al.*, 1999). In addition, the genomic sequence for WÜ284 has been obtained and a preliminary assembly is available. The CD36 hybrid chromosome composed of chromosome 5 and chromosome R described by Jackson *et al.* is not present in WÜ284 (personal communication, Dr. Brenda McManus). In contrast, HE30 displayed a slightly higher tendency to produce true hyphae under inducing conditions and has been found to be a relatively virulent *C. dubliniensis* strain in a murine model of systemic infection (Asmundsdottir *et al.*, 2009). Similar to WÜ284, HE30 has been sequenced and a preliminary assembly is available. SC5314 was chosen as the *C. albicans* reference strain. This has commonly been used as a *C. albicans* reference strain and a GPI-anchored cell wall-associated proteome has been obtained experimentally (Gillum *et al.*, 1984; Heilmann *et al.*, 2011).

Pure cultures of *C. albicans* and *C. dubliniensis* yeast cells were prepared by inoculating a single yeast colony from a 48 h agar plate into YEPD broth, and incubating the culture overnight at 37 °C, 200 r.p.m. After 16 h the cells were centrifuged, washed in 1X PBS and inoculated in fresh YEPD broth to a final density of 1×10^5 cells/ml. These cultures were incubated aerobically at 37 °C, 200 r.p.m., for 18 h. Final culture morphology was confirmed by microscopic visualisation

Cultures comprised purely of *C. albicans* and *C. dubliniensis* hyphal cells were prepared by inoculating a single yeast colony from a 48 h agar plate into Lee's pH 4.5 broth and incubating the culture overnight at 30 °C, 200 r.p.m. After 16 h the cells were centrifuged, washed in 1X PBS and inoculated at a final density of 1×10^5 cells/ml in DUBLIN medium, supplemented with 0.1 % (w/v) galactose and 10 % (v/v) FCS, prewarmed to 37 °C in a 5 % (v/v) CO₂ incubator. Broths were divided into small-scale batches in petri dishes to avoid microenvironment pockets influencing formation of hyphae. Broths were incubated statically at 37 °C under 5 % (v/v) CO₂ for 18 h. Morphology was assessed by microscopic visualisation.

In each case, a reference culture containing standard ^{14}N nitrogen was generated for each strain under each morphological condition. Due to the limitations of hyphal formation of *C. dubliniensis* with a single defined nitrogen source over long time periods, it was necessary to generate a mixed morphology culture to act as the ^{15}N isotope-labelled reference culture. Microscopically, this culture was determined to contain approximately 50 % yeast cells and 50 % hyphal cells by visual biomass estimation. The ^{15}N *C. albicans* reference culture used for this study was kindly supplied by Clemens Heilmann, University of Amsterdam (Heilmann *et al.*, 2011). *Candida* strains were initially grown on YEPD agar for 48 h at 37 °C.

A mixed morphology, single nitrogen source *C. dubliniensis* culture was prepared by inoculating a single WÜ284 colony into Lee's pH 4.5 broth (prepared with ^{15}N ammonium sulphate in place of ^{14}N ammonium sulphate) and incubating the culture overnight at 30 °C with shaking. After 16 h the cells were centrifuged, washed in 1X PBS and inoculated to a final density of 1×10^5 cells/ml in prewarmed ^{15}N growth medium (0.5 g/L ^{15}N ammonium sulphate, 0.07 % (w/v) YNB -aa $-(\text{NH}_4)_2\text{SO}_4$, 0.1 % (w/v) galactose). This ^{15}N culture was also divided into small-scale batches in petri dishes and incubated statically at 37 °C under 5 % (v/v) CO_2 for 18 h.

An aliquot from each culture was examined microscopically to assess morphology. Cultures were centrifuged, cells were washed three times in 1X PBS, snap frozen in liquid nitrogen and stored at -80 °C.

6.2.2. Effective cell disruption and isolation of cellular protein fractions

Yeast and hyphal cell suspensions were centrifuged at $3,500 \times g$ for 7 min, washed three times in cold 1X PBS, and resuspended in 1X PBS. Suspensions (1.5 ml) were divided evenly into 2 ml screw capped Eppendorf tubes and centrifuged at $16,000 \times g$ for 3 min. The supernatant was removed and pellets were resuspended in 400 μl Tris-HCl, pH 7.5, and 5 μl protease inhibitor cocktail (Sigma-Aldrich). This mixture was transferred to fresh 2 ml screw-cap microfuge tubes containing 200 mg glass beads (425 - 600 μm , Sigma). An additional 400 μl Tris-HCl buffer was added to the suspensions. Tubes were transferred to a bead beater (Fastprep FP120) and cells

were broken with interspersed chilling steps on ice. Cell disintegration efficiency was monitored by direct visualisation under a light microscope.

Cold 1 M NaCl was used to rinse and pool the lysed contents of each tube into a 50 ml conical Falcon tube. The contents of the Falcon tube were allowed to settle and the supernatant was transferred to a fresh 50 ml tube. The remaining glass beads and lysed material were washed three times with fresh 1 M NaCl by shaking. The resultant supernatant was also transferred to collect as much of the lysed material as possible. The lysate was centrifuged at $3,500 \times g$ for 7 min, the supernatant, which represents the intracellular protein fraction, was poured into a clean, sterile 50 ml Falcon tube, and stored at $-80\text{ }^{\circ}\text{C}$.

The remaining pellet was resuspended and washed with cold 1 M NaCl a total of six times. The pellet was then washed three times with cold ultrapure water. The supernatant was discarded and the pellet was allowed to equilibrate at room temperature. After 10 min equilibration, 20 ml SDS-extraction buffer with βMe was used to resuspend the pellet completely. The suspension was incubated at $37\text{ }^{\circ}\text{C}$, 200 r.p.m. for 30 min. After 30 min the suspension was centrifuged at $3,500 \times g$ for 7 min and the supernatant was discarded. The pellet was resuspended using 20 ml of fresh SDS extraction buffer. The suspension was incubated at $37\text{ }^{\circ}\text{C}$, 200 r.p.m. overnight. After 12 h the supernatant was discarded, 15 ml SDS-extraction buffer was added and the resuspended mixture was boiled for 10 min. The tubes were allowed to cool at room temperature, centrifuged at $3,500 \times g$ for 10 min, and the supernatant, which represented the SDS-extractable fraction, was stored at $-80\text{ }^{\circ}\text{C}$.

The remaining pellet was boiled in SDS-extraction buffer a total of 5 times. The remaining SDS was removed from the pellet by washing with ultrapure water for a total of 6 washes. The resultant cell wall fraction was resuspended in $500\text{ }\mu\text{l}$ of ultrapure water and aliquoted into Lo-Bind Eppendorfs (Sigma-Aldrich). The tubes were centrifuged at $16,000 \times g$ for 3 min and the supernatant was removed. The cell wall pellets were frozen in liquid nitrogen and freeze-dried (Freezone Triad Freeze Dry System, TCBE, Trinity Biomedical Sciences Institute) overnight for $\sim 12\text{ h}$. The freeze-dried walls were stored at $-80\text{ }^{\circ}\text{C}$.

6.2.3. Sample preparation for mass spectrometry

The pilot study experiments described as follows were performed in the laboratory of Prof. F. Klis, University of Amsterdam, with the invaluable assistance of C. Heilmann and L. de Koning. Subsequent biological replicates were kindly prepared for mass spectrometry and processed by H. Dekker and L. de Koning, with assistance from Prof. F. Klis.

6.2.4. Preparation of peptides

6.2.4.1. Disulphide bond reduction and alkylation

Freeze-dried cell wall pellets were treated with 100 μ l reducing solution (10 mM DTT, 100 mM NH_4HCO_3) and incubated at 55 °C for 1 h to break the disulphide bonds in the cell wall proteins. The solution was allowed to cool at room temperature, centrifuged, and the supernatant was removed. Alkyl groups were added to the cysteine residues to prevent reformation of disulphide bonds by adding 100 μ l alkylating solution (65 mM IAA, 100 mM NH_4HCO_3) to the pellet and incubating at room temperature for 45 min in the dark. The solution was centrifuged and the supernatant was removed. The alkylating reaction was halted by adding 100 μ l quenching solution (55 mM DTT, 100 mM NH_4HCO_3) to the pellet and incubating it at room temperature for 5 min. The solution was centrifuged and the supernatant was removed. Residual DTT and IAA were removed by washing the pellet five times in 50 mM NH_4HCO_3 .

6.2.4.2. Tryptic digestion of cell wall proteins

Enzymatic digestion of reduced, partially unfolded cell wall GPI proteins, to create tryptic peptide passports, was achieved using trypsin enzyme at a ratio of 50:1 (mg protein to mg enzyme). Each cell wall pellet was completely resuspended in 160 μ l of 50 mM NH_4HCO_3 . Trypsin was added to the suspension and incubated overnight at 37 °C with shaking. After 16 h the suspension was centrifuged, and the supernatant containing the digested peptides was transferred to a Lo-Bind Eppendorf tube and stored at -80 °C. The cell wall pellet was also stored at -80 °C.

6.2.4.3. Peptide processing

Processing of the supernatant, containing the peptides, was necessary to desalt and concentrate the peptides for subsequent HPLC and mass spectrometry. This was achieved using an Omix ZipTip column C18 (Varian, Palo Alto, California, USA). A 100 µl ZipTip was activated by pipetting and dispensing 100 µl 60 % (v/v) ACN three times. The column was equilibrated by pipetting and dispensing 100 µl 0.1 % (v/v) TFA three times. 100 µl of the peptide solution was drawn into the column and pipetted and dispensed in the sample Eppendorf tube four times to ensure effective binding of peptide to the column. The column was then washed three times with 0.1 % (v/v) TFA. Column-bound peptides were eluted by pipetting a solution of 20 µl 60 % (v/v) ACN, 0.1 % (v/v) TFA and transferred to Lo-Bind tube. Concentration of peptides was estimated by the A205 method relating absorbance to peptide quantification (Scopes, 1974).

6.2.5. Quadropole Time of Flight mass spectrometry

6.2.5.1. Run conditions

Q-TOF run conditions mirrored those used in previous studies (Heilmann *et al.*, 2011). Briefly, peptides were injected onto an Ultimate 2000nano-HPLC System (LC Packings, Amsterdam, The Netherlands) fitted with a PepMap100 C18 reversed phase column (Dionex, Sunnyvale, CA, USA). The elution flow rate was 0.3 µl/min over a linear gradient of increasing concentration of acetonitrile and eluted peptides were directly ionised in a Q-TOF (Micromass, Whyttenshaw, UK).

6.2.5.2. Data analysis

Masslynx Proteinlynx Software was used to process the resultant spectra. Peak list data in the form of .pkl files were submitted to a licensed version of MASCOT (Matrix Science, UK) and referenced against both *C. albicans* and *C. dubliniensis* proteome databases (CGD). Two miscleavages and a 0.6 Da threshold for peptides and MS/MS were allowed for MASCOT analysis. Peptides and proteins were identified by a system of probabilistic MASCOT scoring with $p < 0.05$ defined as statistically significant.

6.2.6. Fourier Transform mass spectrometry

6.2.6.1. Run conditions

Fourier Transform Mass Spectrometry (FTMS) conditions were identical to those used previously (Heilmann *et al.*, 2011). Briefly, the equipment configuration consisted of an ApexQ Fourier transform ion cyclotron resonance mass spectrometer (Bruker Daltonik, Bremen, Germany) with a 7 T magnet and a Combisource™ coupled to an Ultimate 3000 HPLC system (Dionex, Sunnyvale, CA, USA), with a PepMap 100 C18 precolumn and a PepMap 100 C18 analytical column (Dionex, Sunnyvale, CA, USA). A flow rate of 3 µl/min over a linear gradient (0.1 % (v/v) formic acid/ 100 % (v/v) H₂O to 0.1 % (v/v) formic acid/ 40 % (v/v) ACN/ 60 % (v/v) H₂O) generated a chromatogram of ESI-FT-MS spectra.

6.2.6.2. Data analysis

Data processing was carried out with the Data Analysis 3.4 software program (Bruker Daltonik, Bremen, Germany). Each analysis generated a list of calculated monoisotopic masses and these lists were exported as a MASCOT generic file (.mgf). The .mgf files were imported in the CoolToolBox Software (SILS, University of Amsterdam) and peptide ion chromatograms were generated. Mass and retention time were also calculated from the data. This allowed calculation of isotope abundance over the ion chromatogram. Ion masses were attributed to peptide identifications by matching the isotopic masses within 1.5 p.p.m. from the LC-FT-MS data with the mass of tryptic peptides generated from *in silico* digestion of the *C. albicans* and *C. dubliniensis* proteome databases. ¹⁴N and ¹⁵N peptides were distinguished by a reliable difference in retention time, with the ¹⁵N peptides eluting just before the ¹⁴N peptides due to their larger mass. This enabled the CoolToolBox software to identify ¹⁴N/¹⁵N tryptic peptide pairs and the ratio of their isotopic abundance.

6.2.7. *In silico* protein prediction tools

A number of tools were used to predict potential GPI-anchored cell wall proteins in *C. dubliniensis*. A *C. dubliniensis* proteome database was generated using the ORF translation of the CD36 genome from CGD. This proteome database, and its *C. albicans* counterpart, generated from SC5314 ORF translation, was scanned for GPI

modification sites using the Fungal Big-PI tool (Eisenhaber *et al.*, 2004). Signal peptide cleavage sites were detected using SignalP (Nielsen *et al.*, 1997). Prediction of transmembrane helices was handled by TMHMM (Krogh *et al.*, 2001). The output of these tools were combined with ProFASTA pipeline tool to filter the combined datasets (de Groot & Brandt, 2012). The ProFASTA output for each database was analysed for classic GPI anchored cell wall motifs by amino acid distribution patterns. *Candida albicans* output was compared to experimentally proven data to support validation of the prediction method (Heilmann *et al.*, 2011).

6.3. Results

6.3.1. *In silico* protein prediction

Both *C. albicans* and *C. dubliniensis* proteome databases were analysed in the same way to predict potential cell wall GPI-anchored proteins for comparison. A *C. albicans* database obtained from SC5314 data contained 6201 non-redundant protein entries. Proteins with an isoelectric point (PI) of > 5.0 were filtered out, leaving 2053 proteins. Of these, 111 proteins were predicted to have GPI anchors. Scanning for a signal sequence and the presence of transmembrane helices reduced the final count to 34 potential cell wall GPI-anchored proteins. This represents just 0.6 % of the calculated total protein repertoire of *C. albicans*. *Candida dubliniensis* possesses a proteome of similar size. A total of 5847 protein entries comprised the *C. dubliniensis* proteome database. Only 1207 proteins were calculated to have a PI < 5.0. Of those 1207 proteins, 77 proteins were predicted to possess a GPI-anchor attachment point using Fungal BigPI. Filtering with SignalP and TMHMM revealed a final count of 31 potential cell wall GPI-anchored proteins for *C. dubliniensis*. This represents 0.5 % of the total *C. dubliniensis* protein repertoire.

All but one *C. dubliniensis* protein, encoded by Cd36_65010 (best hit; *CaALS4*), possessed *C. albicans* orthologues (i.e. proteins which evolved from a common ancestral gene). However, only 14 proteins were matched for both *C. dubliniensis* and *C. albicans* potential GPI- protein datasets. The reason for this is unclear although further sequence analysis may identify discrepancies in the GPI-anchor sequences, or signal sequences recognised by the *in silico* algorithms.

ProFASTA analysis of amino acid distribution of the predicted GPI-anchored proteins commonly showed serine/threonine-rich mid-regions. Predicted GPI-proteins also displayed enrichment of hydrophobic amino acid side chains (GAVLIPFMWC) at each end of the protein.

6.3.2. Morphological induction and maintenance

While long-term (18 h) *C. dubliniensis* and *C. albicans* hyphae were successfully generated using DUBLIN medium supplemented with galactose, and grown under 5 % (v/v) CO₂, the resultant biomass was relatively low, reflecting the lack of nutrients.

Addition of FCS to the culture medium at a final concentration of 10 % (v/v) considerably increased the biomass generated and was deemed to be necessary for generation of sufficient cell wall material for analysis by mass spectrometry. These cultures represented the ^{14}N query cultures.

The reference *C. dubliniensis* culture contained ^{15}N labeled ammonium sulfate ($(\text{NH}_4)_2\text{SO}_4$) as the sole nitrogen source. This culture contained a mixture of yeast and hyphal forms. The ratio of yeast to hyphal forms was roughly 1:1. This provided a good mix of yeast-specific, hyphal-specific and morphotype independent proteins for subsequent FTMS identification and relative quantification.

6.3.3. Protein identification by Q-TOF mass spectrometry

Analysis of the *C. dubliniensis* WÜ284 ^{14}N query cultures by Q-TOF generated a distinctive GPI-anchored cell wall protein profile (Table 6.1). A total of 18 proteins were detected with five of those being yeast-specific and 4 hypha-specific proteins. The nine morphotype independent proteins that were detected are predominantly associated with cell wall stability. The yeast-specific profile identified two adhesin proteins (*CdAls2p*, *CdAls4p*), an aspartyl protease (*CdSap9p*), a pH-responsive protein (*CdPhr2p*), and *CdRhd3p*, a protein associated with iron-rich environments and virulence. WÜ284 hyphae were found to specifically express a superoxide dismutase (*CdSod5p*), putative adhesins (*CdHwp1p*, *CdFlo9p*) and a protein of unknown function but with similarity to *Hwp1p* (*CdRbt1p*). The morphotype independent proteins identified included *CdEcm33p*, *CdCrh11p*, *CdCht2p*, *CdUtr2p*, *CdRbt5p*, *CdPga4p*, *CdPir1p*, *CdMp65p*, and *CdSsr1p*. These proteins were found in both yeast and hyphal cells.

A total of 17 GPI- anchored cell wall proteins were detected by Q-TOF analysis of HE30 cells. Similar to WÜ284, HE30 yeast cells specifically displayed the adhesins *CdAls2p* and *CdAls4p*. The aspartyl protease, *CdSap9p*, and pH-responsive, *CdPhr2p*, were identified on HE30 yeast cells alone. Hyphal HE30 cells displayed *CdSod5p* superoxide dismutase, the pH-responsive protein, *CdPhr1p*, and the putative adhesin, *CdFlo9p*, were also detected in filamentous HE30 cell samples. The morphotype independent profile generated matched that seen in WÜ284 cells with one divergence. Interestingly, *CdRhd3p* was identified on both yeast and hyphal cells.

C. albicans SC5314 cells presented a panel of 19 detected GPI-anchored cell wall proteins. SC5314 YEPD-grown yeast cells specifically displayed adhesins (*CaAls1p*, *CaAls4p*), an aspartyl protease (*CaSap9p*), pH-responsive protein (*CaPhr2p*) and iron-associated protein (*CaRhd3p*), similar to WÜ284. However, *CaUtr2p* and *CaMp65p* were designated as being yeast morphology-specific. *CaPga10p* was also detected in the yeast form, however this shares a tryptic peptide identification sequence with *CaRbt5p* leading to identity uncertainty. The hyphal-specific SC5314 profile identified four proteins consisting of adhesins (*CaAls3p*, *CaAls5p*), superoxide dismutase (*CaSod5p*) and a protein associated with protection against host defences (*CaHyr1p*).

Analysis by Q-TOF has identified a core, shared GPI-anchored cell wall protein profile for *C. albicans* and *C. dubliniensis*. In both species, yeast-specific proteins include *Phr2p*, *Als4p* and *Sap9p* while *Sod5p* is expressed specifically on hyphae. Unsurprisingly, the shared core set of proteins contains cell-stability related proteins *Cht2p*, *Pir1p*, *Ecm33p*, *Rbt5p*, *Pga4p*, *Crh11p*, and *Ssr1p*. Other proteins detected vary in expression according to morphotype and may be significant factors in differing virulence of the respective species and strains.

Q-TOF identifications were based on detection of tryptic peptide sequences. Certain tryptic sequences, such as those found in proteins possessing CFEM domains (*Rbt5p*, *Pga10p*) not only produce dominant peaks when analysed by Q-TOF, leading to preferential detection of these proteins, but also make discernment between CFEM proteins difficult without additional identifying peptides.

6.3.4. Relative quantification of proteins by FTMS

6.3.4.1. Interspecies protein variation

While Q-TOF analysis allows identification of peptides and proteins, FTMS analysis provided both identification and a method of relative quantification based on the different isotope mass ratios of ^{15}N nitrogen to ^{14}N nitrogen. As this ratio is dependent on the presence of proteins in both the single-morphology ^{14}N query cultures and the dual morphology ^{15}N reference culture, proteins absent from the ^{14}N

Table 6.1. Identification of GPI-proteins by Q-TOF mass spectrometry.

Protein Name	<i>C. dubliniensis</i> ORF	<i>C. albicans</i> ORF	WÜ284	HE30	SC5314	Protein Function ^a
Phr2	Cd36_00220	orf19.6081	Y	Y	Y	Transglycosylase
Als4	Cd36_64610	orf19.4555	Y	Y	Y	Adhesin
Als2	Cd36_64800	orf19.1907	Y	Y	-	Adhesin
Utr2	Cd36_81610	orf19.1671	Y/H	Y/H	Y	Transglycosylase
Rhd3	Cd36_43810	orf19.5305	Y	Y/H	Y	Unknown, Iron-associated
Pga10	Cd36_40510	orf19.5674	-	-	Y	Iron acquisition
Mp65	Cd36_24090	orf19.1779	Y/H	Y/H	Y	Transglycosylase
Sap9	Cd36_83850	orf19.6928	Y	Y	Y	Protease
Als1	Cd36_64210	orf19.5471	-	-	Y	Adhesin
Cht2	Cd36_53830	orf19.3895	Y/H	Y/H	Y/H	Chitinase
Pir1	Cd36_23050	orf19.220	Y/H	Y/H	Y/H	Unknown, wall integrity
Ecm33	Cd36_02990	orf19.3010.1	Y/H	Y/H	Y/H	Wall integrity
Rbt5	Cd36_40190	orf19.5636	Y/H	Y/H	Y/H	Iron binding
Pga4	Cd36_54990	orf19.4035	Y/H	Y/H	Y/H	Transglycosylase
Crh11	Cd36_42770	orf19.10221	Y/H	Y/H	Y/H	Transglycosylase
Ssr1	Cd36_70800	orf19.7030	Y/H	Y/H	Y/H	Wall integrity
Als3	-	orf19.1816	-	-	H	Adhesin, Iron-binding
Hyr1	-	orf19.4975	-	-	H	Neutrophil resistance
Sod5	Cd36_15620	orf19.9607	H	H	H	Superoxide dismutase
Flo9	Cd36_80540	orf5404.1	H	H	-	Putative adhesin
Hwp1	Cd36_43360	orf19.1321	H	-	-	Adhesin
Rbt1	Cd36_43400	orf19.1327	H	H	-	Unknown, similar to Hwp1
Als5	Cd36_64210	orf19.5736	-	-	H	Adhesin

Proteins were identified as being present in yeast culture only (Y), hyphal culture only (H), or morphology independent (Y/H).

^a Function inferred from *C. albicans* putative functions.

query culture returned a ratio value of 0. For the sake of simplicity, for interspecies comparison, the ratio values for individual morphologies were summed, and protein abundances were expressed as a percentage of the “morphological sum” (Table 6.2). Consequently, the relative abundance of the detected GPI-anchored protein abundance on the cell walls of each morphotype and species were determined (Fig. 6.2).

WÜ284 YEPD-grown yeast displayed 15 GPI-anchored cell wall proteins upon analysis by FTMS. The predominant protein detected was *CdPhr2p*, representing 67.5 % of the GPI-anchored protein present on the cell wall. The second most abundant GPI-protein on the yeast cell surface was *CdPir1p*, followed by *CdRhd3p*, *CdUtr2p*, and *CdEcm33p*. These five proteins represent approximately 90 % of the GPI-protein presence. The remaining 10 % consisted of small amounts of *CdCht2p*, *CdSsr1p*, *CdCrh11p*, *CdPga4p*, *CdAls2p*, *CdAls4p*, *CdMp65p*, *CdPhr1p*, *CdSod5p*, and *CdSsa2p* in descending order of abundance.

Using this methodology, WÜ284 committed hyphae displayed only 13 GPI-anchored proteins. *CdCht2p* and *CdPhr1p* represented 35.6 % and 17.7 % respectively of the GPI-proteins present. The superoxide dismutase *CdSod5p* showed an abundance of 16 %. *CdCrh11p* and *CdPga4p* accounted for 10.3 % and 5.6 % respectively. The final 15 % consisted of *CdEcm33p*, *CdMp65p*, *CdRbt5p*, *CdSap9p*, *CdSsa2p*, *CdRhd3p*, *CdAls2p*, and *CdAls4p*.

Yeast cells from the relatively more virulent *C. dubliniensis* strain HE30 produced 16 detectable GPI-anchored cell wall proteins under the conditions tested. The most abundant protein, similar to WÜ284 yeast, was found to be *CdPhr2p* with 37.9 % share of the GPI-protein abundance. Also similar to WÜ284, the second most abundant protein was *CdPir1*. However, *CdPir1* represented 16.8 % of the HE30 yeast cell wall compared to approximately 8 % on WÜ284 yeast cells with relation to GPI-anchored proteins. *CdAls1p* constituted 10.9 % of the GPI-protein repertoire. The remaining 35 % was comprised of *CdRhd3p*, *CdUtr2p*, *CdEcm33p*, *CdCht2p*, *CdSsr1p*, *CdAls2p*, *CdPga4p*, *CdCrh11p*, *CdMp65p*, *CdAls4p*, *CdPhr1p*, *CdSod5p*, and *CdSsa2p*.

HE30 hyphae from 18 h cultures displayed 15 GPI-anchored cell wall proteins. The single most abundant GPI-protein found was *CdFlo9p*, representing over 75 % of the detectable GPI- protein. Remarkably, *CdFlo9p* was not detected at all on the surface of *C. dubliniensis* WÜ284 hyphae by FTMS, in contrast to the less sensitive Q-TOF. The second most abundant protein on the surface of HE30 hyphae was the chitinase, *CdCht2p*. Similar to WÜ284 hyphae, *CdSod5p* accounted for the third most abundant protein with a 4.8 % share of the HE30 hyphal GPI-protein repertoire. The remaining proteins in descending order of abundance were *CdPhr1p*, *CdCrh11p*, *CdUtr2p*, *CdSap9p*, *CdSsr1p*, *CdPga4p*, *CdRhd3p*, *CdMp65p*, *CdSsa2p*, *CdPga25p*, *CdAls2p*, *CdAls4p*.

SC5314 yeast from 18 h YEPD cultures displayed 18 different GPI-anchored proteins. As observed with both *C. dubliniensis* strains, *C. albicans* SC5314 yeast cells presented *CaPhr2p* as the most abundant protein under these growth conditions, with 42.3 % of the share of detected GPI-proteins. This was followed by *CaUtr2p*, with approximately 20 % abundance. The third most abundant GPI- protein was *CaEcm33p*, representing 8.3 % of the available GPI-anchored cell wall protein. The remaining 30 % were found to consist of *CaPir1p*, *CaCht2p*, *CaMp65p*, *CaCrh11p*, *CaPga4p*, *CaSsr1p*, *CaAls4p*, *CaRhd3p*, *CaRbt5p*, *CaAls2p*, *CaPhr1p*, *CaSsa2p*, *CaSod4p*, *CaRbt1p*, and *CaAls3p*.

SC5314 hyphae from 18 h cultures were observed to display 16 GPI-anchored cell wall proteins. The dominant GPI- protein on the surface of these cells was *CaHyr1p*, covering 72 % of the space allocated to GPI-anchored proteins. *CaAls3p* was the second most abundant protein representing 10.9 % of the GPI- protein on the hyphal cell surface. *CaSod5p* is present in similar proportions to *CaAls3p*. The remainder of the GPI-anchored hyphal cell surface consists of *CaPhr1p*, *CaCrh11p*, *CaPga4p*, *CaRbt5p*, *CaSsr1p*, *CaEcm33p*, *CaCht2p*, *CaRbt1p*, *CaPir1p*, *CaRhd3p*, *CaSod4p*, *CaAls2p*, and *CaAls4p* in descending order of abundance.

6.3.4.2. Intraspecies protein variation

As both WÜ284 and HE30 analyses use the same ¹⁵N reference culture, the resultant data can be directly related to each other. For intraspecies comparison of *C. dubliniensis* strains it was valid to directly compare ¹⁴N/¹⁵N ratios (Table 6.3). Thus it

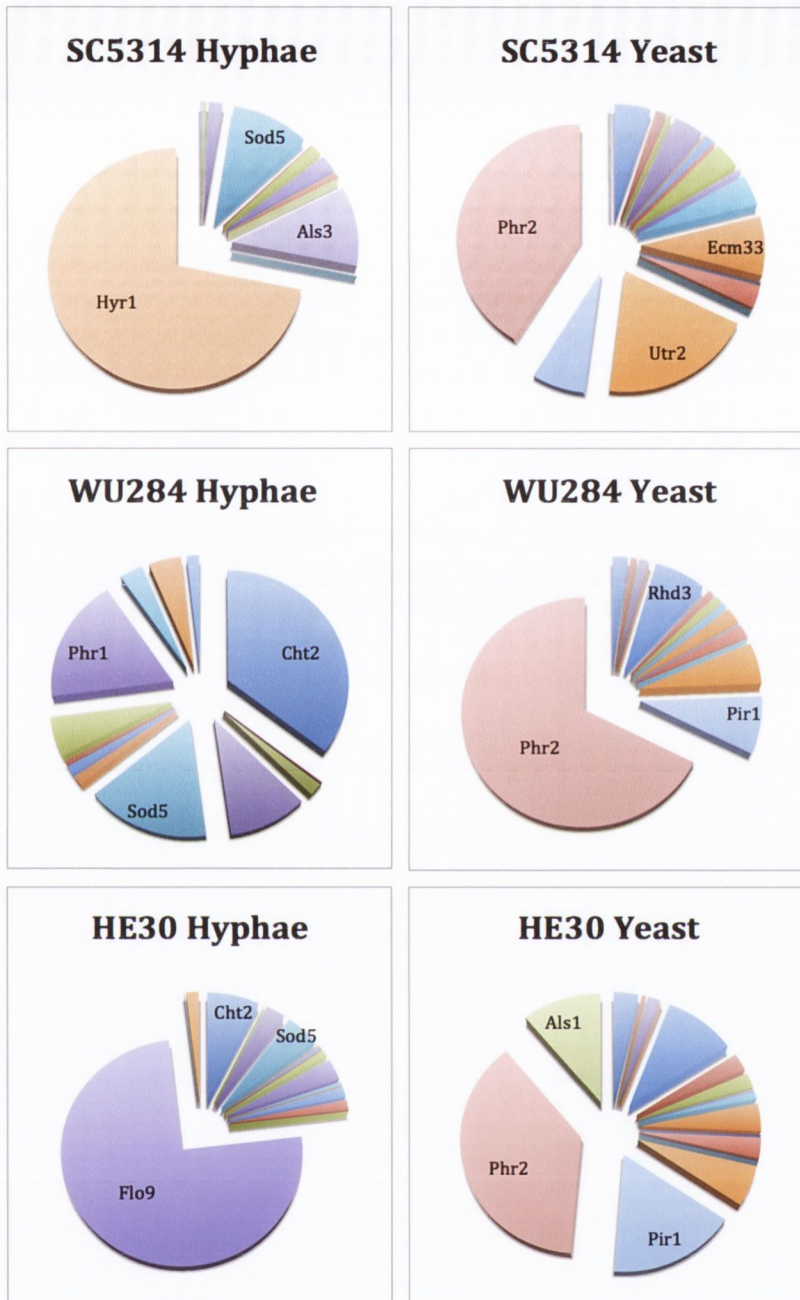


Figure 6.2. Interspecies GPI-protein variation and GPI-protein abundance. Data obtained from FTMS analysis of *C. albicans* and *C. dubliniensis* GPI-anchored cell wall proteomes enabled construction of a GPI-protein profile for yeast and hyphal morphologies. Abundance of specific GPI-proteins, as part of the detected GPI-repertoire, is shown here. For clarity, only the three most abundant GPI-proteins in each case have been labelled.

Table 6.2. Interspecies comparison of GPI-protein abundance by FTMS on *C. albicans* and *C. dubliniensis* cell walls.

Protein Name	SC5314 Hyphae	SC5314 Yeast	WÜ284 Hyphae	WÜ284 Yeast	HE30 Hyphae	HE30 Yeast
Cht2	0.17	4.84	35.60	2.10	7.21	3.44
Als4	0.00	1.48	0.17	0.88	0.03	0.52
Rbt5	0.51	0.49	1.80	-	-	-
Crh11	1.84	4.02	10.31	1.30	2.70	1.72
Sod5	10.20	-	15.99	0.03	4.78	0.05
Ssa2	-	0.10	1.42	0.00	0.18	0.01
Rhd3	0.03	1.22	1.30	7.14	0.49	10.02
Als2	0.00	0.17	0.49	0.89	0.04	2.53
Pga4	1.47	3.69	5.75	1.20	1.06	2.18
Phr1	2.36	0.58	17.72	0.09	3.13	0.14
Mp65	-	4.35	3.24	0.62	0.49	1.08
Ecm33	0.30	8.24	4.52	2.25	-	4.03
Sap9	-	-	1.69	-	1.52	-
Ssr1	0.41	3.10	-	1.94	1.50	2.98
Rbt1	0.06	0.03	-	-	-	-
Flo9	-	-	-	-	75.02	-
Pga25	-	-	-	-	0.08	-
Utr2	-	19.68	-	5.89	1.76	5.81
Pir1	0.03	6.63	-	8.16	-	16.76
Phr2	-	41.30	-	67.50	-	37.86
Als1	-	-	-	-	-	10.87
Als3	10.81	0.01	-	-	-	-
Sod4	0.02	0.05	-	-	-	-
Hyr1	71.78	-	-	-	-	-

% protein abundance determined by sum score distribution
 - Protein not detected in query culture.

was observed that *CdCht2p* relative abundance did not vary significantly between yeast cells from WÜ284 and HE30. There was relatively more *CdCht2p* in HE30 hyphae compared to WÜ284 hyphae, indicating higher levels of cell wall remodeling in HE30 hyphae. In each case there was more *CdCht2p* present in hyphae of either species compared to yeast cells. By the same comparisons, there was almost three times the amount of *CdAls4p* on the surface of WÜ284 yeast cells relative to HE30 yeast cells. While the levels of *CdCrh11p* were stable between HE30 yeast and hyphae, there was half the amount of *CdCrh11p* present on the surface of WÜ284 hyphae compared to WÜ284 yeast. Yeast from both WÜ284 and HE30 displayed low levels of *CdSod5p*. Abundance of *CdSod5* on the surface of hyphae was much higher than yeast cells of both strains, with HE30 hyphae displaying double the amount of *CdSod5p* relative to WÜ284 hyphae. Levels of *CdAls2p* on the surface of yeast highlighted intraspecies differences that may influence virulence, as HE30 yeast possessed double the amount of *CdAls2p* on their cell surface compared to WÜ284 yeast. While HE30 hyphae and yeast both expressed *CdUtr2p* on the surface of their cells, with nearly 4.5 times the amount on hyphae as on yeast, the protein was absent from the surface of WÜ284 hyphae. However WÜ284 yeast displayed almost twice the amount of *CdUtr2p* on their surface relative to HE30 yeast. Similarly WÜ284 yeast displayed almost 3 times the amount of *CdPhr2p* on their surface relative to HE30 yeast.

6.3.5. Gene expression analysis of a hypha-associated GPI-protein

Due to the unexpected abundance of *CdFlo9p* on the surface of *C. dubliniensis* HE30 hyphal cells, qRT-PCR was used to analyse expression of *FLO9* encoding the GPI-anchored cell wall protein in both *C. dubliniensis* and *C. albicans*. Using the improved method for *C. dubliniensis* hyphal induction, developed and described in Chapter 5, RNA was isolated from cells induced to grow exclusively as yeast or hyphae, with conditions matching those used for GPI-anchored cell wall proteome analysis. Expression of *FLO9* in both *C. albicans* and *C. dubliniensis* was assessed to both support proteome findings, and examine the temporal gene expression pattern of this hypha-associated protein.

Analysis of *CdFLO9* gene expression in HE30 hyphal cells yielded results reflecting the proteome findings (Fig. 6.3). In HE30 hyphae, *CdFLO9* was found to be highly

upregulated over the course of 18 h when induced with DUBLIN medium supplemented with galactose and FCS. While HE30 hyphal cells induced with WS displayed upregulation of *CdFLO9* between 3 h and 6 h, this trend did not continue. After 18 h growth in WS, the increase in gene expression had been reduced to levels almost matching those of the initial inoculation culture (T_0), apparently mirroring the trend of morphological reversion of hyphae to yeast. YEPD-grown yeast cells showed little change in expression of *CdFLO9* over the course of 6 h. Between 6 h and 18 h, however, expression levels decreased by over 100-fold relative to T_0 .

As with the proteomic data, the pattern of gene expression of *CdFLO9* in WÜ284 hyphal cells deviated from that observed with HE30 hyphal cells. While hyphal induction with WS followed a similar pattern to HE30 WS-induced hyphae, with gene induction peaking at 6 h and reducing thereafter, induction with DUBLIN medium resulted in a reduction in *CdFLO9* expression by 200-fold after only 1 h. This decrease in gene expression reduced in magnitude over the course of 18 h, with the final measurement yielding a 36-fold reduction in gene expression at T_{18} . The pattern of *CdFLO9* expression in WÜ284 yeast was found to be quite stable, with little deviation from T_0 levels, over the course of 18 h.

Interestingly, *C. albicans* SC5314 hyphae displayed yet another pattern in expression of *FLO9* (*CaFLO9*). DUBLIN-induced SC5314 hyphae initially showed a 9-fold reduction in expression levels. This trend reversed, resulting in a 9-fold increase in gene expression after 6 h, rising to a 11-fold increase after 18 h. WS-induced SC5314 hyphae showed a similar decrease in gene expression after 1 h. Gene expression subsequently increased after 1 h. However, the rate of increase was much slower than that observed with DUBLIN-induced hyphae. Even after 18 h, expression levels did not equal those observed in the initial cell inoculum (T_0). YEPD-grown yeast cells followed the gene expression pattern displayed by WS-induced cells.

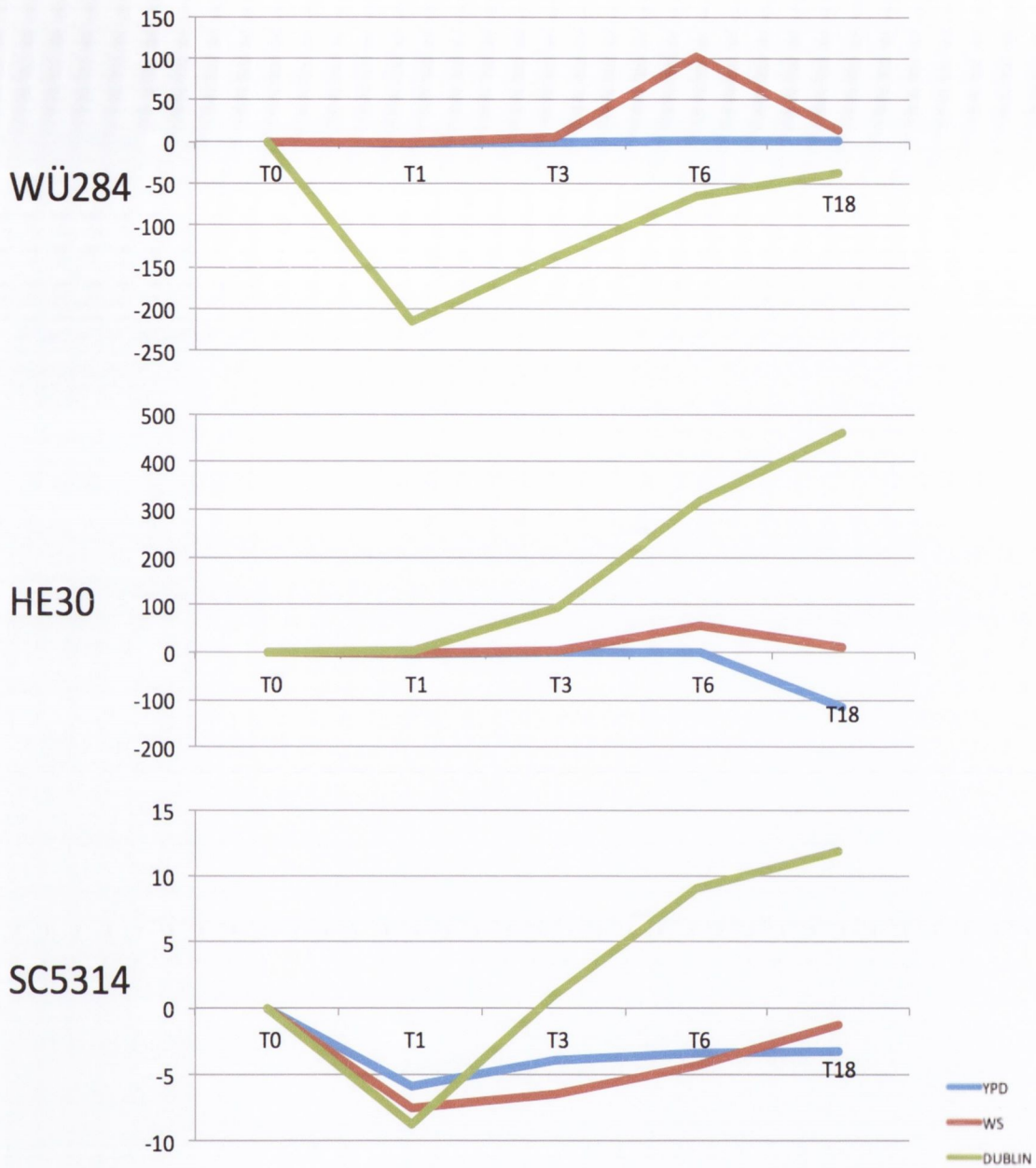


Figure 6.3. Analysis of *C. dubliniensis* and *C. albicans* hypha-associated *FLO9* gene expression. Expression of *FLO9*, encoding a GPI-anchored cell wall protein, was measured by qRT-PCR from *C. dubliniensis* and *C. albicans* cultures grown under different morphology-inducing conditions over the course of 18 h. Data is presented as fold change values ($2^{-\Delta\Delta C_t}$) relative to 0 h i.e. gene expression levels in the cell inoculum.

6.4. Discussion

Due to the close evolutionary relationship between *C. albicans* and *C. dubliniensis*, and the significant similarities shared by the two species at a genetic level, many hypotheses have been made regarding the differences observed in both *Candida* filamentation and virulence (Stokes *et al.*, 2007). However, many of these hypotheses have not been experimentally verified at a protein level. As the first point of contact between fungal cells and host tissues, many GPI-anchored cell wall proteins have been identified as important virulence factors. Therefore identification, relative quantification and comparison of *C. albicans* and *C. dubliniensis* GPI-linked cell wall proteins was carried out. This study has enabled the generation and comparison of a GPI-cell wall anchored proteome for *C. dubliniensis*, and *C. albicans*, under matching conditions, in which cell morphology is induced and maintained over extended time periods (18 h).

6.4.1. Comparison of *in silico* and *in vitro* GPI-protein identification

Prediction of GPI-anchored proteins from proteome databases composed of translated open reading frame entries from the respective genomic databases resulted in a similar number of predictions for both *C. albicans* and *C. dubliniensis*, reflecting the high genomic similarity between the species. These predictions represented 0.5 % and 0.6 % of the *C. dubliniensis* and *C. albicans* total potential proteome respectively. While *in silico* analyses may identify GPI-anchored cell wall protein motifs such as a GPI-cleavage sequence or signal sequence targeting a protein to the fungal cell wall, the ability to assign proteins to various morphological forms currently requires experimental verification. Although more than 30 GPI-proteins were predicted for both *C. albicans* and *C. dubliniensis*, only a subset of these proteins were likely to be expressed in the morphologies, and growth conditions, analysed. Thus, it was unsurprising to find, by Q-TOF analyses of *C. dubliniensis* WÜ284 cultures, 18 distinct proteins were detected, with half of those identified as morphology-specific. Similarly, Q-TOF analysis of HE30 cultures yielded 17 distinct protein identifications, seven of which were dependent on cell morphology. Similar results for *C. albicans*, with over half of the proteins detected identified as morphology specific, highlighted the importance of experimental verification of *in silico* predictions. Correlation between protein predictions and experimental

verification was poor, highlighting the limitations of *in silico* predictions. Identification of morphology-specific proteins has played an important role in understanding the pathogenesis of *C. albicans*. Identification and assignment of *C. dubliniensis* proteins to specific morphologies has the potential to reveal important information about the difference in pathogenesis between *C. dubliniensis* and *C. albicans*.

6.4.2. Identification of GPI-proteins by Q-TOF

6.4.2.1. Morphology-independent protein expression

Protein detection by Q-TOF identified a core set of seven proteins (Cht2p, Pir1, Ecm33p, Rbt5p, Pga4p, Crh11p, Ssr1p) in both *C. dubliniensis* and *C. albicans* that were expressed independently of morphology. The majority of these proteins are associated with cell wall remodeling and integrity and may play a role in *Candida* virulence. The chitinase Cht2p is responsible for remodeling of the chitinous cell wall and thus plays an important role in the response of the fungal cell to changing environments (McCreath *et al.*, 1995). Notably *CHT2* has been found to be negatively regulated by the cAMP signaling pathway in *C. albicans*, indicating a potential mechanism of communication between both *C. albicans* and *C. dubliniensis* hyphal induction and cell wall remodeling (Harcus *et al.*, 2004). A heterozygous *CaPIR1* mutant, constructed by Martinez *et al.*, showed cell wall defects and, although little is known regarding a mechanism of action, Pir1p is thought to play a role in cell wall stability (Martinez *et al.*, 2004). Gene transcription is induced by many different environmental stimuli including hypoxia and low pH, although conversely, studies have shown expression to be decreased during the switch from yeast to hyphal growth (Sorgo *et al.*, 2010). Both cell wall stability and filamentation appear to be influenced by Ecm33p (Martinez-Lopez *et al.*, 2004). Null mutants of *ECM33* in *C. albicans* displayed cell wall defects and are non-filamentous under hypha-inducing conditions. The transglycosylases, Pga4p and Crh11p, likely play an important role in cell wall adaptation through carbohydrate metabolism, providing building blocks for wall remodeling (Alberti-Segui *et al.*, 2004; De Groot *et al.*, 2003). Both proteins are induced in low oxygen growth environments. The role of Ssr1p in *Candida* cells is still undefined, although levels of β -1,3-glucan in a null mutant were increased in what has been described as a “compensatory mechanism”, suggesting a role in cell wall

integrity and stability (Garcera *et al.*, 2005). While these seven core morphology-independent proteins were present in yeast and hyphae of both *C. albicans* and *C. dubliniensis*, three proteins were expressed only in *C. albicans* yeast that showed morphology-independent expression in *C. dubliniensis*. The transglycosylases, Mp65p and Utr2p were expressed in yeast and hyphae of both *C. dubliniensis* WÜ284 and HE30 (Pardini *et al.*, 2006; Sandini *et al.*, 2011). In addition, Rhd3p was found on the surface of HE30 yeast and hyphae. The protein in *C. albicans* is usually repressed during the yeast to hypha switch but is associated with virulence as the *C. albicans* null mutant displayed reduced virulence in a RHE model of infection (de Boer *et al.*, 2010). The presence of Rhd3p on the surface of hyphae may contribute to the relatively high virulence of *C. dubliniensis* HE30.

6.4.2.2. Morphology-dependent protein expression

Generation of a morphology-dependent GPI- cell wall proteome for *C. albicans* and *C. dubliniensis* by Q-TOF confirmed a number of hypotheses about the influencing factors behind the differential virulence *C. albicans* and *C. dubliniensis*. Differences in the yeast-specific proteomes of *C. albicans* and *C. dubliniensis* included detection of Pga10p and Als1p on the surface of *C. albicans* yeast cells but not *C. dubliniensis* yeast cells. Additionally, Als2p was detected on *C. dubliniensis* yeast but not *C. albicans* yeast. Although Als1p and Als2p are both members of the ALS family of adhesins, they are known to bind different substrates and appear to contribute to *Candida* virulence to different degrees (Green *et al.*, 2005; Sheppard *et al.*, 2004). The presence of Pga10p on the surface of *C. albicans* yeast cells also reinforces the increased virulence of *C. albicans*, as the protein is associated with iron utilisation, resulting in a fitness increase in host tissues (Weissman & Kornitzer, 2004). The hypha-specific proteome also identified differential expression of a number of proteins known to influence *Candida* virulence. The absence of *ALS3* and *HYR1* from the *C. dubliniensis* genome and the impact of these putative virulence factors on *Candida* pathogenesis has been discussed in Chapter 3. These proteins were detected on the surface of *C. albicans* hyphae, in addition to Sod5p and Als5p. The presence of Als5p may be an indication of the functional redundancy commonly seen in *C. albicans* or it may be expressed as a substrate-specific adhesin. The superoxide dismutase Sod5p has been shown to protect *C. albicans* against oxidative stress and is strongly expressed in *C. albicans* hyphae (Frohner *et al.*, 2009). Although *C. dubliniensis* hyphae did not express Als5p,

Sod5p was detected under the conditions tested, demonstrating potential to react to general environmental stresses such as reactive oxygen species, but lacking the potential to bind strongly to host-specific substrates. As Als3p and Hyr1 constitute a significant proportion of the *C. albicans* hyphal cell surface, the lack of these proteins from the surface of *C. dubliniensis* hyphae presents an opportunity for alternative proteins to occupy the corresponding space on the hyphal cell surface. Analysis of *C. dubliniensis* hyphae by Q-TOF identified Flo9p on the surface of both WÜ284 and HE30 hyphal cells.

6.4.3. Methodology sensitivity and variation

Relative quantification by FTMS detection of GPI-cell wall anchored proteins further increased our understanding of the yeast and hyphal cell wall proteomes of *C. dubliniensis* and *C. albicans*. While a morphology-specific proteome, with relative quantification of proteins, is available for *C. albicans* grown under a variety of conditions, the conditions used for the current study allowed comparable induction and maintenance of *C. dubliniensis* true hyphae after 18 h (Heilmann *et al.*, 2011). This enabled improved comparisons of *Candida* morphology-specific protein expression. Although both Q-TOF and FTMS analysis identified proteins based on detection of tryptic peptides, FTMS is a more sensitive measurement. Coupled with quantification by comparing ^{14}N and ^{15}N ratios as part of the FTMS detection, there were a small number of differences in proteins detected by the two methods. Specifically, Q-TOF detected Pga10p and Als5p in *C. albicans* hyphae, and Hwp1p in WÜ284 hyphae. These proteins were not detected by FTMS, presumably due to the low levels of protein expression, or in the case of Hwp1p, limitations in detection of valid tryptic peptides. In addition, FTMS detected four proteins not observed by Q-TOF. Low levels of Sod4p, Pga25p and Ssa2p were detected by FTMS. Although Phr1p was not detected by Q-TOF, significant amounts of the protein were detected in hyphal samples analysed by FTMS.

6.4.4. Intra- and inter-species cell wall GPI-protein variation

Analysis of cells by FTMS revealed both interspecies and intraspecies variation in levels of protein expression. Significant differences in protein quantity at the cell surface of either yeast or hyphal cells likely has a large impact on the different levels of virulence associated with each of the strains examined. While five times the

amount of Cht2p was detected on the surface of *C. albicans* SC5314 yeast cells compared to SC5314 hyphae, a different trend was observed for *C. dubliniensis* cells. Hyphal cells from both *C. dubliniensis* strains presented more Cht2p than on the surface of yeast, indicating a higher level, or increased potential for, cell wall remodeling in *C. dubliniensis* hyphae. Whether this is a species-specific adaptation to environmental sensing is unclear. It is perhaps important to note that *CHT2* experiences negative regulation in *C. albicans* as a result of cAMP signaling. It has yet to be investigated whether this apparent regulation mechanism is intact in *C. dubliniensis*. Expression of Crh11p at the *Candida* cell surface presented a number of different trends. Hyphal cells of SC5314 displayed approximately three times the amount of Crh11p on the cell surface of hyphal cells as yeast cells. Conversely WÜ284 hyphae displayed half the amount of Crh11p on the surface of hyphae compared to yeast cells. Cells from either yeast or hyphal cultures of HE30 did not display any change in the levels of Crh11p present on the cell surface. Presumably Crh11p confers a fitness advantage to the fungal cell in specific environmental conditions. The wide-ranging differences in regulation of Crh11p in the samples investigated may indicate evolution of strain-specific adaptation of regulatory mechanisms that are not yet understood. It is possible that this is as a result of adaptation of each strain to specific niches. While Rhd3p is strongly downregulated in both *C. dubliniensis* and *C. albicans* hyphae, the relative abundance of the protein on the surface of *C. dubliniensis* yeast cells compared to *C. albicans* yeast cells is striking. This may be an indication of species-specific response to iron abundance in the growth medium. Regardless, it is not clear what impact this difference in protein quantity has on the relative virulence of *C. albicans* and *C. dubliniensis* yeast cells. Expression levels of Als2p in *C. albicans* were negligible in both yeast and hyphal cells. However, in *C. dubliniensis* yeast Als2p is present in much higher quantities than seen in *C. dubliniensis* hyphae. It has been shown that Als2p is not present on the *C. albicans* surface under many *in vitro* growth conditions (Hoyer *et al.*, 1998b). It has however, been shown to be overexpressed in *C. albicans* biofilms (Nailis *et al.*, 2010). The relatively high levels of Als2p expression in *C. dubliniensis* yeast cells indicate that this adhesin may play a dominant role in the adhesion of cells within *C. dubliniensis* biofilms, perhaps compensating for the lack of *ALS3* and corresponding protein. Levels of Pga4p abundance presented divergent patterns of expression between the two *Candida* species. Hyphal cells of SC5314 displayed twice the amount of Pga4p as was found on the surface of yeast cells.

Conversely, the opposite was true for both *C. dubliniensis* strains. The amount of the transglycosylase Pga4p detected on the surface of *C. dubliniensis* hyphal cells was half the amount detected on the surface of yeast cells. The extent to which Pga4p contributes to hyphal-associated virulence in *C. albicans* and the mechanism by which its expression is regulated is not yet known. However, the protein clearly experiences species-specific regulation and thus may play a role in the differential virulence displayed by the two *Candida* species.

6.4.5. Quantification and relative abundance of GPI-proteins

Visualisation of GPI-anchored cell wall protein abundance for each morphology revealed distinct profiles for each strain. By expressing relative quantitation values i.e. $^{14}\text{N}/^{15}\text{N}$ for each protein as a percentage of the sum $^{14}\text{N}/^{15}\text{N}$, it was possible to gain an insight into the relative contribution of each protein to the GPI-protein repertoire for each morphology. While it is clear from previous work, and the current study, that the virulence-associated proteins Hyr1p and Als3p were highly abundant on the surface of *C. albicans* hyphae, it was notable to find a single protein (Flo9p) with similar abundance on the cell wall surface of *C. dubliniensis* HE30 hyphal cells. This proteomic data was also reflected in qRT-PCR gene expression analysis. In *C. albicans*, CaFlo9p was previously determined to be localised to the plasma membrane (Boisrame *et al.*, 2011). As part of the current study, CaFlo9p was absent from the outer cell wall fraction of either yeast or hyphae of *C. albicans* supporting the theory of retention of CaFlo9p at the plasma membrane of *C. albicans* cells. Analysis of CdFLO9 nucleotide sequence revealed domains similar to the IFF family, most closely related to CaIFF11 (Fig. 6.4). Although CaIFF11 has been found to encode a secreted protein required for cell wall structure and virulence, it is apparent that CdFLO9 encodes a GPI-cell wall-associated protein that may express functionality similar to the virulence-associated Calff11p (Bates *et al.*, 2007). The relatively high virulence of the *C. dubliniensis* HE30 strain, compared to WÜ284, in conjunction with the apparent absence of the protein from the surface of WÜ284 cells, indicate that CdFlo9p may play an important role in *C. dubliniensis* hyphal virulence. Whether CdFlo9p may compensate functionally for the lack of Hyr1p and Als3p, reflecting a *C. dubliniensis* niche-specific adaptation, will be the subject of future investigation.

A

```

Cd36_80540      GTKTDTVIVQVPTPNPQVTVTTTWTGTYVTASTITGDKTDTVIVDVPETTTSCLTNT 480
orf19.5404.1|FLO9  GTKTDTVIVQVPTPNPQITVKKTWTESFITASVTGDKTDTVIVDIPETTTSCLTNT 480
*****          *****:***:***:  :::****:*****:*****:*****

Cd36_80540      WTGEYITTTITSGWVIEIPTESVATYVYVYDTSQVPTPKATATSEVTAVTSATTGNDNTAS 540
orf19.5404.1|FLO9  WTGDYITTTITSGWIIIVEVPTQNVVTVIVYDTSQSTSGKTTTTPVVAETAETATTGNDNTAS 540
***:*****:***:***:.* ***** . *:*. *** *****

Cd36_80540      ATGATGNNNNNDSTTG-ATGNEKNKSTPSTAGNVNTAATTTTGNNGNDSTTGATGNNNNN 599
orf19.5404.1|FLO9  TTDATGKLLTTVTSSNDNTTSTGDDSTTASTGNDNTDSTTTTATVNKN--IDSTTNATDN 598
:*.***:.. .. ::. * . :*.***:*** ** :****. ** :  .:* * .:*

Cd36_80540      DSTTGATGNEKNKSTPSTAGNVNTAATTTTGNNGNDSTTGATGNNNIDSTTGATGNEKNK 659
orf19.5404.1|FLO9  DSKATTTGNDNTDSKTTASG---TDSTTTTGDNNSESTASTGNDNDSTTVTGDDYTT 655
*.: :***:..*..:.* * :*****:*.***:***:  **** :***: ..

Cd36_80540      SPPSTAGNVNTAATTTTGNNGNDSTTGATGNNNIDSTTGATGNNNSAST 719
orf19.5404.1|FLO9  ---VTTDNDNTASTIVT-TGNSNTTLLDATGKDSSTTTDNG-HDESTVTTTGDDD--- 706
*.* ****.* .*.***:.* * ..****.*. : :*** :***:

Cd36_80540      TATTDNVNTASTTGATGKDNDSATTGNVNTASTTNTGNNNNNDSTTGATGNNNNNDSTT 779
orf19.5404.1|FLO9  TATTKDNNTASTTTKTG--DNDTATTVNHSIESTTVTTGDDN----TATTGNDDTASTT 759
****.: ***** ** **:***.:. :*.***:.* *.:***:.. ***

Cd36_80540      GATGNNNNNDSTTGATGNTLSTVTTGNDNTASTTGATGNDNSASTASTTDNVNTASATGA 839
orf19.5404.1|FLO9  DATGNDSTTATTGNSHSIESTPVTTGDDNTATT---GNDDTASTVS-TGNDNSASKTGA 813
.***:.. . :*** . :.***:***:.* ****:***.* *.* *:* **

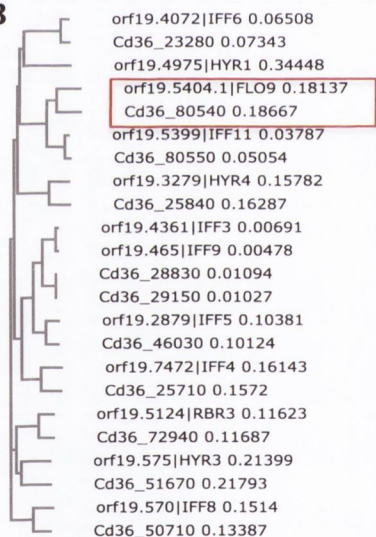
Cd36_80540      TGKGNDSATTGNVNTASTTNTGNNNIDSTTGATGNNNSASTTATDNDVNIASATGAT 899
orf19.5404.1|FLO9  TDTEN--DDTSTGDDDTATTIPTDAPTTFGDFVSSTETKTKKTKTKTKTFEDELTKT 871
*.* * .:***: :***:.* * .. * .: : :.*** * .. : : *

Cd36_80540      GKDNNDSATTGNVNTASTTNTGNNNIDSTTGAPTTSDFSGSTESQSRETKHTKSKNTET 959
orf19.5404.1|FLO9  STSLEASASSSEYPFESTSDQICQCTPVTVTEYIPQSPIPKEVESTTQSTKSFASESSL 931
.. : ***: : : : : : * . * .. ** :*** :***:

Cd36_80540      HKTKLTETSTSLAAISSLEFPFENTSN---LICQCTPVTVTKYIPQSNIPENTESTTQ 1015
orf19.5404.1|FLO9  EPTVSVLSKSESTTDITAETSHESSTEQKSETLDQSTSVVTPATNQESTTDTSSDNNVE 991
. * ..*.* : : : * ..*.*: : *.*.*... :*. :.***:

```

B



C

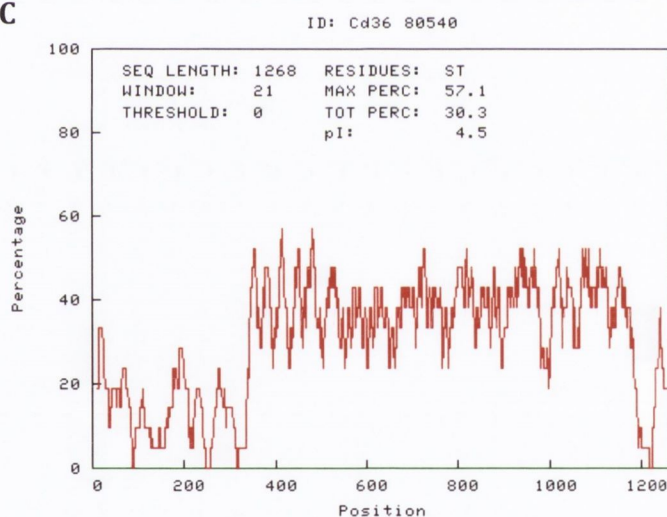


Figure 6.4. Conservation of *FLO9* between *C. albicans* and *C. dubliniensis*.

(A) ClustalW alignment of *CaFLO9* and Cd36_80540 (*CdFLO9*) nucleotide sequences showed significant variation in the N-terminal domain, which is likely to be the functional domain of the translated protein. (B) ClustalW alignment of Cd36_80540 shows that it is an orthologue of *CaFLO9* and related to the *C. albicans IFF* gene family. (C) A ProFASTA amino acid distribution plot showed *CdFlo9p* possesses a serine/threonine-rich mid-region common to GPI-proteins such as *CaHyr1p* and *CaAls3p*.

6.4.6. Cell wall GPI-proteins and vaccine development

GPI-anchored cell wall proteins often act as the first point of interface between the fungal cell and the host. As such it is common for these proteins to be targeted as vaccine candidates. Thus it is important to understand the temporal expression patterns of proteins as part of the *Candida* dimorphic shift in order to assess their potential as vaccine target candidates. Although vaccines targetting Als3p and Sap2p have completed Phase I clinical trials there are concerns about the univalent nature of the protection that they offer (Cassone, 2013). The possibility of fungal adaptation by masking antigens or otherwise evading an immune response is high (Mora-Montes *et al.*, 2011). As indicated by the current study, the lack of *ALS3* and *HYR1* from the *C. dubliniensis* genome may have allowed adaptation of a hypha-specific protein (CdFlo9p), which possesses both putative adhesin function and similarity to members of the *IFF* family, to become a *C. dubliniensis* virulence factor. Although Flo9p is not a surface expressed protein in *C. albicans* SC5314, its *C. dubliniensis* HE30 counterpart has clearly adapted to environmental pressures to express a putative virulence-associated GPI-cell wall protein in the absence of Als3p or Hyr1p. Further investigation of CdFlo9p function will be conducted by deleting the gene from HE30 and WÜ284, and exploring any difference in virulence. This apparent example of evolutionary adaptation highlights the potential for *C. albicans* adaptation to univalent vaccines.

6.4.7. Future directions

This study has, for the first time, enabled experimental identification and analysis GPI-anchored cell wall proteins expressed on the cell surface of both yeast and hyphal cells of *C. dubliniensis* and *C. albicans*. This is an area of study that has until now suffered from a lack of experimental evidence. Similarly, *C. dubliniensis* proteomes such as the secretome, cytosolic proteome and even the chlamydospore-specific proteome, suffer from a distinct absence of experimental support. Proteomic data is now available for the *C. albicans* secretome, biofilm and cells grown under a variety of growth conditions (Ene *et al.*, 2012; Heilmann *et al.*, 2011; Sorgo *et al.*, 2010). Although *C. albicans* and *C. dubliniensis* share a high degree of similarity at a genomic level, this study has shown that there is significant variation in the regulation of proteins associated with the morphogenic shift. Due to the high degree of interconnectivity between filamentation signaling pathways with environmental

sensing, metabolism, and even mating, it is probable that the translation and trafficking of proteins, other than GPI-anchored cell wall proteins, also experiences significant differences between *C. albicans* and *C. dubliniensis*. Investigation of such variation would likely aid in understanding the wider basis behind the differential virulence between *C. albicans* and *C. dubliniensis*. Notably, the data presented here also suggest a high degree of intra-species variation regarding proteome expression. Therefore caution should be used when extrapolating data based on a single strain.

Chapter 7

General discussion

General discussion

Despite the close genetic and phylogenetic relationship between *C. albicans* and *C. dubliniensis*, key differences in virulence-associated features result in a significant difference in pathogenicity between the two *Candida* species. The absence of virulence-associated genes such as *ALS3* and *HYR1*, in combination with its reduced capacity to form true hyphae relative to *C. albicans*, have been suggested as the basis for the reduced virulence of *C. dubliniensis*.

7.1. Molecular cloning methods

7.1.1. Species-specific adaptations and challenges

This study has documented the difficulty in creating *C. dubliniensis* strains expressing the *C. albicans* virulence-associated genes, *CaALS3* and *CaHYR1*. The poor correlation between RNA expression and protein abundance has been documented in other fields of study (Gygi *et al.*, 1999; Vogel & Marcotte, 2012). Translation of RNA into protein is a simplified paradigm. The lack of correlation between *CaALS3* RNA levels, and protein detected by antibody-mediated immunofluorescence, may be due to many factors including RNA or protein modifications, species-specific trafficking and secretion, or even protein presentation on the cell surface, affecting antibody binding. It is clear that numerous processes may have influenced elaboration and detection of protein on the surface of *C. dubliniensis* cells. Attachment of a His or HA-tag to *C. albicans* virulence-associated genes expressed in *C. dubliniensis* would be beneficial for investigation of protein abundance and localisation in the future. This study has also highlighted differences in strength of transcription from promoters. The *CaADH1* promoter has been used as an integral part of many gene expression systems (Bailey *et al.*, 1996; Hiller *et al.*, 2006; Park & Morschhauser, 2005). As molecular methods develop, and alternative gene promoters are chosen for use in gene expression systems, it is important to verify the transcriptional strength of species-specific promoters.

7.2. Filamentation of *C. dubliniensis* and *C. albicans*

7.2.1. Filamentation and strain variation

The reduced ability of *C. dubliniensis* to form true hyphae has been shown previously (O'Connor *et al.*, 2010; Stokes *et al.*, 2007). This current study demonstrated that *C. dubliniensis* strains display a range in their ability to filament although no single *C. dubliniensis* strain was as efficient as *C. albicans* SC5314. It is likely that *C. albicans* strains also show a range in tendency to form true hyphae in response to inducing signals. In order to successfully determine whether there is any correlation between the source of isolation of strains and ability to filament, a much larger panel of *C. dubliniensis* and *C. albicans* strains from various sources would be required for systematic future study. It is intriguing to consider that bloodstream *C. dubliniensis* isolates may be more capable of forming true hyphae compared to oral, gastrointestinal, or even environmental isolates.

7.2.2. Morphology and virulence

By inducing *C. dubliniensis* to form filaments at a higher rate, the contribution of morphology to early adhesion and tissue damage caused by fungal cells in contact with human epithelial cells was investigated. No statistically significant increase in adhesion was found when hyphae were induced. In contrast, tissue damage was increased when fungal cells were induced to develop hyphae at higher rates. Whether this was a result of active penetration as suggested by Wächtler *et al.* for *C. albicans*, or due to the production and secretion of proteases is unclear (Martin *et al.*, 2011b; Wächtler *et al.*, 2012). In order to assess the role of cell surface and secreted proteins in the causation of host tissue damage by *C. dubliniensis* and *C. albicans* hyphae, it would be informative to investigate the cell wall proteome and secretome of *C. dubliniensis* and *C. albicans* hyphae, induced under infection model growth conditions. While there have been some studies regarding actin polymerisation in *C. albicans* hyphae and the role that this may play in the active penetration of host cells, nothing is known concerning the amount of force potentially generated by *C. dubliniensis* hyphae (Hall & Muhlschlegel, 2010; Wolyniak & Sundstrom, 2007). Therefore, the contribution of active penetration of *C. dubliniensis* hyphae to invasion of host cells is currently unclear. Treatment of epithelial cells with cytochalasin D and infection with *C. dubliniensis* hyphae, similar to the method used by Wächtler *et al.* may help

determine the dominant invasion mechanism used by *C. dubliniensis* (Wachtler *et al.*, 2012). Although efforts were made to compare the adhesion and tissue damage caused by similar *C. albicans* and *C. dubliniensis* morphologies, the influence of biomass on pathogenicity should not be overlooked. Due to the requirement for nutrient limitation in the induction of *C. dubliniensis* true hyphae, the growth rate of yeast and hyphal cultures may have played a role in the results observed. The kinetic relationship between hyphal extension and yeast growth rates has not been assessed in *C. dubliniensis* and represents one of the experimental complexities of comparing the virulence of different cell morphologies.

7.2.3. Morphologically stable *C. dubliniensis* hyphae

Although the adhesion and tissue damage of *C. dubliniensis* yeast and hyphae was investigated, the presence of minor cell morphotypes in each culture was significant. Similar to hyphal induction with YPDS and WS, induction of low or high ratios of yeast to hyphae with CDMEM or 10 % (v/v) CDMEM, resulted in mixed morphology cultures. In contrast, *C. albicans* SC5314 grown under each hyphal inducing condition developed consistently higher levels of hyphae. In an effort to reduce conflicting factors in mixed morphology populations in this study, and future studies, a growth medium for maximum, stable induction of *C. dubliniensis* hyphae over extended time periods was developed. Future *in vitro* assays using DUBLIN medium to induce pure *C. dubliniensis* hyphal cultures may more accurately assess the contribution of morphology and morphology-associated genes to the pathogenesis of *C. dubliniensis*, and *C. albicans*. Development of the *C. dubliniensis* hyphal inducing medium highlighted differences in the apparent regulation of *C. albicans* and *C. dubliniensis* hyphae. Reversion of *C. albicans* hyphae to yeast has been documented previously (Heilmann *et al.*, 2011; Lindsay *et al.*, 2012). The current study showed that reversion of *C. dubliniensis* hyphal growth to yeast was more common than *C. albicans* reversion. This observation confirms that not only does *C. dubliniensis* exhibit reduced ability to initiate formation of true hyphae, but the less pathogenic species also shows reduced ability to maintain hyphal growth and extension compared to *C. albicans*. Lu *et al.* demonstrated the importance of relief of *NRG1* transcriptional repression in the two distinct phases of hyphal initiation and maintenance (Lu *et al.*, 2011). Moran *et al.* have also shown that differential regulation of *NRG1* in *C. dubliniensis* contributes to lower rates of filamentation and virulence (Moran *et al.*,

2007). As part of the current study, investigation of the genetic regulatory mechanisms of *C. albicans* and *C. dubliniensis* cells undergoing the dimorphic transition supported the importance of downregulation of *NRG1* for elaboration of *C. albicans* and *C. dubliniensis* filaments. Improved hyphal initiation and maintenance with DUBLIN medium was more effective than WS-mediated downregulation of *NRG1*, removing transcriptional repression of hyphal-specific genes. Analysis of the transcript abundance of major morphogenetic regulators *CPH1* and *EFG1* over the course of 18 h showed a highly complex pattern of regulation of filamentation with differential regulation responses between *C. albicans* and *C. dubliniensis*. Development of hyphae is a dynamic process with temporal effects playing an important role in the maintenance of filamentation. The contributions of *EFG1* and *CPH1*, as effectors of the Ras/cAMP and MAPK pathways respectively, likely combine, fine-tuning hyphal initiation and maintenance. The current study has highlighted interspecies, intraspecies and growth-medium specific differences in the genetic regulation of initiation and maintenance of filamentation. Transcriptomic analyses, using the improved hyphal induction medium, with a wider range of *C. albicans* and *C. dubliniensis* strains, would help clarify the regulatory mechanisms and signaling pathways underlying the dimorphic transition.

7.2.4. A *C. dubliniensis* virulence-associated cell wall GPI-protein

While there have been many *C. albicans* proteomic studies conducted, detailing the secretome, cell wall proteome, and intracellular proteome, very little of the *C. dubliniensis* hypothetical protein repertoire has been verified experimentally (Ene *et al.*, 2012; Heilmann *et al.*, 2011; Kamthan *et al.*, 2012). This current study has identified and quantified the yeast and hyphal GPI-anchored cell wall proteomes for *C. dubliniensis*. Comparison of the *C. dubliniensis* GPI-proteome with *C. albicans* morphology-associated GPI-proteome has highlighted the abundance of known virulence-associated proteins on the surface of *C. albicans* hyphae. By comparing two *C. dubliniensis* strains with varying ability to produce hyphae, and differing virulence in a murine systemic infection model, this study has revealed intraspecies differences in protein identity and abundance on yeast and hyphal cells. Of special note was the discovery of a highly abundant protein (*CdFlo9p*) on the hyphal surface of the relatively virulent *C. dubliniensis* HE30, with levels comparable to *CaHyr1p* on SC5314 hyphal cells. It is possible that *CdFlo9p*, a putative adhesin with similarity to

members of the *IFF* family, is expressed by some *C. dubliniensis* strains in the absence of *ALS3* and *HYR1*, serving a similar function. The presence of this protein on the hyphal cell surface of the relatively virulent HE30 and absence from WÜ284 hyphae suggests that *CdFlo9p* may contribute to *C. dubliniensis* virulence. It is not yet known whether *CdFlo9p* is present on the surface of other systemic or oral *C. dubliniensis* isolates. Future studies will focus on the functionality and prevalence of *CdFlo9p* throughout the *C. dubliniensis* population.

7.3. Filamentation and evolutionary adaptation

7.3.1. Epidemiological source as an indicator of filamentous virulence

Strain variation appears to play an important role in adhesion to epithelial cells and tissue damage. It is important to note that WÜ284 was originally isolated from the oral cavity of a patient suffering from AIDS (Morschhauser *et al.*, 1999). In contrast, both HE30 and SC5314 were isolated from systemic candidiasis infections (Asmundsdottir *et al.*, 2009; Fonzi & Irwin, 1993). Certainly, when investigating the genetic regulatory mechanisms underlying filamentation, *C. dubliniensis* HE30 and *C. albicans* SC5314 displayed similar patterns of gene expression compared to WÜ284. Additionally, GPI-protein distribution on the cell surface of HE30 hyphae displayed similarity to SC5314 in the elaboration of a dominant protein that may function as an adhesin. It is intriguing to consider that “virulent” *C. dubliniensis* bloodstream isolates are more capable of causing disseminated infection as a result of similarities to *C. albicans* systemic isolates in the regulation of filamentation. Further analysis of additional strains, from a variety of sources, will determine whether filamentous virulence of systemic *C. dubliniensis* isolates is the rule or the exception. It would be beneficial to investigate the morphogenetic regulatory patterns exhibited by *C. albicans* oral isolates for comparison with *C. dubliniensis* oral isolates such as WÜ284. Further analysis may help identify convergent or divergent evolutionary patterns exhibited by *C. albicans* and *C. dubliniensis* as a result of adaptation to specific niches.

7.3.2. The importance of host factors

Regardless of elaboration of *Candida* virulence factors, host factors and immune status play an extremely important role in candidiasis. Microenvironments within the human host vary and factors such as carbon source, oxidative stress, pH, CO₂

concentration, and general nutrient levels induce different responses in *C. albicans* and *C. dubliniensis* (Cottier & Muhlschlegel, 2009; Ene *et al.*, 2012; Grahl *et al.*, 2012). The morphological flexibility and redundancy of *C. albicans* in response to many of these signals, readily producing true hyphae capable of invading host tissues, is important for the virulence of the species. The low filamentation efficiency displayed by *C. dubliniensis* in response to the same hypha-inducing signals is clear. This current study suggests that *C. dubliniensis* requires the coordination of many hypha-inducing signals in the host microenvironment in order to initiate and maintain hyphae. This requirement reflects the relatively rare isolation of *C. dubliniensis* from systemic infections compared to *C. albicans*.

7.3.3. Evolutionary and pathogenic divergence

The stark contrast between the reported virulence rates of *C. albicans* and *C. dubliniensis* in conjunction with differential regulation of filamentation and expansion or reduction of gene families associated with virulence presents a view of two related species which have followed functionally distinct evolutionary pathways. While *C. albicans* has expanded its genetic repertoire with relation to virulence-associated genes, the pathogenic species also readily produces hyphae and hypha-specific proteins in response to environmental cues commonly found in the human host, resulting in an organism highly capable of taking advantage of a suppressed immune system, resulting in invasive disease. Although *C. dubliniensis* is closely related to *C. albicans*, the lack of virulence- and hypha-associated genes such as *ALS3* and *HYR1*, coupled with its reduced capacity to produce hyphae in response to physiological cues in the human host, has resulted in an organism that is rarely identified as an opportunistic pathogen. As a consequence of the combined impact of reduced filamentation and lack of virulence genes in *C. dubliniensis*, the species is more suited to growth as a commensal rather than an opportunistic pathogen. However, the selective pressures that have caused this divergent evolution are not defined and some *C. dubliniensis* strains may yet possess the capability to follow the pathogenic path followed by *C. albicans*.

7.4. Future directions and concluding remarks

Further development of *C. dubliniensis* specific molecular tools for heterologous expression of *C. albicans* hypha-regulated virulence genes is required in order to

better assess the importance of hypha-specific genes and proteins in the pathogenesis of filamentous *Candida*. Although gene knockout strains have been created for *C. albicans* filamentation studies, relatively few complementary *C. dubliniensis* strains are available. Deletion of the master morphogenetic regulators, *EFG1* or *CPH1*, would help determine the relative importance of each signaling pathway for hyphal initiation and maintenance. *Candida dubliniensis* filamentation studies have thus far suffered from hyphal reversion to yeast over time, resulting in analysis of mixed morphology populations. Using DUBLIN medium, future studies will be able to investigate the behavior and characteristics of stable *C. dubliniensis* hyphal cultures over extended time periods. Although *C. dubliniensis* transcriptomic data are available, very little data exist confirming the presence and abundance of protein (O'Connor *et al.*, 2010; Spiering *et al.*, 2010). This current study has revealed the nature of the GPI-proteome for yeast and hyphal cell walls. However, alternative morphologies such as chlamyospores, opaque cells and pseudohyphae may present a different protein repertoire, affecting cell behavior and virulence. As previously mentioned, investigation of *C. dubliniensis* intracellular proteins and the secretome may elaborate on the relative lack of pathogenesis of *C. dubliniensis*. Finally, integration of filamentation studies and proteomic data with population structure data would improve epidemiological studies of *C. albicans* and *C. dubliniensis*, furthering our understanding of the mechanisms and selective pressures that have enabled *C. albicans* to become the most successful *Candida* pathogen.

Al Mosaid, A., Sullivan, D. J., Polacheck, I., Shaheen, F. A., Soliman, O., Al Hedaithy, S., Al Thawad, S., Kabadaya, M. & Coleman, D. C. (2005). Novel 5-flucytosine-resistant clade of *Candida dubliniensis* from Saudi Arabia and Egypt identified by Cd25 fingerprinting. *Journal of Clinical Microbiology* **43**, 4026-4036.

Al Thaqafi, A. H., Farahat, F. M., Al Ahmadi, M. I., Al Mowallad, A. F. & Perfect, J. R. (2014). Predictors and outcomes of *Candida* bloodstream infection: eight-year surveillance, western Saudi Arabia. *International Journal of Infectious Diseases* **21**, 5-9.

Alani, E., Cao, L. & Kleckner, N. (1987). A method for gene disruption that allows repeated use of URA3 selection in the construction of multiply disrupted yeast strains. *Genetics* **116**, 541-545.

Alarco, A. M., Marcil, A., Chen, J., Suter, B., Thomas, D. & Whiteway, M. (2004). Immune-deficient *Drosophila melanogaster*: a model for the innate immune response to human fungal pathogens. *J Immunol* **172**, 5622-5628.

Alberti-Segui, C., Morales, A. J., Xing, H., Kessler, M. M., Willins, D. A., Weinstock, K. G., Cottarel, G., Fachtel, K. & Rogers, B. (2004). Identification of potential cell-surface proteins in *Candida albicans* and investigation of the role of a putative cell-surface glycosidase in adhesion and virulence. *Yeast* **21**, 285-302.

Albuquerque, P. & Casadevall, A. (2012). Quorum sensing in fungi--a review. *Medical Mycology* **50**, 337-345.

Alby, K. & Bennett, R. J. (2010). Sexual reproduction in the *Candida* clade: cryptic cycles, diverse mechanisms, and alternative functions. *Cellular and Molecular Life Sciences : CMLS* **67**, 3275-3285.

Almeida, R. S., Brunke, S., Albrecht, A., Thewes, S., Laue, M., Edwards, J. E., Filler, S. G. & Hube, B. (2008). the hyphal-associated adhesin and invasin Als3 of *Candida albicans* mediates iron acquisition from host ferritin. *PLoS Pathogens* **4**, e1000217.

Alnuaimi, A. D., O'Brien-Simpson, N. M., Reynolds, E. C. & McCullough, M. J. (2013). Clinical isolates and laboratory reference *Candida* species and strains have varying abilities to form biofilms. *FEMS Yeast Research* **13**, 689-699.

Alsteens, D., Dague, E., Verbelen, C., Andre, G., Dupres, V. & Dufrene, Y. F. (2009). Nanoscale imaging of microbial pathogens using atomic force microscopy. *Wiley Interdisciplinary Reviews Nanomedicine and Nanobiotechnology* **1**, 168-180.

Alsteens, D., Van Dijck, P., Lipke, P. N. & Dufrene, Y. F. (2013). Quantifying the forces driving cell-cell adhesion in a fungal pathogen. *Langmuir : The ACS Journal of Surfaces and Colloids* **29**, 13473-13480.

Alvarez, F. J. & Konopka, J. B. (2007). Identification of an N-acetylglucosamine transporter that mediates hyphal induction in *Candida albicans*. *Molecular Biology of the Cell* **18**, 965-975.

Arendrup, M., Horn, T. & Frimodt-Moller, N. (2002). *In vivo* pathogenicity of eight medically relevant *Candida* species in an animal model. *Infection* **30**, 286-291.

Argimon, S., Wishart, J. A., Leng, R. & other authors (2007). Developmental regulation of an adhesin gene during cellular morphogenesis in the fungal pathogen *Candida albicans*. *Eukaryotic Cell* **6**, 682-692.

Asmundsdottir, L. R., Erlendsdottir, H., Agnarsson, B. A. & Gottfredsson, M. (2009). The importance of strain variation in virulence of *Candida dubliniensis* and *Candida albicans*: results of a blinded histopathological study of invasive candidiasis. *Clinical Microbiology and Infection* **15**, 576-585.

Bader, O., Weig, M., Taverne-Ghadwal, L., Lugert, R., Gross, U. & Kuhns, M. (2011). Improved clinical laboratory identification of human pathogenic yeasts by matrix-assisted laser desorption ionization time-of-flight mass spectrometry. *Clinical Microbiology and Infection* **17**, 1359-1365.

Baginski, M. & Czub, J. (2009). Amphotericin B and its new derivatives - mode of action. *Current Drug Metabolism* **10**, 459-469.

Bailey, D. A., Feldmann, P. J., Bovey, M., Gow, N. A. & Brown, A. J. (1996). The *Candida albicans* *HYR1* gene, which is activated in response to hyphal development, belongs to a gene family encoding yeast cell wall proteins. *Journal of Bacteriology* **178**, 5353-5360.

Bain, J. M., Stubberfield, C. & Gow, N. A. (2001). Ura-status-dependent adhesion of *Candida albicans* mutants. *FEMS Microbiology Letters* **204**, 323-328.

Banerjee, D., Lelandais, G., Shukla, S., Mukhopadhyay, G., Jacq, C., Devaux, F. & Prasad, R. (2008). Responses of pathogenic and nonpathogenic yeast species to steroids reveal the functioning and evolution of multidrug resistance transcriptional networks. *Eukaryotic Cell* **7**, 68-77.

Barelle, C. J., Priest, C. L., Maccallum, D. M., Gow, N. A., Odds, F. C. & Brown, A. J. (2006). Niche-specific regulation of central metabolic pathways in a fungal pathogen. *Cellular Microbiology* **8**, 961-971.

Basso, L. R., Jr., Bartiss, A., Mao, Y., Gast, C. E., Coelho, P. S., Snyder, M. & Wong, B. (2010). Transformation of *Candida albicans* with a synthetic hygromycin B resistance gene. *Yeast* **27**, 1039-1048.

Bastidas, R. J., Heitman, J. & Cardenas, M. E. (2009). The protein kinase Tor1 regulates adhesin gene expression in *Candida albicans*. *PLoS Pathogens* **5**, e1000294.

Bates, S., de la Rosa, J. M., MacCallum, D. M., Brown, A. J., Gow, N. A. & Odds, F. C. (2007). *Candida albicans* Iff11, a secreted protein required for cell wall structure and virulence. *Infection and Immunity* **75**, 2922-2928.

Bendel, C. M., Hess, D. J., Garni, R. M., Henry-Stanley, M. & Wells, C. L. (2003). Comparative virulence of *Candida albicans* yeast and filamentous forms in orally and intravenously inoculated mice. *Critical Care Medicine* **31**, 501-507.

Berman, J. (2006). Morphogenesis and cell cycle progression in *Candida albicans*. *Current Opinion in Microbiology* **9**, 595-601.

Bertram, G., Swoboda, R. K., Gooday, G. W., Gow, N. A. & Brown, A. J. (1996). Structure and regulation of the *Candida albicans* *ADH1* gene encoding an immunogenic alcohol dehydrogenase. *Yeast* **12**, 115-127.

Biasoli, M. S., Tosello, M. E., Luque, A. G. & Magaro, H. M. (2010). Adherence, colonization and dissemination of *Candida dubliniensis* and other *Candida* species. *Medical Mycology* **48**, 291-297.

Biswas, K. & Morschhauser, J. (2005). The Mep2p ammonium permease controls nitrogen starvation-induced filamentous growth in *Candida albicans*. *Molecular Microbiology* **56**, 649-669.

Biswas, S., Van Dijck, P. & Datta, A. (2007). Environmental sensing and signal transduction pathways regulating morphopathogenic determinants of *Candida albicans*. *Microbiology and Molecular Biology Reviews* : *MMBR* **71**, 348-376.

Blignaut, E., Pujol, C., Joly, S. & Soll, D. R. (2003). Racial distribution of *Candida dubliniensis* colonization among South Africans. *Journal of Clinical Microbiology* **41**, 1838-1842.

Boisrame, A., Cornu, A., Da Costa, G. & Richard, M. L. (2011). Unexpected role for a serine/threonine-rich domain in the *Candida albicans* Iff protein family. *Eukaryotic Cell* **10**, 1317-1330.

Bonhomme, J. & d'Enfert, C. (2013). *Candida albicans* biofilms: building a heterogeneous, drug-tolerant environment. *Current Opinion in Microbiology* **16**, 398-403.

Bougnoux, M. E., Morand, S. & d'Enfert, C. (2002). Usefulness of multilocus sequence typing for characterization of clinical isolates of *Candida albicans*. *Journal of Clinical Microbiology* **40**, 1290-1297.

Bougnoux, M. E., Diogo, D., Francois, N. & other authors (2006). Multilocus sequence typing reveals intrafamilial transmission and microevolutions of *Candida albicans* isolates from the human digestive tract. *Journal of Clinical Microbiology* **44**, 1810-1820.

Boyer, M. & Wisniewski-Dye, F. (2009). Cell-cell signalling in bacteria: not simply a matter of quorum. *FEMS Microbiology Ecology* **70**, 1-19.

Brand, A., MacCallum, D. M., Brown, A. J., Gow, N. A. & Odds, F. C. (2004). Ectopic expression of *URA3* can influence the virulence phenotypes and proteome of *Candida albicans* but can be overcome by targeted reintegration of *URA3* at the *RPS10* locus. *Eukaryotic Cell* **3**, 900-909.

Braun, B. R., Kadosh, D. & Johnson, A. D. (2001). *NRG1*, a repressor of filamentous growth in *C. albicans*, is down-regulated during filament induction. *The EMBO Journal* **20**, 4753-4761.

- Butler, G., Kenny, C., Fagan, A., Kurischko, C., Gaillardin, C. & Wolfe, K. H. (2004).** Evolution of the *MAT* locus and its Ho endonuclease in yeast species. *Proceedings of the National Academy of Sciences of the United States of America* **101**, 1632-1637.
- Butler, G., Rasmussen, M. D., Lin, M. F. & other authors (2009).** Evolution of pathogenicity and sexual reproduction in eight *Candida* genomes. *Nature* **459**, 657-662.
- Butler, G. (2010).** Fungal sex and pathogenesis. *Clinical Microbiology Reviews* **23**, 140-159.
- Cassone, A. (2013).** Development of vaccines for *Candida albicans*: fighting a skilled transformer. *Nature Reviews Microbiology* **11**, 884-891.
- Chabasse, D., Bouchara, J. P., de Gentile, L. & Chennebault, J. M. (1988).** *Candida albicans* chlamydospores observed *in vivo* in a patient with AIDS. *Annales de Biologie Clinique* **46**, 817-818.
- Chaffin, W. L. & Wheeler, D. E. (1981).** Morphological commitment in *Candida albicans*. *Canadian Journal of Microbiology* **27**, 131-137.
- Chaffin, W. L. (1984).** The relationship between yeast cell size and cell division in *Candida albicans*. *Canadian Journal of Microbiology* **30**, 192-203.
- Chao, C. C., Hsu, P. C., Jen, C. F. & other authors (2010).** Zebrafish as a model host for *Candida albicans* infection. *Infection and Immunity* **78**, 2512-2521.
- Chen, H., Fujita, M., Feng, Q., Clardy, J. & Fink, G. R. (2004).** Tyrosol is a quorum-sensing molecule in *Candida albicans*. *Proceedings of the National Academy of Sciences of the United States of America* **101**, 5048-5052.
- Chen, X., Zhao, X., Xiong, Y., Liu, J. & Zhan, C. G. (2011).** Fundamental reaction pathway and free energy profile for hydrolysis of intracellular second messenger adenosine 3',5'-cyclic monophosphate (cAMP) catalyzed by phosphodiesterase-4. *The Journal of Physical Chemistry B* **115**, 12208-12219.
- Cheng, S., Nguyen, M. H., Zhang, Z., Jia, H., Handfield, M. & Clancy, C. J. (2003).** Evaluation of the roles of four *Candida albicans* genes in virulence by using gene disruption strains that express *URA3* from the native locus. *Infection and Immunity* **71**, 6101-6103.
- Citiulo, F., Moran, G. P., Coleman, D. C. & Sullivan, D. J. (2009).** Purification and germination of *Candida albicans* and *Candida dubliniensis* chlamydospores cultured in liquid media. *FEMS Yeast Research* **9**, 1051-1060.
- Cleary, I. A., Reinhard, S. M., Miller, C. L., Murdoch, C., Thornhill, M. H., Lazzell, A. L., Montegudo, C., Thomas, D. P. & Saville, S. P. (2011).** *Candida albicans* adhesin Als3p is dispensable for virulence in the mouse model of disseminated candidiasis. *Microbiology* **157**, 1806-1815.

Clemons, K. V., Gonzalez, G. M., Singh, G., Imai, J., Espiritu, M., Parmar, R. & Stevens, D. A. (2006). Development of an orogastrintestinal mucosal model of candidiasis with dissemination to visceral organs. *Antimicrobial Agents and Chemotherapy* **50**, 2650-2657.

Cottier, F. & Muhlschlegel, F. A. (2009). Sensing the environment: response of *Candida albicans* to the X factor. *FEMS Microbiology Letters* **295**, 1-9.

Dalle, F., Wachtler, B., L'Ollivier, C., Holland, G., Bannert, N., Wilson, D., Labruere, C., Bonnin, A. & Hube, B. (2010). Cellular interactions of *Candida albicans* with human oral epithelial cells and enterocytes. *Cellular Microbiology* **12**, 248-271.

Daniels, K. J., Pujol, C., Srikantha, T. & Soll, D. R. (2012). The "finger," a unique multicellular morphology of *Candida albicans* induced by CO₂ and dependent upon the Ras1-cyclic AMP pathway. *Eukaryotic Cell* **11**, 1257-1267.

De Boer, A. D., de Groot, P. W., Weindl, G. & other authors (2010). The *Candida albicans* cell wall protein Rhd3/Pga29 is abundant in the yeast form and contributes to virulence. *Yeast* **27**, 611-624.

De Groot, P. W., Hellingwerf, K. J. & Klis, F. M. (2003). Genome-wide identification of fungal GPI proteins. *Yeast* **20**, 781-796.

De Groot, P. W., de Boer, A. D., Cunningham, J., Dekker, H. L., de Jong, L., Hellingwerf, K. J., de Koster, C. & Klis, F. M. (2004). Proteomic analysis of *Candida albicans* cell walls reveals covalently bound carbohydrate-active enzymes and adhesins. *Eukaryotic Cell* **3**, 955-965.

De Groot, P. W. & Brandt, B. W. (2012). ProFASTA: a pipeline web server for fungal protein scanning with integration of cell surface prediction software. *Fungal Genetics and Biology* **49**, 173-179.

De Sordi, L. & Muhlschlegel, F. A. (2009). Quorum sensing and fungal-bacterial interactions in *Candida albicans*: a communicative network regulating microbial coexistence and virulence. *FEMS Yeast Research* **9**, 990-999.

Dell, A. & Morris, H. R. (2001). Glycoprotein structure determination by mass spectrometry. *Science* **291**, 2351-2356.

Deveau, A., Piispanen, A. E., Jackson, A. A. & Hogan, D. A. (2010). Farnesol induces hydrogen peroxide resistance in *Candida albicans* yeast by inhibiting the Ras-cyclic AMP signaling pathway. *Eukaryotic Cell* **9**, 569-577.

Deveau, A. & Hogan, D. A. (2011). Linking quorum sensing regulation and biofilm formation by *Candida albicans*. *Methods in Molecular Biology* **692**, 219-233.

Dimopoulos, G., Ntziora, F., Rachiotis, G., Armaganidis, A. & Falagas, M. E. (2008). *Candida albicans* versus non-*albicans* intensive care unit-acquired bloodstream infections: differences in risk factors and outcome. *Anesthesia and Analgesia* **106**, 523-529.

Dodgson, A. R., Dodgson, K. J., Pujol, C., Pfaller, M. A. & Soll, D. R. (2004). Clade-specific flucytosine resistance is due to a single nucleotide change in the *FUR1* gene of *Candida albicans*. *Antimicrobial Agents and Chemotherapy* **48**, 2223-2227.

Doedt, T., Krishnamurthy, S., Bockmuhl, D. P., Tebarth, B., Stempel, C., Russell, C. L., Brown, A. J. & Ernst, J. F. (2004). APSES proteins regulate morphogenesis and metabolism in *Candida albicans*. *Molecular Biology of the Cell* **15**, 3167-3180.

Donnelly, S. M., Sullivan, D. J., Shanley, D. B. & Coleman, D. C. (1999). Phylogenetic analysis and rapid identification of *Candida dubliniensis* based on analysis of *ACT1* intron and exon sequences. *Microbiology* **145 (Pt 8)**, 1871-1882.

Drew, R. H., Townsend, M. L., Pound, M. W., Johnson, S. W. & Perfect, J. R. (2013). Recent advances in the treatment of life-threatening, invasive fungal infections. *Expert Opinion on Pharmacotherapy* **14**, 2361-2374.

Edelmann, A., Kruger, M. & Schmid, J. (2005). Genetic relationship between human and animal isolates of *Candida albicans*. *Journal of Clinical Microbiology* **43**, 6164-6166.

Edwards, J. E., Jr. (2012). Fungal cell wall vaccines: an update. *Journal of Medical Microbiology* **61**, 895-903.

Eisenhaber, B., Schneider, G., Wildpaner, M. & Eisenhaber, F. (2004). A sensitive predictor for potential GPI lipid modification sites in fungal protein sequences and its application to genome-wide studies for *Aspergillus nidulans*, *Candida albicans*, *Neurospora crassa*, *Saccharomyces cerevisiae* and *Schizosaccharomyces pombe*. *Journal of Molecular Biology* **337**, 243-253.

Ene, I. V. & Bennett, R. J. (2009). Hwp1 and related adhesins contribute to both mating and biofilm formation in *Candida albicans*. *Eukaryotic Cell* **8**, 1909-1913.

Ene, I. V., Heilmann, C. J., Sorgo, A. G., Walker, L. A., de Koster, C. G., Munro, C. A., Klis, F. M. & Brown, A. J. (2012). Carbon source-induced reprogramming of the cell wall proteome and secretome modulates the adherence and drug resistance of the fungal pathogen *Candida albicans*. *Proteomics* **12**, 3164-3179.

Ene, I. V., Cheng, S. C., Netea, M. G. & Brown, A. J. (2013). Growth of *Candida albicans* cells on the physiologically relevant carbon source lactate affects their recognition and phagocytosis by immune cells. *Infection and Immunity* **81**, 238-248.

Fang, H. M. & Wang, Y. (2006). RA domain-mediated interaction of Cdc35 with Ras1 is essential for increasing cellular cAMP level for *Candida albicans* hyphal development. *Molecular Microbiology* **61**, 484-496.

Fanning, S. & Mitchell, A. P. (2012). Fungal biofilms. *PLoS Pathogens* **8**, e1002585.

Fidel, P. L., Jr. & Sobel, J. D. (1996). Immunopathogenesis of recurrent vulvovaginal candidiasis. *Clinical Microbiology Reviews* **9**, 335-348.

- Finkel, J. S. & Mitchell, A. P. (2011).** Genetic control of *Candida albicans* biofilm development. *Nature Reviews Microbiology* **9**, 109-118.
- Finley, K. R. & Berman, J. (2005).** Microtubules in *Candida albicans* hyphae drive nuclear dynamics and connect cell cycle progression to morphogenesis. *Eukaryotic Cell* **4**, 1697-1711.
- Fitzpatrick, D. A., Logue, M. E., Stajich, J. E. & Butler, G. (2006).** A fungal phylogeny based on 42 complete genomes derived from supertree and combined gene analysis. *BMC Evolutionary Biology* **6**, 99.
- Fitzpatrick, D. A., O'Gaora, P., Byrne, K. P. & Butler, G. (2010).** Analysis of gene evolution and metabolic pathways using the *Candida* Gene Order Browser. *BMC Genomics* **11**, 290.
- Flevari, A., Theodorakopoulou, M., Velegraki, A., Armaganidis, A. & Dimopoulos, G. (2013).** Treatment of invasive candidiasis in the elderly: a review. *Clinical Interventions in Aging* **8**, 1199-1208.
- Fonzi, W. A. & Irwin, M. Y. (1993).** Isogenic strain construction and gene mapping in *Candida albicans*. *Genetics* **134**, 717-728.
- Fradin, C., Poulain, D. & Jouault, T. (2000).** Beta-1,2-linked oligomannosides from *Candida albicans* bind to a 32-kilodalton macrophage membrane protein homologous to the mammalian lectin galectin-3. *Infection and Immunity* **68**, 4391-4398.
- Free, S. J. (2013).** Fungal cell wall organization and biosynthesis. *Advances in Genetics* **81**, 33-82.
- Frohner, I. E., Bourgeois, C., Yatsyk, K., Majer, O. & Kuchler, K. (2009).** *Candida albicans* cell surface superoxide dismutases degrade host-derived reactive oxygen species to escape innate immune surveillance. *Molecular Microbiology* **71**, 240-252.
- Fu, Y., Phan, Q. T., Luo, G., Solis, N. V., Liu, Y., Cormack, B. P., Edwards, J. E., Jr., Ibrahim, A. S. & Filler, S. G. (2013).** Investigation of the function of *Candida albicans* Als3 by heterologous expression in *Candida glabrata*. *Infection and Immunity* **81**, 2528-2535.
- Fuchs, B. B., Eby, J., Nobile, C. J., El Khoury, J. B., Mitchell, A. P. & Mylonakis, E. (2010).** Role of filamentation in *Galleria mellonella* killing by *Candida albicans*. *Microbes and Infection / Institut Pasteur* **12**, 488-496.
- Gallagher, P. J., Bennett, D. E., Henman, M. C., Russell, R. J., Flint, S. R., Shanley, D. B. & Coleman, D. C. (1992).** Reduced azole susceptibility of oral isolates of *Candida albicans* from HIV-positive patients and a derivative exhibiting colony morphology variation. *Journal of General Microbiology* **138**, 1901-1911.
- Ganguly, S., Bishop, A. C., Xu, W., Ghosh, S., Nickerson, K. W., Lanni, F., Patton-Vogt, J. & Mitchell, A. P. (2011).** Zap1 control of cell-cell signaling in *Candida albicans* biofilms. *Eukaryotic Cell* **10**, 1448-1454.

Garcera, A., Castillo, L., Martinez, A. I., Elorza, M. V., Valentin, E. & Sentandreu, R. (2005). Anchorage of *Candida albicans* Ssr1 to the cell wall, and transcript profiling of the null mutant. *Research in Microbiology* **156**, 911-920.

Garcia, M. G., O'Connor, J. E., Garcia, L. L., Martinez, S. I., Herrero, E. & del Castillo Agudo, L. (2001). Isolation of a *Candida albicans* gene, tightly linked to *URA3*, coding for a putative transcription factor that suppresses a *Saccharomyces cerevisiae aft1* mutation. *Yeast* **18**, 301-311.

Gee, S. F., Joly, S., Soll, D. R., Meis, J. F., Verweij, P. E., Polacheck, I., Sullivan, D. J. & Coleman, D. C. (2002). Identification of four distinct genotypes of *Candida dubliniensis* and detection of microevolution *in vitro* and *in vivo*. *Journal of Clinical Microbiology* **40**, 556-574.

Geiger, J., Wessels, D., Lockhart, S. R. & Soll, D. R. (2004). Release of a potent polymorphonuclear leukocyte chemoattractant is regulated by white-opaque switching in *Candida albicans*. *Infection and Immunity* **72**, 667-677.

Gerami-Nejad, M., Zacchi, L. F., McClellan, M., Matter, K. & Berman, J. (2013). Shuttle vectors for facile gap repair cloning and integration into a neutral locus in *Candida albicans*. *Microbiology* **159**, 565-579.

Gilfillan, G. D., Sullivan, D. J., Haynes, K., Parkinson, T., Coleman, D. C. & Gow, N. A. (1998). *Candida dubliniensis*: phylogeny and putative virulence factors. *Microbiology* **144**, 829-838.

Gillum, A. M., Tsay, E. Y. & Kirsch, D. R. (1984). Isolation of the *Candida albicans* gene for orotidine-5'-phosphate decarboxylase by complementation of *S. cerevisiae ura3* and *E. coli pyrF* mutations. *Molecular and General Genetics* **198**, 179-182.

Goshorn, A. K. & Scherer, S. (1989). Genetic analysis of prototrophic natural variants of *Candida albicans*. *Genetics* **123**, 667-673.

Gossen, M., Freundlieb, S., Bender, G., Muller, G., Hillen, W. & Bujard, H. (1995). Transcriptional activation by tetracyclines in mammalian cells. *Science* **268**, 1766-1769.

Gow, N. A., van de Veerdonk, F. L., Brown, A. J. & Netea, M. G. (2012). *Candida albicans* morphogenesis and host defence: discriminating invasion from colonization. *Nature Reviews Microbiology* **10**, 112-122.

Grahl, N., Shepardson, K. M., Chung, D. & Cramer, R. A. (2012). Hypoxia and fungal pathogenesis: to air or not to air? *Eukaryotic Cell* **11**, 560-570.

Green, C. B., Zhao, X., Yeater, K. M. & Hoyer, L. L. (2005). Construction and real-time RT-PCR validation of *Candida albicans* PALS-GFP reporter strains and their use in flow cytometry analysis of *ALS* gene expression in budding and filamenting cells. *Microbiology* **151**, 1051-1060.

Gunasekera, A., Alvarez, F. J., Douglas, L. M., Wang, H. X., Rosebrock, A. P. & Konopka, J. B. (2010). Identification of *GIG1*, a GlcNAc-induced gene in *Candida*

albicans needed for normal sensitivity to the chitin synthase inhibitor nikkomycin Z. *Eukaryotic Cell* **9**, 1476-1483.

Gygi, S. P., Rochon, Y., Franza, B. R. & Aebersold, R. (1999). Correlation between protein and mRNA abundance in yeast. *Molecular and Cellular Biology* **19**, 1720-1730.

Hall, R. A., De Sordi, L., Maccallum, D. M. & other authors (2010). CO₂ acts as a signalling molecule in populations of the fungal pathogen *Candida albicans*. *PLoS Pathogens* **6**, e1001193.

Hall, R. A. & Muhlschlegel, F. A. (2010). A multi-protein complex controls cAMP signalling and filamentation in the fungal pathogen *Candida albicans*. *Molecular Microbiology* **75**, 534-537.

Hall, R. A. & Gow, N. A. (2013). Mannosylation in *Candida albicans*: role in cell wall function and immune recognition. *Molecular Microbiology* **90**, 1147-1161.

Harcus, D., Nantel, A., Marcil, A., Rigby, T. & Whiteway, M. (2004). Transcription profiling of cyclic AMP signaling in *Candida albicans*. *Molecular Biology of the Cell* **15**, 4490-4499.

Harriott, M. M. & Noverr, M. C. (2011). Importance of *Candida*-bacterial polymicrobial biofilms in disease. *Trends in Microbiology* **19**, 557-563.

Hauser, M., Hess, J. & Belohradsky, B. H. (2003). Treatment of *Candida albicans* endocarditis: case report and a review. *Infection* **31**, 125-127.

Hazan, I., Sepulveda-Becerra, M. & Liu, H. (2002). Hyphal elongation is regulated independently of cell cycle in *Candida albicans*. *Molecular Biology of the Cell* **13**, 134-145.

Hazen, K. C. (2004). Relationship between expression of cell surface hydrophobicity protein 1 (CSH1p) and surface hydrophobicity properties of *Candida dubliniensis*. *Current Microbiology* **48**, 447-451.

Heilmann, C. J., Sorgo, A. G., Siliakus, A. R., Dekker, H. L., Brul, S., de Koster, C. G., de Koning, L. J. & Klis, F. M. (2011). Hyphal induction in the human fungal pathogen *Candida albicans* reveals a characteristic wall protein profile. *Microbiology* **157**, 2297-2307.

Henriques, M., Martins, M., Azeredo, J. & Oliveira, R. (2007). Effect of farnesol on *Candida dubliniensis* morphogenesis. *Letters in Applied Microbiology* **44**, 199-205.

Hernandez, R., Nombela, C., Diez-Orejas, R. & Gil, C. (2004). Two-dimensional reference map of *Candida albicans* hyphal forms. *Proteomics* **4**, 374-382.

Hiller, D., Sanglard, D. & Morschhauser, J. (2006). Overexpression of the *MDR1* gene is sufficient to confer increased resistance to toxic compounds in *Candida albicans*. *Antimicrobial Agents and Chemotherapy* **50**, 1365-1371.

Hiyari, S. & Bennett, K. M. (2011). Dental diagnostics: molecular analysis of oral biofilms. *Journal of Dental Hygiene* **85**, 256-263.

Hogan, D. A., Vik, A. & Kolter, R. (2004). A *Pseudomonas aeruginosa* quorum-sensing molecule influences *Candida albicans* morphology. *Molecular Microbiology* **54**, 1212-1223.

Hogan, D. A. & Sundstrom, P. (2009). The Ras/cAMP/PKA signaling pathway and virulence in *Candida albicans*. *Future Microbiology* **4**, 1263-1270.

Hope, W. W., Taberner, L., Denning, D. W. & Anderson, M. J. (2004). Molecular mechanisms of primary resistance to flucytosine in *Candida albicans*. *Antimicrobial Agents and Chemotherapy* **48**, 4377-4386.

Horak, J. (2013). Regulations of sugar transporters: insights from yeast. *Current Genetics* **59**, 1-31.

Hornby, J. M. & Nickerson, K. W. (2004). Enhanced production of farnesol by *Candida albicans* treated with four azoles. *Antimicrobial Agents and Chemotherapy* **48**, 2305-2307.

Hoyer, L. L., Payne, T. L., Bell, M., Myers, A. M. & Scherer, S. (1998a). *Candida albicans* *ALS3* and insights into the nature of the *ALS* gene family. *Current Genetics* **33**, 451-459.

Hoyer, L. L., Payne, T. L. & Hecht, J. E. (1998b). Identification of *Candida albicans* *ALS2* and *ALS4* and localization of als proteins to the fungal cell surface. *Journal of Bacteriology* **180**, 5334-5343.

Hoyer, L. L. (2001). The *ALS* gene family of *Candida albicans*. *Trends in Microbiology* **9**, 176-180.

Hoyer, L. L., Fundyga, R., Hecht, J. E., Kapteyn, J. C., Klis, F. M. & Arnold, J. (2001). Characterization of agglutinin-like sequence genes from non-*albicans* *Candida* and phylogenetic analysis of the *ALS* family. *Genetics* **157**, 1555-1567.

Hoyer, L. L., Green, C. B., Oh, S. H. & Zhao, X. (2008). Discovering the secrets of the *Candida albicans* agglutinin-like sequence (*ALS*) gene family--a sticky pursuit. *Medical Mycology* **46**, 1-15.

Huang, G., Wang, H., Chou, S., Nie, X., Chen, J. & Liu, H. (2006). Bistable expression of *WOR1*, a master regulator of white-opaque switching in *Candida albicans*. *Proceedings of the National Academy of Sciences of the United States of America* **103**, 12813-12818.

Huang, G., Srikantha, T., Sahni, N., Yi, S. & Soll, D. R. (2009). CO₂ regulates white-to-opaque switching in *Candida albicans*. *Current Biology* **19**, 330-334.

Huang, H., H Marcus, D. & Whiteway, M. (2008). Transcript profiling of a MAP kinase pathway in *C. albicans*. *Microbiological Research* **163**, 380-393.

Hunter, P. R. (1991). A critical review of typing methods for *Candida albicans* and their applications. *Critical Reviews in Microbiology* **17**, 417-434.

Ibrahim, A. S., Spellberg, B. J., Avanesian, V., Fu, Y. & Edwards, J. E., Jr. (2006). The anti-*Candida* vaccine based on the recombinant N-terminal domain of Als1p is broadly active against disseminated candidiasis. *Infection and Immunity* **74**, 3039-3041.

Inglis, D. O., Arnaud, M. B., Binkley, J. & other authors (2012). The *Candida* genome database incorporates multiple *Candida* species: multispecies search and analysis tools with curated gene and protein information for *Candida albicans* and *Candida glabrata*. *Nucleic Acids Research* **40**, D667-674.

Jabra-Rizk, M. A., Falkler, W. A., Jr., Merz, W. G., Kelley, J. I., Baqui, A. A. & Meiller, T. F. (1999). *Candida dubliniensis* and *Candida albicans* display surface variations consistent with observed intergeneric coaggregation. *Revista Iberoamericana de Micologia* **16**, 187-193.

Jabra-Rizk, M. A., Falkler, W. A., Jr., Merz, W. G., Baqui, A. A., Kelley, J. I. & Meiller, T. F. (2000). Retrospective identification and characterization of *Candida dubliniensis* isolates among *Candida albicans* clinical laboratory isolates from human immunodeficiency virus (HIV)-infected and non-HIV-infected individuals. *Journal of Clinical Microbiology* **38**, 2423-2426.

Jackson, A.P., Gamble, J.A., Yeomans, T., Moran, G.P., Saunders, D., Harris, D., Aslett, M., Barrell, J.F., Butler, G., Citiulo, F., Coleman, D.C., de Groot, P.W., Goodwin, T.J., Quail, M.A., McQuillan, J., Munro, C.A., Pain, A., Poulter, R.T., Rajandream, M.A., Renauld, H., Spiering, M.J., Tivey, A., Gow, N.A., Barrell, B., Sullivan, D.J., Berriman, M. (2009). Comparative genomics of the fungal pathogens *Candida dubliniensis* and *Candida albicans*. *Genome Research* **19**, 2231-2244.

Jansons, V. K. & Nickerson, W. J. (1970a). Induction, morphogenesis, and germination of the chlamyospore of *Candida albicans*. *Journal of Bacteriology* **104**, 910-921.

Jansons, V. K. & Nickerson, W. J. (1970b). Chemical composition of chlamyospores of *Candida albicans*. *Journal of Bacteriology* **104**, 922-932.

Jayatilake, J. A., Samaranayake, Y. H. & Samaranayake, L. P. (2008). A comparative study of candidal invasion in rabbit tongue mucosal explants and reconstituted human oral epithelium. *Mycopathologia* **165**, 373-380.

Joly, S., Pujol, C., Rysz, M., Vargas, K. & Soll, D. R. (1999). Development and characterization of complex DNA fingerprinting probes for the infectious yeast *Candida dubliniensis*. *Journal of Clinical Microbiology* **37**, 1035-1044.

Jordan, R. P., Williams, D. W., Moran, G. P., Coleman, D. C. & Sullivan, D. J. (2014). Comparative adherence of *Candida albicans* and *Candida dubliniensis* to human buccal epithelial cells and extracellular matrix proteins. *Medical Mycology* **52**, 254-263.

Kadosh, D. & Johnson, A. D. (2005). Induction of the *Candida albicans* filamentous growth program by relief of transcriptional repression: a genome-wide analysis. *Molecular Biology of the Cell* **16**, 2903-2912.

Kamthan, M., Mukhopadhyay, G., Chakraborty, N., Chakraborty, S. & Datta, A. (2012). Quantitative proteomics and metabolomics approaches to demonstrate N-acetyl-D-glucosamine inducible amino acid deprivation response as morphological switch in *Candida albicans*. *Fungal Genetics and Biology* **49**, 369-378.

Kamthan, M., Kamthan, A., Ruhela, D., Maiti, P., Bhavesh, N. S. & Datta, A. (2013). Upregulation of galactose metabolic pathway by N-acetylglucosamine induced endogenous synthesis of galactose in *Candida albicans*. *Fungal Genetics and Biology* **54**, 15-24.

Kapteyn, J. C., Hoyer, L. L., Hecht, J. E., Muller, W. H., Andel, A., Verkleij, A. J., Makarow, M., Van Den Ende, H. & Klis, F. M. (2000). The cell wall architecture of *Candida albicans* wild-type cells and cell wall-defective mutants. *Molecular Microbiology* **35**, 601-611.

Kapuscinski, J. (1995). DAPI: a DNA-specific fluorescent probe. *Biotechnic & Histochemistry* **70**, 220-233.

Kibbler, C. C., Seaton, S., Barnes, R. A., Gransden, W. R., Holliman, R. E., Johnson, E. M., Perry, J. D., Sullivan, D. J. & Wilson, J. A. (2003). Management and outcome of bloodstream infections due to *Candida* species in England and Wales. *The Journal of Hospital Infection* **54**, 18-24.

Kim, J. O., Garofalo, L., Blecker-Shelly, D. & McGowan, K. L. (2003). *Candida dubliniensis* infections in a pediatric population: retrospective identification from clinical laboratory isolates of *Candida albicans*. *Journal of Clinical Microbiology* **41**, 3354-3357.

Kirkpatrick, W. R., Revankar, S. G., McAtee, R. K. & other authors (1998). Detection of *Candida dubliniensis* in oropharyngeal samples from human immunodeficiency virus-infected patients in North America by primary CHROMagar candida screening and susceptibility testing of isolates. *Journal of Clinical Microbiology* **36**, 3007-3012.

Klengel, T., Liang, W. J., Chaloupka, J. & other authors (2005). Fungal adenylyl cyclase integrates CO₂ sensing with cAMP signaling and virulence. *Current Biology* **15**, 2021-2026.

Klis, F. M., de Groot, P. & Hellingwerf, K. (2001). Molecular organization of the cell wall of *Candida albicans*. *Medical Mycology* **39 Suppl. 1**, 1-8.

Klis, F. M., Sosinska, G. J., de Groot, P. W. & Brul, S. (2009). Covalently linked cell wall proteins of *Candida albicans* and their role in fitness and virulence. *FEMS Yeast Research* **9**, 1013-1028.

Kohler, G. A., White, T. C. & Agabian, N. (1997). Overexpression of a cloned IMP dehydrogenase gene of *Candida albicans* confers resistance to the specific inhibitor mycophenolic acid. *Journal of Bacteriology* **179**, 2331-2338.

Korting, H. C. (1989). Clinical spectrum of oral candidosis and its role in HIV-infected patients. *Mycoses* **32 Suppl. 2**, 23-29.

Korting, H. C., Hube, B., Oberbauer, S., Januschke, E., Hamm, G., Albrecht, A., Borelli, C. & Schaller, M. (2003). Reduced expression of the hyphal-independent *Candida albicans* proteinase genes *SAP1* and *SAP3* in the *efg1* mutant is associated with attenuated virulence during infection of oral epithelium. *Journal of Medical Microbiology* **52**, 623-632.

Krcmery, V. & Barnes, A. J. (2002). Non-*albicans* *Candida* spp. causing fungaemia: pathogenicity and antifungal resistance. *The Journal of Hospital Infection* **50**, 243-260.

Krogh, A., Larsson, B., von Heijne, G. & Sonnhammer, E. L. (2001). Predicting transmembrane protein topology with a hidden Markov model: application to complete genomes. *Journal of Molecular Biology* **305**, 567-580.

Kumamoto, C. A. (2002). *Candida* biofilms. *Current Opinion in Microbiology* **5**, 608-611.

Kumamoto, C. A. (2011). Inflammation and gastrointestinal *Candida* colonization. *Current Opinion in Microbiology* **14**, 386-391.

Kumar, M. J., Jamaluddin, M. S., Natarajan, K., Kaur, D. & Datta, A. (2000). The inducible N-acetylglucosamine catabolic pathway gene cluster in *Candida albicans*: discrete N-acetylglucosamine-inducible factors interact at the promoter of *NAG1*. *Proceedings of the National Academy of Sciences of the United States of America* **97**, 14218-14223.

Kuss, S. K., Best, G. T., Etheredge, C. A., Pruijssers, A. J., Frierson, J. M., Hooper, L. V., Dermody, T. S. & Pfeiffer, J. K. (2011). Intestinal microbiota promote enteric virus replication and systemic pathogenesis. *Science* **334**, 249-252.

Lafleur, M. D., Qi, Q. & Lewis, K. (2010). Patients with long-term oral carriage harbor high-persistence mutants of *Candida albicans*. *Antimicrobial Agents and Chemotherapy* **54**, 39-44.

Langford, M. L., Atkin, A. L. & Nickerson, K. W. (2009). Cellular interactions of farnesol, a quorum-sensing molecule produced by *Candida albicans*. *Future Microbiology* **4**, 1353-1362.

Laniado-Laborin, R. & Cabrales-Vargas, M. N. (2009). Amphotericin B: side effects and toxicity. *Revista Iberoamericana de Micologia* **26**, 223-227.

Lay, J., Henry, L. K., Clifford, J., Koltin, Y., Bulawa, C. E. & Becker, J. M. (1998). Altered expression of selectable marker *URA3* in gene-disrupted *Candida albicans* strains complicates interpretation of virulence studies. *Infection and Immunity* **66**, 5301-5306.

- Leberer, E., Harcus, D., Dignard, D., Johnson, L., Ushinsky, S., Thomas, D. Y. & Schroppel, K. (2001).** Ras links cellular morphogenesis to virulence by regulation of the MAP kinase and cAMP signalling pathways in the pathogenic fungus *Candida albicans*. *Molecular Microbiology* **42**, 673-687.
- Lee, K. L., Buckley, H. R. & Campbell, C. C. (1975).** An amino acid liquid synthetic medium for the development of mycelial and yeast forms of *Candida albicans*. *Sabouraudia* **13**, 148-153.
- Lewis, K. (2010).** Persister cells. *Annual Review of Microbiology* **64**, 357-372.
- Liachko, I. & Dunham, M. J. (2013).** An autonomously replicating sequence for use in a wide range of budding yeasts. *FEMS Yeast Research*.
- Lindsay, A. K., Deveau, A., Piispanen, A. E. & Hogan, D. A. (2012).** Farnesol and cyclic AMP signaling effects on the hypha-to-yeast transition in *Candida albicans*. *Eukaryotic Cell* **11**, 1219-1225.
- Liu, H., Kohler, J. & Fink, G. R. (1994).** Suppression of hyphal formation in *Candida albicans* by mutation of a *STE12* homolog. *Science* **266**, 1723-1726.
- Liu, Y. & Filler, S. G. (2011).** *Candida albicans* Als3, a multifunctional adhesin and invasin. *Eukaryotic Cell* **10**, 168-173.
- Liu, Z. H., Li, M., Lu, X. L., She, X. D., Hu, S. Q., Chen, W. & Liu, W. D. (2010).** Higher concentration of CO₂ and 37°C stabilize the less virulent opaque cell of *Candida albicans*. *Chinese Medical Journal* **123**, 2446-2450.
- Lo, H. J., Kohler, J. R., DiDomenico, B., Loebenberg, D., Cacciapuoti, A. & Fink, G. R. (1997).** Nonfilamentous *C. albicans* mutants are avirulent. *Cell* **90**, 939-949.
- Loreto, E. S., Scheid, L. A., Nogueira, C. W., Zeni, G., Santurio, J. M. & Alves, S. H. (2010).** *Candida dubliniensis*: epidemiology and phenotypic methods for identification. *Mycopathologia* **169**, 431-443.
- Losberger, C. & Ernst, J. F. (1989).** Sequence and transcript analysis of the *C. albicans* *URA3* gene encoding orotidine-5'-phosphate decarboxylase. *Current Genetics* **16**, 153-158.
- Lovering, A. L., Safadi, S. S. & Strynadka, N. C. (2012).** Structural perspective of peptidoglycan biosynthesis and assembly. *Annual Review of Biochemistry* **81**, 451-478.
- Lu, Y., Su, C., Wang, A. & Liu, H. (2011).** Hyphal development in *Candida albicans* requires two temporally linked changes in promoter chromatin for initiation and maintenance. *PLoS Biology* **9**, e1001105.
- Luo, G., Ibrahim, A. S., Spellberg, B., Nobile, C. J., Mitchell, A. P. & Fu, Y. (2010).** *Candida albicans* Hyr1p confers resistance to neutrophil killing and is a potential vaccine target. *The Journal of Infectious Diseases* **201**, 1718-1728.

- Luo, G., Ibrahim, A. S., French, S. W., Edwards, J. E., Jr. & Fu, Y. (2011).** Active and passive immunization with rHyr1p-N protects mice against hematogenously disseminated candidiasis. *PLoS One* **6**, e25909.
- Luo, S., Skerka, C., Kurzai, O. & Zipfel, P. F. (2013).** Complement and innate immune evasion strategies of the human pathogenic fungus *Candida albicans*. *Molecular Immunology* **56**, 161-169.
- Mackenzie, D. W. (1962).** Serum tube identification of *Candida albicans*. *Journal of Clinical Pathology* **15**, 563-565.
- Magee, B. B. & Magee, P. T. (2000).** Induction of mating in *Candida albicans* by construction of MTL α and MTL α strains. *Science* **289**, 310-313.
- Magee, B. B., Sanchez, M. D., Saunders, D., Harris, D., Berriman, M. & Magee, P. T. (2008).** Extensive chromosome rearrangements distinguish the karyotype of the hypovirulent species *Candida dubliniensis* from the virulent *Candida albicans*. *Fungal Genetics and Biology* **45**, 338-350.
- Martchenko, M., Levitin, A., Hogues, H., Nantel, A. & Whiteway, M. (2007).** Transcriptional rewiring of fungal galactose-metabolism circuitry. *Current biology* **17**, 1007-1013.
- Martin, R., Moran, G. P., Jacobsen, I. D., Heyken, A., Domey, J., Sullivan, D. J., Kurzai, O. & Hube, B. (2011a).** The *Candida albicans*-specific gene *EED1* encodes a key regulator of hyphal extension. *PLoS One* **6**, e18394.
- Martin, R., Wachtler, B., Schaller, M., Wilson, D. & Hube, B. (2011b).** Host-pathogen interactions and virulence-associated genes during *Candida albicans* oral infections. *International Journal of Medical Microbiology* **301**, 417-422.
- Martinez, A. I., Castillo, L., Garcera, A., Elorza, M. V., Valentin, E. & Sentandreu, R. (2004).** Role of Pir1 in the construction of the *Candida albicans* cell wall. *Microbiology* **150**, 3151-3161.
- Martinez-Lopez, R., Monteoliva, L., Diez-Orejas, R., Nombela, C. & Gil, C. (2004).** The GPI-anchored protein CaEcm33p is required for cell wall integrity, morphogenesis and virulence in *Candida albicans*. *Microbiology* **150**, 3341-3354.
- Martins, M., Henriques, M., Azeredo, J., Rocha, S. M., Coimbra, M. A. & Oliveira, R. (2007).** Morphogenesis control in *Candida albicans* and *Candida dubliniensis* through signaling molecules produced by planktonic and biofilm cells. *Eukaryotic Cell* **6**, 2429-2436.
- Massey, S. E., Moura, G., Beltrao, P., Almeida, R., Garey, J. R., Tuite, M. F. & Santos, M. A. (2003).** Comparative evolutionary genomics unveils the molecular mechanism of reassessment of the CTG codon in *Candida* spp. *Genome Research* **13**, 544-557.

Matsumoto, H., Nagao, J., Cho, T. & Kodama, J. (2013). Evaluation of pathogenicity of *Candida albicans* in germination-ready states using a silkworm infection model. *Medical Mycology Journal* **54**, 131-140.

Mayer, F. L., Wilson, D. & Hube, B. (2013). *Candida albicans* pathogenicity mechanisms. *Virulence* **4**, 119-128.

Mayor, S. & Riezman, H. (2004). Sorting GPI-anchored proteins. *Nature Reviews Molecular Cell Biology* **5**, 110-120.

McCreath, K. J., Specht, C. A. & Robbins, P. W. (1995). Molecular cloning and characterization of chitinase genes from *Candida albicans*. *Proceedings of the National Academy of Sciences of the United States of America* **92**, 2544-2548.

McManus, B. A., Coleman, D. C., Moran, G. & other authors (2008). Multilocus sequence typing reveals that the population structure of *Candida dubliniensis* is significantly less divergent than that of *Candida albicans*. *Journal of Clinical Microbiology* **46**, 652-664.

McManus, B. A., Sullivan, D. J., Moran, G. P., d'Enfert, C., Bougnoux, M. E., Nunn, M. A. & Coleman, D. C. (2009). Genetic differences between avian and human isolates of *Candida dubliniensis*. *Emerging Infectious Diseases* **15**, 1467-1470.

McManus, B. A. & Coleman, D. C. (2014). Molecular epidemiology, phylogeny and evolution of *Candida albicans*. *Infection, Genetics and Evolution* **21**, 166-178.

Mear, J. B., Kipnis, E., Faure, E., Dessein, R., Schurtz, G., Faure, K. & Guery, B. (2013). *Candida albicans* and *Pseudomonas aeruginosa* interactions: more than an opportunistic criminal association? *Medecine et Maladies Infectieuses* **43**, 146-151.

Merson-Davies, L. A. & Odds, F. C. (1989). A morphology index for characterization of cell shape in *Candida albicans*. *Journal of General Microbiology* **135**, 3143-3152.

Miller, S. E., Spurlock, B. O. & Michaels, G. E. (1974). Electron microscopy of young *Candida albicans* chlamydospores. *Journal of Bacteriology* **119**, 992-999.

Milne, S. W., Cheetham, J., Lloyd, D., Aves, S. & Bates, S. (2011). Cassettes for PCR-mediated gene tagging in *Candida albicans* utilizing nourseothricin resistance. *Yeast* **28**, 833-841.

Miranda, I., Silva-Dias, A., Rocha, R. & other authors (2013). *Candida albicans* CUG mistranslation is a mechanism to create cell surface variation. *MBio* **4**.

Mitchell, L. H. & Soll, D. R. (1979). Commitment to germ tube or bud formation during release from stationary phase in *Candida albicans*. *Experimental Cell Research* **120**, 167-179.

Moazeni, M., Khorramizadeh, M. R., Teimoori-Toolabi, L., Noorbakhsh, F., Fallahi, A. A. & Rezaie, S. (2012). Down-regulation of the *ALS3* gene as a consequent effect of RNA-mediated silencing of the *EFG1* gene in *Candida albicans*. *Iranian Biomedical Journal* **16**, 172-178.

- Mora-Montes, H. M., Netea, M. G., Ferwerda, G. & other authors (2011).** Recognition and blocking of innate immunity cells by *Candida albicans* chitin. *Infection and Immunity* **79**, 1961-1970.
- Moran, G., Sullivan, D., Morschhauser, J. & Coleman, D. (2002).** The *Candida dubliniensis* *CdCDR1* gene is not essential for fluconazole resistance. *Antimicrobial Agents and Chemotherapy* **46**, 2829-2841.
- Moran, G., Stokes, C., Thewes, S., Hube, B., Coleman, D. C. & Sullivan, D. (2004).** Comparative genomics using *Candida albicans* DNA microarrays reveals absence and divergence of virulence-associated genes in *Candida dubliniensis*. *Microbiology* **150**, 3363-3382.
- Moran, G. P., Sanglard, D., Donnelly, S. M., Shanley, D. B., Sullivan, D. J. & Coleman, D. C. (1998).** Identification and expression of multidrug transporters responsible for fluconazole resistance in *Candida dubliniensis*. *Antimicrobial Agents and Chemotherapy* **42**, 1819-1830.
- Moran, G. P., MacCallum, D. M., Spiering, M. J., Coleman, D. C. & Sullivan, D. J. (2007).** Differential regulation of the transcriptional repressor *NRG1* accounts for altered host-cell interactions in *Candida albicans* and *Candida dubliniensis*. *Molecular Microbiology* **66**, 915-929.
- Moran, G. P., Coleman, D. C. & Sullivan, D. J. (2012).** *Candida albicans* versus *Candida dubliniensis*: Why Is *C. albicans* More Pathogenic? *International Journal of Microbiology* **2012**, 205921.
- Moreno-Ruiz, E., Galan-Diez, M., Zhu, W., Fernandez-Ruiz, E., d'Enfert, C., Filler, S. G., Cossart, P. & Veiga, E. (2009).** *Candida albicans* internalization by host cells is mediated by a clathrin-dependent mechanism. *Cellular Microbiology* **11**, 1179-1189.
- Morschhauser, J., Ruhnke, M., Michel, S. & Hacker, J. (1999).** Identification of CARE-2-negative *Candida albicans* isolates as *Candida dubliniensis*. *Mycoses* **42**, 29-32.
- Mosel, D. D., Dumitru, R., Hornby, J. M., Atkin, A. L. & Nickerson, K. W. (2005).** Farnesol concentrations required to block germ tube formation in *Candida albicans* in the presence and absence of serum. *Applied and Environmental Microbiology* **71**, 4938-4940.
- Mukherjee, P. K., Chandra, J., Kuhn, D. M. & Ghannoum, M. A. (2003).** Mechanism of fluconazole resistance in *Candida albicans* biofilms: phase-specific role of efflux pumps and membrane sterols. *Infection and Immunity* **71**, 4333-4340.
- Mukherjee, P. K., Zhou, G., Munyon, R. & Ghannoum, M. A. (2005).** *Candida* biofilm: a well-designed protected environment. *Medical Mycology* **43**, 191-208.
- Mukherjee, P. K., Mohamed, S., Chandra, J. & other authors (2006).** Alcohol dehydrogenase restricts the ability of the pathogen *Candida albicans* to form a biofilm on catheter surfaces through an ethanol-based mechanism. *Infection and Immunity* **74**, 3804-3816.

- Munro, C. A., Schofield, D. A., Gooday, G. W. & Gow, N. A. (1998).** Regulation of chitin synthesis during dimorphic growth of *Candida albicans*. *Microbiology* **144**, 391-401.
- Munro, C. A., Winter, K., Buchan, A., Henry, K., Becker, J. M., Brown, A. J., Bulawa, C. E. & Gow, N. A. (2001).** Chs1 of *Candida albicans* is an essential chitin synthase required for synthesis of the septum and for cell integrity. *Molecular Microbiology* **39**, 1414-1426.
- Murad, A. M., Lee, P. R., Broadbent, I. D., Barelle, C. J. & Brown, A. J. (2000).** Clp10, an efficient and convenient integrating vector for *Candida albicans*. *Yeast* **16**, 325-327.
- Murad, A. M., d'Enfert, C., Gaillardin, C. & other authors (2001).** Transcript profiling in *Candida albicans* reveals new cellular functions for the transcriptional repressors CaTup1, CaMig1 and CaNrg1. *Molecular Microbiology* **42**, 981-993.
- Naglik, J. R., Fidel, P. L., Jr. & Odds, F. C. (2008a).** Animal models of mucosal *Candida* infection. *FEMS Microbiology Letters* **283**, 129-139.
- Naglik, J. R., Moyes, D., Makwana, J. & other authors (2008b).** Quantitative expression of the *Candida albicans* secreted aspartyl proteinase gene family in human oral and vaginal candidiasis. *Microbiology* **154**, 3266-3280.
- Nailis, H., Kucharikova, S., Ricicova, M., Van Dijck, P., Deforce, D., Nelis, H. & Coenye, T. (2010).** Real-time PCR expression profiling of genes encoding potential virulence factors in *Candida albicans* biofilms: identification of model-dependent and -independent gene expression. *BMC Microbiology* **10**, 114.
- Negredo, A., Monteoliva, L., Gil, C., Pla, J. & Nombela, C. (1997).** Cloning, analysis and one-step disruption of the *ARG5,6* gene of *Candida albicans*. *Microbiology* **143**, 297-302.
- Netea, M. G., Brown, G. D., Kullberg, B. J. & Gow, N. A. (2008).** An integrated model of the recognition of *Candida albicans* by the innate immune system. *Nature Reviews Microbiology* **6**, 67-78.
- Nett, J. E., Crawford, K., Marchillo, K. & Andes, D. R. (2010).** Role of Fks1p and matrix glucan in *Candida albicans* biofilm resistance to an echinocandin, pyrimidine, and polyene. *Antimicrobial Agents and Chemotherapy* **54**, 3505-3508.
- Nielsen, H., Engelbrecht, J., Brunak, S. & von Heijne, G. (1997).** A neural network method for identification of prokaryotic and eukaryotic signal peptides and prediction of their cleavage sites. *International Journal of Neural Systems* **8**, 581-599.
- Nielsen, K. & Heitman, J. (2007).** Sex and virulence of human pathogenic fungi. *Advances in Genetics* **57**, 143-173.

- Nigro, G., Fazio, L. L., Martino, M. C. & other authors (2008).** Muramylpeptide shedding modulates cell sensing of *Shigella flexneri*. *Cellular Microbiology* **10**, 682-695.
- Nobbs, A. H., Vickerman, M. M. & Jenkinson, H. F. (2010).** Heterologous expression of *Candida albicans* cell wall-associated adhesins in *Saccharomyces cerevisiae* reveals differential specificities in adherence and biofilm formation and in binding oral *Streptococcus gordonii*. *Eukaryotic Cell* **9**, 1622-1634.
- Nobile, C. J. & Mitchell, A. P. (2006).** Genetics and genomics of *Candida albicans* biofilm formation. *Cellular Microbiology* **8**, 1382-1391.
- Nobile, C. J., Nett, J. E., Andes, D. R. & Mitchell, A. P. (2006).** Function of *Candida albicans* adhesin Hwp1 in biofilm formation. *Eukaryotic Cell* **5**, 1604-1610.
- Nobile, C. J., Nett, J. E., Hernday, A. D., Homann, O. R., Deneault, J. S., Nantel, A., Andes, D. R., Johnson, A. D. & Mitchell, A. P. (2009).** Biofilm matrix regulation by *Candida albicans* Zap1. *PLoS Biology* **7**, e1000133.
- Nobile, C. J., Fox, E. P., Nett, J. E., Sorrells, T. R., Mitrovich, Q. M., Hernday, A. D., Tuch, B. B., Andes, D. R. & Johnson, A. D. (2012).** A recently evolved transcriptional network controls biofilm development in *Candida albicans*. *Cell* **148**, 126-138.
- Nunn, M. A., Schaefer, S. M., Petrou, M. A. & Brown, J. R. (2007).** Environmental source of *Candida dubliniensis*. *Emerging Infectious Diseases* **13**, 747-750.
- O'Connor, L., Caplice, N., Coleman, D. C., Sullivan, D. J. & Moran, G. P. (2010).** Differential filamentation of *Candida albicans* and *Candida dubliniensis* is governed by nutrient regulation of *UME6* expression. *Eukaryotic Cell* **9**, 1383-1397.
- Odds, F. C. (1985).** Morphogenesis in *Candida albicans*. *Critical Reviews in Microbiology* **12**, 45-93.
- Odds, F. C. & Bernaerts, R. (1994).** CHROMagar *Candida*, a new differential isolation medium for presumptive identification of clinically important *Candida* species. *Journal of Clinical Microbiology* **32**, 1923-1929.
- Odds, F. C. (2010).** Molecular phylogenetics and epidemiology of *Candida albicans*. *Future Microbiology* **5**, 67-79.
- Oeser, C., Vergnano, S., Naidoo, R. & other authors (2014).** Neonatal invasive fungal infection in England 2004-2010. *Clinical Microbiology and Infection* In press.
- Oh, S. H., Cheng, G., Nuessen, J. A., Jajko, R., Yeater, K. M., Zhao, X., Pujol, C., Soll, D. R. & Hoyer, L. L. (2005).** Functional specificity of *Candida albicans* Als3p proteins and clade specificity of *ALS3* alleles discriminated by the number of copies of the tandem repeat sequence in the central domain. *Microbiology* **151**, 673-681.
- Otoo, H. N., Lee, K. G., Qiu, W. & Lipke, P. N. (2008).** *Candida albicans* Als adhesins have conserved amyloid-forming sequences. *Eukaryotic Cell* **7**, 776-782.

- Padmanabhan, S., Thakur, J., Siddharthan, R. & Sanyal, K. (2008).** Rapid evolution of Cse4p-rich centromeric DNA sequences in closely related pathogenic yeasts, *Candida albicans* and *Candida dubliniensis*. *Proceedings of the National Academy of Sciences of the United States of America* **105**, 19797-19802.
- Palige, K., Linde, J., Martin, R. & other authors (2013).** Global transcriptome sequencing identifies chlamyospore specific markers in *Candida albicans* and *Candida dubliniensis*. *PLoS One* **8**, e61940.
- Papon, N., Courdavault, V., Clastre, M., Simkin, A. J., Creche, J. & Giglioli-Guivarc'h, N. (2012).** *Deus ex Candida* genetics: overcoming the hurdles for the development of a molecular toolbox in the CTG clade. *Microbiology* **158**, 585-600.
- Papon, N., Courdavault, V., Clastre, M. & Bennett, R. J. (2013).** Emerging and emerged pathogenic *Candida* species: beyond the *Candida albicans* paradigm. *PLoS Pathogens* **9**, e1003550.
- Pardini, G., De Groot, P. W., Coste, A. T., Karababa, M., Klis, F. M., de Koster, C. G. & Sanglard, D. (2006).** The *CRH* family coding for cell wall glycosylphosphatidylinositol proteins with a predicted transglycosidase domain affects cell wall organization and virulence of *Candida albicans*. *The Journal of Biological Chemistry* **281**, 40399-40411.
- Park, H., Liu, Y., Solis, N. & other authors (2009).** Transcriptional responses of *Candida albicans* to epithelial and endothelial cells. *Eukaryotic Cell* **8**, 1498-1510.
- Park, Y. N. & Morschhauser, J. (2005).** Tetracycline-inducible gene expression and gene deletion in *Candida albicans*. *Eukaryotic Cell* **4**, 1328-1342.
- Pearce, M. A. & Howell, S. A. (1991).** Restriction fragment length polymorphism analysis of azole-resistant and azole-susceptible *Candida albicans* strains. *Journal of Clinical Microbiology* **29**, 1364-1367.
- Pfaller, M. A. & Diekema, D. J. (2007).** Epidemiology of invasive candidiasis: a persistent public health problem. *Clinical Microbiology Reviews* **20**, 133-163.
- Pfaller, M. A., Diekema, D. J., Gibbs, D. L., Newell, V. A., Ellis, D., Tullio, V., Rodloff, A., Fu, W. & Ling, T. A. (2010).** Results from the ARTEMIS DISK Global Antifungal Surveillance Study, 1997 to 2007: a 10.5-year analysis of susceptibilities of *Candida* species to fluconazole and voriconazole as determined by CLSI standardized disk diffusion. *Journal of Clinical Microbiology* **48**, 1366-1377.
- Pfaller, M. A. (2012).** Antifungal drug resistance: mechanisms, epidemiology, and consequences for treatment. *The American Journal of Medicine* **125**, S3-13.
- Phan, Q. T., Fratti, R. A., Prasadarao, N. V., Edwards, J. E., Jr. & Filler, S. G. (2005).** N-cadherin mediates endocytosis of *Candida albicans* by endothelial cells. *The Journal of Biological Chemistry* **280**, 10455-10461.
- Phan, Q. T., Myers, C. L., Fu, Y., Sheppard, D. C., Yeaman, M. R., Welch, W. H., Ibrahim, A. S., Edwards, J. E., Jr. & Filler, S. G. (2007).** Als3 is a *Candida albicans*

invasin that binds to cadherins and induces endocytosis by host cells. *PLoS Biology* **5**, e64.

Piispanen, A. E. & Hogan, D. A. (2008). PEPped up: induction of *Candida albicans* virulence by bacterial cell wall fragments. *Cell Host and Microbe* **4**, 1-2.

Piispanen, A. E., Grahl, N., Hollomon, J. M. & Hogan, D. A. (2013). Regulated proteolysis of *Candida albicans* Ras1 is involved in morphogenesis and quorum sensing regulation. *Molecular Microbiology* **89**, 166-178.

Pinjon, E., Sullivan, D., Salkin, I., Shanley, D. & Coleman, D. (1998). Simple, inexpensive, reliable method for differentiation of *Candida dubliniensis* from *Candida albicans*. *Journal of Clinical Microbiology* **36**, 2093-2095.

Pinney, J. H. & Hawkins, P. N. (2012). Amyloidosis. *Annals of Clinical Biochemistry* **49**, 229-241.

Pujol, C., Joly, S., Lockhart, S. R., Noel, S., Tibayrenc, M. & Soll, D. R. (1997). Parity among the randomly amplified polymorphic DNA method, multilocus enzyme electrophoresis, and Southern blot hybridization with the moderately repetitive DNA probe Ca3 for fingerprinting *Candida albicans*. *Journal of Clinical Microbiology* **35**, 2348-2358.

Pujol, C., Pfaller, M. & Soll, D. R. (2002). Ca3 fingerprinting of *Candida albicans* bloodstream isolates from the United States, Canada, South America, and Europe reveals a European clade. *Journal of Clinical Microbiology* **40**, 2729-2740.

Pujol, C., Daniels, K. J., Lockhart, S. R., Srikantha, T., Radke, J. B., Geiger, J. & Soll, D. R. (2004). The closely related species *Candida albicans* and *Candida dubliniensis* can mate. *Eukaryotic Cell* **3**, 1015-1027.

Pukkila-Worley, R., Peleg, A. Y., Tampakakis, E. & Mylonakis, E. (2009). *Candida albicans* hyphal formation and virulence assessed using a *Caenorhabditis elegans* infection model. *Eukaryotic Cell* **8**, 1750-1758.

Quinto-Aleman, D., Canerina-Amaro, A., Hernandez-Abad, L. G., Machin, F., Romesberg, F. E. & Gil-Lamaignere, C. (2012). Yeasts acquire resistance secondary to antifungal drug treatment by adaptive mutagenesis. *PloS One* **7**, e42279.

Ragni, E., Calderon, J., Fascio, U., Sipiczki, M., Fonzi, W. A. & Popolo, L. (2011). Phr1p, a glycosylphosphatidylinositol-anchored beta(1,3)-glucanoyltransferase critical for hyphal wall formation, localizes to the apical growth sites and septa in *Candida albicans*. *Fungal Genetics and Biology* **48**, 793-805.

Ramage, G., Mowat, E., Jones, B., Williams, C. & Lopez-Ribot, J. (2009). Our current understanding of fungal biofilms. *Critical Reviews in Microbiology* **35**, 340-355.

Reuss, O., Vik, A., Kolter, R. & Morschhauser, J. (2004). The SAT1 flipper, an optimized tool for gene disruption in *Candida albicans*. *Gene* **341**, 119-127.

Richard, M. L., Nobile, C. J., Bruno, V. M. & Mitchell, A. P. (2005). *Candida albicans* biofilm-defective mutants. *Eukaryotic Cell* **4**, 1493-1502.

Richard, M. L. & Plaine, A. (2007). Comprehensive analysis of glycosylphosphatidylinositol-anchored proteins in *Candida albicans*. *Eukaryotic Cell* **6**, 119-133.

Robbins, N., Uppuluri, P., Nett, J., Rajendran, R., Ramage, G., Lopez-Ribot, J. L., Andes, D. & Cowen, L. E. (2011). Hsp90 governs dispersion and drug resistance of fungal biofilms. *PLoS Pathogens* **7**, e1002257.

Rocha, C. R., Schroppel, K., Harcus, D., Marcil, A., Dignard, D., Taylor, B. N., Thomas, D. Y., Whiteway, M. & Leberer, E. (2001). Signaling through adenylyl cyclase is essential for hyphal growth and virulence in the pathogenic fungus *Candida albicans*. *Molecular Biology of the Cell* **12**, 3631-3643.

Rotrosen, D., Edwards, J. E., Jr., Gibson, T. R., Moore, J. C., Cohen, A. H. & Green, I. (1985). Adherence of *Candida* to cultured vascular endothelial cells: mechanisms of attachment and endothelial cell penetration. *The Journal of Infectious Diseases* **152**, 1264-1274.

Ruddock, L. W. & Molinari, M. (2006). N-glycan processing in ER quality control. *Journal of Cell Science* **119**, 4373-4380.

Saghrouni, F., Ben Abdeljelil, J., Boukadida, J. & Ben Said, M. (2013). Molecular methods for strain typing of *Candida albicans*: a review. *Journal of Applied Microbiology* **114**, 1559-1574.

Sambrook, J. & Russell, D. W. (2006). Preparation and Transformation of Competent *E. coli* Using Calcium Chloride. *CSH Protocols* **2006**.

Sandini, S., Stringaro, A., Arancia, S., Colone, M., Mondello, F., Murtas, S., Girolamo, A., Mastrangelo, N. & De Bernardis, F. (2011). The *MP65* gene is required for cell wall integrity, adherence to epithelial cells and biofilm formation in *Candida albicans*. *BMC Microbiology* **11**, 106.

Santos, M. A. & Tuite, M. F. (1995). The CUG codon is decoded *in vivo* as serine and not leucine in *Candida albicans*. *Nucleic Acids Research* **23**, 1481-1486.

Sanyal, K., Baum, M. & Carbon, J. (2004). Centromeric DNA sequences in the pathogenic yeast *Candida albicans* are all different and unique. *Proceedings of the National Academy of Sciences of the United States of America* **101**, 11374-11379.

Saville, S. P., Lazzell, A. L., Monteagudo, C. & Lopez-Ribot, J. L. (2003). Engineered control of cell morphology *in vivo* reveals distinct roles for yeast and filamentous forms of *Candida albicans* during infection. *Eukaryotic Cell* **2**, 1053-1060.

Schaller, M., Schackert, C., Korting, H. C., Januschke, E. & Hube, B. (2000). Invasion of *Candida albicans* correlates with expression of secreted aspartic proteinases during experimental infection of human epidermis. *The Journal of Investigative Dermatology* **114**, 712-717.

Schaller, M., Zakikhany, K., Naglik, J. R., Weindl, G. & Hube, B. (2006). Models of oral and vaginal candidiasis based on *in vitro* reconstituted human epithelia. *Nature Protocols* **1**, 2767-2773.

Schmittgen, T. D. & Livak, K. J. (2008). Analyzing real-time PCR data by the comparative C_T method. *Nature Protocols* **3**, 1101-1108.

Scigelova, M., Hornshaw, M., Giannakopoulos, A. & Makarov, A. (2011). Fourier transform mass spectrometry. *Molecular and Cellular Proteomics* **10**, M111 009431.

Scopes, R. K. (1974). Measurement of protein by spectrophotometry at 205 nm. *Analytical Biochemistry* **59**, 277-282.

Selmecki, A., Forche, A. & Berman, J. (2010). Genomic plasticity of the human fungal pathogen *Candida albicans*. *Eukaryotic Cell* **9**, 991-1008.

Sevilla, M. J. & Odds, F. C. (1986). Development of *Candida albicans* hyphae in different growth media--variations in growth rates, cell dimensions and timing of morphogenetic events. *Journal of General Microbiology* **132**, 3083-3088.

Shannon, J. L. (1981). Scanning and transmission electron microscopy of *Candida albicans* chlamydospores. *Journal of General Microbiology* **125**, 199-203.

Shen, J., Guo, W. & Kohler, J. R. (2005). *CaNAT1*, a heterologous dominant selectable marker for transformation of *Candida albicans* and other pathogenic *Candida* species. *Infection and Immunity* **73**, 1239-1242.

Sheppard, D. C., Yeaman, M. R., Welch, W. H. & other authors (2004). Functional and structural diversity in the Als protein family of *Candida albicans*. *The Journal of Biological Chemistry* **279**, 30480-30489.

Sheth, C. C., Hall, R., Lewis, L., Brown, A. J., Odds, F. C., Erwig, L. P. & Gow, N. A. (2011). Glycosylation status of the *C. albicans* cell wall affects the efficiency of neutrophil phagocytosis and killing but not cytokine signaling. *Medical Mycology* **49**, 513-524.

Shevchenko, A., Loboda, A., Shevchenko, A., Ens, W. & Standing, K. G. (2000). MALDI quadrupole time-of-flight mass spectrometry: a powerful tool for proteomic research. *Analytical Chemistry* **72**, 2132-2141.

Silva, S., Negri, M., Henriques, M., Oliveira, R., Williams, D. W. & Azeredo, J. (2011). Adherence and biofilm formation of non-*Candida albicans* *Candida* species. *Trends in Microbiology* **19**, 241-247.

Singh, V., Satheesh, S. V., Raghavendra, M. L. & Sadhale, P. P. (2007). The key enzyme in galactose metabolism, UDP-galactose-4-epimerase, affects cell-wall integrity and morphology in *Candida albicans* even in the absence of galactose. *Fungal Genetics and Biology* **44**, 563-574.

- Slutsky, B., Staebell, M., Anderson, J., Risen, L., Pfaller, M. & Soll, D. R. (1987).** "White-opaque transition": a second high-frequency switching system in *Candida albicans*. *Journal of Bacteriology* **169**, 189-197.
- Soll, D. R., Stasi, M. & Bedell, G. (1978).** The regulation of nuclear migration and division during pseudo-mycelium outgrowth in the dimorphic yeast *Candida albicans*. *Experimental Cell Research* **116**, 207-215.
- Soll, D. R. & Pujol, C. (2003).** *Candida albicans* clades. *FEMS Immunology and Medical Microbiology* **39**, 1-7.
- Sorgo, A. G., Heilmann, C. J., Dekker, H. L., Brul, S., de Koster, C. G. & Klis, F. M. (2010).** Mass spectrometric analysis of the secretome of *Candida albicans*. *Yeast* **27**, 661-672.
- Southern, E. M. (1975).** Detection of specific sequences among DNA fragments separated by gel electrophoresis. *Journal of Molecular Biology* **98**, 503-517.
- Spellberg, B., Ibrahim, A. S., Yeaman, M. R. & other authors (2008).** The antifungal vaccine derived from the recombinant N terminus of Als3p protects mice against the bacterium *Staphylococcus aureus*. *Infection and Immunity* **76**, 4574-4580.
- Spellberg, B. J., Ibrahim, A. S., Avanesian, V., Fu, Y., Myers, C., Phan, Q. T., Filler, S. G., Yeaman, M. R. & Edwards, J. E., Jr. (2006).** Efficacy of the anti-*Candida* rAls3p-N or rAls1p-N vaccines against disseminated and mucosal candidiasis. *The Journal of Infectious Diseases* **194**, 256-260.
- Spiering, M. J., Moran, G. P., Chauvel, M. & other authors (2010).** Comparative transcript profiling of *Candida albicans* and *Candida dubliniensis* identifies *SFL2*, a *C. albicans* gene required for virulence in a reconstituted epithelial infection model. *Eukaryotic Cell* **9**, 251-265.
- Staab, J. F., Bradway, S. D., Fidel, P. L. & Sundstrom, P. (1999).** Adhesive and mammalian transglutaminase substrate properties of *Candida albicans* Hwp1. *Science* **283**, 1535-1538.
- Staab, J. F., Datta, K. & Rhee, P. (2013).** Niche-specific requirement for hyphal wall protein 1 in virulence of *Candida albicans*. *PLoS One* **8**, e80842.
- Staebell, M. & Soll, D. R. (1985).** Temporal and spatial differences in cell wall expansion during bud and mycelium formation in *Candida albicans*. *Journal of General Microbiology* **131**, 1467-1480.
- Staib, P., Moran, G. P., Sullivan, D. J., Coleman, D. C. & Morschhauser, J. (2001).** Isogenic strain construction and gene targeting in *Candida dubliniensis*. *Journal of Bacteriology* **183**, 2859-2865.
- Staib, P. & Morschhauser, J. (2005a).** Liquid growth conditions for abundant chlamydo-spore formation in *Candida dubliniensis*. *Mycoses* **48**, 50-54.

Staib, P. & Morschhauser, J. (2005b). Differential expression of the *NRG1* repressor controls species-specific regulation of chlamyospore development in *Candida albicans* and *Candida dubliniensis*. *Molecular Microbiology* **55**, 637-652.

Staib, P. & Morschhauser, J. (2007). Chlamyospore formation in *Candida albicans* and *Candida dubliniensis*--an enigmatic developmental programme. *Mycoses* **50**, 1-12.

Statland, B. E., Winkel, P. & Killingsworth, L. M. (1976). Factors contributing to intra-individual variation of serum constituents: Physiological day-to-day variation in concentrations of 10 specific proteins in sera of healthy subjects. *Clinical Chemistry* **22**, 1635-1638.

Stokes, C., Moran, G. P., Spiering, M. J., Cole, G. T., Coleman, D. C. & Sullivan, D. J. (2007). Lower filamentation rates of *Candida dubliniensis* contribute to its lower virulence in comparison with *Candida albicans*. *Fungal Genetics and Biology* **44**, 920-931.

Stoldt, V. R., Sonneborn, A., Leuker, C. E. & Ernst, J. F. (1997). Efg1p, an essential regulator of morphogenesis of the human pathogen *Candida albicans*, is a member of a conserved class of bHLH proteins regulating morphogenetic processes in fungi. *The EMBO Journal* **16**, 1982-1991.

Sudbery, P., Gow, N. & Berman, J. (2004). The distinct morphogenic states of *Candida albicans*. *Trends in Microbiology* **12**, 317-324.

Sudbery, P. E. (2001). The germ tubes of *Candida albicans* hyphae and pseudohyphae show different patterns of septin ring localization. *Molecular Microbiology* **41**, 19-31.

Sudbery, P. E. (2011). Growth of *Candida albicans* hyphae. *Nature Reviews Microbiology* **9**, 737-748.

Sullivan, D. & Coleman, D. (1998). *Candida dubliniensis*: characteristics and identification. *Journal of Clinical Microbiology* **36**, 329-334.

Sullivan, D. J., Westerneng, T. J., Haynes, K. A., Bennett, D. E. & Coleman, D. C. (1995). *Candida dubliniensis* sp. nov.: phenotypic and molecular characterization of a novel species associated with oral candidosis in HIV-infected individuals. *Microbiology* **141**, 1507-1521.

Sullivan, D. J., Moran, G. P., Pinjon, E., Al-Mosaïd, A., Stokes, C., Vaughan, C. & Coleman, D. C. (2004). Comparison of the epidemiology, drug resistance mechanisms, and virulence of *Candida dubliniensis* and *Candida albicans*. *FEMS Yeast Research* **4**, 369-376.

Sullivan, D. J., Moran, G. P. & Coleman, D. C. (2005). *Candida dubliniensis*: ten years on. *FEMS Microbiology Letters* **253**, 9-17.

Sullivan, D. J. & Moran, G. P. (2011). Differential virulence of *Candida albicans* and *C. dubliniensis*: A role for Tor1 kinase? *Virulence* **2**, 77-81.

Sundstrom, P., Balish, E. & Allen, C. M. (2002a). Essential role of the *Candida albicans* transglutaminase substrate, hyphal wall protein 1, in lethal oroesophageal candidiasis in immunodeficient mice. *The Journal of Infectious Diseases* **185**, 521-530.

Sundstrom, P., Cutler, J. E. & Staab, J. F. (2002b). Reevaluation of the role of *HWP1* in systemic candidiasis by use of *Candida albicans* strains with selectable marker *URA3* targeted to the *ENO1* locus. *Infection and Immunity* **70**, 3281-3283.

Suzuki, T., Miyamae, Y. & Ishida, I. (1991). Variation of colony morphology and chromosomal rearrangement in *Candida tropicalis* pK233. *Journal of General Microbiology* **137**, 161-167.

Szabo, E. K. & MacCallum, D. M. (2011). The contribution of mouse models to our understanding of systemic candidiasis. *FEMS Microbiology Letters* **320**, 1-8.

Taff, H. T., Mitchell, K. F., Edward, J. A. & Andes, D. R. (2013). Mechanisms of *Candida* biofilm drug resistance. *Future Microbiology* **8**, 1325-1337.

Takemoto, K., Yamamoto, Y. & Ueda, Y. (2006). Evaluation of antifungal pharmacodynamic characteristics of AmBisome against *Candida albicans*. *Microbiology and Immunology* **50**, 579-586.

Tavanti, A., Gow, N. A., Senesi, S., Maiden, M. C. & Odds, F. C. (2003). Optimization and validation of multilocus sequence typing for *Candida albicans*. *Journal of Clinical Microbiology* **41**, 3765-3776.

Tavanti, A., Davidson, A. D., Fordyce, M. J., Gow, N. A., Maiden, M. C. & Odds, F. C. (2005). Population structure and properties of *Candida albicans*, as determined by multilocus sequence typing. *Journal of Clinical Microbiology* **43**, 5601-5613.

Taxis, C. & Knop, M. (2006). System of centromeric, episomal, and integrative vectors based on drug resistance markers for *Saccharomyces cerevisiae*. *BioTechniques* **40**, 73-78.

Tebarth, B., Doedt, T., Krishnamurthy, S., Weide, M., Monterola, F., Dominguez, A. & Ernst, J. F. (2003). Adaptation of the Efg1p morphogenetic pathway in *Candida albicans* by negative autoregulation and PKA-dependent repression of the *EFG1* gene. *Journal of Molecular Biology* **329**, 949-962.

Thompson, D. S., Carlisle, P. L. & Kadosh, D. (2011). Coevolution of morphology and virulence in *Candida* species. *Eukaryotic Cell* **10**, 1173-1182.

Uppuluri, P., Chaturvedi, A. K., Srinivasan, A., Banerjee, M., Ramasubramaniam, A. K., Kohler, J. R., Kadosh, D. & Lopez-Ribot, J. L. (2010). Dispersion as an important step in the *Candida albicans* biofilm developmental cycle. *PLoS Pathogens* **6**, e1000828.

Urban, C., Sohn, K., Lottspeich, F., Brunner, H. & Rupp, S. (2003). Identification of cell surface determinants in *Candida albicans* reveals Tsa1p, a protein differentially localized in the cell. *FEBS Letters* **544**, 228-235.

Vermes, A., Guchelaar, H. J. & Dankert, J. (2000). Flucytosine: a review of its pharmacology, clinical indications, pharmacokinetics, toxicity and drug interactions. *The Journal of Antimicrobial Chemotherapy* **46**, 171-179.

Vidotto, V., Bruatto, M., Accattatis, G. & Caramello, S. (1996). Observation on the nucleic acids in the chlamydospores of *Candida albicans*. *The New Microbiologica* **19**, 327-334.

Vilela, M. M., Kamei, K., Sano, A., Tanaka, R., Uno, J., Takahashi, I., Ito, J., Yarita, K. & Miyaji, M. (2002). Pathogenicity and virulence of *Candida dubliniensis*: comparison with *C. albicans*. *Medical Mycology* **40**, 249-257.

Viudes, A., Peman, J., Canton, E., Ubeda, P., Lopez-Ribot, J. L. & Gobernado, M. (2002). Candidemia at a tertiary-care hospital: epidemiology, treatment, clinical outcome and risk factors for death. *European Journal of Clinical Microbiology and Infectious Diseases* **21**, 767-774.

Vogel, C. & Marcotte, E. M. (2012). Insights into the regulation of protein abundance from proteomic and transcriptomic analyses. *Nature Reviews Genetics* **13**, 227-232.

Wachtler, B., Wilson, D., Haedicke, K., Dalle, F. & Hube, B. (2011). From attachment to damage: defined genes of *Candida albicans* mediate adhesion, invasion and damage during interaction with oral epithelial cells. *PloS One* **6**, e17046.

Wachtler, B., Citiulo, F., Jablonowski, N., Forster, S., Dalle, F., Schaller, M., Wilson, D. & Hube, B. (2012). *Candida albicans*-epithelial interactions: dissecting the roles of active penetration, induced endocytosis and host factors on the infection process. *PloS One* **7**, e36952.

Waldorf, A. R. & Polak, A. (1983). Mechanisms of action of 5-fluorocytosine. *Antimicrobial Agents and Chemotherapy* **23**, 79-85.

Walker, L. A., Gow, N. A. & Munro, C. A. (2013). Elevated chitin content reduces the susceptibility of *Candida* species to caspofungin. *Antimicrobial Agents and Chemotherapy* **57**, 146-154.

Wang, Y. & Xu, X. L. (2008). Bacterial peptidoglycan-derived molecules activate *Candida albicans* hyphal growth. *Communicative and Integrative Biology* **1**, 137-139.

Warendt, A. J. & Konopka, J. B. (2002). Septin function in *Candida albicans* morphogenesis. *Molecular Biology of the Cell* **13**, 2732-2746.

Weber, K., Schulz, B. & Ruhnke, M. (2010). The quorum-sensing molecule *E,E*-farnesol--its variable secretion and its impact on the growth and metabolism of *Candida* species. *Yeast* **27**, 727-739.

Weissman, Z. & Kornitzer, D. (2004). A family of *Candida* cell surface haem-binding proteins involved in haemin and haemoglobin-iron utilization. *Molecular Microbiology* **53**, 1209-1220.

Wilson, L. S., Reyes, C. M., Stolpman, M., Speckman, J., Allen, K. & Beney, J. (2002). The direct cost and incidence of systemic fungal infections. *Value in Health : the Journal of the International Society for Pharmacoeconomics and Outcomes Research* **5**, 26-34.

Wilson, R. B., Davis, D., Enloe, B. M. & Mitchell, A. P. (2000). A recyclable *Candida albicans* *URA3* cassette for PCR product-directed gene disruptions. *Yeast* **16**, 65-70.

Wirsching, S., Michel, S. & Morschhauser, J. (2000). Targeted gene disruption in *Candida albicans* wild-type strains: the role of the *MDR1* gene in fluconazole resistance of clinical *Candida albicans* isolates. *Molecular Microbiology* **36**, 856-865.

Wolyniak, M. J. & Sundstrom, P. (2007). Role of actin cytoskeletal dynamics in activation of the cyclic AMP pathway and *HWP1* gene expression in *Candida albicans*. *Eukaryotic Cell* **6**, 1824-1840.

Wu, W., Lockhart, S. R., Pujol, C., Srikantha, T. & Soll, D. R. (2007). Heterozygosity of genes on the sex chromosome regulates *Candida albicans* virulence. *Molecular Microbiology* **64**, 1587-1604.

Xie, J., Tao, L., Nobile, C. J. & other authors (2013). White-opaque switching in natural MTL α /alpha isolates of *Candida albicans*: evolutionary implications for roles in host adaptation, pathogenesis, and sex. *PLoS Biology* **11**, e1001525.

Zehm, S., Schweinitz, S., Wurzner, R., Colvin, H. P. & Rieder, J. (2012). Detection of *Candida albicans* by mass spectrometric fingerprinting. *Current Microbiology* **64**, 271-275.

Zhang, A., Petrov, K. O., Hyun, E. R., Liu, Z., Gerber, S. A. & Myers, L. C. (2012). The Tlo proteins are stoichiometric components of *Candida albicans* mediator anchored via the Med3 subunit. *Eukaryotic Cell* **11**, 874-884.

Zhao, X., Oh, S. H., Cheng, G., Green, C. B., Nuessen, J. A., Yeater, K., Leng, R. P., Brown, A. J. & Hoyer, L. L. (2004). *ALS3* and *ALS8* represent a single locus that encodes a *Candida albicans* adhesin; functional comparisons between Als3p and Als1p. *Microbiology* **150**, 2415-2428.

Zhao, X., Oh, S. H., Yeater, K. M. & Hoyer, L. L. (2005). Analysis of the *Candida albicans* Als2p and Als4p adhesins suggests the potential for compensatory function within the Als family. *Microbiology* **151**, 1619-1630.

Zhu, W. & Filler, S. G. (2010). Interactions of *Candida albicans* with epithelial cells. *Cellular Microbiology* **12**, 273-282.

Zordan, R. E., Miller, M. G., Galgoczy, D. J., Tuch, B. B. & Johnson, A. D. (2007). Interlocking transcriptional feedback loops control white-opaque switching in *Candida albicans*. *PLoS Biology* **5**, e256.